ENHANCED PROTONATION OF PEPTIDES

USING TRIVALENT CHROMIUM IN

MASS SPECTROMETRY

by

NNENNA ENYIDIYA DIEKE

CAROLYN J. CASSADY, COMMITTEE CHAIR
YUPING BAO
DAVID A. DIXON
GREGORY J. SZULCZEWSKI
JOHN B. VINCENT

A DISSERTATION

Submitted in partial fulfillment of the requirements
for the degree of Doctor of Philosophy
in the Department of Chemistry and Biochemistry
in the Graduate School of
The University of Alabama

TUSCALOOSA, ALABAMA

2022

ABSTRACT

Ionization of peptides is an important step in mass spectrometry (MS)-based bottom-up proteomics. Electrospray ionization (ESI) is a common method of converting peptide ions into the gas phase. ESI is known to produce multiply protonated ions. The addition of trivalent chromium, Cr(III), to peptide solutions undergoing ESI was discovered to increase their protonation. This dissertation contains fundamental studies of peptide ionization using Cr(III) as an additive.

The mechanism of Cr(III) enhanced protonation in ESI was deduced experimentally using model peptides. Carboxylic acid groups are involved in the coordination of Cr(III) to the peptide zwitterion. The protonation of model peptide amides containing no carboxyl groups are enhanced by Cr(III). This indicates that carboxyl and amide groups are involved in the mechanism. Cr(III) was ineffective at enhancing the protonation of phosphorylated model peptides.

A survey of twenty-seven biological peptides was completed to gauge the analytical utility of Cr(III) in MS-based proteomics. Cr(III) enhanced the protonation of eleven of the peptides studied. The protonation of the remaining peptides was either suppressed or not affected by Cr(III). The interactions between sidechains of biological peptides are of higher complexity and can prevent binding and/or dissociation of Cr(III) from the peptide. Post-column addition or doping the nebulizing gas with Cr(III) are potential methods of delivering Cr(III) into the source region in proteomic workflows.

Dissociation of protonated ions formed by Cr(III) were also studied. The electron transfer dissociation (ETD) products of precursor ions generated with Cr(III) did not differ from those generated using 1% acetic acid. Higher charge states generate better sequence coverage than lower charge states. Certain residues direct fragmentation and the type of product ions produced in ETD. This residue effect subsides with higher charge states.

Matrix-assisted laser desorption ionization (MALDI) is another method of ionizing peptides. Singly protonated ions are generally formed in MALDI. Additional protons are not expected to be added with Cr(III), but rather an increase in the intensity of singly protonated ion. The effect of Cr(III) as an additive in MALDI for peptides was inconclusive due to poor reproducibility, which is common in MALDI.

DEDICATION

This dissertation is dedicated to my mother, Elizabeth Dieke. I cannot thank her enough for the love and support she has shown me throughout this process. During my lowest moments, she built me back up and reminded me of my greatness. I could not have completed this dissertation without her.

LIST OF ABBREVIATIONS AND SYMBOLS

°C	degree Celsius
$[M + 2H]^{2+}$	doubly protonated ion
$[M + 3H]^{3+}$	triply protonated ion
$[M + 4H]^{4+}$	quadruply protonated ion
$[M + H]^{+}$	singly protonated ion
$[M + nH]^{n+}$	multiply protonated ion
[v/v]	volume/volume
2-NPG	2-nitrophloroglucinol
A.I	absolute intensity
AC	alternating current
Ala	alanine (A)
Ar	argon gas
Arg	arginine (R)
Asn	asparagine (N)
Asp	aspartic acid (D)
ATP	adenosine triphosphate
BNA	1, 1-bi-2-naphthylamine
BNA	1, 1-bi-2-napthylamine
CHCA	α-cyano-4-hydroxycinnamic acid
CID	collision-induced dissociation

cm	centimeter
Cr(III)	chromium trivalent cation
CRM	charge residue model
Cys	cysteine (C)
DFT	density functional theory
DHB	2, 5-dihydroxybenzoic acid
DIC	1,3-diisopropylcarbodiimide
DMF	N, N-dimethylformamide
DMSO	dimethyl sulfoxide
e	electron
ECD	electron capture dissociation
ESI	electrospray ionization
ETD	electron transfer dissociation
ETnoD	electron transfer no dissociation
eV	electron volt
Fmoc	9-fluoroenylmethoxycarbonyl
FT-ICR	Fourier transform ion cyclotron resonance
Gln	glutamine (Q)
Glu	glutamic acid (E)
Gly	glycine (G)
HCT	high capacity trap
He	helium gas
HGP	Human Genome Project

His	histidine (H)
HNBA	3-hydroxy-4-nitrobenzoic acid
HOBt	1-hydroxybenzotriazole
HPLC	high-performance liquid chromatography
hr	hour
HUGO	Human Genome Organization
HUPO	Human Proteome Organization
ICC	ion charge control
Ile	isoleucine (I)
kcal	kilocalorie
KE	kinetic energy
kHz	kilohertz
l	length
L	liter
LC	liquid chromatography
Leu	leucine (L)
Lys	lysine (K)
m	mass
M	molar
m-NBA	*m*-nitrobenzyl alcohol
m/z	mass-to-charge ratio
MALDI	matrix-assisted laser desorption ionization
MeOH	methanol

Met	methionine (M)
min	minute
mol	mole
MS	mass spectrometry
ms	milliseconds
MS/MS	tandem mass spectrometry
MSA	6-methoxysalicylic acid
N_2	nitrogen gas
nCI	negative chemical ionization
Nd:YAG	neodymium-doped yttrium aluminum garnet
NMP	N-methyl-2-pyrrolidinone
NNA	4-nitro-1-napthylamine
pE	pyroglutamic acid
PEEK	Polyether Ether-Ketone
Phe	phenylalanine (F)
pI	isoelectric point
PIP	piperidine
Pro	proline (P)
psi	pound per square inch
PTM	post-translational modification
pY	phosphorylated tyrosine
QIT	quadrupole ion trap
r	radius

rf	radiofrequency
S/N	signal-to-noise ratio
sDHB	super 2,5-dihydroxybenzoic acid
Ser	serine (S)
SPPS	solid-phase peptide synthesis
t	time
TFA	trifluoroacetic acid
THAP	2, 4, 6-trihydroxyacetophenone
Thr	threonine (T)
TIPS	trisoproylsilane
TOF	time-of-flight
Trp	tryptophan (W)
Tyr	tyrosine (Y)
UW	Utah-Washington
V	voltage
Val	valine (V)
ZDV	zero dead volume
μ	micro (prefix)
ω	frequency

ACKNOWLEDGEMENTS

I would like to express my sincere gratitude to my advisor, Dr. Carolyn J. Cassady, for not only giving me the opportunity to work in her group, but also believing in my success. I have had a wonderful experience with her as a mentor. I also would like to extend my appreciation to Dr. Yuping Bao, Dr. David A. Dixon, Dr. Gregory Szulczewski, and Dr. John B. Vincent for serving on my committee in addition to their support and valuable input throughout my time here.

I would like to acknowledge the National Science Foundation (CHE-1609764) for funding my research, including support for the purchase of the Bruker HCTultra PTM discovery system (CHE-0639003) and the Bruker rapifleX (CHE-1726812). The financial support from the Department of Education GAANN Fellowship along with mentorship from Dr. Silas Blackstock is much appreciated.

Many thanks to my colleagues in the Cassady group: Dr. Juliette Commodore, Dr. Ranelle Schaller-Duke, Dr. Xinyao Jing, Dr. Can Cui, Matthew Mireles, Surakshya Thapa, Ramesh Karki, and Chioma Akor. I appreciate their support, assistance, and conversations as we navigated through this process together.

God has blessed me with the amazing people I call family. I am eternally grateful and do not take it for granted. I am thankful for the prayers and love from my extended family in Nigeria. I am forever appreciative of my siblings for the laughter, tears, and prayers we have shared together. No amount of thanks can suffice when it comes to my parents. Their sacrifices were not in vain. I am thankful for the foundation that they built for me. The process has been

a rollercoaster ride, but one thing that has remained constant is their love and reminders that I belong here and God will not fail me.

Lastly, I would like to thank my fiancé, Ibukun Afon, for his prayers, patience, love, and reassurance. You made my time in Alabama easier, and I have enjoyed every moment being with you. I am looking forward to our next chapter together.

CONTENTS

LIST OF TABLES

LIST OF FIGURES

CHAPTER 1. INTRODUCTION AND DISSERTATION OVERVIEW

In the early 2000s, the Human Proteome Organization (HUPO) was launched to "increase awareness of, and support for, large-scale protein analysis, in scientific, political and financial circles".[1] The organization was developed after the completion of Human Genome Project (HGP), which was organized in 1990 by the Human Genome Organization (HUGO). The HGP was a publicly funded global effort to map out the entire human genome. The success of the HGP led to interest in understanding the human proteome. Consequently, the Human Proteome Project was launched at the 2011 World Congress of Proteomics in Geneva, Switzerland.[2] Studying the human proteome is more challenging than the human genome due to its size and complexity; yet, as of 2020, nearly a decade after launch, >90% of the human proteome coded in the human genome has been sequenced.[3-5] *De novo* sequencing using MS/MS data or direct database searches can identify the primary structure of the protein or peptide. Of the proteins detected, 95% were validated by *de novo* sequencing or database searching using MS/MS datasets. In addition to the human proteome, an understanding of other proteomes, such as those of agricultural crops[6-8] and livestocks,[9,10] is important.

Proteins or polypeptides are biomolecules comprised of amino acid residues held together by peptide bonds. A protein's structure can be broken down into four levels: (1) primary, (2) secondary, (3) tertiary, and (4) quaternary structures.[11,12] The primary structure of a protein refers to the amino acid sequence that makes up the protein. Twenty standard amino acids make up proteins.[13] The structures of these amino acids are provided in Section 2.8. Secondary protein

structures describe the conformation of the peptide backbone. Protein conformations involve the interaction between sites along the peptide backbone, which includes formation of α-helices and β-sheets. Tertiary structures depict the spatial arrangement of atoms in three-dimensions as the secondary structures non-covalently interact. Large proteins can be comprised of multiple polypeptide chains that are called subunits. These proteins can have a quaternary structure, which is the spatial arrangement of the protein's different subunits.

To understand a protein's overall function and higher orders of structure, an understanding of the protein's primary structure is required.[14-16] Protein sequencing involves elucidating the primary structure, or amino acid sequence, of a protein. Amino acids are small organic molecules comprised of a carboxylic acid and an amine group each bonded to an α-carbon. The α-carbon on each of the 20 essential amino acids has a sidechain unique to that amino acid. Polypeptide chains are formed by multiple amino acids linked together by the carbonyl carbon and the amine nitrogen to create a peptide bond. Short chains of amino acids are referred to as peptides. The end of the peptide with the free amino group is called the N-terminus, while the free carboxylic acid group end is the C-terminus.

Two methods of determining a protein's primary structure exist: Edman degradation and MS. Edman degradation is named after Pehr Edman, who reported the process in 1950.[17,18] In Edman degradation, a peptide is sequenced from the N-terminus, and each residue is cleaved one at a time. The Edman degradation cycle of experiments involves coupling, cleaving, and conversion. Phenyl isothiocyanate is coupled to the peptide via the N-terminus, which is then cleaved under acidic conditions to create a cyclic compound containing the phenyl isothiocyanate and the cleaved amino acid. This compound is then hydrolyzed to reveal the identity of the amino acid. Although Edman degradation has now been automated, the technique

is still time-consuming and requires the peptide to be linear with a free amino group at the N-terminus.

With the advancement of ionization methods, MS has become the preferred method of peptide and protein sequencing.[19,20] MS-based proteomics provides high sensitivity and a high throughput of analysis.[16] Two approaches are used to study the primary structures of proteins by MS. The most common method is called the bottom-up approach.[21-23] A bottom-up approach on a complex mixture of proteins is often named shotgun proteomics.[23-25] Figure 1.1 illustrates a typical bottom-up workflow. In this approach, proteins are first isolated from a biological sample and then enzymatically digested to produce a collection of peptides. Digestion is accomplished using a site-specific enzyme, such as trypsin, pepsin, Lys-N, or chymotrypsin, to cleave the peptide bonds at a specific type of amino acid residue.[26-30] Following digestion, the peptides can be separated by high-performance liquid chromatography (HPLC).[31-33] After separation, MS is used to ionize the peptides and detect the mass-to-charge ratio (m/z) of their quasi-molecular ions. The peptide ions can be fragmented in a second mass analyzer using tandem mass spectrometry (MS/MS) dissociation techniques, such as collision-induced dissociation (CID),[25,34-36] to deduce the amino acid sequence of the peptide. The final step in the process often involves database searches to identify the protein.

Though a robust methodology, the bottom-up approach has its disadvantages. Contamination is a major issue; common contaminants are detergents used for cleaning glassware, phthalates from plastics and fittings, and keratins from skin and dust.[37-39] These contaminants ionize readily in MS and produce abundant ions that can interfere with mass spectral analysis and interpretation. Another disadvantage of the bottom-up approach is that

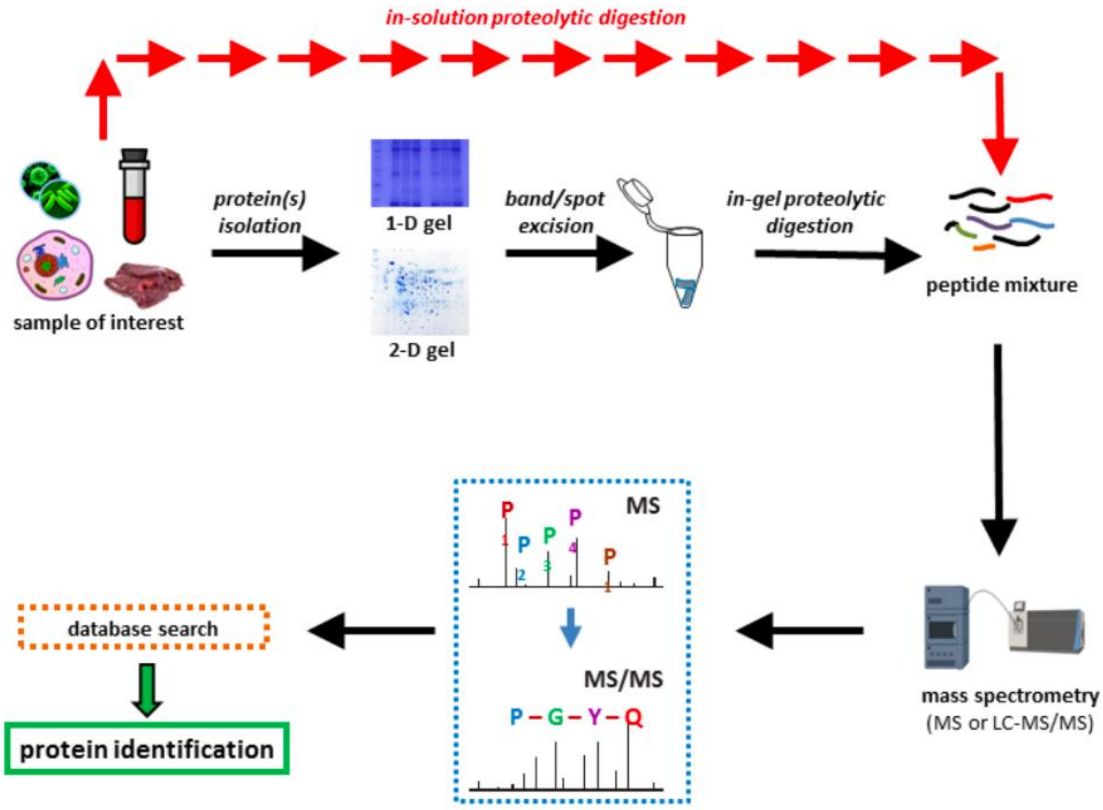

Figure 0.1. Typical bottom-up proteomics workflow (available open access from reference 22).

often large pieces of the sequence, which can contain critical information (i.e., post-translational modifications (PTMs)) about the protein's function and structure, are missing or misidentified.[40,41] In spite of these disadvantages, the bottom-up approach is routinely used in protein analysis in labs across the world and was critical to the completion of the first draft of the Human Proteome Project, which included tens of thousands liquid chromatography (LC) MS/MS data sets from human tissues, cell lines, body fluids.[4,5]

The second approach in protein analysis by MS is the top-down approach. This method involves the direct MS analysis of intact native proteins and their fragment ions.[41] Top-down proteomics typically gives 100% sequence coverage and full characterization of protein modifications and variations. Native proteins are fragmented using electron capture dissociation (ECD)[42-45] or electron transfer dissociation (ETD), which can impart sufficient energy for fragmentation if the protein ions are multiply charged.[46] Top-down proteomics can be time-consuming from preparation to the extensive mass spectral interpretation, and is therefore suited for single proteins and simple mixtures.[47] Analysis of complex mixtures at the intact protein level is difficult because separation of intact proteins is cumbersome and requires multiple separation steps.[41,48,49] In addition to that, high performance mass analyzers that provide high resolution and mass accuracy are needed to determine the exact m/z of the fragment ions for their identification and for distinguishing between sequence variations and modifications.[41]

Regardless of the approach used, MS plays a critical role in the characterization of proteins. The introduction of electrospray ionization (ESI) by Fenn[50,51] and matrix-assisted laser desorption ionization (MALDI) by Tanaka[52] and by Hillenkamp and Karas,[20,53] in the 1980s led to the widespread use of mass spectrometry for the analysis of large biomolecules. After the digestion and separation of peptides, the peptides are ionized in the mass spectrometer, mass

analyzed, and detected. The most common method of peptide fragmentation is CID due to its ease of implementation on many commercial mass spectrometers.[35,54,55] Electron-based dissociation techniques such as electron-transfer dissociation (ETD) and electron-capture dissociation (ECD) require multiply charged precursor ions, which can be generated by ESI. Multiply charged ions have advantages over singly charged ions in single stage MS and MS/MS analysis of proteins. The higher charged ions shift the m/z of ions to a lower range where resolution is optimal and allows for the use of lower m/z mass analyzers.[56] Higher charge states usually require less energy to dissociate and provide more sequence informative cleavage.[57-59] However, not all peptides generate multiply charged ions by ESI. Acidic peptides sometimes do not readily form multiply charged ions by ESI in the positive mode due to their preference for deprotonation.[60,61] Acidic peptides are peptides that contain more acidic residues (aspartic acid, D, or glutamic acid, E) as well as phosphorylated or sulfonated residues than basic residues (arginine, lysine, or histidine). Deprotonation occurs more readily than protonation due to their high acidic nature. While negative mode MS/MS of peptides can be accomplished, the technique often yields sidechain loss and uninformative neutral losses that greatly complicate mass spectral interpretation.[62-64]

Volatile organic acids (e.g., acetic acid, trifluoroacetic acid, formic acid) are often added to peptide solutions to increase the ionic charge states formed and the ion intensities. The charge state of ions (n) produced by ESI can also be increased using various other methods. The term "supercharging" is used to describe increasing the highest charge state observed for a protein in ESI-MS. Protein supercharging has been pioneered by the Williams group of the University of California, Berkeley.[65-70] This research almost exclusively involves positive protonated ions produced by ESI, $[M + nH]^{n+}$. Several methods have been developed by the Williams group to

supercharge proteins in ESI. Electrochemical supercharging is one method used to increase protein charge states; this method involves the unfolding of native proteins in ESI by using aqueous salt solutions and increasing the ESI spray potential.[68,69,71] The proteins are thermally denatured (unfolded) by the increased temperature of the capillary entrance, spray potential, and the ionic strength of the buffer. An increase in maximum charge state and charge distribution is observed. The Williams group also determined that the addition of lanthanum chloride, $LaCl_3$, to native protein solutions results in supercharging by forming high charge state metal-adducted protein ions.[70] ECD on these metal-adducted protein ions results in improved sequence coverage.[70]

The most common method of increasing charge states, which was also discovered by the Williams group, is by the addition of supercharging reagents to protein solutions undergoing ESI.[72] Supercharging reagents are small organic molecules with boiling points higher than water. Common supercharging reagents are *m*-nitrobenzyl alcohol (*m*-NBA),[65-67,72] glycerol,[72] and sulfolane.[73-76] Supercharging reagents have been reported to produce stable higher charged protein ion signals in ESI.[65,66,74,75,77-80] Different theories exist to explain the mechanism of supercharging. One theory is that organic supercharging reagents increase the surface tension of ESI droplets.[81] The increase in the surface tension causes an increase in the charge density of the droplet; therefore, more charges accumulate on the droplet before the Rayleigh limit is reached.[81] The Rayleigh limit is defined as the maximum amount of charge a droplet can carry. Here, the mechanism proceeds to follow the charge residue model (CRM) for ion formation by ESI, which involves solvent evaporation of droplets containing a single analyte ion at the Rayleigh limit.[82,83] The final charge of the ion is determined by the Rayleigh limit of the droplet generated during the spraying process. Another theory is that supercharging reagents in aqueous solutions undergo

solvent segregation in ESI droplets.[84] The supercharging reagent surrounds the aqueous core that contains the protein and decreases the rate at which the ion ejection model proceeds and traps the charges within the aqueous core. In the ion ejection model, smaller droplets are ejected from the droplet until only the charged analyte remains.[85] As ion ejection is inhibited, charge carriers bind to the protein and the charged protein is released upon evaporation of the supercharging reagent. Denaturing of proteins in the gas phase by supercharging reagents have also been proposed as a mechanism for protein supercharging,[75,78,86] as well as the interaction between analyte and supercharging reagent[73,87,88] to form a proton bridge that facilitates protonation.

In 2014, the Donald group at the University of New South Wales reported the use of low concentrations of organic carbonates to induce extreme supercharging of protein ions in ESI.[89,90] The term "extreme supercharging" was given because higher charge states were observed compared to organic supercharging reagents. The addition of organic carbonates narrows the charge state distribution for protein ions and adds on more charges than is predicted based upon the number of highly basic sites available for protonation.[89]

All supercharging methods mentioned involve native proteins and, therefore, are beneficial in top-down proteomics. In 2015, the Cassady group reported that addition of trivalent chromium, Cr(III), to peptide solutions undergoing ESI increases protonation by increasing the maximum charge state and/or signal intensity of the protonated peptide ion.[91] The model peptide AAAEAAA (A3EA3) is an acidic peptide that forms singly charged protonated ions, $[M + H]^+$, by ESI. Figure 1.2(a) is typical ESI mass spectrum for A3EA3. Addition of chromium(III) nitrate, $[Cr(H_2O)_6](NO_3)_3 \bullet 3H_2O$, to A3EA3, Figure 1.2(b), yields abundant $[M + 2H]^{2+}$ that could not be achieved by the addition of the organic supercharging reagents *m*-NBA and dimethylsulfoxide (DMSO). An experimental parameter optimization study revealed the

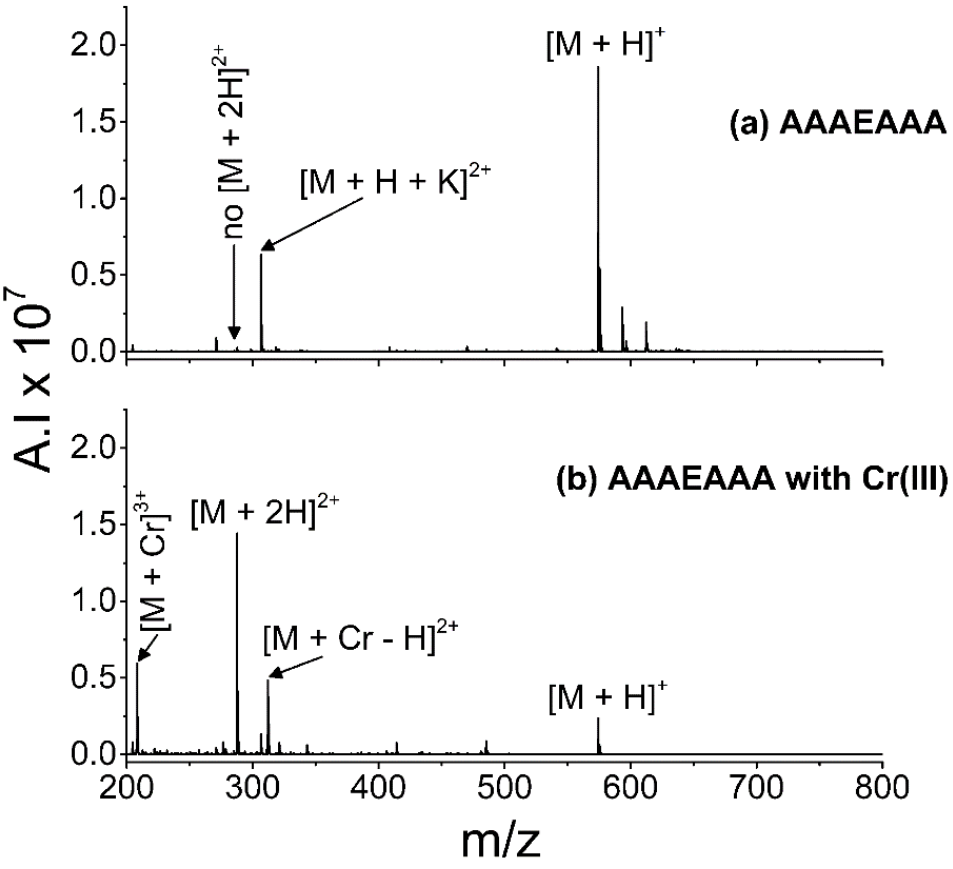

Figure 0.2. ESI mass spectra of 10 uM AAAEAAA in 50:50 [v/v] acetonitrile:water containing (a) no Cr(III) and (b) Cr(III) in a 10:1 molar ratio of metal:peptide.

importance of the ESI drying gas flow rate and nebulizing gas pressure, which leads to the idea that Cr(III) is enhancing the protonation of the peptides in the gas phase during the ESI desolvation stage.[92] Multiple Cr(III) complexes have been studied, and the best complexes for peptide protonation were determined to be $[Cr(H_2O)_6](NO_3)_3 \bullet 3H_2O$ and $[Cr(THF)_3]Cl_3$. These complexes successfully enhance protonate peptides in aqueous solvent systems, which implies that water plays a critical role in the mechanism.[93] The work in this dissertation will build upon this discovery to explore the analytical utility of Cr(III) in proteomics to enhance the ionization of peptides and the mechanism by which the process occurs.

Chapter 2 will start by introducing the instrumentation and experimental methods utilized in this dissertation. Two mass spectrometers were employed in this work; their components (i.e., ionization method and mass analyzers) will be individually described. Afterwards, two common dissociation methods for peptide sequencing, CID and ETD, will be discussed along with the peptide fragmentation nomenclature. Some of the model peptides studied were synthesized using solid-phase peptide synthesis. A detailed description of the peptide synthesis protocol will be included. The chapter concludes with structures of the 20 essential amino acids.

Chapter 3 investigates the impact of peptide structure on the degree of enhanced protonation using Cr(III) and the implications for the mechanism involved. Several model peptides were synthesized in the Cassady lab or commercially purchased to study the effects of specific amino acid residues (i.e., acidic residues, proline, tyrosine, and phosphorylated tyrosine), the positioning of acidic residues along the peptide backbone, and the importance of the C-terminal carboxylic acid group. Previous work by the Cassady group shows that Cr(III) does not enhance the protonation of peptide methyl esters, which lack carboxylic acid groups.[91]

Carboxylic acid groups can be found at the sidechains of acidic residues or at the C-terminus. Methyl esterification was performed to determine whether the location of the carboxyl group matters. Experimental studies were combined with computational studies[94] from the Dixon group to propose a mechanism for Cr(III) enhanced protonation of peptides.

Typically, mixing peptide and Cr(III) in a 1:10 peptide-to-Cr(III) molar ratio in the solution undergoing ESI is enough to induce enhanced protonation. Over time Cr(III) can accumulate in the mass spectrometer's ion source and cause enhanced protonation of peptide solutions that do not contain added Cr(III). In Chapter 4, the method of Cr(III) delivery into the ESI source is evaluated. Three different methods will be discussed: (i) coating or swabbing the ESI spray shield with Cr(III), (ii) creating a co-axial inlet design that introduces the Cr(III) solution into the source independently from the peptide solution, and (iii) introducing Cr(III) through the ESI drying gas. Using these methods, the addition of Cr(III) might be integrated into the typical bottom-up approach between separation and mass analysis of the sample. By adding Cr(III) post-column, the chromatographic separation is not affected, and typical buffer LC systems can be used.

Next, the ability of Cr(III) to enhance the protonation of peptides in MALDI will be explored in Chapter 5. MALDI rarely forms $[M + 2H]^+$ for small peptides, instead forming singly protonated ions, $[M + H]^+$. Therefore, an increase is charge state is not expected. Rather, preliminary data shows that Cr(III) may increase the signal intensity of $[M + H]^+$.[95] The work discussed in this chapter is an attempt to construct a procedure for enhancing peptide ion signals produced by MALDI while using Cr(III). Sample preparation, which includes the method of depositing the sample on the target plate and choosing the correct organic MALDI matrix, plays a huge factor in MALDI analysis. In the absence of a matrix, peptide/Cr(III) samples do not

ionize; therefore, Cr(III) does not replace the matrix. Several matrices, with varying functional groups, have been studied, along with the method of mixing Cr(III), matrix, and peptide for deposition on the target plate.

To evaluate the utility of Cr(III) in proteomic studies, twenty-seven commercial biological peptides were analyzed in Chapter 6. Compared to the model peptides studied in Chapter 3, the biological peptides are more diverse in the type of amino acid residues present in the sequence. The interactions between the different sidechains add another level of complexity. The scope of Cr(III) for proteomics will be discussed. In addition, metabolomics is a growing area of research seeking to understand small molecules derived from cellular metabolic processes. Understanding these metabolites can lead to insight into different facets of cellular physiology.[96,97] Similar to proteomics, metabolomics uses MS to identify and characterize metabolites. This chapter will also discuss the ability to enhance the protonation of glycans, steroids, and lipids (e.g., types of metabolites) using Cr(III) in ESI.

Peptides can be dissociated using a number of MS/MS techniques to determine their amino acid sequences. Chapter 7 will study the dissociation by ETD of peptide ions following enhanced protonation using Cr(III). Biological peptides from Chapter 6 were chosen to study their dissociation patterns after Cr(III)-enhanced protonation. This work takes advantage of the fact that Cr(III) can cause an increase in the peptide charge state produced by ESI or an increase in the ion abundance of the higher charge states. The effect of charge state on ETD of peptides will be examined by comparing product ion formation and sequence coverage of higher charge states to $[M + 2H]^{2+}$. In this work, fragmentation trends due to specific amino acids will be discussed.

Chapter 8 summarizes the most important aspects of the research described in this dissertation. The impact of Cr(III) on enhancing the protonation of peptides in MS and its relevance to proteomics will be discussed. Furthermore, future prospective projects will be proposed to expand on the concepts presented in this work.

References

1. Abbott, A. And Now for the Proteome. . .. *Nature* **2001**, *409*, 747.

2. Omenn, G. S. The HUPO Human Proteome Project (HPP), a Global Health Research Collaboration. *Cent. Asian J. Glob. Health* **2012**, *1*, 37.

3. Omenn, G. S.; Lane, L.; Overall, C. M.; Cristea, I. M.; Corrales, F. J.; Lindskog, C.; Paik, Y.; Van Eyk, J. E.; Liu, S.; Pennington, S. R.; Snyder, M. P.; Baker, M. S.; Bandeira, N.; Aebersold, R.; Moritz, R. L.; Deutsch, E. W. Research on the Human Proteome Reaches a Major Milestone: >90% of Predicted Human Proteins Now Credibly Detected, According to the HUPO Human Proteome Project. *J. Proteome Res.* **2020**, *19*, 4735-4746.

4. Kim, M.; Pinto, S. M.; Getnet, D.; Nirujogi, R. S.; Manda, S. S.; Chaerkady, R.; Madugundu, A. K.; Kelkar, D. S.; Isserlin, R.; Jain, S.; Thomas, J. K.; Muthusamy, B.; Leal-Rojas, P.; Kumar, P.; Sahasrabuddhe, N. A.; Balakrishnan, L.; Advani, J.; George, B.; Renuse, S.; Selvan, L. D. N.; Patil, A. H.; Nanjappa, V.; Radhakrishnan, A.; Prasad, S.; Subbannayya, T.; Raju, R.; Kumar, M.; Sreenivasamurthy, S. K.; Marimuthu, A.; Sathe, G. J.; Chavan, S.; Datta, K. K.; Subbannayya, Y.; Sahu, A.; Yelamanchi, S. D.; Jayaram, S.; Rajagopalan, P.; Sharma, J.; Murthy, K. R.; Syed, N.; Goel, R.; Khan, A. A.; Ahmad, S.; Dey, G.; Mudgal, K.; Chatterjee, A.; Huang, T.; Zhong, J.; Wu, X.; Shaw, P. G.; Freed, D.; Zahari, M. S.; Mukherjee, K. K.; Shankar, S.; Mahadevan, A.; Lam, H.; Mitchell, C. J.; Shankar, S. K.; Satishchandra, P.; Schroeder, J. T.; Sirdeshmukh, R.; Maitra, A.; Leach, S. D.; Drake, C. G.; Halushka, M. K.; Prasad, T. S. K.; Hruban, R. H.; Kerr, C. L.; Bader, G. D.; Iacobuzio-Donahue, C.; Gowda, H.; Pandey, A. A Draft Map of the Human Proteome. *Nature* **2014**, *509*, 575-581.

5. Wilhelm, M.; Schlegl, J.; Hahne, H.; Gholami, A. M.; Lieberenz, M.; Savitski, M. M.; Ziegler, E.; Butzmann, L.; Gessulat, S.; Marx, H.; Mathieson, T.; Lemeer, S.; Schnatbaum, K.; Reimer, U.; Wenschuh, H.; Mollenhauer, M.; Slotta-Huspenina, J.; Boese, J.; Bantscheff, M.; Gerstmair, A.; Faerber, F.; Kuster, B. Mass-Spectrometry-Based Draft of the Human Proteome. *Nature* **2014**, *509*, 582-587.

6. Kottapalli, K. R.; Rakwal, R.; Shibato, J.; Burow, G.; Tissue, D.; Burke, J.; Puppala, N.; Burow, M.; Payton, P. Physiology and Proteomics of the Water-Deficit Stress Response in Three Contrasting Peanut Genotypes. *Plant, Cell Environ.* **2009**, *32*, 380-407.

7. Cheng, L.; Wang, Y.; He, Q.; Li, H.; Zhang, X.; Zhang, F. Comparative Proteomics Illustrates the Complexity of Drought Resistance Mechanisms in Two Wheat (Triticum Aestivum L.) Cultivars Under Dehydration and Rehydration. *BMC Plant Biol.* **2016**, *16*, 188.

8. Hao, P.; Zhu, J.; Gu, A.; Lv, D.; Ge, P.; Chen, G.; Li, X.; Yan, Y. An Integrative Proteome Analysis of Different Seedling Organs in Tolerant and Sensitive Wheat Cultivars Under Drought Stress and Recovery. *Proteomics* **2015**, *15*, 1544-1563.

9. Bendixen, E.; Danielsen, M.; Larsen, K.; Bendixen, C. Advances in Porcine Genomics and Proteomics—a Toolbox for Developing the Pig as a Model Organism for Molecular Biomedical Research. *Brief Funct. Genomics* **2010**, *9*, 208-219.

10. Picard, B.; Berri, C.; Lefaucheur, L.; Molette, C.; Sayd, T.; Terlouw, C. Skeletal Muscle Proteomics in Livestock Production. *Brief Funct. Genomics* **2010**, *9*, 259-278.

11. Nelson, D. L.; Cox, M. M., Eds.; In *Lehninger Principles of Biochemistry;* W. H. Freeman: New York, 2004.

12. Sun, P. D.; Foster, C. E.; Boyington, J. C. Overview of Protein Structural and Functional Folds. *Curr. Protoc. Protein Sci.* **2004**, 17.1.1-17.1.189.

13. Voet, D.; Voet, J. G. *Biochemistry;* John Wiley & Sons: New York, 1995.

14. Anfinsen Christian, B. Principles that Govern the Folding of Protein Chains. *Science* **1973**, *181*, 223-230.

15. Aebersold, R.; Goodlett, D. R. Mass Spectrometry in Proteomics. *Chem. Rev.* **2001**, *101*, 269-296.

16. Aebersold, R.; Mann, M. Mass Spectrometry-Based Proteomics. *Nature* **2003**, *422*, 198-207.

17. Edman, P.; Begg, G. A Protein Sequenator. *Eur. J. Biochem.* **1967**, *1*, 80-91.

18. Biemann, K. Contributions of Mass-Spectrometry to Peptide and Protein-Structure. *Biomed. Environ. Mass Spectrom.* **1988**, *16*, 99-111.

19. Fenn, J. B.; Mann, M.; Meng, C. K.; Wong, S. F.; Whitehouse, C. M. Electrospray Ionization for Mass Spectrometry of Large Biomolecules. *Science* **1989**, *246*, 64-71.

20. Karas, M.; Hillenkamp, F. Laser Desorption Ionization of Proteins with Molecular Masses Exceeding 10,000 Daltons. *Anal. Chem.* **1988**, *60*, 2299-2301.

21. Hunt, D. F.; Yates, J. R.; Shabanowitz, J.; Winston, S.; Hauer, C. R. Protein Sequencing by Mass Spectrometry. *Proc. Natl. Acad. Sci. USA* **1986**, *83*, 6233-6237.

22. Dupree, E. J.; Jayathirtha, M.; Yorkey, H.; Mihasan, M.; Petre, B. A.; Darie, C. C. A Critical Review of Bottom-Up Proteomics: The Good, the Bad, and the Future of this Field. *Proteomes* **2020**, *8*, 14.

23. Zhang, Y.; Fonslow, B. R.; Shan, B.; Baek, M.; Yates, J. R. Protein Analysis by Shotgun/Bottom-Up Proteomics. *Chem. Rev.* **2013**, *113*, 2343-2394.

24. McDonald, W. H.; Yates, J. R. Shotgun Proteomics and Biomarker Discovery. *Dis. Markers* **1900**, *18*, 505397.

25. Purvine, S.; Eppel, J.; Yi, E. C.; Goodlett, D. R. Shotgun Collision-Induced Dissociation of Peptides using a Time of Flight Mass Analyzer. *Proteomics* **2003**, *3*, 847-850.

26. Olsen, J. V.; Ong, S. E.; Mann, M. Trypsin Cleaves Exclusively C-Terminal to Arginine and Lysine Residues. *Mol. Cell. Proteomics* **2004**, *3*, 608-614.

27. Saveliev, S.; Bratz, M.; Zubarev, R.; Szapacs, M.; Budamgunta, H.; Urh, M. Trypsin/Lys-C Protease Mix for Enhanced Protein Mass Spectrometry Analysis. *Nat. Methods* **2013**, *10*, i-ii.

28. Ahn, J.; Cao, M.; Yu, Y. Q.; Engen, J. R. Accessing the Reproducibility and Specificity of Pepsin and Other Aspartic Proteases. *Biochim. Biophys. Acta Proteins Proteom.* **2013**, *1834*, 1222-1229.

29. Taouatas, N.; Drugan, M. M.; Heck, A. J. R.; Mohammed, S. Straightforward Ladder Sequencing of Peptides using a Lys-N Metalloendopeptidase. *Nat. Methods* **2008**, *5*, 405-407.

30. Giansanti, P.; Tsiatsiani, L.; Low, T. Y.; Heck, A. J. R. Six Alternative Proteases for Mass Spectrometry–based Proteomics Beyond Trypsin. *Nat. Protoc.* **2016**, *11*, 993-1006.

31. Nilsson, T.; Mann, M.; Aebersold, R.; Yates, J. R.; Bairoch, A.; Bergeron, J. J. M. Mass Spectrometry in High-Throughput Proteomics: Ready for the Big Time. *Nat. Methods* **2010**, *7*, 681-685.

32. Eeltink, S.; Geiser, L.; Svec, F.; Fréchet, J. M. J. Optimization of the Porous Structure and Polarity of Polymethacrylate-Based Monolithic Capillary Columns for the LC-MS Separation of Enzymatic Digests. *J. Sep. Science* **2007**, *30*, 2814-2820.

33. Covey, T. R.; Huang, E. C.; Henion, J. D. Structural Characterization of Protein Tryptic Peptides Via Liquid Chromatography/Mass Spectrometry and Collision-Induced Dissociation of their Doubly Charged Molecular Ions. *Anal. Chem.* **1991**, *63*, 1193-1200.

34. Liu, C.; Lai, C. Effects of Electron-Transfer Coupled with Collision-Induced Dissociation (ET/CID) on Doubly Charged Peptides and Phosphopeptides. *J. Am. Soc. Mass Spectrom.* **2011**, *22*, 57-66.

35. Mitchell Wells, J.; McLuckey, S. A. Collision-Induced Dissociation (CID) of Peptides and Proteins. *Meth. Enzymol.* **2005**, *402*, 148-185.

36. Smith, R. D.; Loo, J. A.; Barinaga, C. J.; Edmonds, C. G.; Udseth, H. R. Collisional Activation and Collision-Activated Dissociation of Large Multiply Charged Polypeptides and Proteins Produced by Electrospray Ionization. *J. Am. Soc. Mass Spectrom.* **1990**, *1*, 53-65.

37. Rogers, J. C.; Bomgarden, R. D. Sample Preparation for Mass Spectrometry-Based Proteomics; from Proteomes to Peptides. *Adv. Exp. Med. Biol.* **2016**, *919*, 43-62.

38. Hodge, K.; Have, S. T.; Hutton, L.; Lamond, A. I. Cleaning Up the Masses: Exclusion Lists to Reduce Contamination with HPLC-MS/MS. *J. Proteomics* **2013**, *88*, 92-103.

39. Bell, A. W.; Deutsch, E. W.; Au, C. E.; Kearney, R. E.; Beavis, R.; Sechi, S.; Nilsson, T.; Bergeron, J. J. M.; Beardslee, T. A.; Chappell, T.; Meredith, G.; Sheffield, P.; Gray, P.; Hajivandi, M.; Pope, M.; Predki, P.; Kullolli, M.; Hincapie, M.; Hancock, W. S.; Jia, W.; Song, L.; Li, L.; Wei, J.; Yang, B.; Wang, J.; Ying, W.; Zhang, Y.; Cai, Y.; Qian, X.; He, F.; Meyer, H. E.; Stephan, C.; Eisenacher, M.; Marcus, K.; Langenfeld, E.; May, C.; Carr, S. A.; Ahmad, R.; Zhu, W.; Smith, J. W.; Hanash, S. M.; Struthers, J. J.; Wang, H.; Zhang, Q.; An, Y.; Goldman, R.; Carlsohn, E.; van der Post, S.; Hung, K. E.; Sarracino, D. A.; Parker, K.; Krastins, B.; Kucherlapati, R.; Bourassa, S.; Poirier, G. G.; Kapp, E.; Patsiouras, H.; Moritz, R.; Simpson, R.; Houle, B.; LaBoissiere, S.; Metalnikov, P.; Nguyen, V.; Pawson, T.; Wong, C. C. L.; Cociorva, D.; Yates III, J.,R.; Ellison, M. J.; Lopez-Campistrous, A.; Semchuk, P.; Wang, Y.; Ping, P.; Elia, G.; Dunn, M. J.; Wynne, K.; Walker, A. K.; Strahler, J. R.; Andrews, P. C.; Hood, B. L.; Bigbee, W. L.; Conrads, T. P.; Smith, D.; Borchers, C. H.; Lajoie, G. A.; Bendall, S. C.; Speicher, K. D.; Speicher, D. W.; Fujimoto, M.; Nakamura, K.; Paik, Y.; Cho, S. Y.; Kwon, M.; Lee, H.; Jeong, S.; Chung, A. S.; Miller, C. A.; Grimm, R.; Williams, K.; Dorschel, C.; Falkner, J. A.; Martens, L.; Vizcaíno, J. A.; HUPO Test Sample, Working Group A HUPO Test Sample Study Reveals Common Problems in Mass Spectrometry–based Proteomics. *Nat. Methods* **2009**, *6*, 423-430.

40. Yates, J. R.; Ruse, C. I.; Nakorchevsky, A. Proteomics by Mass Spectrometry: Approaches, Advances, and Applications. *Annu. Rev. Biomed. Eng.* **2009**, *11*, 49-79.

41. Catherman, A. D.; Skinner, O. S.; Kelleher, N. L. Top Down Proteomics: Facts and Perspectives. *Biochem. Biophys. Res. Commun.* **2014**, *445*, 683-693.

42. Li, H.; Wolff, J. J.; Van Orden, S. L.; Loo, J. A. Native Top-Down Electrospray Ionization-Mass Spectrometry of 158 kDa Protein Complex by High-Resolution Fourier Transform Ion Cyclotron Resonance Mass Spectrometry. *Anal. Chem.* **2014**, *86*, 317-320.

43. Li, H.; Nguyen, H. H.; Ogorzalek Loo, R. R.; Campuzano, I. D. G.; Loo, J. A. An Integrated Native Mass Spectrometry and Top-Down Proteomics Method that Connects Sequence to Structure and Function of Macromolecular Complexes. *Nat. Chem.* **2018**, *10*, 139-148.

44. Breuker, K.; McLafferty, F. W. Native Electron Capture Dissociation for the Structural Characterization of Noncovalent Interactions in Native Cytochrome C. *Angew. Chem. Int. Ed.* **2003**, *42*, 4900-4904.

45. Zhang, H.; Cui, W.; Wen, J.; Blankenship, R. E.; Gross, M. L. Native Electrospray and Electron-Capture Dissociation in FTICR Mass Spectrometry Provide Top-Down Sequencing of a Protein Component in an Intact Protein Assembly. *J. Am. Soc. Mass Spectrom.* **2010**, *21*, 1966-1968.

46. Riley, N. M.; Coon, J. J. The Role of Electron Transfer Dissociation in Modern Proteomics. *Anal. Chem.* **2018**, *90*, 40-64.

47. Melby, J. A.; Roberts, D. S.; Larson, E. J.; Brown, K. A.; Bayne, E. F.; Jin, S.; Ge, Y. Novel Strategies to Address the Challenges in Top-Down Proteomics. *J. Am. Soc. Mass Spectrom.* **2021**, *32*, 1278-1294.

48. Capriotti, A. L.; Cavaliere, C.; Foglia, P.; Samperi, R.; Laganà, A. Intact Protein Separation by Chromatographic and/Or Electrophoretic Techniques for Top-Down Proteomics. *J. Chromatogr. A* **2011**, *1218*, 8760-8776.

49. Wu, Z.; Wei, B.; Zhang, X.; Wirth, M. J. Efficient Separations of Intact Proteins using Slip-Flow with Nano-Liquid Chromatography-Mass Spectrometry. *Anal. Chem.* **2014**, *86*, 1592-1598.

50. Fenn, J. B.; Mann, M.; Meng, C. K.; Wong, S. F. Electrospray Ionization--Principles and Practice. *Mass Spectrom. Rev.* **1990**, *9*, 37-70.

51. Wong, S. F.; Meng, C. K.; Fenn, J. B. Multiple Charging in Electrospray Ionization of Poly(Ethylemen Glycols). *J. Phys. Chem.* **1988**, *92*, 546-550.

52. Tanaka, K.; Waki, H.; Ido, Y.; Akita, S.; Yoshida, Y.; Yohida, T. Protein and Polymer Analyses Up to M/Z 100,000 by Laser Ionization Time-of-Flight Mass Spectrometry. *Rapid Commun. Mass Spectrom.* **1988**, *2*, 151-153.

53. Hillenkamp, F.; Karas, M. Matrix-Assisted Laser Desorption/Ionisation, an Experience. *Int. J. Mass Spectrom.* **2000**, *200*, 71-77.

54. Yates III, J. R. Mass Spectrometry and the Age of the Proteome. *J. Mass Spectrom.* **1998**, *33*, 1-19.

55. Hunt, D. F.; Yates, J. R.; Shabanowitz, J.; Winston, S.; Hauer, C. R. Protein Sequencing by Tandem Mass Spectrometry. *Proc. Natl. Acad. Sci. USA* **1986**, *83*, 6233-6237.

56. Marshall, A. G.; Hendrickson, C. L. Charge Reduction Lowers Mass Resolving Power for Isotopically Resolved Electrospray Ionization Fourier Transform Ion Cyclotron Resonance Mass Spectra. *Rapid Commun. Mass Spectrom.* **2001**, *15*, 232-235.

57. Dongre, A. R.; Jones, J. L.; Somogyi, A.; Wysocki, V. H. Influence of Peptide Composition, Gas-Phase Basicity, and Chemical Modification on Fragmentation Efficiency: Evidence for the Mobile Proton Model. *J. Am. Chem. Soc.* **1996**, *118*, 8365-8374.

58. Madsen, J. A.; Brodbelt, J. S. Comparison of Infrared Multiphoton Dissociation and Collision-Induced Dissociation of Supercharged Peptides in Ion Traps. *J. Am. Soc. Mass Spectrom.* **2009**, *20*, 349-358.

59. Kjeldsen, F.; Giessing, A. M. B.; Ingrell, C. R.; Jensen, O. N. Peptide Sequencing and Characterization of Post-Translational Modifications by Enhanced Ion-Charging and Liquid Chromatography Electron-Transfer Dissociation Tandem Mass Spectrometry. *Anal. Chem.* **2007**, *79*, 9243-9252.

60. Gao, J.; Cassady, C. J. Negative Ion Production from Peptides and Proteins by Matrix-Assisted Laser Desorption/Ionization Time-of-Flight Mass Spectrometry. *Rapid Commun. Mass Spectrom.* **2008**, *22*, 4066-4072.

61. Huzarska, M.; Ugalde, I.; Kaplan, D. A.; Hartmer, R.; Easterling, M. L.; Polfer, N. C. Negative Electron Transfer Dissociation of Deprotonated Phosphopeptide Anions: Choice of Radical Cation Reagent and Competition between Electron and Proton Transfer. *Anal. Chem.* **2010**, *82*, 2873-2878.

62. Ganisl, B.; Valovka, T.; Hartl, M.; Taucher, M.; Bister, K.; Breuker, K. Electron Detachment Dissociation for Top-Down Mass Spectrometry of Acidic Proteins. *Chem. Eur. J.* **2011**, *17*, 4460-4469.

63. Kalli, A.; Grigorean, G.; Håkansson, K. Electron Induced Dissociation of Singly Deprotonated Peptides. *J. Am. Soc. Mass Spectrom.* **2011**, *22*, 2209-2221.

64. Huzarska, M.; Ugalde, I.; Kaplan, D. A.; Hartmer, R.; Easterling, M. L.; Polfer, N. C. Negative Electron Transfer Dissociation of Deprotonated Phosphopeptide Anions: Choice of Radical Cation Reagent and Competition between Electron and Proton Transfer. *Anal. Chem.* **2010**, *82*, 2873-2878.

65. Iavarone, A. T.; Jurchen, J. C.; Williams, E. R. Supercharged Protein and Peptide Ions Formed by Electrospray Ionization. *Anal. Chem.* **2001**, *73*, 1455-1460.

66. Sterling, H. J.; Williams, E. R. Origin of Supercharging in Electrospray Ionization of Noncovalent Complexes from Aqueous Solution. *J. Am. Soc. Mass Spectrom.* **2009**, *20*, 1933-1943.

67. Iavarone, A. T.; Williams, E. R. Collisionally Activated Dissociation of Supercharged Proteins Formed by Electrospray Ionization. *Anal. Chem.* **2003**, *75*, 4525-4533.

68. Cassou, C. A.; Sterling, H. J.; Susa, A. C.; Williams, E. R. Electrothermal Supercharging in Mass Spectrometry and Tandem Mass Spectrometry of Native Proteins. *Anal. Chem.* **2013**, *85*, 138-146.

69. Sterling, H. J.; Cassou, C. A.; Susa, A. C.; Williams, E. R. Electrothermal Supercharging of Proteins in Native Electrospray Ionization. *Anal. Chem.* **2012**, *84*, 3795-3801.

70. Flick, T. G.; Williams, E. R. Supercharging with Trivalent Metal Ions in Native Mass Spectrometry. *J. Am. Soc. Mass Spectrom.* **2012**, *23*, 1885-1895.

71. Mortensen, D. N.; Williams, E. R. Electrothermal Supercharging of Proteins in Native MS: Effects of Protein Isoelectric Point, Buffer, and nanoESI-Emitter Tip Size. *Analyst* **2016**, *141*, 5598-5606.

72. Iavarone, A. T.; Williams, E. R. Supercharging in Electrospray Ionization: Effects on Signal and Charge. *Int. J. Mass Spectrom.* **2002**, *219*, 63-72.

73. Douglass, K. A.; Venter, A. R. Investigating the Role of Adducts in Protein Supercharging with Sulfolane. *J. Am. Soc. Mass Spectrom.* **2012**, *23*, 489-497.

74. Lomeli, S. H.; Peng, I. X.; Yin, S.; Ogorzalek Loo, R. R.; Loo, J. A. New Reagents for Increasing ESI Multiple Charging of Proteins and Protein Complexes. *J. Am. Soc. Mass Spectrom.* **2010**, *21*, 127-131.

75. Sterling, H. J.; Daly, M. P.; Feld, G. K.; Thoren, K. L.; Kintzer, A. F.; Krantz, B. A.; Williams, E. R. Effects of Supercharging Reagents on Noncovalent Complex Structure in Electrospray Ionization from Aqueous Solutions. *J. Am. Soc. Mass Spectrom.* **2010**, *21*, 1762-1774.

76. Zhang, J.; Loo, R. R. O.; Loo, J. A. Increasing Fragmentation of Disulfide-Bonded Proteins for Top-Down Mass Spectrometry by Supercharging. *Int. J. Mass Spectrom.* **2015**, *377*, 546-556.

77. Lomeli, S. H.; Yin, S.; Ogorzalek Loo, R. R.; Loo, J. A. Increasing Charge while Preserving Noncovalent Protein Complexes for ESI-MS. *J. Am. Soc. Mass Spectrom.* **2009**, *20*, 593-596.

78. Sterling, H. J.; Kintzer, A. F.; Feld, G. K.; Cassou, C. A.; Krantz, B. A.; Williams, E. R. Supercharging Protein Complexes from Aqueous Solution Disrupts their Native Conformations. *J. Am. Soc. Mass Spectrom.* **2012**, *23*, 191-200.

79. Sterling, H. J.; Prell, J. S.; Cassou, C. A.; Williams, E. R. Protein Conformation and Supercharging with DMSO from Aqueous Solution. *J. Am. Soc. Mass Spectrom.* **2011**, *22*, 1178-1186.

80. Going, C. C.; Xia, Z.; Williams, E. R. New Supercharging Reagents Produce Highly Charged Protein Ions in Native Mass Spectrometry. *Analyst* **2015**, *140*, 7184-7194.

81. Iavarone, A. T.; Williams, E. R. Mechanism of Charging and Supercharging Molecules in Electrospray Ionization. *J. Am. Chem. Soc.* **2003**, *125*, 2319-2327.

82. Dole, M.; Mack, L. L.; Hines, R. L. Molecular Beams of Macroions. *J. Chem. Phys.* **1968**, *49*, 2240.

83. Mack, L. L.; Kralik, P.; Rheude, A.; Dole, M. Molecular Beams of Macroions. II. *J. Chem. Phys.* **1970**, *52*, 4977-4986.

84. Metwally, H.; McAllister, R. G.; Popa, V.; Konermann, L. Mechanism of Protein Supercharging by Sulfolane and M-Nitrobenzyl Alcohol: Molecular Dynamics Simulations of the Electrospray Process. *Anal. Chem.* **2016**, *88*, 5345-5354.

85. Iribarne, J. V.; Thomson, B. A. On the Evaporation of Small Ions from Charged Droplets. *J. Chem. Phys.* **1976**, *64*, 2287-2294.

86. Sterling, H. J.; Cassou, C. A.; Trnka, M. J.; Burlingame, A. L.; Krantz, B. A.; Williams, E. R. The Role of Conformational Flexibility on Protein Supercharging in Native Electrospray Ionization. *Phys. Chem. Chem. Phys.* **2011**, *13*, 18288-18296.

87. Douglass, K. A.; Venter, A. R. On the Role of a Direct Interaction between Protein Ions and Solvent Additives during Protein Supercharging by Electrospray Ionization Mass Spectrometry. *Eur. J. Mass Spectrom.* **2015**, *21*, 641-647.

88. Picotti, P.; Aebersold, R.; Domon, B. The Implications of Proteolytic Background for Shotgun Proteomics. *Mol. Cell. Proteomics* **2007**, *6*, 1589-1598.

89. Teo, C. A.; Donald, W. A. Solution Additives for Supercharging Proteins Beyond the Theoretical Maximum Proton-Transfer Limit in Electrospray Ionization Mass Spectrometry. *Anal. Chem.* **2014**, *86*, 4455-4462.

90. Zenaidee, M. A.; Donald, W. A. Extremely Supercharged Proteins in Mass Spectrometry: Profiling the pH of Electrospray Generated Droplets, Narrowing Charge State Distributions, and Increasing Ion Fragmentation. *Analyst* **2015**, *140*, 1894-1905.

91. Feng, C.; Commodore, J. J.; Cassady, C. J. The use of Chromium(III) to Supercharge Peptides by Protonation at Low Basicity Sites. *J. Am. Soc. Mass Spectrom.* **2015**, *26*, 347-358.

92. Commodore, J. J.; Jing, X.; Cassady, C. J. Optimization of Electrospray Ionization Conditions to Enhance Formation of Doubly Protonated Peptide Ions with and without Addition of Chromium(III). *Rapid Commun. Mass Spectrom.* **2017**, *31*, 1129-1136.

93. Jing, X.; Edwards, K. C.; Vincent, J. B.; Cassady, C. J. The use of Chromium(III) Complexes to Enhance Peptide Protonation by Electrospray Ionization Mass Spectrometry. *J. Mass Spectrom.* **2018**, *53*, 1198-1206.

94. Persaud, R. R.; Dieke, N. E.; Jing, X.; Lambert, S.; Parsa, N.; Hartmann, E.; Vincent, J. B.; Cassady, C. J.; Dixon, D. A. Mechanistic Study of Enhanced Protonation by Chromium(III) in Electrospray Ionization: A Superacid Bound to a Peptide. *J. Am. Soc. Mass Spectrom.* **2020**, *31*, 308-318.

95. Perkins, T.; Puckett, S.; Cassady, C. J. University of Alabama, Tuscaloosa, AL. Unpublished work, **2017.**

96. Liu, X.; Locasale, J. W. Metabolomics: A Primer. *Trends Biochem. Sci.* **2017**, *42*, 274-284.

97. Griffiths, W.; Koal, T.; Wang, Y.; Kohl, M.; Enot, D.; Deigner, H. Targeted Metabolomics for Biomarker Discovery. *Angew. Chem. Int. Ed.* **2010**, *49*, 5426-5445.

CHAPTER 2. EXPERIMENTAL AND INSTRUMENTATIONAL METHODS

2.1 Overview

Mass spectrometry (MS) is a powerful analytical tool used for the identification and characterization of molecules. An extensive range of organic and inorganic compounds can be analyzed by MS, which makes it a frequently used technique across many fields of science. Analysis by MS can be divided into three main parts: ionization method, mass analyzer, and detector. This chapter will cover the ionization methods and mass analyzers for all instruments used in this dissertation, as well as dissociation techniques used to study peptide fragmentation. Experimental methodology, including solid-phase synthesis of peptides and solution-phase modification of peptides, will also be discussed. Amino acid structures are provided at the end of the chapter as a reference.

2.2 Ionization Methods

2.2.1 Electrospray ionization

Converting the sample into the gas phase is the first step of MS. Multiple ways exist to ionize the analyte of interest depending on the properties of the analyte. Electrospray ionization (ESI) is the most commonly used ionization method for low volatility compounds in MS and was first reported by Dole and coworkers in 1968.[1] The technique was further developed and popularized by John Fenn[2-6] in the 1980s, which led to Fenn being awarded the Nobel Prize

in Chemistry in 2002. ESI is an efficient method of analyzing low volatility samples such as biomolecules and has propelled the field of MS. ESI is considered a soft ionization method, which means that little to no fragmentation of the analyte is observed during the ionization process.

Performed under atmospheric pressure, a solution is introduced into the electrospray chamber through a stainless-steel needle. The solution is sprayed into a strong electric field, where it is nebulized, and charged droplets are generated by the potential difference between the needle and capillary. All ESI experiments in this dissertation were performed on a Bruker (Billerica, MA, USA) HCTultra PTM Discovery system in the positive mode with a high voltage (-3000 to -4000 V) applied to the endcap and capillary entrance while the needle is kept at ground. A second source design exists that places the high voltage on the needle and the capillary entrance and endplate are at ground.

The most accepted mechanism for the formation of ions by ESI is the charged residue model (CRM), illustrated in Figure 2.1, which was proposed by Dole.[1] The potential difference within the source region causes the solution being sprayed to form a pointed meniscus at the tip of the ESI emitter called a Taylor cone.[7] A nebulizer gas (flowing parallel to the sample solution) can aid in the creation of charged droplets but is not necessary. The research described in this dissertation utilizes nitrogen as the nebulizer gas. After droplet formation, a counter-current drying gas is introduced to facilitate solvent evaporation. As the solvent evaporates, the size of the droplets decrease, and the charge at the surface increases until the droplets reach their Rayleigh limit. The Rayleigh limit describes the maximum charge a droplet can acquire before Coulombic repulsion breaks down the droplets to form quasi-molecular ions.[8-10] These ions

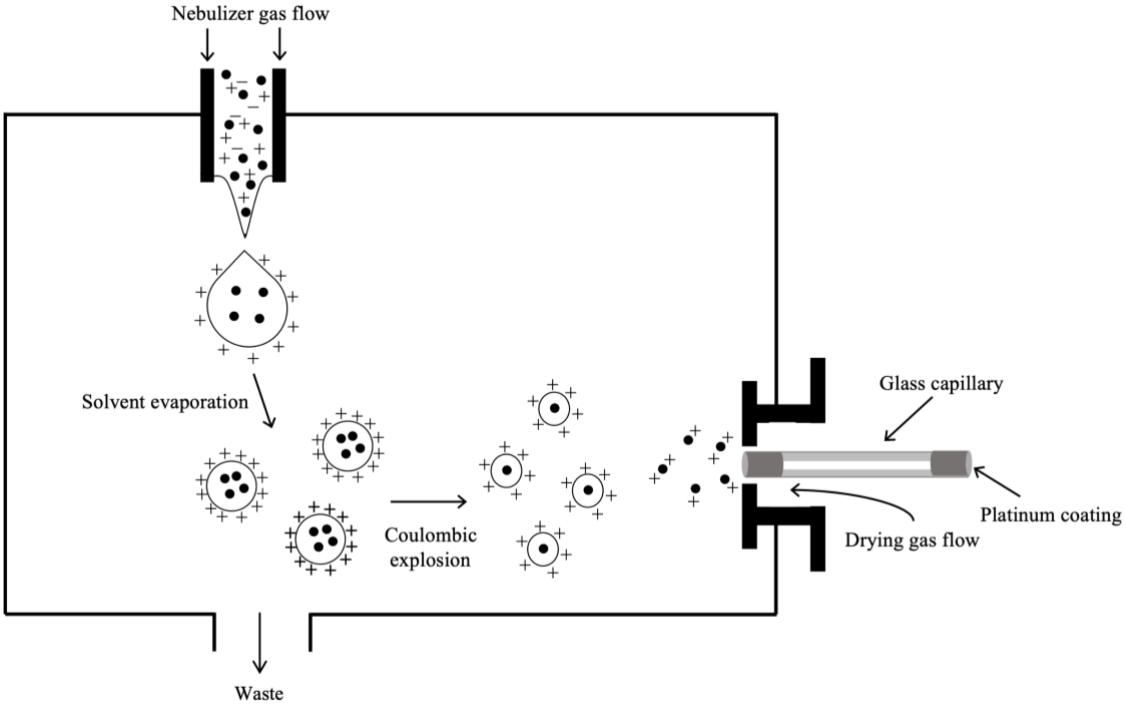

Figure 2.1. Diagram of ESI source design depicting the proposed CRM for ion formation in positive ion mode.

travel through a glass capillary coated with platinum on both ends into a storage octupole where they are held before mass analysis.

Formation of multiply charged ions by ESI is advantageous because it shifts the m/z of ions to a range that that can be detected by all mass analyzers.[11] Multiply charged ions also serve as precursor ions in electron-based tandem mass spectrometry (MS/MS) experiments such as electron transfer dissociation (ETD) (discussed further in Section 2.4.2). In addition to its ability to produce multiply charged ions, the coupling of ESI to separation techniques such as liquid chromatography (LC) has further advance the field of mass spectrometry.[3,12] Samples in solutions can be separated by chromatography then flowed into the mass spectrometer for mass analysis.

2.2.2 Matrix-assisted laser desorption ionization

Another commonly used ionization technique for proteomics is matrix-assisted laser desorption ionization (MALDI). The concept was first reported by Hillenkamp and Karas in 1985,[13,14] and Tanaka received the 2002 Nobel Prize in Chemistry for its application to protein analysis.[15,16] MALDI is a soft ionization technique, which ionizes the analyte by irradiation with a laser. The use of a light absorbing medium, termed matrix, is essential for the generation of ions.[17] MALDI is known for producing predominantly singly charged ions in contrast to ESI; therefore, MALDI spectra can be less complicated in regard to interpretation than ESI spectra. In MALDI, spectral results are heavily dependent on sample preparation. Matrix selection, analyte-to-matrix ratio, and method of deposition onto the target plates are factors that influence the quality of MALDI spectra.

The matrix serves multiple purposes in MALDI. Matrices can serve as a source of protons for the analyte. The matrix is added in excess with a typical analyte-to-matrix molecular

ratio of 1: (100-10,000), which minimizes cluster formation of analyte by separating analyte molecules and also aids in the cooling down ions through collisions. A good matrix is one that absorbs light at the same wavelength as the laser and transfers that energy to the analyte. The best MALDI matrices are low volatile solids that are soluble in common solvents.

The matrix can be introduced to the analyte in many ways. The most common method is the dried droplet method, which is when the analyte and matrix are mixed in a microcentrifuge tube before depositing the mixture onto the steel target plate and allowing the spot to dry. Usually, the volumetric ratio of analyte to matrix is between 1:1 and 1:10. Another method, the thin-layer method, involves depositing the matrix and analyte separately onto the target plate and allowing for dry time between each component. Depending on the matrix and analyte of interest, different deposition methods can influence the quality of the spectrum.

After the matrix and analyte has co-crystallized on the target plate, the plate is then inserted in the vacuum chamber and a pulsed laser irradiates the crystals. All MALDI experiments in this dissertation were performed on a Bruker (Billerica, MA, USA) rapifleX MALDI-TOF/TOF mass spectrometer equipped with a Nd:YAG laser (355 nm) that can fire at a repetition of up to 10 kHz. Once irradiated, the matrix transfers energy to the analyte leading to matrix/analyte clusters desorbing off the surface of the target plate. As desolvation occurs, proton transfer from the matrix to the analyte produces ions that can then be mass analyzed. A schematic of the ionization process in MALDI is presented in Figure 2.2. Poor shot-to-shot reproducibility is a major disadvantage of MALDI. The ability to couple MALDI and chromatography online has been a difficult feat and is a current active area of research. Offline LC-MALDI workflows have been developed to overcome this challenge.[18] MALDI does have

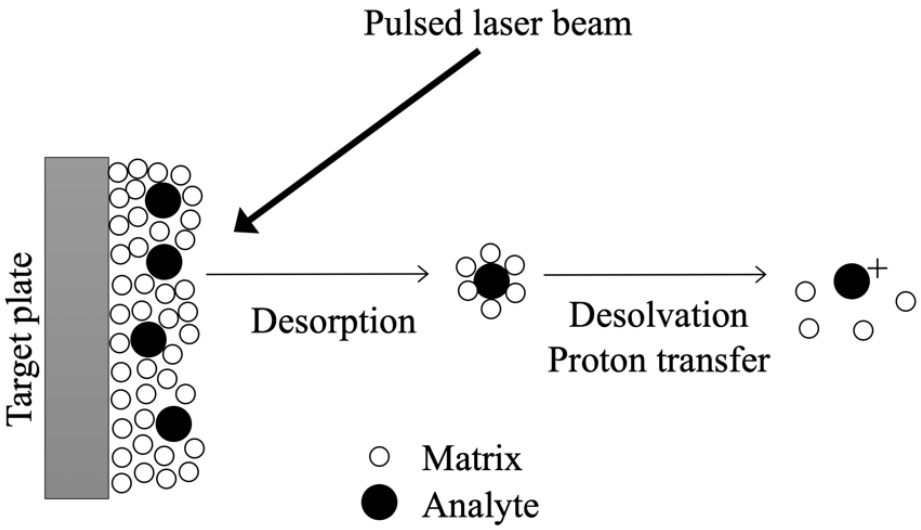

Figure 2.2. Schematic of MALDI ionization process.

advantages over ESI, especially in polymer characterization where the formation of multiply charged ions in ESI can complicate mass spectra. MALDI provides mass spectra of the polymer mass distribution. Other advantages of MALDI include simple sample preparation and ease of automation to perform high through-put analysis.

2.3 Mass analyzers

2.3.1 Quadrupole ion trap

In this dissertation, ions produced by ESI were mass analyzed and dissociated in a quadrupole ion trap (QIT). Introduced in 1958 by Wolfgang Paul, who was awarded the 1989 Nobel Prize in Physics for its development,[19] the QIT consists of two identical dome-shaped end cap electrodes and a central ring electrode where an alternating current (AC) voltage in the radiofrequency (rf) range is applied. The endcaps contain a small hole where ions can enter and exit the ion trap. Ions formed in ESI reach the trap by way of electrostatic focusing using two octopole ion guides and a lens system. Ions are trapped by applying a rf frequency potential to the central ring electrode. The QIT is capable of simultaneously trapping positive and negative ions, which makes it the preferred mass analyzer for ETD experiments. When the frequency (ω) of the rf voltage is fixed, the m/z range that is contained in the trap depends on the amplitude of voltage, V. The AC voltage guides the ions to the center of the trap forming an ion cloud. A bath gas, He, dampens the motion of the ions by reducing their kinetic energy, causing the ions to be trapped in the center of the trap. The motion of the ion cloud is described by solutions of Mathieu's second-order linear differential equation.[20]

Solutions to the Mathieu second order differential equation can be represented graphically in the Mathieu Diagram, which is given in Figure 2.3. The Mathieu diagram in terms

of the trapping parameters, a_u and q_u, indicates regions of stability where ions of a particular m/z range will be confined to the trap.[21]

The relationship between m/z, voltage (V) and frequency (ω) can be expressed as

$$\frac{m}{z} = \frac{4eV}{q_{max}\omega^2 r_0^2} \tag{2.1}$$

where e is the charge of an electron, r represents the radius of the central ring electrode, and q_{max} is defined for all QIT configurations and for most QITs is 0.908. Excitation occurs by placing an auxiliary voltage on the exit endcap, which moves the ions away from the center of the trap.

This work uses a high capacity spherical ion trap (HCT),[22] which is a type of QIT. The purpose of the HCT is to focus ions into a spherical cloud in the center of the trap, thereby increasing the storage capacity of the trap, sensitivity, and interactions between the ions especially for MS/MS experiments. Ions are detected by applying an RF voltage to the endcap electrodes which increases their frequency and orbital radius. Ions are then ejected from the trap and are detected by a Daly photomultiplier.

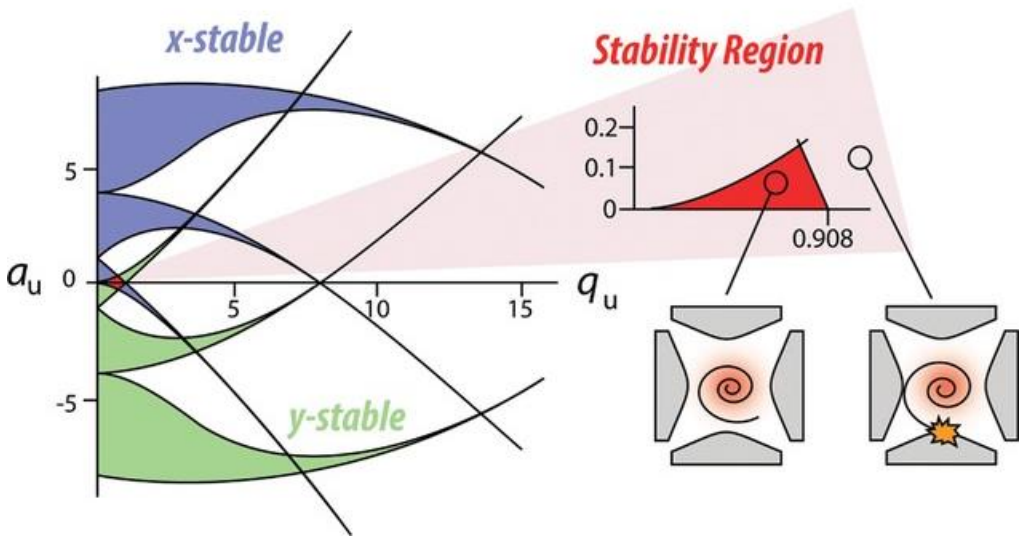

Figure 2.3. Mathieu stability diagram (used with permission from Reference 21).

2.3.2 Time-of-flight mass spectrometer

Time-of-flight (TOF) is a pulsed mass analyzer that separates ions based on their flight time from the ion source to the detector within a flight tube. TOF was developed by Cameron and Eggers in the 1950s.[23] During the ionization process a range of kinetic energy (KE) is imparted on the ions. An extraction electrode applies an accelerating voltage, V, to the ions as they leave the source. The accelerating voltage is usually 20-25 kV, which is large enough to minimize the KE spread of the ions. Consequentially, time spread is minimized because all the ions will have a similar KE derived from the accelerating voltage. Compared to other mass analyzers, TOF analyzers are conceptually the simplest mass analyzer.

As ions are accelerated out of the source, the KE of the ions can be expressed as

$$\frac{mv^2}{2} = zV \tag{2.2}$$

where m and z are the mass and charge of the ion, respectively, v is the velocity of the ion, and V is the accelerating voltage. The accelerated ions travel through a flight tube and the time it takes for the ion to reach the detector is defined as

$$t = \frac{l}{v} \tag{2.3}$$

where t is time it takes to travel the flight tube and L is the length of the flight tube. For the Bruker rapifleX MALDI-TOF/TOF, l = 25 cm for the first TOF and ~3 m for the second TOF. Rearranging Equation 2.2 in terms of v and substituting the expression into Equation 2.3 gives

$$t = \frac{l}{\left(\frac{m}{2zV}\right)^{1/2}} \tag{2.4}$$

which can be rearranged in terms of mass-to-charge, m/z, to give

$$\frac{m}{z} = \frac{2t^2V}{l^2} \tag{2.5}$$

TOF mass analyzers can be operated in two different modes: linear and reflectron mode. The principle of linear mode TOF is described above. In linear mode, the flight spread among ions with the same m/z can cause broadening of peaks due to the ions arriving at the detector at different times. To combat this, delayed extraction, also known as pulsed ion extraction, and the use of a reflectron were developed as a means of minimizing the time spread of ions of the same m/z. Delayed extraction was developed by Wiley and McLaren in the 1950s[24] and involves the accumulation of all ions produced during ionization prior to the ions collectively being extracted from the source. Ions are held for tens or hundreds of nanoseconds before being pulsed into the

TOF. By controlling when the ions leave the source, the time spread can be decreased for ions of the same m/z.

Time spread can also be decreased by means of a reflectron (or reflector).[25] In reflectron mode, an electric field is placed in the middle of the flight path utilizing a series of stainless-steel ring electrodes also known as a reflectron. The reflectron acts as an ion mirror that deflects ions back to the second detector. If two ions have the same m/z, the one that has a slightly higher velocity will travel further down the flight tube before being deflected towards the detector on the opposite end, which increases the ion's flight time. The ion that is moving slower will not penetrate as deep into the electric field before being deflected to the detector, thus allowing the slower ion to catch up to the faster ion with the same m/z. As a result of this, the time spread between ions of the same m/z is minimized, which also decreases peak broadening and improves mass resolution. TOFs are high resolution mass analyzers.

Unlike QIT analyzers, MS/MS experiments cannot be performed inside the flight tube. Instead, two TOF analyzers are placed in tandem with a collision cell placed in between the two flight tubes. The first TOF, a linear region about 25 cm long, are where ions are first separated by their m/z. A time-gated ion selector isolates the precursor ion that will be dissociated in the collision cell. After dissociation, the fragment ions are re-accelerated into the second TOF, ~3 meters in total length, to be mass analyzed before detection by a discrete dynode electron multiplier.

2.4 Tandem mass spectrometry

2.4.1 Collision-induced dissociation

Collision-induced dissociation (CID), first introduced in the 1960s, is the most common dissociation technique and is commonly used in proteomic research due to its widespread

availability on most commercial mass spectrometers.[23] Fundamental structural, kinetic, and energetic properties of biomolecules can be probed by performing CID experiments. The technique involves the dissociation of peptide/protein ions in the gas phase by collisions with neutral gas molecules (e.g. He, N_2, or Ar). In CID, translational energy is converted into internal energy that leads to dissociation and the formation of product ions. The technique can be classified as either high- or low-energy CID depending on the amount of energy that is used to accelerate the precursor ion into the neutral gas molecule. The amount of energy used in acceleration can dictate the rate and extent of fragmentation.[26] In low-energy CID, the collision energy is in the range of 0-100 eV; whereas with high-energy CID, the energy can go into the keV range.

CID is a two-step process that involves collisional activation of the precursor ion followed by unimolecular dissociation of the isolated precursor ion as shown in Equations 2.6 and 2.7.

Collisional activation: $$m_1^+ + He \rightarrow [m_1^+]^* + He/ \quad (2.6)$$

Unimolecular dissociation: $$[m_1^+]^* \rightarrow m_2^+ + m_3 \quad (2.7)$$

The precursor ion is represented by m_1^+. The precursor ion after the added energy is $[m_1^+]^*$. The collision gas is helium: He before collision with the precursor ion and $He/$ after. The product ion and neutral formed are represented by m_2^+ and m_3, respectively. During collisional activation, the precursor ion is excited by applying an AC voltage to the endcap electrodes of the QIT. The kinetic energy gained during excitation results in the ion colliding with the inert collision gas that is present in the trap. As collisions occur, the precursor ion's kinetic energy is converted into internal vibrational energy that is distributed among the bonds leading to unimolecular dissociation and often results in the breaking of the weakest bonds within the ion, which for

peptides are the backbone amide bonds. Cleavage of the amide bond is believed to be charge directed and motivated by the mobile proton model.[27]

The mobile proton model is widely used to describe the fragmentation process in CID of peptides. Energy deposited into the ion can mobilize a proton located at a basic site on the peptide such as the sidechain of arginine, histidine, or lysine or the N-terminus. The mobilized proton is subsequently transferred to a backbone amide nitrogen or carbonyl oxygen, which causes weakening of the amide bond. Cleavage at amide bonds form b- and y-ions.[27,28] (Peptide fragmentation nomenclature will be discussed later in Section 2.5.) Low-energy CID experiments are routinely performed in trapping mass analyzers, such as multi-pole devices, QIT, or Fourier transform ion cyclotron resonance (FT-ICR) mass analyzers, where the precursor ion and collision gas can collide with one another. The gas pressure is optimized to increase the number of collisions within the mass analyzer.

2.4.2 Electron transfer dissociation

Introduced by Hunt and co-workers in 2004,[29] electron transfer dissociation (ETD) is a more recently developed technique for proteomic research. Unlike CID that involves internal energy randomization, ETD is a nonergodic process where internal energy is localized to elicit fragmentation nearby. In ETD, a low-energy electron is made by negative chemical ionization (nCI) then transferred to the QIT, where the isolated precursor ions are trapped. Multiply charged precursor ions are required to prevent neutralization of the ion after the addition of the electron. Low-energy electrons are generated in a nCI source that is located outside of the trap. First, an electron filament at 75 eV produces high energy electrons, which interact with methane (CH_4) gas to produce low-energy electrons (e^{-*}), Equation 2.15.

$$CH_4 + e^- \rightarrow {CH_4}^+ + e^- + e^{-*} \qquad (2.15)$$

An ETD reagent with a low electron affinity captures the low-energy electron and transfers it to the precursor ion through an ion/ion reaction. Common ETD reagent ions are fluoranthene, azobenzene, and anthracene.[29-31] Fluoranthene is the ETD reagent gas used in this research. The fluoranthene molecule captures the low-energy electron to form a radical anion, Figure 2.4. The reagent anion is transferred from the nCI source into the QIT by means of electrostatic focusing. Once in the trap, ion/ion reactions between the anions and the multiply charged precursor ions occur and result in cleavage of the N-C_α bond to produce c-and z-ions.

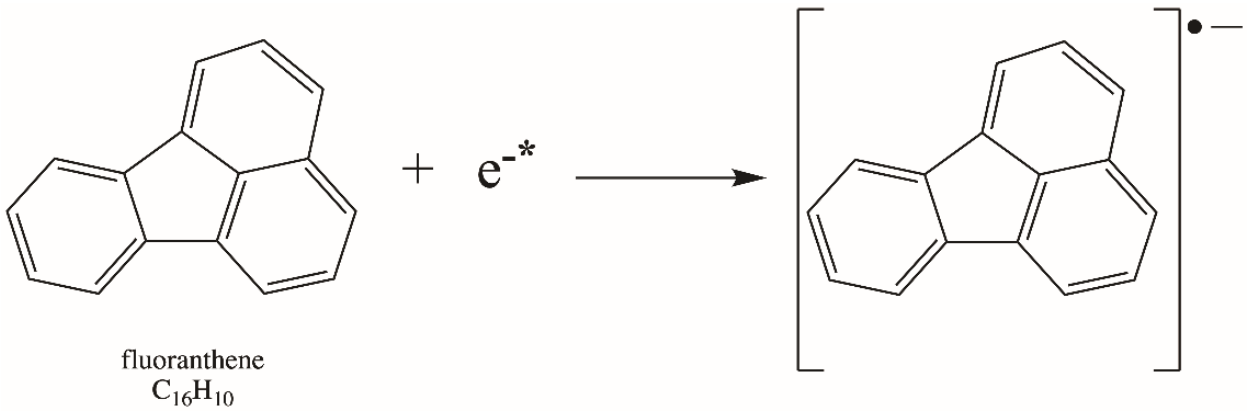

Figure 2.4. Formation of fluoranthene anion.

The mechanism of fragmentation in ETD is similar to the mechanism of electron capture dissociation (ECD), which is another electron-induced dissociation technique that is performed in FT-ICR mass spectrometers. Instead of using a reagent to transfer a low-energy electron to the analyte ion, ECD transfers an electron generated by an electron filament directly to the multiply charged precursor ion. Fragmentation is induced, and the ECD process produces c- and z-ions similar to ETD. Currently, two mechanisms have been developed to explain fragmentation by

ETD and ECD: the Cornell mechanism and the Utah-Washington (UW) mechanism. The Cornell mechanism was proposed by McLafferty and coworkers in 1998,[32] and requires the presence of basic amino acid residues. The positively charged side chains of arginine (R), lysine (K), and histidine (H) residues sequester the captured or transferred low-energy electron to form an odd electron species. A proton migrates to an amide carbonyl group to form an aminoketyl radical intermediate, which triggers N-C_α bond cleavage and produces c- and z-ions.[33] The Cornell mechanism is limited by the fact that a basic residue must be present for the mechanism to proceed; however, dissociation by ETD can be observed with peptides without basic residues.

The UW mechanism was developed independently by Tureck and Syrstad [34] and Simons and coworkers[35] to explain ETD fragmentation of all peptides regardless of the type of residues present. Figure 2.5 illustrates the UW mechanism, which has become the accepted mechanism for fragmentation by ETD. In the UW mechanism, an electron can be captured and stabilized by the π^* orbital of the amide backbone to form the aminoketyl radical-anion. Fragmentation can occur via two different pathways as shown in Figure 2.5. A proton can first be transferred to the aminoketyl radical-anion followed by cleavage of the N-C_α bond or N-C_α bond cleavage occurs first followed by proton transfer to give the c- and z-ions. In comparison to CID, ETD has the advantage of generating extensive backbone cleavage at nearly every residue while maintaining post-translational modifications (PTMs) such as phosphorylation and glycosylation.

2.5 Peptide fragmentation nomenclature

The peptide fragmentation nomenclature used to describe CID and ETD spectra in this dissertation was introduced by Roepstorff and Fohlman.[36] Figure 2.6 illustrates the symbolism used in describing peptide fragmentation. The three locations for peptide backbone cleavage are: the C_α-C(carbonyl) bond (a- and z-ions), the amide bond (b- and y-ions), and the N-C_α bond (c-

and z-ions). Product ions are classified into two categories: ions retaining the charge on the N-terminus side of the peptide (a-, b-, and c-ions) and ions retaining the charge on the C-terminal side (x-, y-, and z-ions). The location of the cleavage relative to the amino acid sequence is indicated by the subscript n. For example, c_8 means cleavage of the N-C_α bond of the eighth amino acid residue from the N-terminus. Fragment ions can gain or lose hydrogen during the fragmentation process, which is signified by the prime symbol before (loss of hydrogens) or after (gain of hydrogens) the letter. For example, $z_n^{/+}$ and $^{//}b_n^+$ stands for $[z_n + H]^+$ and $[b_n - 2H]^+$, respectively.

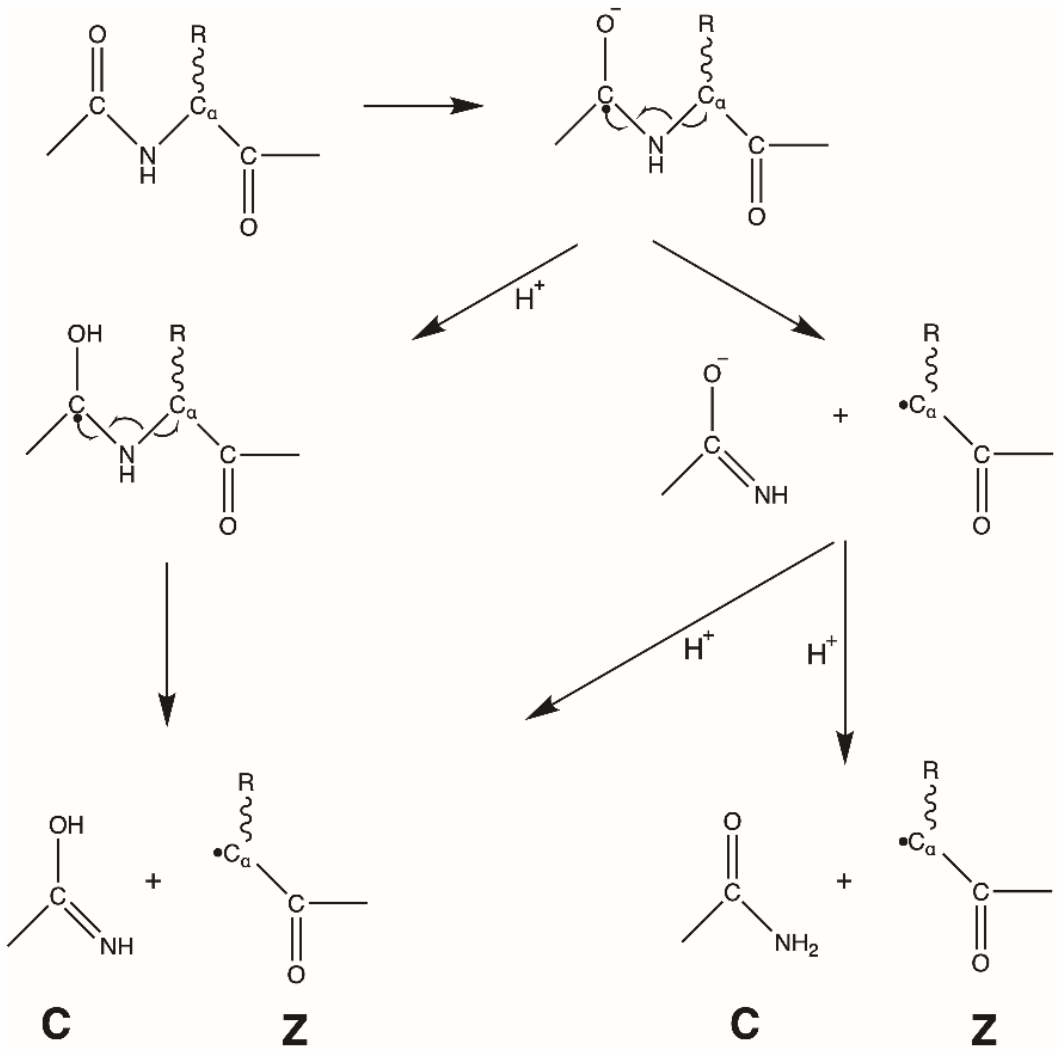

Figure 2.5. Utah Washington mechanism for N-Ca bond cleavage in ETD of peptides.

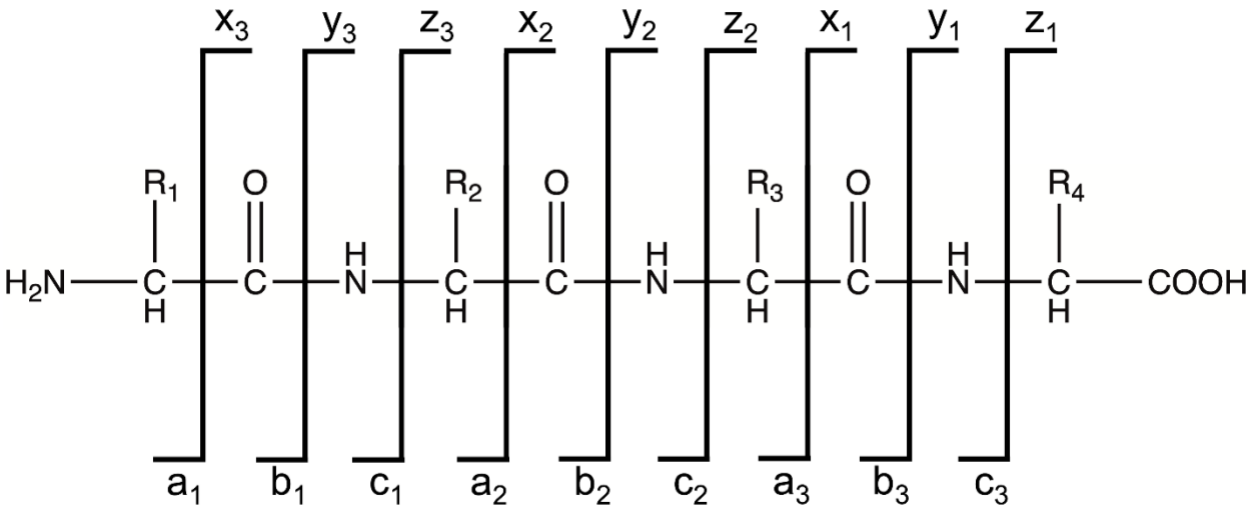

Figure 2.6. Peptide sequencing nomenclature.

2.6 Fmoc solid-phase peptide synthesis

Model peptides were synthesized on an Advanced ChemTech Model 90 synthesizer (Louisville, KY, USA) by Fmoc solid-phase peptide synthesis (SPPS), which was established by Merrifield in 1963.[37] In Fmoc SPPS, peptides are synthesized using an insoluble support resin from the C-terminus to the N-terminus. The C-terminus residue is attached to a Wang resin, which is a porous polystyrene resin bead. Internal residues are bonded to a labile 9-fluoroenylmethoxycarbonyl (Fmoc) group to prevent side reactions from occurring at the sidechain. Figure 2.7 shows that structure of the Fmoc protecting group. Multiple steps of washing, deprotecting, and coupling are involved in the synthesis of the polypeptide chain.

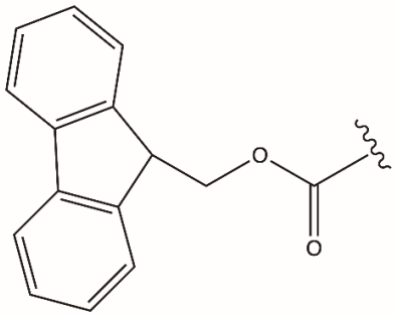

Figure 2.7. Fmoc protecting group.

SPPS protocol requires the use of multiple reagents. Solutions of the amino acid residues and Wang resin are made in 1-hydroxybenzotriazole (HOBt) to a final concentration of 0.5 M in N-methyl-2-pyrrolidinone (NMP) and placed in separate vessels attached to the synthesizer. The Wang resin is washed using N,N-dimethylformamide (DMF) and methanol (MeOH). After washing, the Fmoc protecting group is removed using a solution of 20% piperidine (PIP) in DMF [v/v]. Following deprotection, the next amino acid in the sequence was coupled to the Wang resin by introducing the Fmoc amino acid solution into the reaction vessel containing the deprotected Wang resin and allowing the mixture to shake for 60-75 minutes. During the process of coupling, a 0.5 M solution of 1,3-diisopropylcarbodiimide (DIC) in NMP was added to the reaction vessel to activate the carboxyl group of the Fmoc amino acid. After coupling, the DMF and MeOH wash steps are repeated before the next residue was coupled to the chain until the sequence is complete. After synthesis, the Wang resin is cleaved from the C-terminus amino acid residue using a solution of 92% trifluoroacetic acid (TFA), 5% Milli-Q 18 MΩ water, and 3% trisopropylsilane (TIPS). Cooled diethyl ether and acetone were added to the solution to cause the peptide to precipitate out of solution. The solution was centrifuged, and the organic layer was

decanted leaving behind the free acid peptide. The peptide is placed in a desiccator and allowed to dry overnight. No additional purification step was necessary.

2.7 Methyl esterification of peptides

To test the importance of the carboxylic acid group in the mechanism of Cr(III) enhanced protonation, peptide acids (-COOH) were converted to methyl esters (-COOMe) by conventional solution-phase chemistry.[38] Figure 2.8 shows the process of methyl esterification for peptides. The free acid peptide was mixed with a solution containing 5 μL of acetic anhydride, 6 μL of 12 M hydrochloric acid, and 96 μL of dry MeOH. The reaction proceeds overnight at room temperature. The solution containing the peptide methyl ester was directly used for mass analysis without further purification.

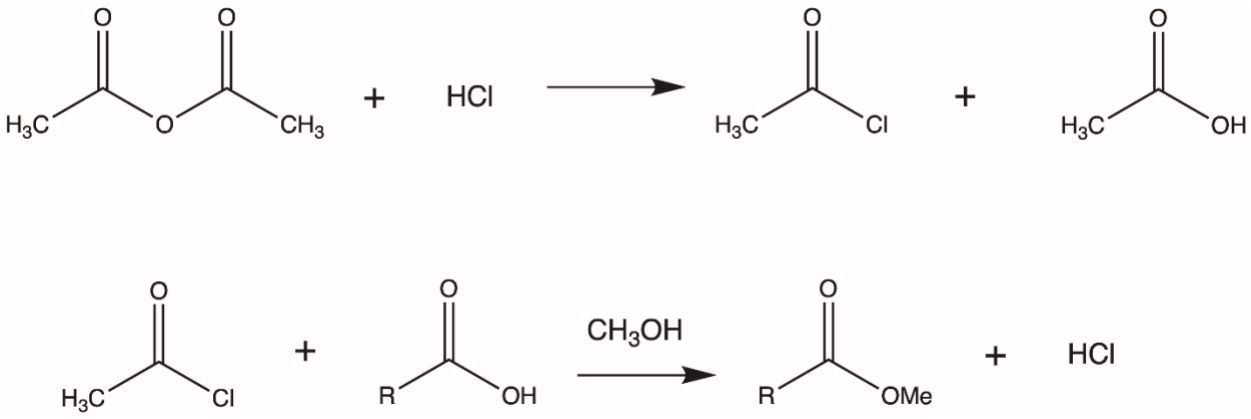

Figure 2.8. Methyl esterification of peptides (R-COOH).

2.8 Amino acid structures

Peptides are biopolymers that are made up from the 20 naturally occurring amino acids linked together by an amide bond, also known as a peptide bond. Figures 2.9 through 2.13 illustrates the 20 common amino acids and their 3- and 1- letter codes. Also included is phosphorylated tyrosine, which was used in this dissertation, Figure 2.14.

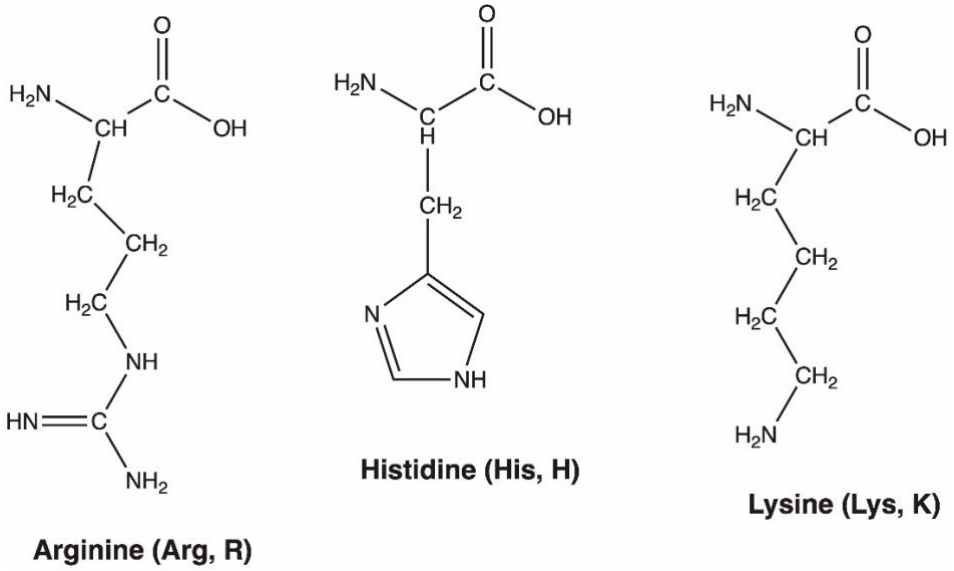

Figure 2.9. Amino acids with basic side chains.

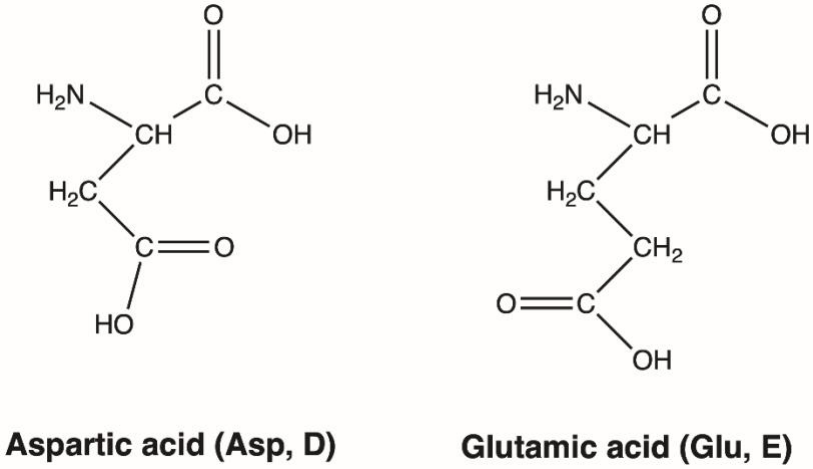

Figure 2.10. Amino acids with acidic side chains.

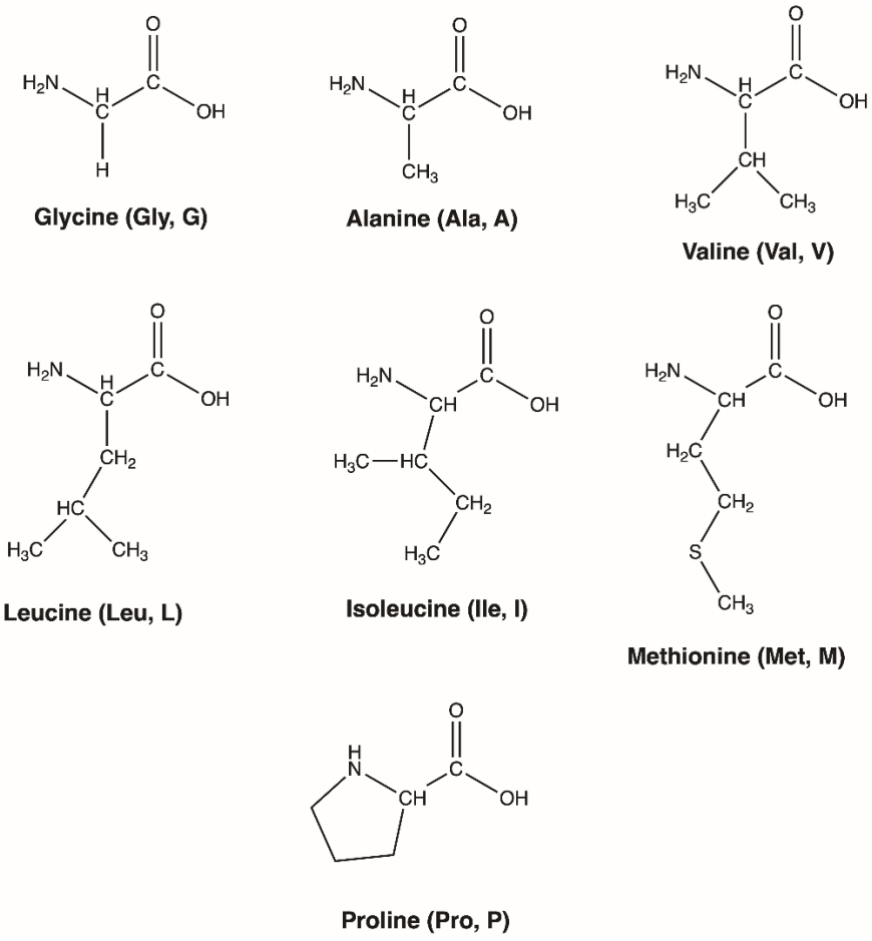

Figure 2.11. Amino acids with hydrophobic aliphatic side chains.

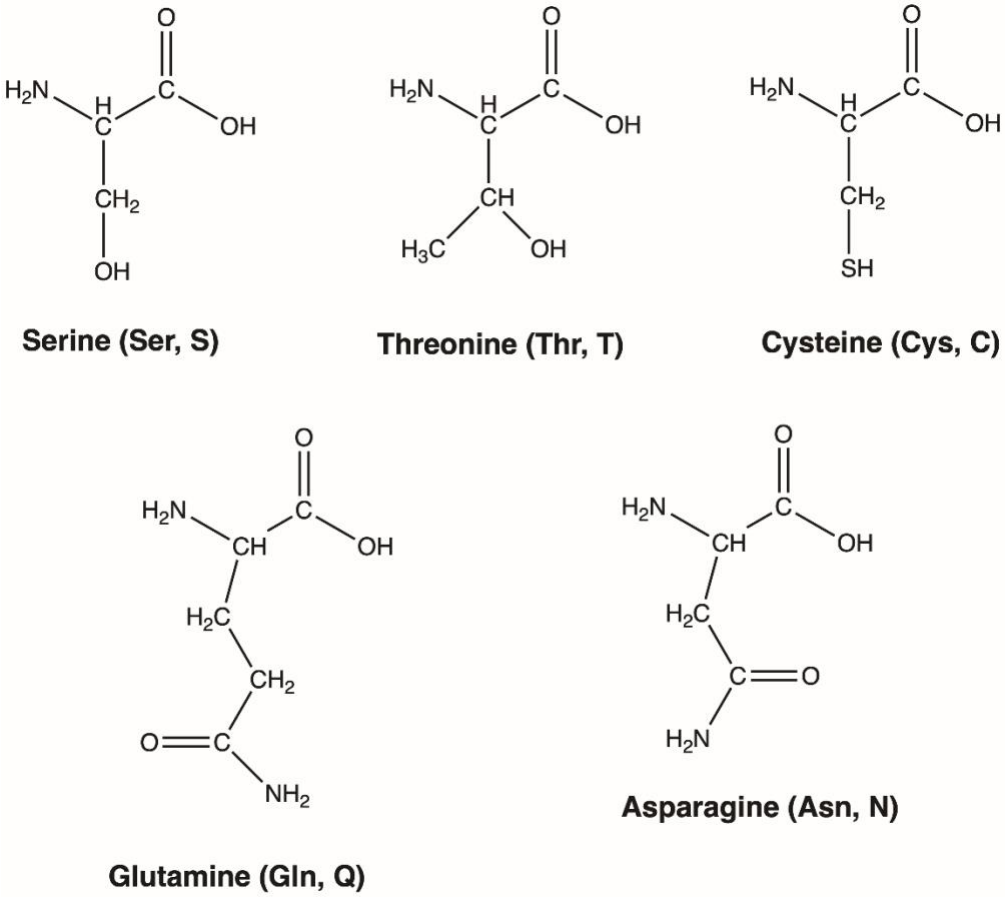

Figure 2.12. Amino acids with uncharged hydrophilic side chains.

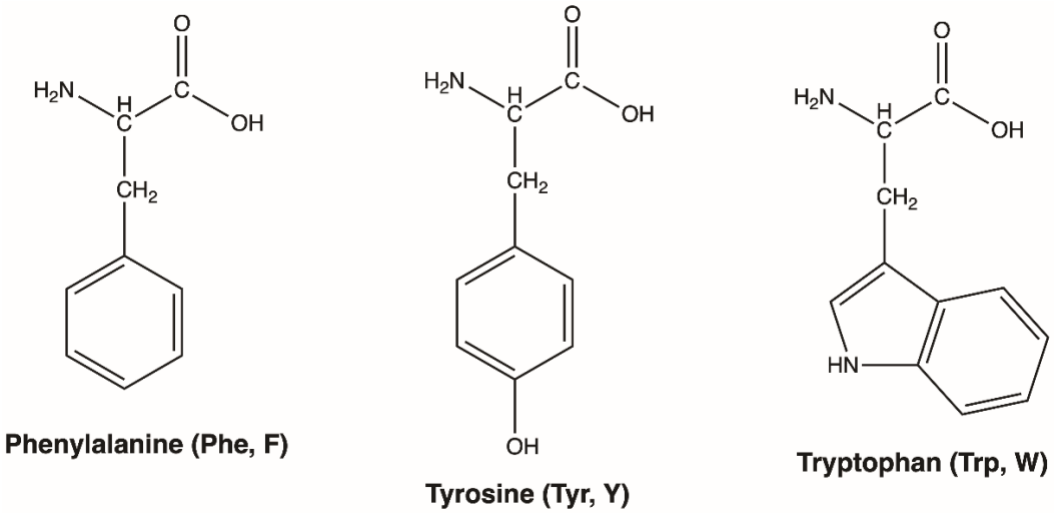

Figure 2.13. Amino acids with aromatic side chains.

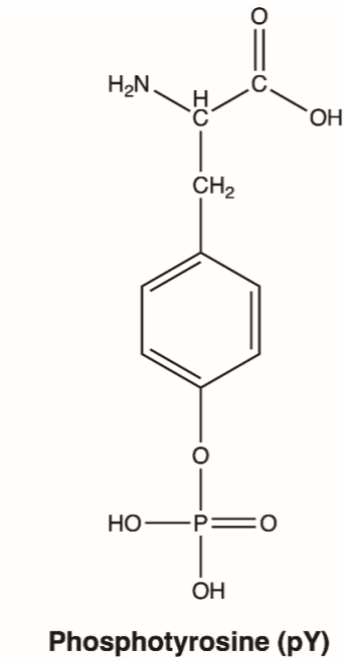

Figure 2.14. Structure of phosphorylated tyrosine.

References

1. Dole, M.; Mack, L. L.; Hines, R. L. Molecular Beams of Macroions. *J. Chem. Phys.* **1968**, *49*, 2240.

2. Yamashita, M.; Fenn, J. B. Negative-Ion Production with the Electrospray Ion-Source. *J. Phys. Chem.* **1984**, *88*, 4671-4675.

3. Whitehouse, C. M.; Dreyer, R. N.; Yamashita, M.; Fenn, J. B. Electrospray Ionization for Liquid Chromatographs and Mass Spectrometers. *Anal. Chem.* **1985**, *57*, 675-679.

4. Fenn, J. B.; Mann, M.; Meng, C. K.; Wong, S. F. Electrospray Ionization--Principles and Practice. *Mass Spectrom. Rev.* **1990**, *9*, 37-70.

5. Fenn, J. B.; Mann, M.; Meng, C. K.; Wong, S. F.; Whitehouse, C. M. Electrospray Ionization for Mass Spectrometry of Large Biomolecules. *Science* **1989**, *246*, 64-71.

6. Fenn, J. B.; Mann, M.; Meng, C. K.; Wong, S. F.; Whitehouse, C. M. Electrospray Ionization for Mass-Spectrometry of Large Biomolecules. *Science* **1989**, *246*, 64-71.

7. Wilm, M. S.; Mann, M. Electrospray and Taylor-Cone Theory, Dole's Beam of Macromolecules at Last? *Int. J. Mass Spectrom. Ion Processes* **1994**, *136*, 167-180.

8. Wilm, M. S.; Mann, M. Electrospray and Taylor-Cone Theory, Doles Beam of Macromolecules at Last. *Int. J. Mass Spectrom.* **1994**, *136*, 167-180.

9. Gomez, A.; Tang, K. Q. Charge and Fission of Droplets in Electrostatic Sprays. *Phys. Fluids* **1994**, *6*, 404-414.

10. Tang, K.; Gomez, A. On the Structure of an Electrostatic Spray of Monodisperse Droplets. *Phys. Fluids* **1994**, *6*, 2317-2332.

11. Marshall, A. G.; Hendrickson, C. L. Charge Reduction Lowers Mass Resolving Power for Isotopically Resolved Electrospray Ionization Fourier Transform Ion Cyclotron Resonance Mass Spectra. *Rapid Commun. Mass Spectrom.* **2001**, *15*, 232-235.

12. Ikonomou, M. G.; Blades, A. T.; Kebarle, P. Investigations of the Electrospray Interface for Liquid-Chromatography Mass-Spectrometry. *Anal. Chem.* **1990**, *62*, 957-967.

13. Karas, M.; Bachmann, D.; Hillenkamp, F. Influence of the Wavelength in High-Irradiance Ultraviolet-Laser Desorption Mass-Spectrometry of Organic-Molecules. *Anal. Chem.* **1985**, *57*, 2935-2939.

14. Karas, M.; Hillenkamp, F. Laser Desorption Ionization of Proteins with Molecular Masses Exceeding 10,000 Daltons. *Anal. Chem.* **1988**, *60*, 2299-2301.

15. Tanaka, K.; Waki, H.; Ido, Y.; Akita, S.; Yoshida, Y.; Yohida, T. Protein and Polymer Analyses Up to M/Z 100,000 by Laser Ionization Time-of-Flight Mass Spectrometry. *Rapid Commun. Mass Spectrom.* **1988**, *2*, 151-153.

16. Tanaka, K. The Origin of Macromolecule Ionization by Laser Irradiation (Nobel Lecture). *Angew. Chem. Int. Ed.* **2003**, *42*, 3860-3870.

17. Fukuyama, Y. MALDI Matrix Research for Biopolymers. *Mass Spectrom. (Tokyo)* **2015**, *4*, A0037.

18. Mueller, D. R.; Voshol, H.; Waldt, A.; Wiedmann, B.; van Oostrum, J. LC-MALDI MS and MS/MS — An Efficient Tool in Proteome Analysis. *Subcellular Proteomics: From Cell Deconstruction to System Reconstruction;* Springer Netherlands: Dordrecht, 2007; pp 355-380.

19. Paul, W. Electromagnetic Traps for Charged and Neutral Particles. *Rev. Mod. Phys.* **1990**, *62*, 531-540.

20. March, R. E. An Introduction to Quadrupole Ion Trap Mass Spectrometry. *J. Mass Spectrom.* **1997**, *32*, 351-369.

21. Savaryn, J. P.; Toby, T. K.; Kelleher, N. L. A Researcher's Guide to Mass Spectrometry-Based Proteomics. *Proteomics* **2016**, *16*, 2435-2443.

22. Bruker Daltonics *HCTultra PTM Discovery System User Manual;* Billerica, MA, 2006.

23. Hoffmann, E. d.; Stroobant, V. *Mass Spectrometry Principles and Applications;* John Wiley & Sons, Ltd: New York, 2007.

24. Wiley, W. C.; McLaren, I. H. Time-of-Flight Mass Spectrometer with Improved Resolution. *Rev. Sci. Instrum.* **1955**, *26*, 1150-1157.

25. Mamyrin, B. A. Time-of-Flight Mass Spectrometry (Concepts, Achievements, and Prospects). *Int. J. Mass Spectrom.* **2001**, *206*, 251-266.

26. Mitchell Wells, J.; McLuckey, S. A. Collision-Induced Dissociation (CID) of Peptides and Proteins. *Meth. Enzymol.* **2005**, *402*, 148-185.

27. Wysocki, V. H.; Tsaprailis, G.; Smith, L. L.; Breci, L. A. Mobile and Localized Protons: A Framework for Understanding Peptide Dissociation. *J. Mass Spectrom.* **2000**, *35*, 1399-1406.

28. Paizs, B.; Suhai, S. Fragmentation Pathways of Protonated Peptides. *Mass Spectrom. Rev.* **2005**, *24*, 508-548.

29. Syka, J. E. P.; Coon, J. J.; Schroeder, M. J.; Shabanowitz, J.; Hunt, D. F. Peptide and Protein Sequence Analysis by Electron Transfer Dissociation Mass Spectrometry. *Proc. Natl. Acad. Sci. USA* **2004**, *101*, 9528-9533.

30. Gunawardena, H. P.; Gorenstein, L.; Erickson, D. E.; Xia, Y.; McLuckey, S. A. Electron Transfer Dissociation of Multiply Protonated and Fixed Charge Disulfide Linked Polypeptides. *Int. J. Mass Spectrom.* **2007***, 265*, 130-138.

31. Swaney, D. L.; McAlister, G. C.; Wirtala, M.; Schwartz, J. C.; Syka, J. E. P.; Coon, J. J. Supplemental Activation Method for High-Efficiency Electron-Transfer Dissociation of Doubly Protonated Peptide Precursors. *Anal. Chem.* **2007**, *79*, 477-485.

32. Zubarev, R. A.; Kelleher, N. L.; McLafferty, F. W. Electron Capture Dissociation of Multiply Charged Protein Cations. A Nonergodic Process. *J. Am. Chem. Soc.* **1998**, *120*, 3265-3266.

33. Zubarev, R. A. Reactions of Polypeptide Ions with Electrons in the Gas Phase. *Mass Spectrom. Rev.* **2003**, *22*, 57-77.

34. Syrstad, E. A.; Tureček, F. Toward a General Mechanism of Electron Capture Dissociation. *J. Am. Soc. Mass Spectrom.* **2005**, *16*, 208-224.

35. Sobczyk, M.; Anusiewicz, I.; Berdys-Kochanska, J.; Sawicka, A.; Skurski, P.; Simons, J. Coulomb-Assisted Dissociative Electron Attachment: Application to a Model Peptide. *J. Phys. Chem. A* **2005**, *109*, 250-258.

36. Roepstorff, P.; Fohlman, J. Proposal for a Common Nomenclature for Sequence Ions in Mass Spectra of Peptides. *Biomed. Mass Spectrom.* **1984**, *11*, 601.

37. Merrifield, R. B. Solid Phase Peptide Synthesis. I. the Synthesis of a Tetrapeptide. *J. Am. Chem. Soc.* **1963**, *85*, 2149-2154.

38. Greene, T. W.; Wuts, P. G. M., Eds.; In *Protective Groups in Organic Synthesis;* John Wiley & Sons, Inc.: New York, 1991.

CHAPTER 3. THE EFFECTS OF PEPTIDE STRUCTURE ON ENHANCED PROTONATION UPON ADDITION OF TRIVALENT CHROMIUM DURING ELECTROSPRAY IONIZATION MASS SPECTROMETRY

3.1 Introduction

Electrospray ionization (ESI) is a widely utilized ionization method in mass spectrometry (MS) for the analysis of large biomolecules owing to its ability to generate multiply charged protonated ions, $[M + nH]^{n+}$.[1] Formation of $[M +nH]^{n+}$ is advantageous in tandem mass spectrometry (MS/MS) analysis of peptides and proteins because multiply charged ions require less energy to dissociate and have been shown to be more sequence informative than singly charged ions.[2-6] In addition, multiply charged protonated ions can be dissociated using electron-based dissociation techniques such as electron transfer dissociation (ETD)[7-9] and electron capture dissociation (ECD),[2,10,11] unlike $[M + H]^+$, which will be charge neutralized upon the addition of an electron.

Different approaches have been taken to form multiply charged protein ions by ESI. Chapter 1 discusses these approaches and the mechanisms involved in supercharging proteins using organic supercharging reagents. The focus of these supercharging studies has been with large proteins [12-14] For work with peptides, the addition of chromium(III) nitrate, $[Cr(H_2O)_6](NO_3)_3{\cdot}3H_2O$, and chromium(III) chloride tetrahydrofuran complex, $[Cr(THF)_3]Cl_3$, to peptide solutions undergoing ESI has been reported by the Cassady and Vincent groups to increase protonation efficiency.[15-17] These Cr(III) complexes in aqueous solutions exist as hydrated chromic ions, $[Cr(H_2O)_6]^{3+}$ and are kinetically inert.[18-20] Cr(III)-induced protonation is

observed with peptide sequences greater than or equal to seven amino acid residues. For example, the model peptide heptaalanine (AAAAAAA, A7) forms exclusively $[M + H]^+$ by ESI in the absence of Cr(III), but the addition of Cr(III) results in the formation of $[M + 2H]^{2+}$ in an optimized 2+ to 1+ signal intensity ratio of 4:1.[15] Protonation of acidic and neutral peptides benefit the most from addition of Cr(III). In positive mode ESI, acidic peptides are often difficult to multiply protonate (or sometimes even singly protonate) due to their preference for deprotonation.[21,22] The addition of Cr(III) to acidic model peptides that formed only $[M + H]^+$ often results in the formation of $[M + 2H]^{2+}$.[15]

Factors such as time, solvent, ESI source parameters, and sample preparation that may influence protonation induced by Cr(III) have been previously studied.[16,17] The amount of time that Cr(III) and the peptide are allowed to interact in solution was determined to not be a factor in the extent of enhanced protonation. The presence of water in the solvent system as well as water bound to Cr(III) is critical to the mechanism. In the absence of water, A7 did not generate $[M + 2H]^{2+}$. A mass spectrometry parameter optimization study for enhanced protonation with Cr(III) revealed that the ESI drying flow rate was also important and suggests that the ESI desolvation stage is essential to the mechanism.[16]

Carboxylic acid groups were discovered to be important to the mechanism after the peptide A7 was converted to a methyl ester and enhanced protonation was not observed.[15] The work in this chapter will further investigate the importance of the carboxylic acid group to better understand the mechanism and the analytical utility of enhanced protonation with Cr(III). The position of acidic residues, which contain carboxylic acid groups on their sidechain, was varied. The effect of peptide size will also be studied to determine whether a size limit exists where enhanced protonation by Cr(III) ceases. Lastly, model peptides containing tyrosine, proline, and

phosphorylated amino acids were synthesized to determine any effects of these rather unique residues on the process.

3.2 Experimental

3.2.1 Peptides and sample preparation

The following peptides were purchased from Biomatik USA (Cambridge, ON, Canada): DAAAAAA, AAADAAA, AAAAAAD, EAAAAAA, AAAEAAA, AAAAAAE, AAAAAAA-NH_2, AAAEAAA-NH_2, and EDDpYDEEN. Bovine ubiquitin (8.5 kDa in molecular mass) and bovine cytochrome c (12 kDa) were obtained from Sigma-Aldrich (St. Louis, MO, USA). Equine myoglobin (18 kDa) was purchased from Fluka Chemical Corp (Ronkonkoma, NY, USA). All other peptides were synthesized in the Cassady group laboratory on an Advanced ChemTech (Louisville, KY, USA) Model 90 automated peptide synthesizer using standard Fmoc procedures.[23] The peptides were used as synthesized, without further purifications, which accounts for impurity peaks in the mass spectra. All peptide synthesis reagents were purchased from Advanced ChemTech or VWR International (Radnor, PA, USA). Peptide methyl esters were produced by acid-catalyzed esterification with methanol.[24] Chromium(III) nitrate nonahydrate and chromium(III) chloride tetrahydrofuran were purchased from VWR International.

Stock peptide solutions were prepared in Ultrapure Milli-Q water at a concentration of 1 mg/mL. The solutions studied contained a final peptide concentration of 10 μM in 50:50 [v/v] acetonitrile: water. Solutions containing Cr(III) were in a 1:10 peptide-to-metal molar ratio except where otherwise indicated. Acidified solutions contained 1% (by volume) acetic acid.

3.2.2 Mass spectrometry

All experiments were performed on a Bruker (Billerica, MA, USA) HCTultra PTM Discovery System high-capacity quadrupole ion trap (QIT) mass spectrometer. Solutions were directly infused at a flow rate of 180 µL/hr using a KD Scientific (Holliston, MA, USA) syringe pump. Mass spectra were obtained in the positive mode with a high voltage of -4.0 kV applied to the platinum coated capillary entrance, stainless steel entrance cap, and endplate. The ESI needle was held at ground. Nitrogen was used as both the nebulizer gas and the drying gas. The drying gas flow rate was varied from 5 to 10 L/min, and the temperature was set to 300°C. The nebulizer gas pressure was between 5 to 10 psi. Final mass spectra were the result of signal averaging 300 scans. Means and standard deviations presented are the result of three independent replications.

3.3 Results and discussion

3.3.1 Effects of acidic residue position

The effect of the location of acidic residues on enhanced protonation was investigated using model heptapeptides. The acidic residue position was varied for the heptapeptides with the general sequences of XAAAAAA (XA6), AAAXAAA (A3XA3), and AAAAAAX (A6X), where A is alanine and X is glutamic (E) or aspartic (D) acid. In the absence of Cr(III), all six hexapeptides produce exclusively $[M + H]^+$ by ESI. Adding 1% acetic acid to the peptide solutions does not lead to the formation of $[M + 2H]^{2+}$; therefore, production of $[M + 2H]^{2+}$ using Cr(III) is not a result of lowered solution-phase pH The absolute intensities (A.I) for the protonated and metal-adducted peptide ions are presented in Table 3.1. Addition of Cr(III) results in the formation of $[M + 2H]^{2+}$ for all six heptapeptides.

Regardless of the type of acidic residue (E or D), when the acidic residue is located at the C-terminus, A6D and A6E, addition of Cr(III) produces the largest ratio of 2+ to 1+. Figure 3.1 illustrates the formation of $[M + 2H]^{2+}$ after Cr(III) is added to a solution containing the model peptide A6E. For 2+ to 1+ ions, a peak intensity ratio of 8:1 is observed for A6E. The aspartic acid analog produces a 2+ to 1+ ratio of 6:1. Trivalent metal ions have been shown to bind to peptides through coordination of the metal ion with the carboxyl group of the peptide to create a metal-ion complex.[6,25] Aspartic acid and glutamic acid have been reported to coordinate transition metal ions along with histidine and cysteine residues.[26,27] The presence of $[M + Cr – H]^{2+}$ in the ESI spectra for the six peptides also indicates that a metal-peptide ion complex forms and that a direct interaction exists between the metal ion and the peptide. The carboxylic acid groups at the C-terminus and sidechain are potential sites for Cr(III) to bind. Possibly, the two carboxylates in A6D and A6E are in close proximity and can simultaneously bind Cr(III) to more readily create a chelate complex with a bidentate ligand. Polydentate complexes are more stable than their analogous monodentate complex.[28] The data suggests that for heptapeptides with an acidic residue near the C-terminus simultaneous binding of Cr(III) to carboxylic acid groups at the C-terminus and at a sidechain increases proton transfer efficiency and leads to a greater extent of protonation than for heptapeptides with the acidic residue located away from the C-terminus.

Table 3.1. ESI results containing absolute intensities of peptides studied with and without Cr(III).

Peptide Name	Peptide Sequence	No Cr(III), A.I[a] x 10^6			Cr(III), A.I x 10^6				
		$[M + H]^+$	$[M + 2H]^{2+}$	$[M + 2H]^{2+}$ to $[M + H]^+$ Ratio	$[M + H]^+$	$[M + 2H]^{2+}$	$[M + Cr]^{3+}$	$[M + Cr - H]^{2+}$	$[M + 2H]^{2+}$ to $[M + H]^+$ Ratio
EA6	EAAAAAA	17 ± 6[b]	0	-[c]	1.0 ± 0.1	1.9 ± 0.1	0.3 ± 0.0	1.4 ± 0.1	2 ± 0
A3EA3	AAAEAAA	17 ± 1	0	-	2.4 ± 0.5	14 ± 0	4.9 ± 0.8	8.2 ± 1.2	6 ± 1
A6E	AAAAAAE	14 ± 5	0	-	0.7 ± 0.3	5.5 ± 2.3	1.7 ± 0.4	0.9 ± 0.1	8 ± 0
DA6	DAAAAAA	1.9 ± 0.8	0	-	0.1 ± 0.1	0.6 ± 0.2	0.2 ± 0.0	0.4 ± 0.0	6 ± 1
A3DA3	AAADAAA	13 ± 1	0	-	1.1 ± 0.5	4.7 ± 1.5	1.2 ± 0.3	3.4 ± 1.4	4 ± 1
A6D	AAAAAAD	0.5 ± 0.2	0	-	0.1 ± 0.1	0.4 ± 0.5	0.3 ± 0.0	0.4 ± 0.0	7 ± 1
YA6	YAAAAAA	3.0 ± 0.4	0	-	0.3 ± 0.1	1.4 ± 0.6	0.7 ± 0.1	0.76 ± 0.04	5 ± 1
pYA7	pYAAAAAAA	0	0	-	0	0	0	0	-
EDDpYDEEN	EDDpYDEEN	0.6 ± 0.2	0	-	0	0	0.44 ± 0.06	0.30 ± 0.01	-
A3PA3	AAAPAAA	15 ± 4	0.15 ± 0.02	0.01 ± 0.00	1.1 ± 0.5	4.5 ± 1.1	0.7 ± 0.0	1.0 ± 0.2	3 ± 1
A7-OH	AAAAAAA-OH	7.3 ± 1.3	0	-	1.1 ± 0.4	3.7 ± 1.3	1.1 ± 0.3	0.9 ± 0.3	3 ± 1
A7-NH_2	AAAAAAA-NH_2	45 ± 5	0	-	0.24 ± 0.04	1.4 ± 0.3	0.89 ± 0.03	0.76 ± 0.03	5 ± 1

[a]AI = absolute intensity

[b]Mean +/- one standard deviation from three independent replicates

[c] "-" signifies that the ratio is unable to be calculated due to lack of signal for the 2+ ion.

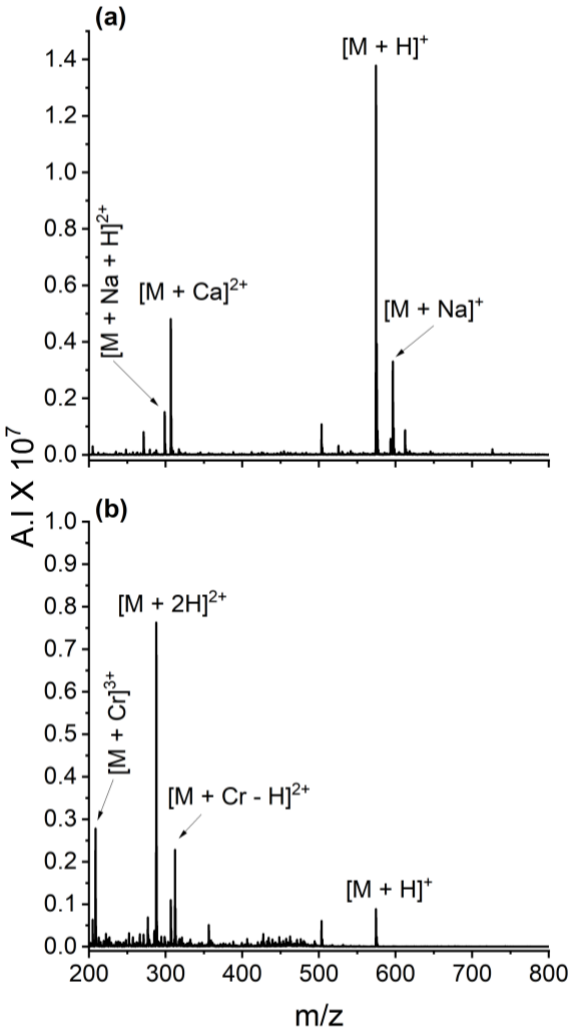

Figure 3.1. ESI mass spectra of A6E with (a) no Cr(III) and (b) Cr(III) at a 1:10 peptide-to-Cr(III) molar ratio.

3.3.2 The role of the carboxyl group in enhanced protonation by Cr(III)

The importance of carboxylic acids groups to the mechanism of enhanced protonation using Cr(III) was further studied. Methyl esterification of model peptides A7, AAVAAAA, and AAIAAAA (i.e., converting -OH to -OCH_3) was completed in a prior study to investigate the role of carboxylic acid groups in the mechanism for Cr(III) enhanced protonation.[15] Methylated peptides did not exhibit any enhanced protonation with Cr(III), which confirms the involvement of the carboxylic acid group in the mechanism. The model peptide A3EA3 contains a carboxylic acid group at both the C-terminus and sidechain of the glutamic acid residue. Methylation of one carboxylic acid group and the addition of Cr(III) to the peptide solution produces $[M + 2H]^{2+}$ that is not formed in the absence of Cr(III). However, methylation of both carboxylic acid groups yields no $[M +2H]^{2+}$, Figure 3.2.

The peptide A3EA3-NH_2 was custom synthesized to study the effects of the location of the carboxylic group by converting the C-terminus to an amide so that the only carboxylic acid group is at the central sidechain of glutamic acid (E). Addition of Cr(III) to solutions containing A3EA3-NH_2 results in the formation of $[M + 2H]^{2+}$, which are not observed in the absence of Cr(III), as shown in Figure 3.3. The enhance protonation of A3EA3-NH_2 with Cr(III) provides further evidence that either (1) the carboxylic acid group does not need to be located at the C-terminus and/or (2) amide groups can facilitate enhanced protonation.

A collaboration with the Dixon, Vincent, and Cassady groups utilized experimental and computational methods to deduce a mechanism to describe enhanced protonation with Cr(III).[29] The proposed mechanism involves the coordination of a carboxylate with a Cr(III)-hexaaqua complex, which facilitates proton transfer. Figure 3.4 illustrates the process of forming the peptide-metal complex. Cr(III) exists as a hexaaqua complex, $[Cr(H_2O)_6]^{3+}$, in solution. During

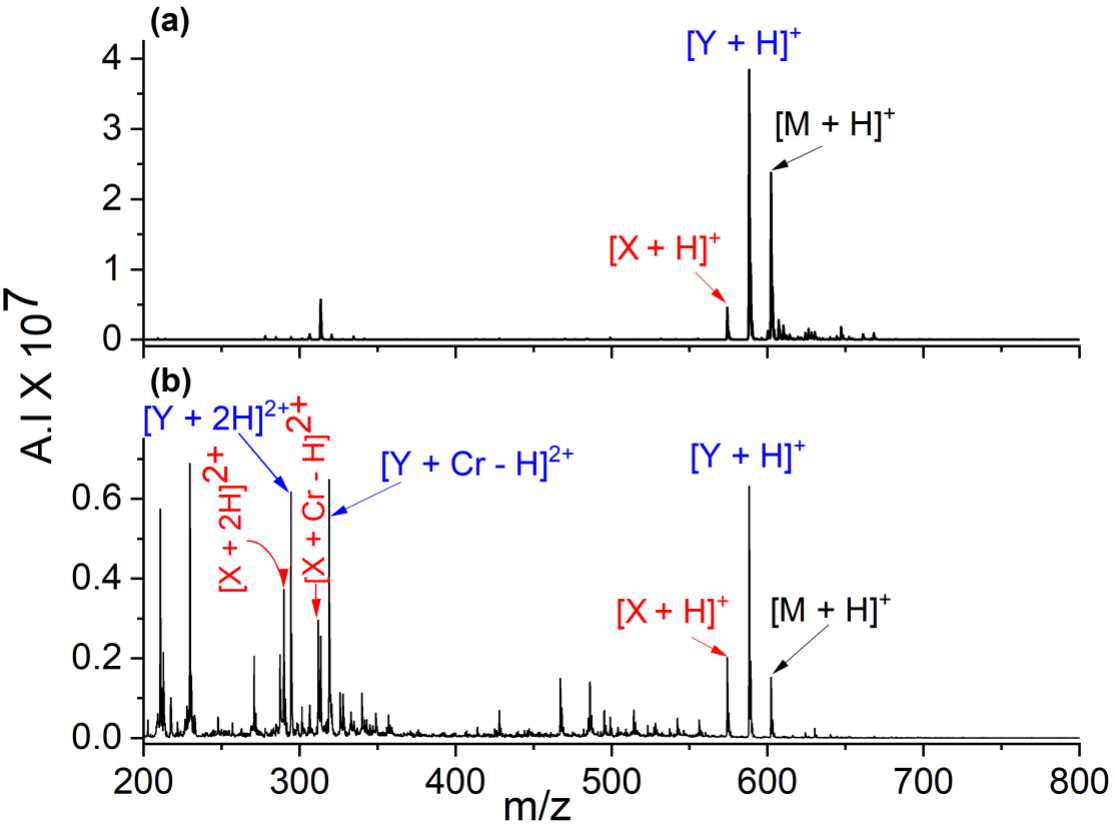

Figure 3.2. ESI mass spectra of A3EA3 after methyl esterification using (a) no Cr(III) and (b) with Cr(III) in a 1:10 peptide-to-Cr(III) molar ratio. A3EA3 with both carboxylic acid groups methylated is represented by M, one carboxylic acid group methylated is Y, and free acid A3EA3 is X.

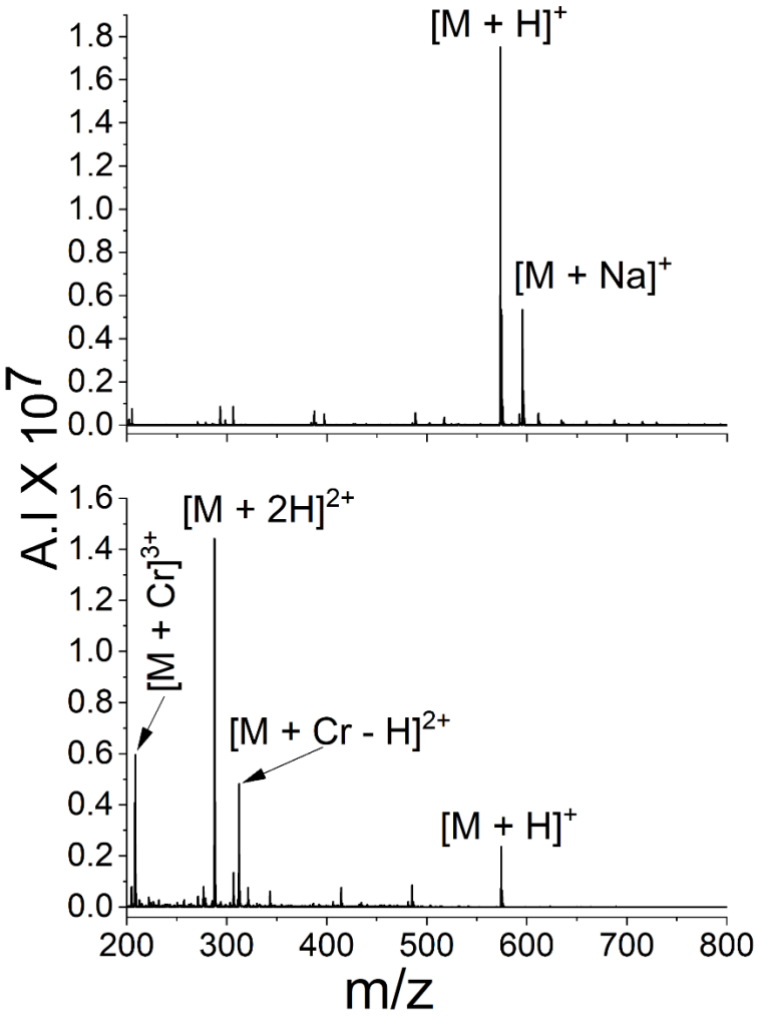

Figure 3.3. ESI spectra of AAAEAAA-NH_2 with (a) no Cr(III) and (b) Cr(III) in a 1:10 peptide-to-Cr(III) molar ratio.

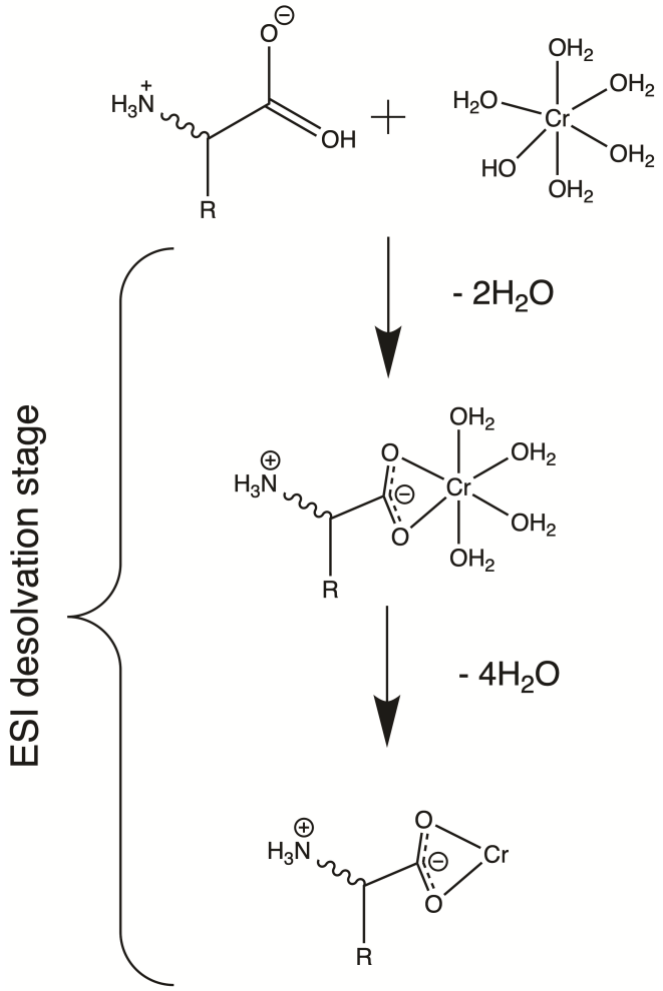

Figure 3.4. Formation of Cr(III)-peptide complex in ESI during desolvation.

the desolvation stage, water ligands are stripped from the complex. Peptide zwitterions bind to Cr(III) after the removal of two water ligands to form a peptide-metal complex, $[Cr(peptide)(H_2O)_4]^{3+}$. The direct binding of Cr(III) to the peptide is experimentally observed in the formation of Cr(III) adducts by ESI. A carboxylic acid group located at a sidechain or the C-terminus coordinates to Cr(III) as the remaining water ligands are removed from the complex. Electronic structure calculations at the density functional theory (DFT) level were performed by Dr. Rudradatt Persaud of the Dixon group to predict the energetics of the Cr(III) complex.[29] As the complex loses water the acidity of the complex increases drastically. The pK_a of the Cr(III) complex with one water molecule attached reaches -84.7. Protons produced by the highly acidic environment are transferred to basic sites on the peptide. The final step in the mechanism involves the dissociation of Cr(III) from the protonated peptide ion. Cr(III) can make the proton transfer process more efficient by increasing the signal intensity of protonated ions or adding on additional protons to increase charge state.

ESI mass spectra for A7-NH_2 with and without Cr(III) are presented in Figure 3.5. A7-NH_2 does not have a carboxylic acid group and exclusively produces $[M + H]^+$ by ESI in the absence of Cr(III). Addition of Cr(III) results in the formation of $[M + 2H]^{2+}$, which was unexpected. The ratio of 2+ to 1+ for A7-NH2 is 6:1 compared to 3:1 for A7-OH, as summarized in Table 3.1. The C-terminal amide group may be playing a similar role to the carboxyl group in the mechanism. Amide nitrogens have been reported to coordinate metal ions[30] and can also deprotonate in the gas phase.[31-33] In the case of A7-NH_2, which does not have a carboxylic acid group, the amide nitrogen can deprotonate and function as site of Cr(III) coordination to the peptide. The gas-phase acidity of alanine is 334.6 kcal/mol[34] compared to 351.1 kcal/mol[32] for its amide, and both molecules can deprotonate to form $[M - H]^-$ by ESI.

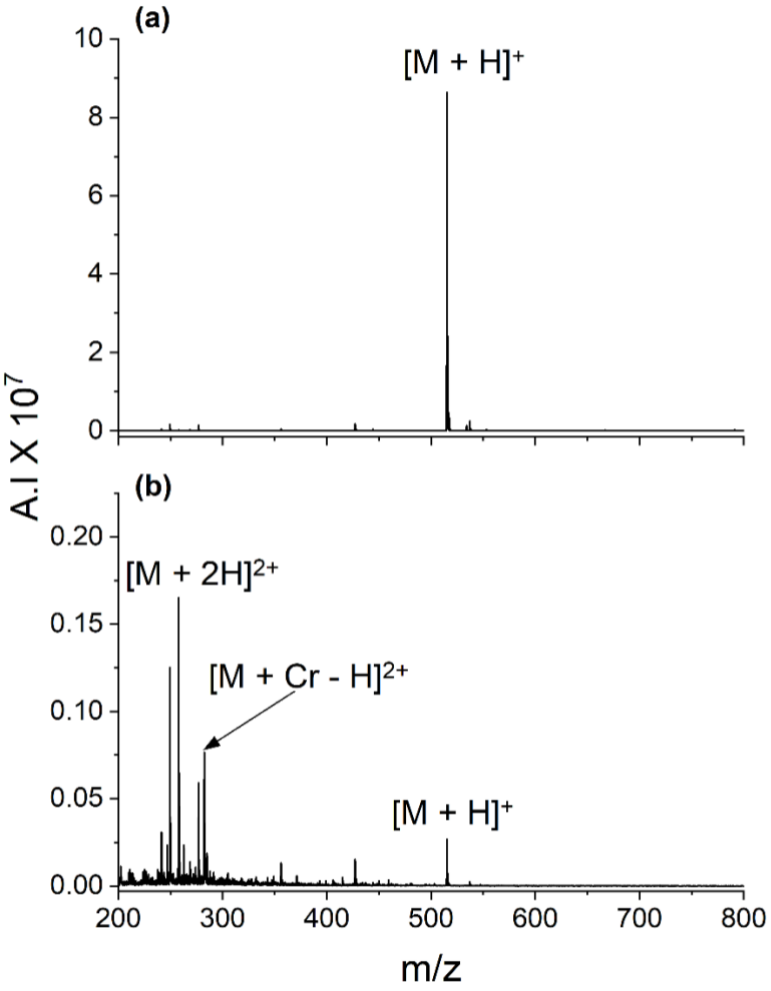

Figure 3.5. ESI spectra of AAAAAAA-NH_2 with (a) no Cr(III) and (b) Cr(III) in a 1:10 peptide-to-Cr(III) molar ratio.

3.3.3 Effects of residue identity

The amino acid composition of a protein dictates its complexity in terms of functionality and structure. Proline (P) is unique in that it is the only common amino acid residue that has its sidechain cyclized onto the backbone amide nitrogen. This cyclization results in a restricted torsion angle for the N-Cα bond of proline and can lead to kinks and bends in α-helices.[35] The structure of proline is provided in Figure 2.12, Section 2.8. Kinks due to proline residues account for ~60% of helix deformations.[36] In peptide sequencing by collision-induced dissociation (CID) MS, the presence of a proline residue causes selective cleavage to occur N-terminal to the proline residue. Intense y_n^+, which is indicative of cleavage at the amide bond N-terminal to proline, dominates the CID spectrum. This preferential cleavage is termed the "proline effect".[37-40] Because of the distinctive properties of proline, the ability of Cr(III) to enhance the protonation of peptides can potentially be impacted by the presence of proline. Figure 3.6 shows mass spectra for A3PA3 without additives, with 1% (by volume) acetic acid, and with Cr(III). Without any additives, A3PA3 forms abundant $[M + H]^+$ and a minute amount of $[M + 2H]^{2+}$ by ESI, Figure 3.6(a). The ratio of 2+ to 1+ ions is 0.01:1. Addition of acetic acid quadruples the intensity of $[M + 2H]^{2+}$ and results in nearly a 1:1 ratio for +2 to +1 ions, Figure 3.6(b). Peptide solutions containing Cr(III) generated the largest 2+ to 1+ ratio of 4:1, Figure 3.6(c). The presence of Cr(III) in peptide solutions causes a 30-fold increase in the absolute intensity of $[M + 2H]^{2+}$ for A3PA3; however, these results are comparable to those of heptaalanine (A7), Table 3.1. Thus, proline residues seem to have negligible impact on the use of Cr(III) to enhance protonate peptides.

The aromatic amino acids tyrosine (Y), tryptophan (W), and phenylalanine (F) can participate in non-covalent π-π interactions that lead to π stacking of biomolecules.[41,42] These

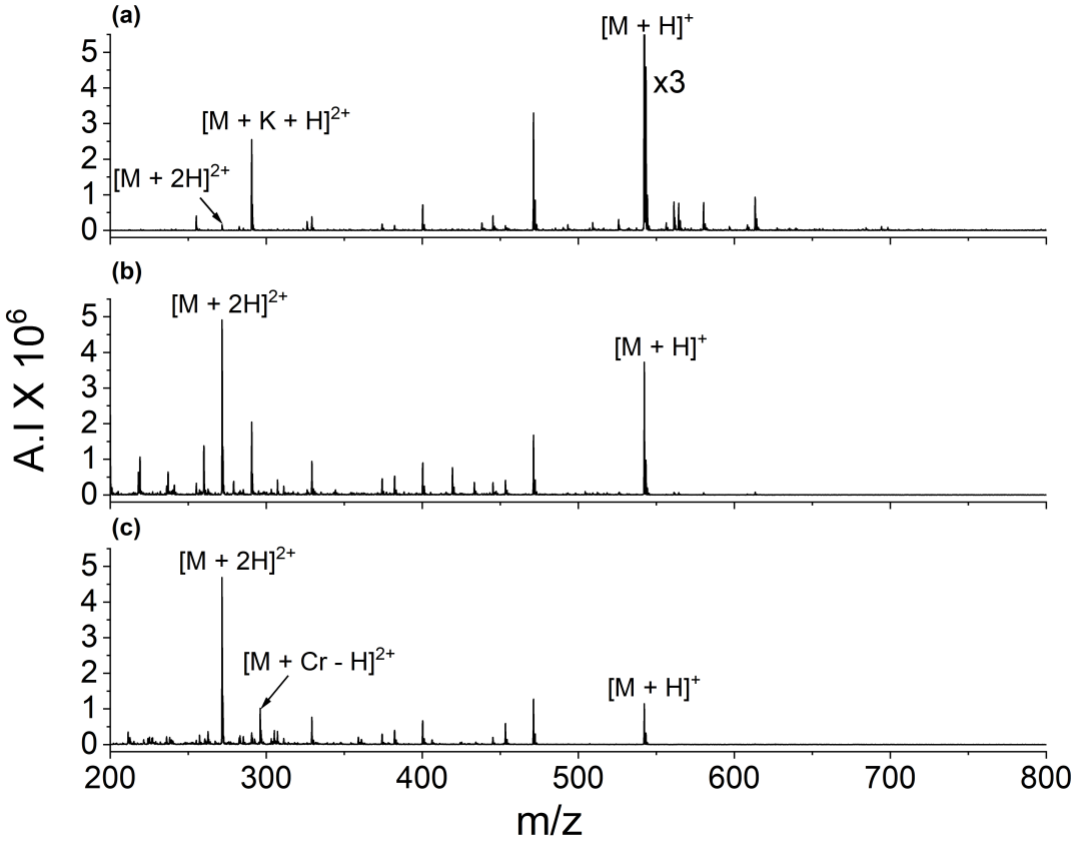

Figure 3.6. ESI mass spectra of AAAPAAA with (a) no Cr(III), (b) 1% acetic acid, and (c) Cr(III) in a 1:10 peptide-to-Cr(III) molar ratio.

amino acids can also make contributions to cation- π interactions with alkali metals.[43-48] There is potential for the π system of tyrosine to help stabilize the interaction between the Cr(III)-aqua complex and the peptide in order for proton transfer to occur. In addition, the phenolic acid chain of tyrosine can serve as an acidic deprotonation site for ESI-MS.[49] The peptide YA6 was synthesized to determine the impact of tyrosine compared to A7. Mass spectra for YA6 are shown in Figure 3.7. In the absence of Cr(III), $[M + 2H]^{2+}$ is not observed for YA6, Figure 3.7(a). The addition of Cr(III) leads to the formation of the doubly protonated ion, Figure 3.7(b). The ratio of 2+ to 1+ for YA6 is the same (4:1) as that of A7. Therefore, although the presence of the π system tyrosine residue may allow for cation-π interactions, it does not appreciably improve the efficiency of proton transfer involving Cr(III) when compared to a peptide with only alanine residues (i.e., only the C-terminus to coordinate to Cr(III)).

Phosphorylation of the hydroxy groups on the sidechains of tyrosine (Y), serine (S), or threonine (T) is a common post-translational modification for peptides and proteins. Phosphopeptides play a role in regulating gene expression and protein synthesis as well as in signaling pathways.[50] Compared to their non-phosphorylated counterparts, phosphopeptides are about 13 to 27 kcal/mol more acidic.[51] The acidic nature of the phosphopeptides contributes to their difficulty in producing protonated ions by ESI and potentially makes them a good candidate for enhanced protonation with Cr(III). The peptides pYA7 and EDDpYDEEN produced little to no protonated ions with and without Cr(III), as shown in the data of Table 3.1. Mass spectra of EDDpYDEEN are presented in Figure 3.8. The inability of Cr(III) to enhance the protonation of phosphopeptides could be a result of Cr(III) forming insoluble salts with phosphates in solution.[52] Cr(III) has been shown to bind DNA[53,54] along the phosphate backbone as well as ATP.[55] Zhitkovich and coworkers noticed a decrease in Cr(III)-DNA binding in the

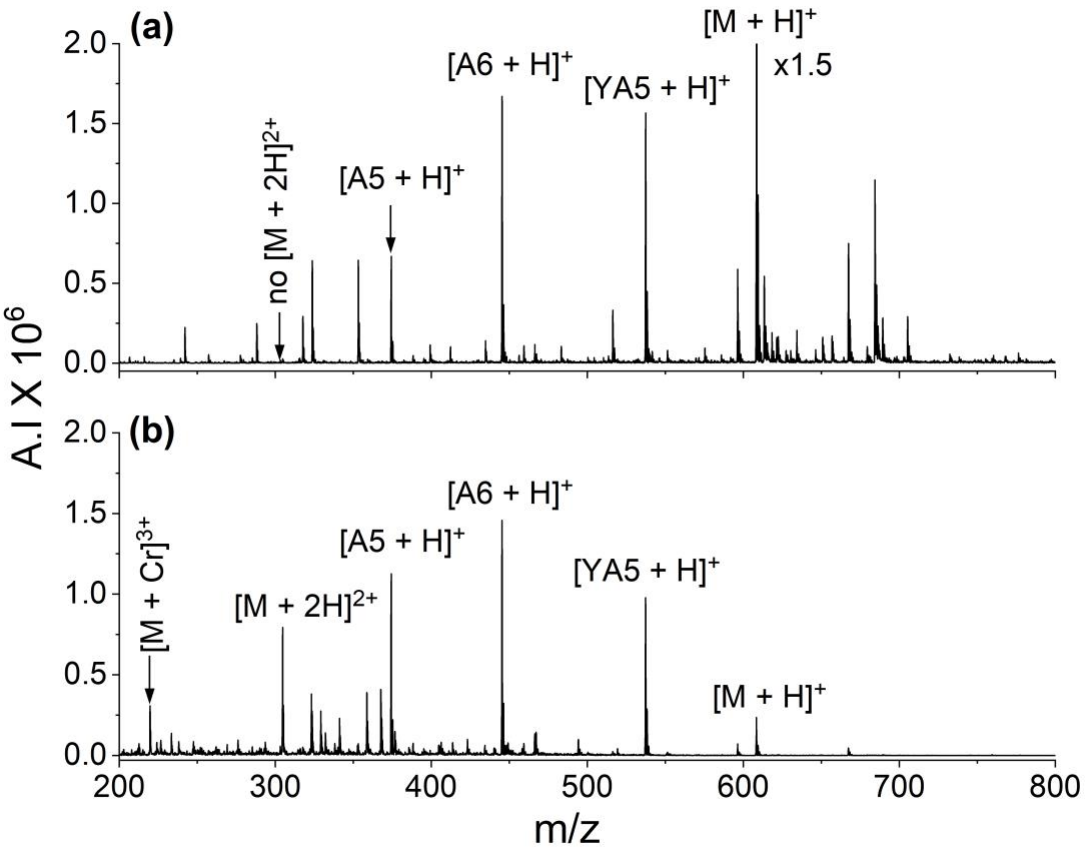

Figure 3.7. ESI mass spectra of YA6 with (a) no Cr(III) and (b) Cr(III) in a 1:10 peptide-to-Cr(III) molar ratio. The peptide was synthesized in the Cassady lab using solid-phase chemistry with no further purification steps, which accounts for impurities in the mass spectra. No $[M + 2H]^{2+}$ is present for A5, A6, and YA5, which is consistent with a previous study that revealed Cr(III) enhances protonation peptides with seven or more amino acid residues.[15]

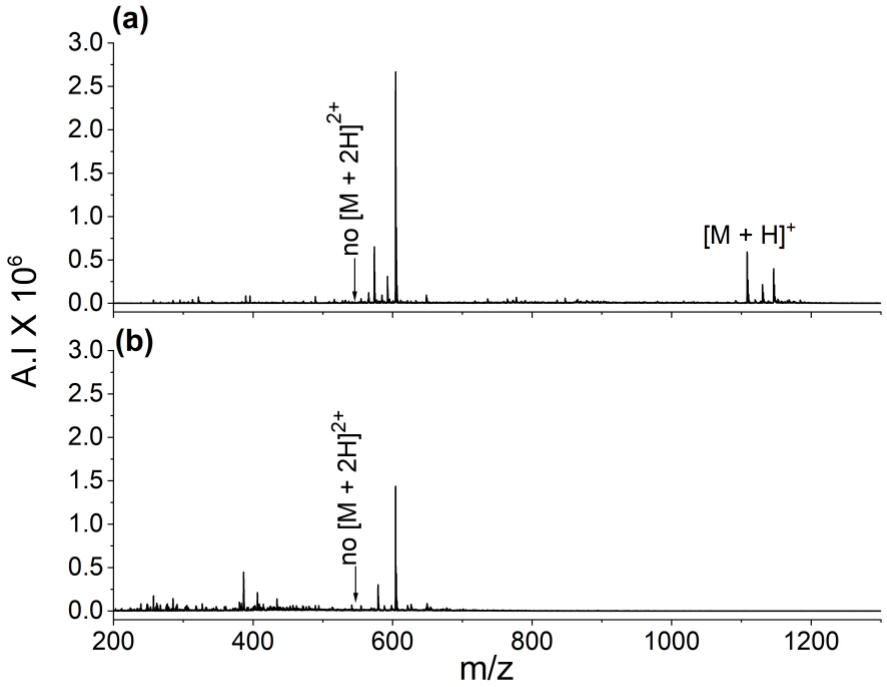

Figure 3.8. ESI mass spectra of for the biological phosphopeptide EDDpYDEEN with (a) no Cr(III) and (b) Cr(III) in a 1:10 peptide-to-Cr(III) molar ratio. Note the total absence of peptide ions when Cr(III) is added to the solution of part (b).

presence of inorganic phosphate buffer.[54] They attributed it to the coordination of Cr(III) to the ionized phosphate oxygen, which may have precipitated out of solution due to Cr(III) phosphate's low solubility. The Cr(III) adducts, $[M + Cr]^{3+}$ and $[M + Cr - H]^{2+}$, are present in the mass spectrum of EDDpYDEEN with Cr(III). This implies that the phospho group binds Cr(III) to the peptide. The possibility exists that Cr(III)-phospho binding is strong enough to inhibit proton transfer by not allowing for the dissociation of Cr(III) from the peptide after complex formation. In this dissertation research, no visible precipitation of a phosphate salt was observed, but this could be attributed to the low concentrations (i.e., micromolar range) being used.

3.3.4 Effect of peptide size

The proteins myoglobin, cytochrome c, and ubiquitin were employed to determine the effect of Cr(III) on the analysis of protein solutions. Previously, Cr(III) was reported to have no effect on the protonation of myoglobin and cytochrome c when added in a 1:10 protein-to-Cr(III) molar ratio.[15] Compared to peptides, proteins possess a myriad of amino acid sidechains with varying functional groups that may tie up Cr(III) and, thus, more Cr(III) may be needed to observe an effect. To test this hypothesis the concentration of Cr(III) was increased for the protein solutions.

Figure 3.9 illustrates the effects of adding Cr(III) in a 1:300 peptide-to-Cr(III) molar ratio to solutions containing cytochrome c. Cytochrome c is a highly conserved protein (i.e., few historical mutations) with 104 amino acids and a molecular mass of ~12 kDa. Without Cr(III), the $[M + nH]^{n+}$ charge states observed are between 10+ and 17+ with the distribution centered at 12+, as shown in Figure 3.9(a). Adding 1% acetic acid increases the maximum charge state to 20+ and shifts the distribution to center around 16+, Figure 3.9(b). Addition of Cr(III) in a 1:300

protein to Cr(III) molar ratio also increases the charge state to 20+ and shifts the center of the distribution to 15+, Figure 3.9(c). Acetic acid increased the overall absolute intensity by 900%, whereas Cr(III) increases the absolute intensity by 33%. Figure 3.10 demonstrates the result of Cr(III) on solutions containing myoglobin. Myoglobin is a heme protein with a mass of ~18 kDa that forms charge states between 12+ and 22+ by ESI, Figure 3.10(a). The distribution is centered around 16+. As shown in Figure 3.10(b), addition of 1% acetic acid increases the maximum charge state to 27 + and shifts the distribution center to 23+. Addition of Cr(III) increases the maximum charge state to 25+ and the distribution centers around 21+, Figure 3.10(c). Both acid and Cr(III) increases the absolute intensity for myoglobin. Cr(III) also increases the maximum charge state for ubiquitin (~8.5 kDa) from 12+ to 13+ and shifts the distribution center from 9+ to 11+, Figure 3.11. The overall absolute intensity of the protonated ions increases with the addition of Cr(III). The three proteins all form $[M + Cr + nH]^{n+}$ signifying the direct binding of Cr(III) to the protein in the gas phase.

Table 3.2. pH of protein solutions undergoing ESI.

Peptide	pH			
	No additives	With 1% acetic acid	1:10 protein-to-Cr(III)	1:300 protein-to-Cr(III)
Cytochrome c	6.23	2.98	6.07	4.20
Myoglobin	5.73	3.21	5.82	4.50
Ubiquitin	5.20	3.18	5.28	4.25

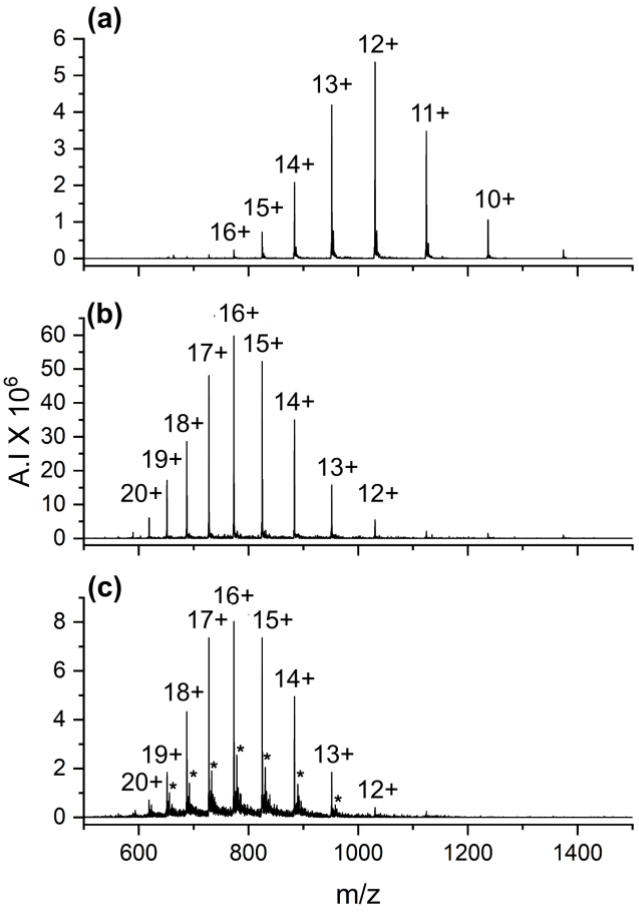

Figure 3.9. ESI spectra of cytochrome c with (a) no Cr(III), (b) 1% acetic acid, and (c) Cr(III) in a 1:300 peptide-to-Cr(III) molar ratio. Protonated protein ions are labeled with their charge. Cr(III) adducted protein ions are labeled with an asterisk.

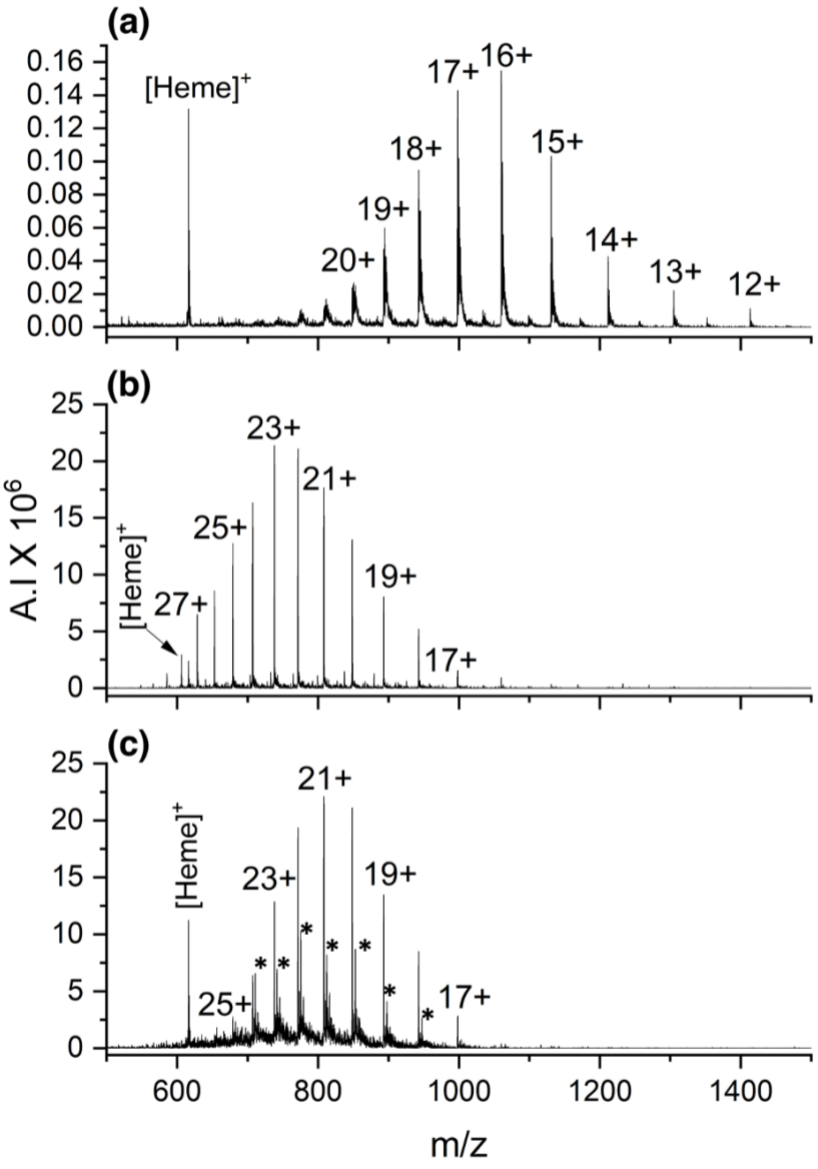

Figure 3.10. ESI spectra of myoglobin with (a) no Cr(III), (b) 1% acetic acid, and (c) Cr(III) in a 1:300 peptide-to-Cr(III) molar ratio. Protonated protein ions are labeled with their charge. Cr(III) adducted protein ions are labeled with an asterisk.

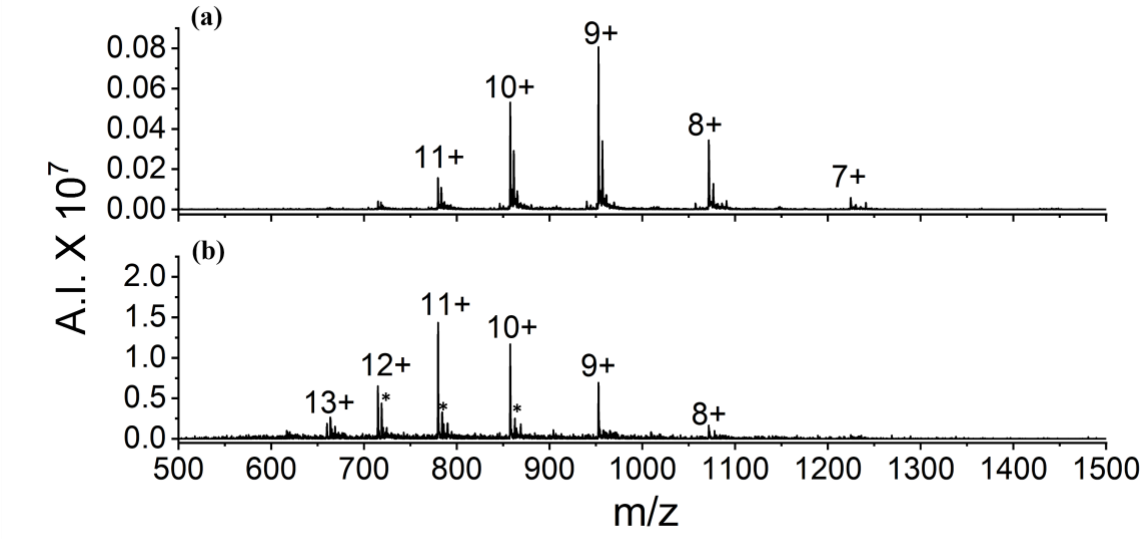

Figure 3.11. ESI mass spectra of ubiquitin with (a) no Cr(III) and (b) Cr(III) in a 1:300 peptide-to-Cr(III) molar ratio. Protonated protein ions are labeled with their charge. Cr(III) adducted protein ions are labeled with an asterisk.

These results show that Cr(III) can be used to increase protonation of proteins by ESI; however, pH measurements reveal that the increase in protonation is caused by a pH effect similar to adding acetic acid. Table 3.2 contains pH values for the protein solutions with no additives, 1% acetic acid, 1:10, and 1:300 protein-to-Cr(III) molar ratio. Adding Cr(III) in a 1:10 protein-to-Cr(III) molar ratio does not change the pH of the solution. At a 1:300 protein-to-Cr(III) molar ratio a decrease in pH is seen. This is consistent with the pH effect of adding 1% acetic acid. Though metal adducts are seen alongside the protonated protein ions, the increase in protonation seems to be a pH effect rather than Cr(III)-inducing enhanced protonation. For this reason, Cr(III) is more beneficial for peptide analysis by ESI than for protein analysis. Proteins benefit most from organic supercharging reagents, which may denature the protein to assist in protonation.[14,56,57]

3.4 Conclusions

Addition of Cr(III) to peptide solutions undergoing ESI increases protonation and often produces additional ion charge states for acidic and neutral peptides. Carboxylic acid groups were shown to be a key factor in the mechanism of protonation induced by Cr(III). Carboxylic acid groups located at the sidechains of glutamic and aspartic acid residues and at the C-terminus can participate in coordinating the metal ion to the peptide to create a Cr(III)-peptide bridge that facilitates proton transfer to a basic site on the peptide. Proton transfer is more efficient when two carboxylic acid groups are located near each other, which further emphasizes the importance of these groups in metal coordination. Peptide amides can also enhance protonation with Cr(III), perhaps by coordinating the metal to the carbonyl oxygen and amide nitrogen. Regardless of

whether Cr(III) is binding to a carboxyl or an amide group, desolvation of the Cr(III)-peptide complex results in a highly acidic environment that enables additional charges to be added to the peptide.

The extent of protonation is affected by size, the identity of amino acid residues present, and the presence of carboxylic acid and amide groups. Acidic residues effect enhanced protonation the most due to their sidechains having a carboxyl group. Phosphorylated peptides did not undergo enhanced protonation with the addition of Cr(III), which is believed to be caused by strong Cr(III) binding to the phosphate group, perhaps resulting in precipitation of a phosphate salt. Higher concentrations of Cr(III) are needed to increase the maximum charge state observed by ESI and shift the charge distribution for proteins, but this was found to be consistent with a pH effect as opposed to a Cr(III)-complexation effect. The presence of Cr(III) adducts and other impurities from the Cr(III) solution decreases the signal-to-noise (S/N) ratio in protein analysis. This suggests that Cr(III) is more suitable for peptide analysis, whereas proteins benefit more from organic supercharging reagents.[12,13,15,58]

References

1. Fenn, J. B.; Mann, M.; Meng, C. K.; Wong, S. F.; Whitehouse, C. M. Electrospray Ionization-Principles and Practice. *Mass Spectrom. Rev.* **1990**, *9*, 37-70.

2. Iavarone, A. T.; Paech, K.; Williams, E. R. Effects of Charge State and Cationizing Agent on the Electron Capture Dissociation of a Peptide. *Anal. Chem.* **2004**, *76*, 2231-2238.

3. Rožman, M.; Gaskell, S. J. Charge State Dependent Top-Down Characterisation using Electron Transfer Dissociation. *Rapid Commun. Mass Spectrom.* **2012**, *26*, 282-286.

4. Madsen, J. A.; Brodbelt, J. S. Comparison of Infrared Multiphoton Dissociation and Collision-Induced Dissociation of Supercharged Peptides in Ion Traps. *J. Am. Soc. Mass Spectrom.* **2009**, *20*, 349-358.

5. Wells, J. M.; Stephenson Jr., J. L.; McLuckey, S. A. Charge Dependence of Protonated Insulin Decompositions. *Int. J. Mass Spectrom.* **2000**, *203*, A1-A9.

6. Flick, T. G.; Donald, W. A.; Williams, E. R. Electron Capture Dissociation of Trivalent Metal Ion-Peptide Complexes. *J. Am. Soc. Mass Spectrom.* **2013**, *24*, 193-201.

7. Liu, J.; McLuckey, S. A. Electron Transfer Dissociation: Effects of Cation Charge State on Product Partitioning in Ion/Ion Electron Transfer to Multiply Protonated Polypeptides. *Int. J. Mass Spectrom.* **2012**, *330-332*, 174-181.

8. Riley, N. M.; Coon, J. J. The Role of Electron Transfer Dissociation in Modern Proteomics. *Anal. Chem.* **2018**, *90*, 40-64.

9. Zhurov, K. O.; Fornelli, L.; Wodrich, M. D.; Laskay, U. A.; Tsybin, Y. O. Principles of Electron Capture and Transfer Dissociation Mass Spectrometry Applied to Peptide and Protein Structure Analysis. *Chem. Soc. Rev.* **2013**, *42*, 5014-5030.

10. Zubarev, R. A.; Kelleher, N. L.; McLafferty, F. W. Electron Capture Dissociation of Multiply Charged Protein Cations. A Nonergodic Process. *J. Am. Chem. Soc.* **1998**, *120*, 3265-3266.

11. Zubarev, R. A.; Horn, D. M.; Fridriksson, E. K.; Kelleher, N. L.; Kruger, N. A.; Lewis, M. A.; Carpenter, B. K.; McLafferty, F. W. Electron Capture Dissociation for Structural Characterization of Multiply Charged Protein Cations. *Anal. Chem.* **2000**, *72*, 563-573.

12. Iavarone, A. T.; Jurchen, J. C.; Williams, E. R. Supercharged Protein and Peptide Ions Formed by Electrospray Ionization. *Anal. Chem.* **2001**, *73*, 1455-1460.

13. Lomeli, S. H.; Peng, I. X.; Yin, S.; Ogorzalek Loo, R. R.; Loo, J. A. New Reagents for Increasing ESI Multiple Charging of Proteins and Protein Complexes. *J. Am. Soc. Mass Spectrom.* **2010**, *21*, 127-131.

14. Sterling, H. J.; Kintzer, A. F.; Feld, G. K.; Cassou, C. A.; Krantz, B. A.; Williams, E. R. Supercharging Protein Complexes from Aqueous Solution Disrupts their Native Conformations. *J. Am. Soc. Mass Spectrom.* **2012**, *23*, 191-200.

15. Feng, C.; Commodore, J. J.; Cassady, C. J. The use of Chromium(III) to Supercharge Peptides by Protonation at Low Basicity Sites. *J. Am. Soc. Mass Spectrom.* **2015**, *26*, 347-358.

16. Commodore, J. J.; Jing, X.; Cassady, C. J. Optimization of Electrospray Ionization Conditions to Enhance Formation of Doubly Protonated Peptide Ions with and without Addition of Chromium(III). *Rapid Commun. Mass Spectrom.* **2017**, *31*, 1129-1136.

17. Jing, X.; Edwards, K. C.; Vincent, J. B.; Cassady, C. J. The use of Chromium(III) Complexes to Enhance Peptide Protonation by Electrospray Ionization Mass Spectrometry. *J. Mass Spectrom.* **2018**, *53*, 1198-1206.

18. Drljaca, A.; Spiccia, L. Early Stages of the Hydrolysis of Chromium(III) in Aqueous Solution. XII. Kinetics of Cleavage of the Trimer and Tetramer in Acidic Solution. *Polyhedron* **1996**, *15*, 4373-4385.

19. Taube, H. Rates and Mechanisms of Substitution in Inorganic Complexes in Solution. *Chem. Rev.* **1952**, *50*, 69-126.

20. Aksoy, M. S.; Oezer, U. Potentiometric and Spectroscopic Studies with Chromium(III) Complexes of Hydroxysalicylic Acid Derivatives in Aqueous Solution. *Turk. J. Chem.* **2003**, *27*, 667-673.

21. Gao, J.; Cassady, C. J. Negative Ion Production from Peptides and Proteins by Matrix-Assisted Laser Desorption/Ionization Time-of-Flight Mass Spectrometry. *Rapid Commun. Mass Spectrom.* **2008**, *22*, 4066-4072.

22. Huzarska, M.; Ugalde, I.; Kaplan, D. A.; Hartmer, R.; Easterling, M. L.; Polfer, N. C. Negative Electron Transfer Dissociation of Deprotonated Phosphopeptide Anions: Choice of Radical Cation Reagent and Competition between Electron and Proton Transfer. *Anal. Chem.* **2010**, *82*, 2873-2878.

23. Chan, W. C.; White, P. D. *Fmoc Solid Phase Peptide Synthesis A Practical Approach;* Oxford University Press Inc.: New York, 2000.

24. Greene, T. W.; Wuts, P. G. M., Eds.; In *Protective Groups in Organic Synthesis;* John Wiley & Sons, Inc.: New York, 1991.

25. Commodore, J. J.; Cassady, C. J. The Effects of Trivalent Lanthanide Cationization on the Electron Transfer Dissociation of Acidic Fibrinopeptide B and its Analogs. *J. Am. Soc. Mass Spectrom.* **2016**, *27*, 1499-1509.

26. Cao, X.; Hu, X.; Zhang, X.; Gao, S.; Ding, C.; Feng, Y.; Bao, W. Identification of Metal Ion Binding Sites Based on Amino Acid Sequences. *PloS one* **2017**, *12*, e0183756.

27. Ivan, D.; Mile, S.; Sanja, T. Metals in Proteins: Correlation between the Metal-Ion Type, Coordination Number and the Amino-Acid Residues Involved in the Coordination. *Acta Crystallogr. D* **2008**, *64*, 257-263.

28. Martell, A. E. Chapter 19: The Chelate Effect. *Werner Centennial;* American Chemical Society: Washington, DC, 1967; Vol. 62, pp 272-294.

29. Persaud, R. R.; Dieke, N. E.; Jing, X.; Lambert, S.; Parsa, N.; Hartmann, E.; Vincent, J. B.; Cassady, C. J.; Dixon, D. A. Mechanistic Study of Enhanced Protonation by Chromium(III) in Electrospray Ionization: A Superacid Bound to a Peptide. *J. Am. Soc. Mass Spectrom.* **2020**, *31*, 308-318.

30. Sigel, H.; Martin, R. B. Coordinating Properties of the Amide Bond. Stability and Structure of Metal Ion Complexes of Peptides and Related Ligands. *Chem. Rev.* **1982**, *82*, 385-426.

31. Bokatzian-Johnson, S. S.; Stover, M. L.; Dixon, D. A.; Cassady, C. J. A Comparison of the Effects of Amide and Acid Groups at the C-Terminus on the Collision-Induced Dissociation of Deprotonated Peptides. *J. Am. Soc. Mass Spectrom.* **2012**, *23*, 1544-1557.

32. Plummer, C. E.; Stover, M. L.; Bokatzian, S. S.; Davis, J. T. M.; Dixon, D. A.; Cassady, C. J. An Experimental and Computational Study of the Gas-Phase Acidities of the Common Amino Acid Amides. *J. Phys. Chem. B* **2015**, *119*, 9661-9669.

33. Li, Z.; Matus, M. H.; Velazquez, H. A.; Dixon, D. A.; Cassady, C. J. Gas-Phase Acidities of Aspartic Acid, Glutamic Acid, and their Amino Acid Amides. *Int. J. Mass Spectrom.* **2007**, *265*, 213-223.

34. Stover, M. L.; Jackson, V.; Matus, M.; Adams, M.; Cassady, C. J.; Dixon, D. A. Fundamental Thermochemical Properties of Amino Acids: Gas-Phase and Aqueous Acidities and Gas-Phase Heats of Formation. *J. Phys. Chem. B* **2012**, *116*, 2905-2916.

35. Reiersen, H.; Rees, A. R. The Hunchback and its Neighbours: Proline as an Environmental Modulator. *Trends Biochem. Sci.* **2001**, *26*, 679-684.

36. Yohannan, S.; Faham, S.; Yang, D.; Whitelegge, J. P.; Bowie, J. U. The Evolution of Transmembrane Helix Kinks and the Structural Diversity of G Protein-Coupled Receptors. *Proc. Natl. Acad. Sci. U. S. A.* **2004**, *101*, 959-963.

37. Schwartz, B. L.; Bursey, M. M. Some Proline Substituent Effects in the Tandem Mass Spectrometry of Protonated Pentaalanine. *Biol. Mass Spectrom.* **1992**, *21*, 92-96.

38. Vaisar, T.; Urban, J. Probing the Proline Effect in CID of Protonated Peptides. *J. Mass Spectrom.* **1996**, *31*, 1185-1187.

39. Grewal, R. N.; El Aribi, H.; Harrison, A. G.; Siu, K. W. M.; Hopkinson, A. C. Fragmentation of Protonated Tripeptides: The Proline Effect Revisited. *J. Phys. Chem. B* **2004**, *108*, 4899-4908.

40. Reid, G. E.; Wu, J.; Chrisman, P. A.; Wells, J. M.; McLuckey, S. A. Charge-State-Dependent Sequence Analysis of Protonated Ubiquitin Ions Via Ion Trap Tandem Mass Spectrometry. *Anal. Chem.* **2001**, *73*, 3274-3281.

41. Serrano, L.; Bycroft, M.; Fersht, A. R. Aromatic-Aromatic Interactions and Protein Stability: Investigation by Double-Mutant Cycles. *J. Mol. Biol.* **1991**, *218*, 465-475.

42. Burley, S.; Petsko, G. Aromatic-Aromatic Interaction: A Mechanism of Protein Structure Stabilization. *Science* **1985**, *229*, 23-28.

43. Ryzhov, V.; Dunbar, R. C.; Cerda, B.; Wesdemiotis, C. Cation-Pi Effects in the Complexation of Na+ and K+ with Phe, Tyr, and Trp in the Gas Phase. *J. Am. Soc. Mass Spectrom.* **2000**, *11*, 1037-1046.

44. Ruan, C.; Rodgers, M. T. Cation−π Interactions: Structures and Energetics of Complexation of Na+ and K+ with the Aromatic Amino Acids, Phenylalanine, Tyrosine, and Tryptophan. *J. Am. Chem. Soc.* **2004**, *126*, 14600-14610.

45. Nicholas, J. B.; Hay, B. P.; Dixon, D. A. Ab Initio Molecular Orbital Study of Cation−π Binding between the Alkali-Metal Cations and Benzene. *J. Phys. Chem. A* **1999**, *103*, 1394-1400.

46. Gallivan Justin, P.; Dougherty Dennis, A. Cation-Π Interactions in Structural Biology. *Proc. Natl. Acad. Sci. U. S. A.* **1999**, *96*, 9459-9464.

47. Dougherty, D. A. The Cation−π Interaction. *Acc. Chem. Res.* **2013**, *46*, 885-893.

48. Gokel, G. W.; De Wall, S. L.; Meadows, E. S. Experimental Evidence for Alkali Metal Cation−π Interactions. *Eur. J. Org. Chem.* **2000**, *2000*, 2967-2978.

49. Bokatzian, S. S.; Stover, M. L.; Plummer, C. E.; Dixon, D. A.; Cassady, C. J. An Experimental and Computational Investigation into the Gas-Phase Acidities of Tyrosine and Phenylalanine: Three Structures for Deprotonated Tyrosine. *J. Phys. Chem. B* **2014**, *118*, 12630-12643.

50. Yan, J. X.; Packer, N. H.; Gooley, A. A.; Williams, K. L. Protein Phosphorylation: Technologies for the Identification of Phosphoamino Acids. *J Chromatogr A.* **1998**, *808*, 23.

51. Stover, M. L.; Plummer, C. E.; Miller, S. R.; Cassady, C. J.; Dixon, D. A. Gas-Phase Acidities of Phosphorylated Amino Acids. *J. Phys. Chem. B* **2015**, *119*, 14604-14621.

52. Brauer; Georg *Handbook of Preparative Inorganic Chemistry;* Academic Press: New York & London, 1963.

53. Salnikow, K.; Zhitkovich, A.; Costa, M. Analysis of the Binding Sites of Chromium to DNA and Protein in Vitro and in Intact Cells. *Carcinogenesis* **1992**, *13*, 2341-2346.

54. Zhitkovich, A.; Shrager, S.; Messer, J. Reductive Metabolism of Cr(VI) by Cysteine Leads to the Formation of Binary and Ternary Cr−DNA Adducts in the Absence of Oxidative DNA Damage. *Chem. Res. Toxicol.* **2000**, *13*, 1114-1124.

55. Kortenkamp, A.; O'Brien, P. Studies of the Binding of Chromium(III) Complexes to Phosphate Groups of Adenosine Triphosphate. *Carcinogenesis* **1991**, *12*, 921-926.

56. Sterling, H. J.; Cassou, C. A.; Trnka, M. J.; Burlingame, A. L.; Krantz, B. A.; Williams, E. R. The Role of Conformational Flexibility on Protein Supercharging in Native Electrospray Ionization. *Phys. Chem. Chem. Phys.* **2011**, *13*, 18288-18296.

57. Sterling, H. J.; Daly, M. P.; Feld, G. K.; Thoren, K. L.; Kintzer, A. F.; Krantz, B. A.; Williams, E. R. Effects of Supercharging Reagents on Noncovalent Complex Structure in Electrospray Ionization from Aqueous Solutions. *J. Am. Soc. Mass Spectrom.* **2010**, *21*, 1762-1774.

58. Teo, C. A.; Donald, W. A. Solution Additives for Supercharging Proteins Beyond the Theoretical Maximum Proton-Transfer Limit in Electrospray Ionization Mass Spectrometry. *Anal. Chem.* **2014**, *86*, 4455-4462.

CHAPTER 4. ALTERNATIVE METHODS OF CHROMIUM DELIVERY INTO ELECTROSPRAY IONIZATION SOURCE

4.1 Introduction

Liquid chromatography (LC) is a common separation method used in mass spectrometry (MS) based-proteomics for the analysis of complex mixtures.[1,2] Electrospray ionization (ESI) and matrix-assisted laser desorption ionization (MALDI) are the two most popular methods of ionizing peptides.[3-6] ESI is a continuous ionization method where a liquid stream is flowed into the source, whereas MALDI is a pulsed technique. The coupling of ESI with LC is easily accomplished online by directly introducing the LC flow into the ESI chamber.[7] This is not the case for MALDI, which requires offline analysis where fractions are collected after eluting from the LC column and then analyzed by MALDI-MS.[8,9]

Volatile organic acids such as trifluoroacetic acid (TFA) are often added to LC mobile phases to change the pH and improve chromatographic separation by acting as an ion-pairing agent.[10,11] The acid anion forms ion pairs with basic molecules, which causes the molecules to appear to have a neutral charge. Because of this, the molecules are retained longer on silica-based reverse-phase columns leading to sharper chromatography peaks.[12] However, the ion pairing of TFA to molecules suppresses the analyte signal in ESI.[13-15] Neutralization of the molecules with TFA renders the molecule undetectable in MS. To remedy this problem, Loo and coworkers[16] reported the addition of small amounts of organic supercharging reagents (e.g., *m*-nitrobenzyl alcohol and propylene carbonate) in the mobile phase to counteract the effects of

TFA. The supercharging reagent decreases the concentration of TFA anions in the droplet during desolvation, and LC separation is not disturbed by the addition of supercharging reagents to the mobile phase.

After the discovery that trivalent chromium, Cr(III), can serve as an additive to increase the protonation of peptides in ESI,[17] a previous Cassady group member, Matthew Mireles, attempted to introduce Cr(III) to peptide solutions via the LC mobile phase.[18] The chromatographic resolution and separation ability were affected by Cr(III), and the project was unsuccessful. Infusion experiments with Cr(III) involved peptide solutions containing Cr(III) in an optimized 1:10 peptide to Cr(III) molar ratio.[17] Experimental and computational results indicated that Cr(III) enhances the protonation of peptides during the ESI desolvation phase and not strictly in the solution phase.[19,20] Therefore, Cr(III) does not necessarily have to be in same solution as the peptide for enhanced protonation to occur.

Post-column additives have been reported to decrease TFA suppression of chromatographic quality.[12,21] Goodley and coworkers[10,12] introduced a solution containing propionic acid in isopropyl alcohol into the LC flow after elution from the column. Addition of the solutions was reported to increase the signal intensity for a mixture of proteins. Another post-column method involves doping the ESI drying gas with organic solvents.[22-24] Drying gas enriched with polar solvent vapor enhances ion formation in ESI. In a study reported by Fenn[22] on the mechanism of ion formation in ESI, addition of polar solvents to the drying gas increased the ion formation of amino acids and peptides. The solvent vapor increases the rate at which the analyte desorbs from the ESI droplet during desolvation. In general, post-column additives allow for LC workflows to go undisturbed while enhancing ionization. Since adding Cr(III) to the mobile phase interferes with the chromatography, post-column addition is a logical option here.

The work presented in this chapter provides alternative methods of delivering Cr(III) into the ESI source independent of the peptide solution. The model peptide A7 was employed to study three different methods of Cr(III) introduction: (1) coating of the spray shield and capillary cap of the ESI source with Cr(III) solution, (2) co-axial entrance of peptide and Cr(III) solutions into the source, and (3) doping the nebulizing gas with Cr(III). These methods should allow for direct analysis using Cr(III) of peptide mixtures eluted from the LC column without Cr(III).

4.2 Experimental

Experiments were performed on a Bruker (Billerica, MA, USA) HCTultra post-translational modification (PTM) Discovery System high capacity quadrupole ion trap (QIT) mass spectrometer. The high voltage is applied on the stainless-steel capillary entrance cap, endplate, and the platinum coating at the entrance of the ESI capillary, while the ESI needle is held at ground. Experiments were performed in the positive ion mode. The parameters altered in this study includes the nebulizing gas pressure and drying gas flow. Peptide and Cr(III) solutions were introduced using a syringe pump from KD Scientific (Holliston, MA, USA). The flow rate varied for each method that was studied. Final peptide solutions were 10 μM in 50:50 [v/v] acetonitrile:water, and the concentration of Cr(III) varied. The peptide A7 was custom synthesized by Biomatik (Cambridge, Ontario, CA). Chromium(III) nitrate nonahydrate was purchased from Alfa Aesar (Tewksbury, MA, USA).

4.3 Results

4.3.1 Coating of capillary end cap with chromium(III)

The experiments were accomplished by immersing the capillary endcap and spray shield in solutions containing Cr(III) in varying concentrations. These ESI source parts were submerged in the Cr(III) solution for 15 min and directly placed back on the instrument. A 10 μM solution

of A7 was infused into the ESI source. Refer to Figure 2.1. The ESI spectrum obtained with no Cr(III) after cleaning the ESI source, capillary, and skimmer is presented in Figure 4.2(a). Figure 4.2(b) is the ESI spectrum after submerging the capillary cap and spray shield in a 0.1 M solution of Cr(III). At 0.1 M Cr(III), the ESI capillary (through which ions travel into the vacuum chamber) began to clog from the accumulation of Cr(III) salt, and the analyte signal was lost after a while. At lower concentrations of Cr(III), formation of $[M + 2H]^{2+}$ is not observed. To reduce the amount of Cr(III), a polyester tipped swab (Puritan Medical Co. LLC, Guilford, ME, USA) was used to swab a small amount of the 0.1 M Cr(III) solution directly on the spray shield. Figure 4.3 contains the ESI mass spectra for A7 without Cr(III) and with 0.1 M Cr(III) swabbed onto the spray shield.

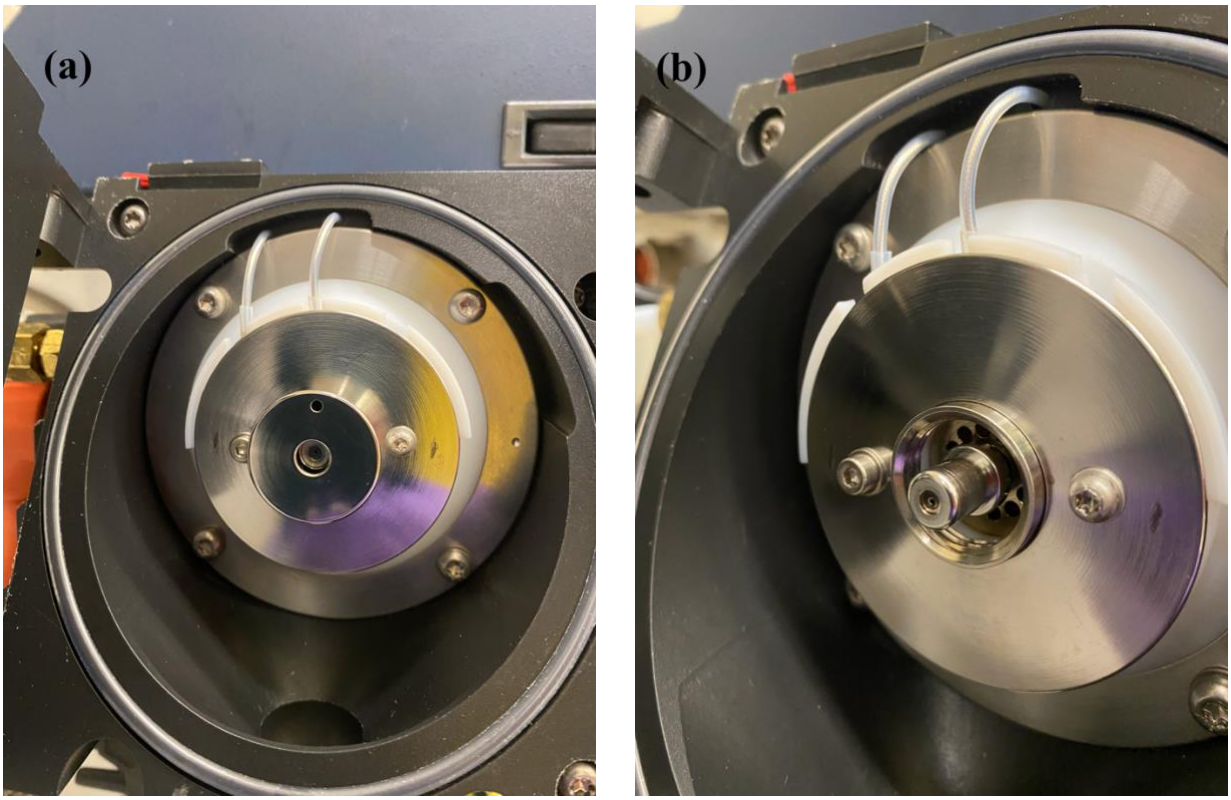

Figure 4.1. Opened ESI source with (a) spray shield exposed and (b) capillary cap exposed after removal of the spray shield.

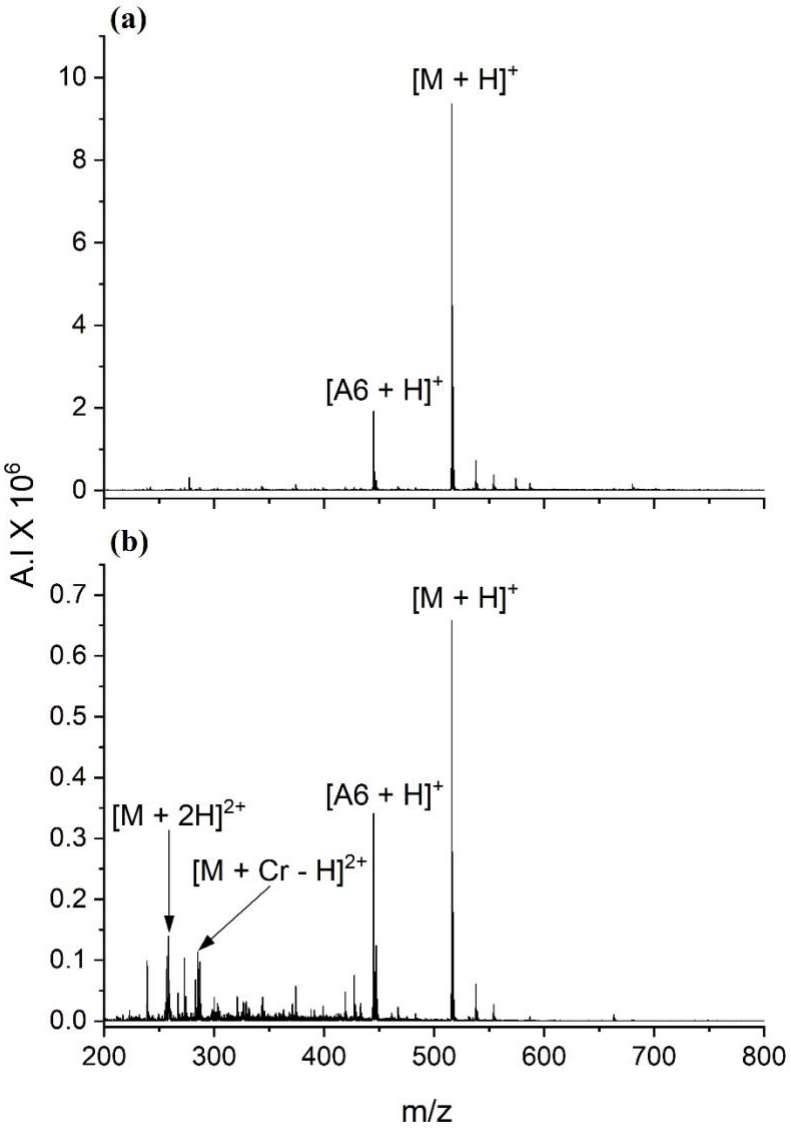

Figure 4.2. ESI mass spectra of A7 with (a) no Cr(III) and (b) spray shield and endcap submerged in 0.1 M Cr(III) solution.

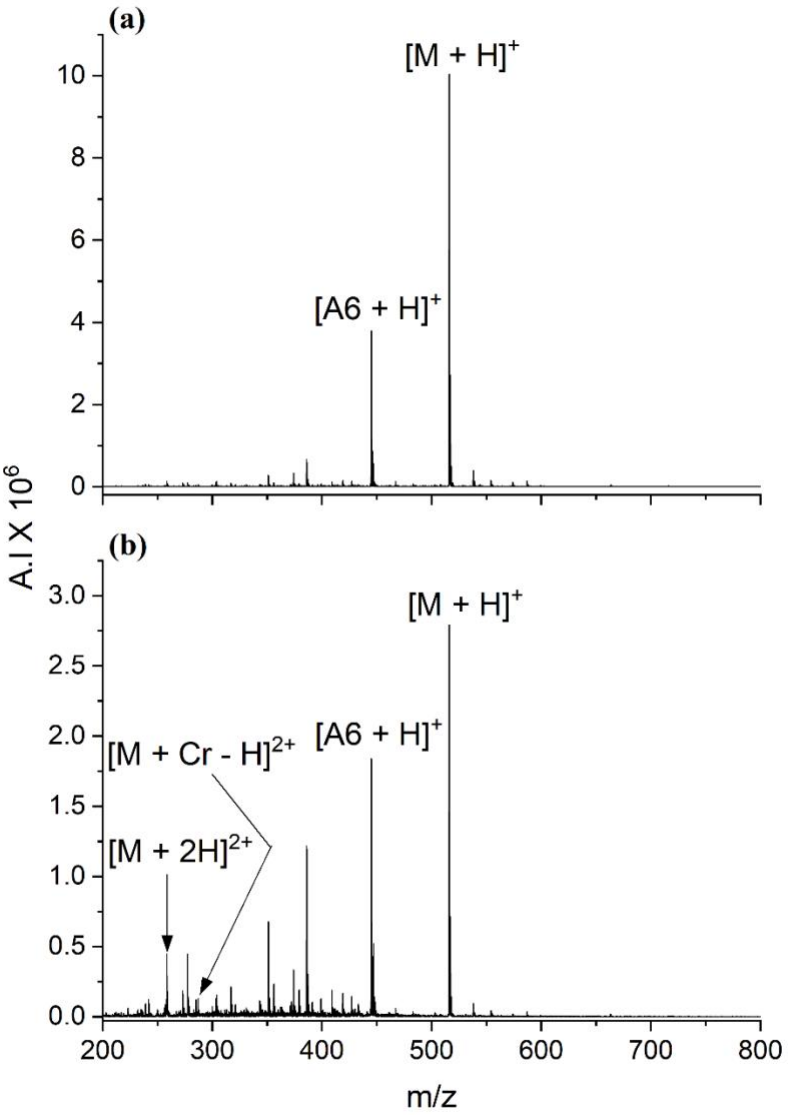

Figure 4.3. ESI mass spectra of A7 with (a) no Cr(III) and (b) 0.1 M Cr(III) swabbed on the spray shield.

4.3.2 Co-axial introduction of solutions into the ESI source

For the co-axial introduction of Cr(III) into the ESI source, as shown in Figure 4.4, a Swagelok (Solon, OH, USA) 1/16" union tee was connected to the ESI needle with a zero dead volume (ZDV) union. Two syringe pumps were employed to introduce the peptide solution and the Cr(III) solution separately. The flow rate was set to 1.5 μL/min for both solutions. At the optimized 1:10 peptide to Cr(III) molar ratio, no enhanced protonation is observed. The addition of Cr(III) in a 1:50 molar ratio results in the formation of $[M + 2H]^{2+}$. Figure 4.5 shows the ESI mass spectra for A7 with (a) no Cr(III) and (b) infusion of a 500 μM Cr(III) solution.

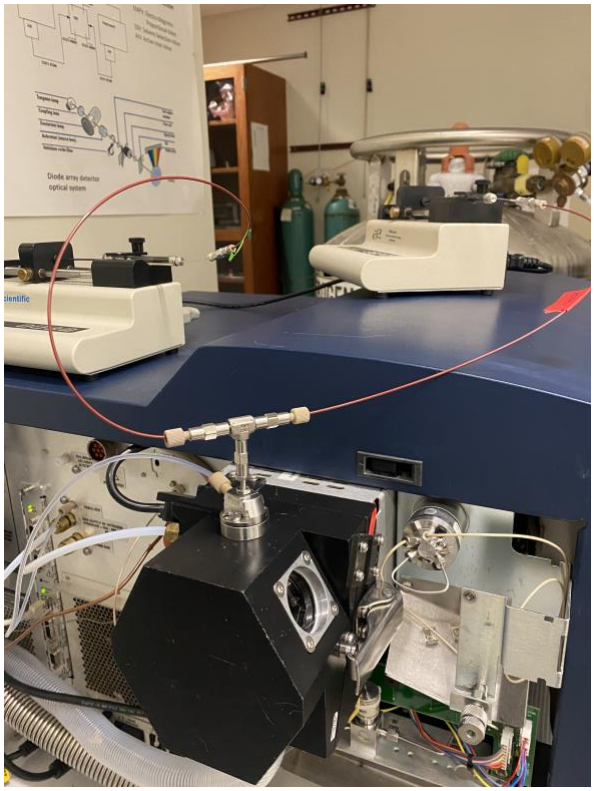

Figure 4.4. Image of co-axial introduction of peptide solution and Cr(III) solution into the ESI chamber.

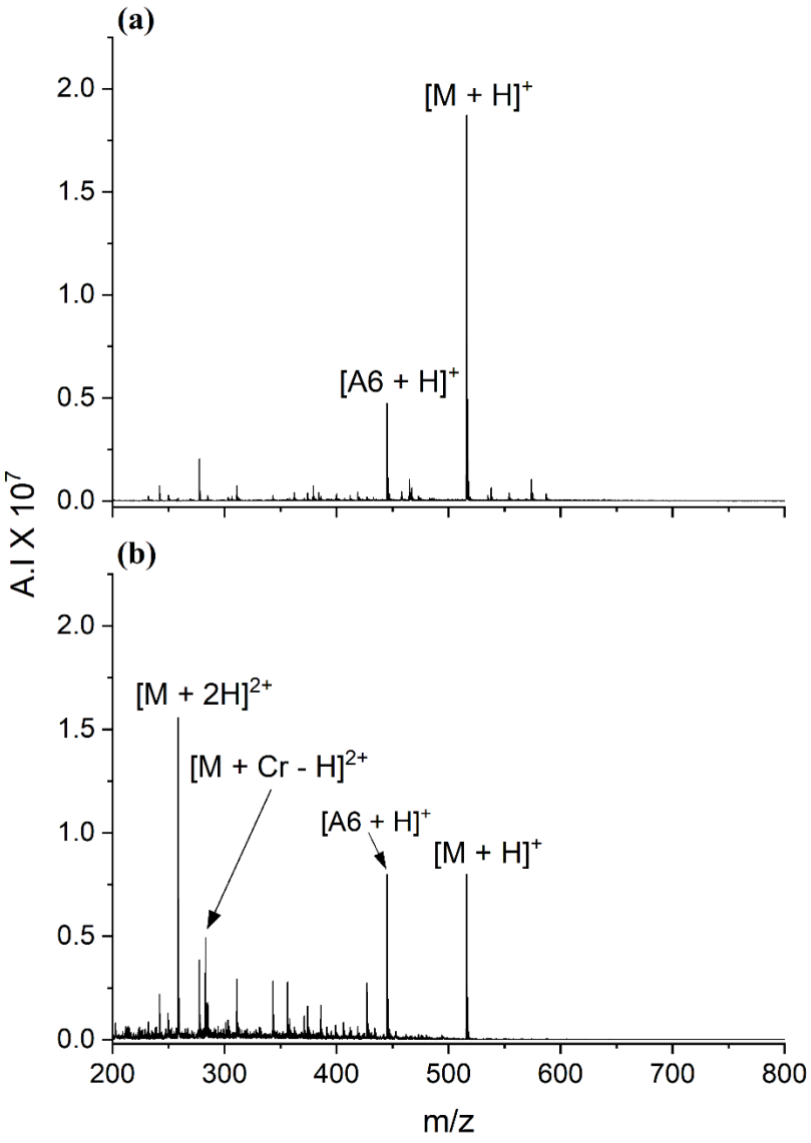

Figure 4.5. ESI mass spectra of A7 using the co-axial design with (a) no Cr(III) and (b) 500 uM Cr(III) solution.

4.3.3 Doping the nebulizing gas with chromium(III)

When adding Cr(III) directly to solutions containing A7, the nebulizer gas pressure was found to be important for increasing the intensity of $[M + 2H]^{2+}$.[25] Introducing Cr(III) into the gas phase via the nebulizer gas was investigated using nitrogen as the nebulizer gas. A Peek™ (Lancashire, UK) tee high pressure LC connection was used to introduce a solution containing Cr(III) in water into the nebulizing gas flow path. Figure 4.6 is an image of the PEEK connection with the red line carrying Cr(III) solution. The drying gas flow rate, nebulizer gas pressure, peptide and Cr(III) solution flow rate, and Cr(III) concentration was varied until $[M + 2H]^{2+}$ formation was observed. A decrease in absolute intensity is observed after addition of Cr(III) to the nebulizer gas flow, and $[M + 2H]^{2+}$ forms with 0.02 M Cr(III) solution at a flow rate of 3.5 μL/min. The peptide solution was infused at a flow rate of 1.5 μL/min. The drying gas flow rate was set to 5 L/min and the nebulizing gas pressure at 12 psi. Figure 4.7 is the mass spectra for A7 with no Cr(III) and with a 0.02 M Cr(III) solution doped into the nebulizer gas flow.

4.4 Discussion

After multiple ESI-MS experiments have been conducted using peptide solutions containing Cr(III), residual Cr(III) in the mass spectrometer can cause enhanced protonation to still occur with peptide solutions containing no Cr(III). (This was a hindrance to conducting the experiments discussed in Chapters 3 and 6.) A thorough cleaning of the mass spectrometer is required between each trial to avoid residual Cr(III) affecting results, especially in cases where absolute intensities are being compared. This led to the realization that Cr(III) does not need to be in the peptide solution to achieve enhanced protonation and could instead be introduced by depositing Cr(III) onto the spray shield and capillary endcap of the Bruker HCTultra's ESI

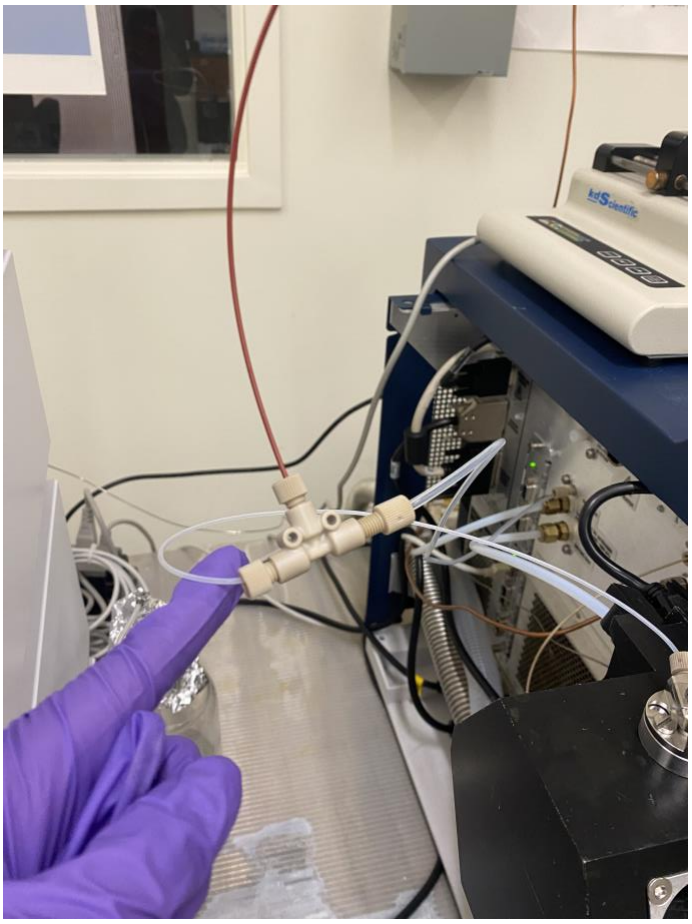

Figure 4.6. Image of Cr(III)-doped nebulizing gas setup. The red line contains Cr(III) solution.

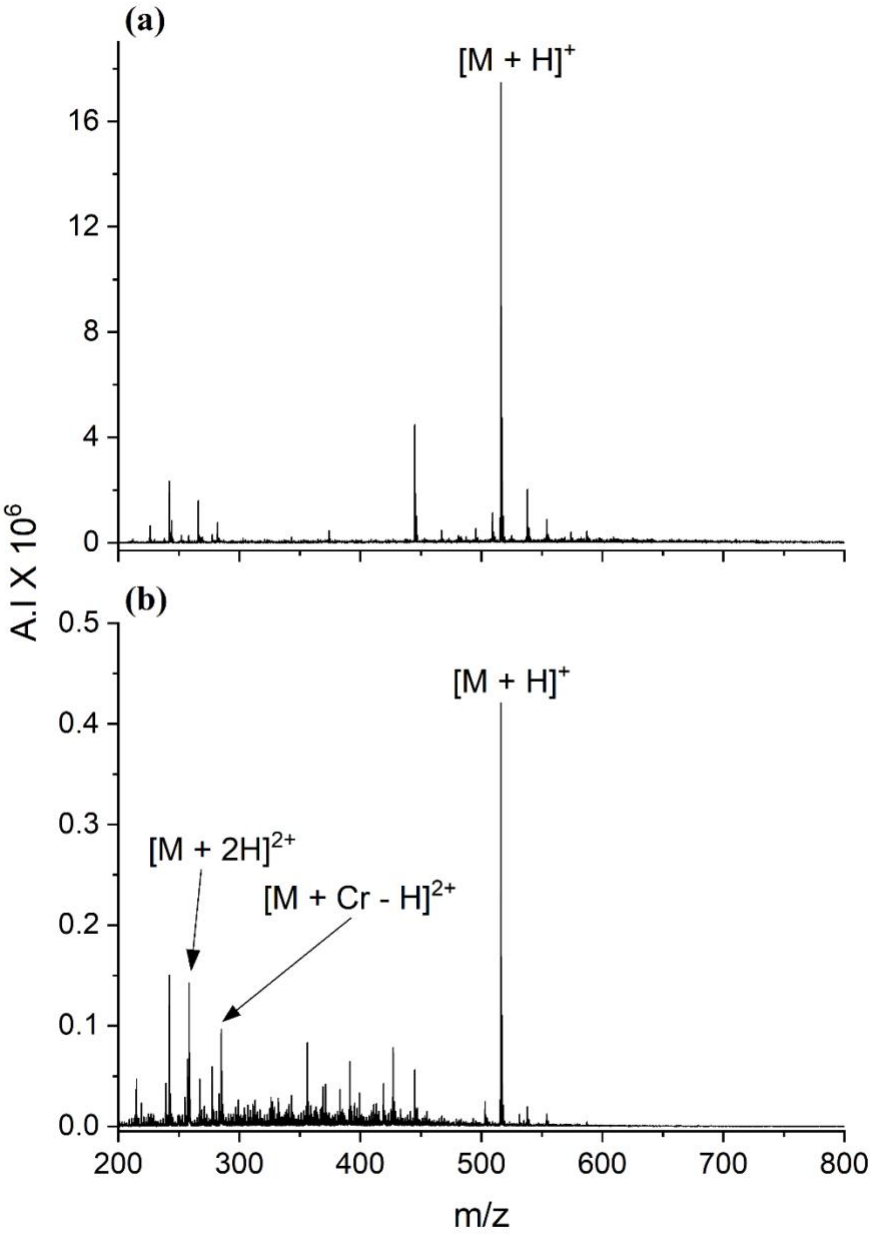

Figure 4.7. ESI mass spectra of A7 with (a) no Cr(III) and (b) 0.02 μM Cr(III) doped into the nebulizing gas flow.

source. An image of the Bruker HCTultra spray shield and endcap is provided in Figure 4.1. The endcap and spray shield were chosen due to their location at the entrance of the glass capillary and the drying gas flow path. The drying gas conditions were determined to be a critical factor in enhanced protonation using Cr(III).[25]

An overall decrease in absolute signal intensity for A7 is observed when swabbing Cr(III) on the spray shield or doping the nebulizing gas flow with Cr(III). This may be due to the use high concentrations of Cr(III) that is required to observe formation of $[M + 2H]^{2+}$. Dr. Changgeng Feng, a previous group member, reported the optimal molar ratio of 1:10 peptide to Cr(III) and noted a decline in the signal intensity of $[M + H]^{+}$ and $[M + 2H]^{2+}$ at higher concentrations.[17] This indicates that high concentrations of Cr(III) may be suppressing ionization of A7. The drastic decrease in signal intensity is not observed with the co-axial introduction of Cr(III), which uses 500 μM Cr(III) compared to 0.1 and 0.02 M Cr(III) used with swabbing the spray shield and doping the nebulizing gas flow, respectively. However, the concentrations are not directly comparable because coaxial introduction involves Cr(III) in solution, while coating of source parts results in introduction of Cr(III) from the heated solid salt that remains after the solvent has evaporated.

When swabbing the spray shield with Cr(III), the absolute intensity of $[M + 2H]^{2+}$ decreases over time. Another factor that may be causing the decrease in signal intensity could be the quick melting of $[Cr(H_2O)_6](NO_3)_3 \bullet 3H_2O$, which begins at 60ºC.[26] Control over the temperature when swabbing Cr(III) onto the spray shield with the ESI source door open is limited; thus, the drying gas temperature fluctuates between 250 to 300ºC. At this temperature range, Cr(III) goes into the gas phase instantaneously and begins to interact with peptide ions. As time progresses, the concentration of Cr(III) in the source decreases resulting is less Cr(III) and

peptide interactions. Ultimately the formation of $[M + 2H]^{2+}$ decreases. A time effect was observed when Cr(III) was swabbed on the spray shield. The effect time has on $[M + 2H]^{2+}$ formation is illustrated in Figure 4.8 where the absolute intensity is plotted over a time span of 5 min. As time elapses, the absolute intensity of $[M + 2H]^{2+}$ decreases by 65%. Depositing Cr(III) on the spray shield may not be the best method of introducing Cr(III) because of the need of a constant supply of Cr(III) in the source region to keep enhanced protonation going. However, this experiment does confirm the general concept that Cr(III) can be introduced in the gas phase as opposed to being adding only to a peptide solution.

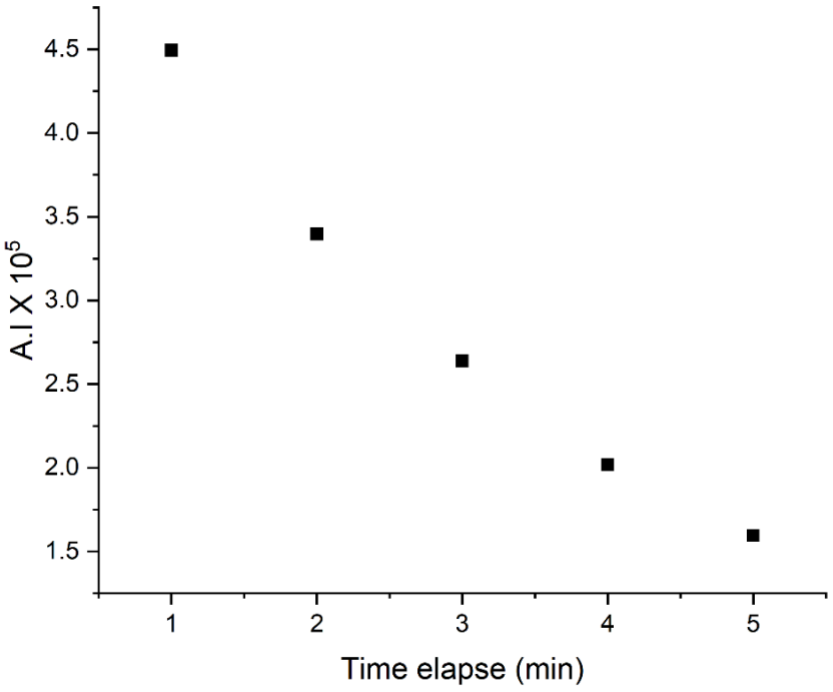

Figure 4.8. Absolute intensity of $[M + 2H]^{2+}$ for A7 as a function of time (min) elapsed from closing of the ESI source door.

The greatest degree of enhanced protonation was observed using the co-axial introduction of Cr(III) solution into the ESI needle. Formation of $[M + 2H]^{2+}$ forms at ~ 2:1 ratio of $[M + 2H]^{2+}$ to $[M + H]^{+}$. Unlike the other two methods, the optimized ESI conditions for enhanced protonation of A7 [25] could be used in the co-axial design with no modifications. The 1:50 peptide to Cr(III) molar ratio is slightly higher than the 1:10 optimized ratio; but in the case of two separate solutions, the amount of solvent increases and dilutes the peptide and Cr(III) ions. In addition, mixing of peptide and Cr(III) is not as thorough with co-axial introduction as it is when both species are in the same .

4.5 Conclusions

Enhanced protonation of A7 was observed using all three methods of Cr(III) delivery albeit to different extents. These results give additional support that the mechanism is occurring during the desolvation phase in the ESI source. Although enhanced protonation is observed with depositing Cr(III) onto the spray shield, the decrease in signal intensity overtime as the amount of Cr(III) diminishes and the high concentration of Cr(III) required resulting in the ESI capillary clogging does not make it a good method of choice. The most promising methods are the co-axial introduction of Cr(III) solution and the doping of the nebulizing gas. As the work in this chapter is a proof-of-concept experiment, additional parameter and design optimization needs to be done. In addition, other peptides that undergo enhanced protonation with Cr(III) should be investigated. In all, these results look hopeful for the incorporation of Cr(III) into LC-MS workflows as a post-separation additive to increase protonation efficiency of peptides.

References

1. Xie, F.; Smith, R. D.; Shen, Y. Advanced Proteomic Liquid Chromatography. *J. Chromatogr. A* **2012**, *1261*, 78-90.

2. Shi, Y.; Xiang, R.; Horváth, C.; Wilkins, J. A. The Role of Liquid Chromatography in Proteomics. *J. Chromatogr. A* **2004**, *1053*, 27-36.

3. Jabbour, R. E.; Snyder, A. P. Mass Spectrometry-Based Proteomics Techniques for Biological Identification. *Woodhead Publ. Ser. Electron. Opt. Mater.* **2014**, *59*, 370-430.

4. Kollipara, S.; Agarwal, N.; Varshney, B.; Paliwal, J. Technological Advancements in Mass Spectrometry and its Impact on Proteomics. *Anal. Lett.* **2011**, *44*, 1498-1520.

5. Nilsson, T.; Mann, M.; Aebersold, R.; Yates, J. R.; Bairoch, A.; Bergeron, J. J. M. Mass Spectrometry in High-Throughput Proteomics: Ready for the Big Time. *Nat. Methods* **2010**, *7*, 681-685.

6. Zhang, Y.; Fonslow, B. R.; Shan, B.; Baek, M.; Yates, J. R. Protein Analysis by Shotgun/Bottom-Up Proteomics. *Chem. Rev.* **2013**, *113*, 2343-2394.

7. Creese, A. J.; Cooper, H. J. Liquid Chromatography Electron Capture Dissociation Tandem Mass Spectrometry (LC-ECD-MS/MS) Versus Liquid Chromatography Collision-Induced Dissociation Tandem Mass Spectrometry (LC-CID-MS/MS) for the Identification of Proteins. *J. Am. Soc. Mass Spectrom.* **2007**, *18*, 891-897.

8. Neubert, H.; Bonnert, T. P.; Rumpel, K.; Hunt, B. T.; Henle, E. S.; James, I. T. Label-Free Detection of Differential Protein Expression by LC/MALDI Mass Spectrometry. *J. Proteome Res.* **2008**, *7*, 2270-2279.

9. Zhen, Y.; Xu, N.; Richardson, B.; Becklin, R.; Savage, J. R.; Blake, K.; Peltier, J. M. Development of an LC-MALDI Method for the Analysis of Protein Complexes. *J. Am. Soc. Mass Spectrom.* **2004**, *15*, 803-822.

10. Apffel, A.; Fischer, S.; Goldberg, G.; Goodley, P. C.; Kuhlmann, F. E. Enhanced Sensitivity for Peptide Mapping with Electrospray Liquid Chromatography-Mass Spectrometry in the Presence of Signal Suppression due to Trifluoroacetic Acid-Containing Mobile Phases. *J. Chromatogr. A* **1995**, *712*, 177-190.

11. Chen, Y.; Mehok, A. R.; Mant, C. T.; Hodges, R. S. Optimum Concentration of Trifluoroacetic Acid for Reversed-Phase Liquid Chromatography of Peptides Revisited. *J. Chromatogr. A* **2004**, *1043*, 9-18.

12. Kuhlmann, F. E.; Apffel, A.; Fischer, S. M.; Goldberg, G.; Goodley, P. C. Signal Enhancement for Gradient Reverse-Phase High-Performance Liquid Chromatography-Electrospray Ionization Mass Spectrometry Analysis with Trifluoroacetic and Other Strong Acid Modifiers by Postcolumn Addition of Propionic Acid and Isopropanol. *J. Am. Soc. Mass Spectrom.* **1995**, *6*, 1221-1225.

13. Eshraghi, J.; Chowdhury, S. K. Factors Affecting Electrospray Ionization of Effluents Containing Trifluoroacetic Acid for High-Performance Liquid Chromatography/Mass Spectrometry. *Anal. Chem.* **1993**, *65*, 3528-3533.

14. Chowdhury, S. K.; Chait, B. T. Method for the Electrospray Ionization of Highly Conductive Aqueous-Solutions. *Anal. Chem.* **1991**, *63*, 1660-1664.

15. Mirza, U. A.; Chait, B. T. Effects of Anions on the Positive Ion Electrospray Ionization Mass Spectra of Peptides and Proteins. *Anal. Chem.* **1994**, *66*, 2898-2904.

16. Nshanian, M.; Lakshmanan, R.; Chen, H.; Loo, R. R. O.; Loo, J. A. Enhancing Sensitivity of Liquid Chromatography-Mass Spectrometry of Peptides and Proteins using Supercharging Agents. *Int. J. Mass Spectrom.* **2018**, *427*, 157-164.

17. Feng, C.; Commodore, J. J.; Cassady, C. J. The use of Chromium(III) to Supercharge Peptides by Protonation at Low Basicity Sites. *J. Am. Soc. Mass Spectrom.* **2015**, *26*, 347-358.

18. Mireles, M.; Cassady, C. J. The University of Alabama, Tuscaloosa, AL. Unpublished work, **2019.**

19. Persaud, R. R.; Dieke, N. E.; Jing, X.; Lambert, S.; Parsa, N.; Hartmann, E.; Vincent, J. B.; Cassady, C. J.; Dixon, D. A. Mechanistic Study of Enhanced Protonation by Chromium(III) in Electrospray Ionization: A Superacid Bound to a Peptide. *J. Am. Soc. Mass Spectrom.* **2020**, *31*, 308-318.

20. Jing, X.; Edwards, K. C.; Vincent, J. B.; Cassady, C. J. The use of Chromium(III) Complexes to Enhance Peptide Protonation by Electrospray Ionization Mass Spectrometry. *J. Mass Spectrom.* **2018**, *53*, 1198-1206.

21. Xu, C.; Zang, L.; Weiskopf, A. Size-Exclusion Chromatography-Mass Spectrometry with M-Nitrobenzyl Alcohol as Post-Column Additive for Direct Characterization of Size Variants of Monoclonal Antibodies. *J. Chromatogr. B* **2014**, *960*, 230-238.

22. Steve, N.; Fenn John, B. Gas-Phase Ions of Solute Species from Charged Droplets of Solutions. *Proc. Natl. Acad. Sci. U.S.A.* **2007**, *104*, 1111-1117.

23. Kammeijer, G. S. M.; Kohler, I.; Jansen, B. C.; Hensbergen, P. J.; Mayboroda, O. A.; Falck, D.; Wuhrer, M. Dopant Enriched Nitrogen Gas Combined with Sheathless Capillary Electrophoresis–Electrospray Ionization-Mass Spectrometry for Improved Sensitivity and Repeatability in Glycopeptide Analysis. *Anal. Chem.* **2016**, *88*, 5849-5856.

24. Iavarone, A. T.; Jurchen, J. C.; Williams, E. R. Effects of Solvent on the Maximum Charge State and Charge State Distribution of Protein Ions Produced by Electrospray Ionization. *J. Am. Soc. Mass Spectrom.* **2000**, *11*, 976-985.

25. Commodore, J. J.; Jing, X.; Cassady, C. J. Optimization of Electrospray Ionization Conditions to Enhance Formation of Doubly Protonated Peptide Ions with and without Addition of Chromium(III). *Rapid Commun. Mass Spectrom.* **2017**, *31*, 1129-1136.

26. Gubrynowicz, L.; Strömich, T. Study on the Thermal Decomposition of Chromium(III) Nitrate Nonahydrate (CNN). *Thermochim. Acta* **1987**, *115*, 137-151.

CHAPTER 5. ENHANCED PROTONATION WITH TRIVALENT CHROMIUM IN MATRIX-ASSISTED LASER DESORPTION IONIZATION MASS SPECTROMETRY

5.1 Introduction

Matrix-assisted laser desorption ionization (MALDI) is a soft ionization technique routinely used in the analysis of biomolecules and polymers by mass spectrometry (MS). Introduced in the 1980s by Tanaka,[1] Hillenkamp, and Karas,[2] MALDI can analyze large molecules and has a high tolerance for sample contamination.[3,4] Unlike electrospray ionization (ESI), MALDI produces primarily singly charged ions, usually $[M + H]^+$.[4,5] The analyte is generally mixed with an excess of matrix molecules before being spotted on a target plate to dry and co-crystallize. In MALDI, the target plate is placed into the mass spectrometer and the sample spot is irradiated with a pulsed laser, which results in desorption of the analyte and matrix from the target plate. The matrix, which absorbs at the wavelength of the laser, serves the purpose of absorbing the laser's energy and transferring the energy to the analyte. The matrix also prevents cluster formation of the analyte and provides an additional source of protons for protonation of the analyte.[6] MALDI matrices are categorized into three different general classes: solid organic matrices, liquid crystalline matrices, and inorganic matrices.[7] Solid crystalline organic matrices are most often used in the analysis of peptides (as well as other biomolecules). The most common matrices are 2,5-dihydroxybenzoic acid (DHB) and α-cyano-4-hydroxycinnamic acid (CHCA).[8,9]

A previous member of the Cassady group, Dr. Xinyao Jing, determined that trivalent chromium, Cr(III), as a matrix alone results in poor crystal formation and poor reproducibility of

peptide ion intensities.[10] However, preliminary data showed that Cr(III) as an additive used with an organic matrix has the potential to enhance the ionization of the biological peptides bradykinin, bradykinin (1-7), and substance P in MALDI-MS.[11] Although promising, these results could not be consistently reproduced. Poor sample-to-sample and shot-to-shot reproducibility is a major disadvantage of MALDI and has limited quantitative analysis using MALDI.[12,13] Poor reproducibility stems from the heterogenous co-crystallization of the matrix and analyte on the target plate leading to signal variations over the surface of the sample spot. The perfect matrix will promote homogenous co-crystallization with the analyte and give consistent signal intensity throughout the sample spot. New MALDI matrices are constantly being developed.

Besides the matrix, another factor that influences MALDI analysis is the method of depositing the sample and matrix on the target plate. The most common method is the dried droplet method;[5] in this method, a solution containing the matrix and sample is spotted on the target plate and dried (i.e., evaporation of the solvent). Although widely used in qualitative analysis, the dried droplet method produces heterogeneous crystallization that results in poor reproducibility making it a poor choice for quantitative analysis.[14,15] In another method, an analyte solution is spotted and dried on the target plate; then, the matrix solution is spotted on top of the analyte layer and dried to create a thin film. This process can be done in the reverse. Termed the two or thin-layer method,[16-18] this method was reported to produce homogeneous co-crystallization and improve quantitative MALDI analysis of DNA.[19] Sample preparation in MALDI-MS is not a one size fits all protocol. Matrix selection and deposition method differs depending on the analyte of interest. Determining the best sample preparation method can at times be based on trial and error.

In this chapter, Cr(III) will be investigated as an additive in positive ion mode MALDI-MS for the enhanced protonation of peptides. Various matrices and sample deposition methods will be studied in an effort to determine the best sample preparation method to use for increasing the absolute intensity of $[M + H]^+$. Because MALDI rarely produces multiply charged ions, supercharging by production of $[M + nH]^{n+}$ is not expected to occur.

5.2 Experimental

5.2.1 Mass spectrometry

All MALDI experiments were performed on a Bruker (Billerica, MA, USA) rapifleX MALDI-TOF/TOF mass spectrometer equipped with a smartbeam™ 3D Nd:YAG (355 nm) laser. Mass spectra were acquired in reflectron positive ion mode by signal averaging 10,000 scans per spectrum. The laser power varied between 30 to 70% of the total laser power and was set to automatic random walk mode across the sample spot surface. External mass-to-charge calibration was performed using the peptide calibration standard solution from Bruker.

5.2.2 Peptides, Cr(III) complex, and MALDI matrices

The peptide heptaalanine amide, A7-NH_2, was custom synthesized by Biomatik USA (Wilmington, Delaware, USA). Substance P acid was purchased from ThermoFisher (Waltham, MA, USA). Peptide solutions contained a final concentration of 5-10 µL peptide in 50:50 [v/v] acetonitrile: Milli-Q water. Chromium(III) nitrate nonahydrate was purchased from VWR International (Radnor, PA) and was dissolved in Milli-Q water. The concentration of Cr(III) was varied to determine the optimal ratio of matrix-to-Cr(III).

The matrices 2,5-dihydroxybenzoic acid (DHB) and 5-methoxysalicylic acid (MSA) were obtained from Acros Organics (Fair Lawn, NJ, USA). 1,1-Bi-2-naphthylamine (BNA), 3-hydroxy-4-nitrobenzoic acid (HNBA), and α-cyano-4-hydroxycinnamic acid (CHCA) were

purchased from Alfa Aesar (Haverhill, MA, USA). 2-Nitrophloroglucinol (2-NPG) came from Chem-Impex International Inc. (Wood Dale, IL, USA). 2,4,6-Trihydroxyacetophenone (THAP) was acquired from TCI Chemicals (Portland, OR, USA); and 4-nitro-1-naphthylamine (NNA), from Sigma-Aldrich (St. Louis, MO, USA). DHB (20 mg/mL) and CHCA (10 mg/mL) were dissolved in 30:70 [v/v] acetonitrile: 0.1% trifluoracetic acid in Milli-Q water. MSA was dissolved in 3:1 [v/v] acetonitrile: Milli-Q water to a final concentration of 17 mg/mL. Super-DHB (sDHB) was prepared by making a solution of 9:1 [v/v] DHB: MSA. The matrices THAP (25 mg/mL), 2-NPG (10 mg/mL), HNBA (10 mg/mL), NNA (10 mg/mL), and BNA (10 mg/mL) were prepared in 50:50 [v/v] acetonitrile: 0.1% trifluoracetic acid in Milli-Q water.

5.2.3 Sample preparation

For the dried droplet method, 1 uL of peptide solution was mixed with 1 uL of each matrix; afterwards, 1 uL of the mixture was deposited onto the target plate and dried at room temperature. For Cr(III) analysis, 1 uL of Cr(III) solution was added to the peptide-matrix mixture, and 1uL of the total solution was deposited onto the target plate. The thin-layer method consisted of separately depositing 1 µL each of matrix, peptide, and Cr(III) solutions onto the target plate allowing for each layer to dry at room temperature before loading the next layer. In another formulation, each matrix was also mixed with Cr(III) in a 1:1 [v/v] ratio, then 1 µL of the mixture was deposited on the target plate. Once dried, 1 µL of peptide solution was loaded as the final layer.

5.3 Results and discussion

The results of the work discussed in Chapter 3 demonstrated the importance of carboxylic acid groups to the mechanism of Cr(III) enhanced protonation. Many common peptide matrices contain a carboxylic acid group (e.g. DHB, CHCA). Nine matrices with varying functional

groups were studied to determine the appropriate matrix to use in conjunction with Cr(III). Table 5.1 contains information on the nine matrices used in this study.

These matrices were chosen for various reasons. In routine peptide analysis using MALDI, the most widely used matrices are DHB and CHCA; therefore, these matrices were employed in the study.[20] Interaction between Cr(III) and the peptide is important; thus, adequate time is needed for proton transfer to occur. The matrix BNA was chosen due to its aromatic π system that could potentially stabilize the Cr(III)-peptide complex giving time for proton transfer to occur. To eliminate competition between the peptide and matrix for Cr(III) binding, the matrices THAP, NNA, and 2-NPG were chosen. These matrices do not have carboxylic acid groups. Besides not having a carboxylic acid group, 2-NPG as a matrix was reported to form highly charged protein ions in MALDI and to increase protonated ion abundance.[21-24] Several studies have demonstrated the softness of MSA in oligonucleotide analysis by MALDI.[25-27] A "soft" matrix transfers less energy to the sample and, therefore, results in a decrease chance of bonds breaking (i.e., product or fragment ion formation); whereas, a "hard" matrix can transfer enough energy to break bonds. Using a soft matrix like MSA may help in extending the lifetime of the Cr(III)-peptide complex compared to hot matrices (e.g. CHCA) that, after irradiation, may break apart the complex before proton transfer has occurred. MSA can also serve as additive to DHB to achieve more homogeneous crystal formation compared to DHB and MSA alone.[28] This mixture is commonly known as sDHB and is reported to enhance ionization. The addition of MSA disrupts the lattice structure of DHB causing 'softer' desorption of the analyte and matrix. For this reason, sDHB was added to the present study. Lastly, the matrix HNBA is a benzoic acid derivative similar to DHB that and available in our lab.

Table 5.1. List of MALDI matrices studied.

Name	Abbreviation	MW (Da)	Structure
α-cyano-4-hydroxycinnamic acid	CHCA	189.2	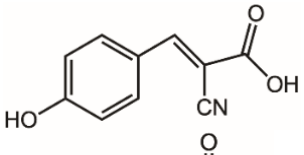
2,5-dihydroxybenzoic acid	DHB	154.1	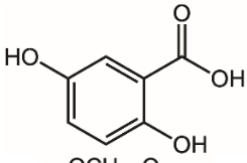
6-methoxysalicylic acid	MSA	168.2	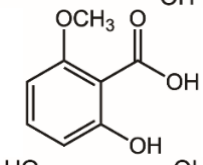
2-nitrophloroglucinol	2-NPG	171.1	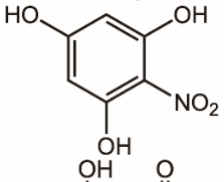
2,4,6-trihydroxyacetophenone	THAP	186.2	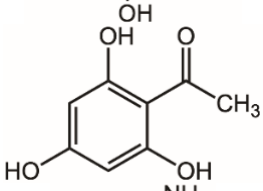
4-nitro-1-naphthylamine	4-NNA	188.2	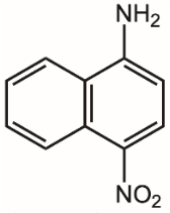
3-hydroxy-4-nitrobenzoic acid	HNBA	183.1	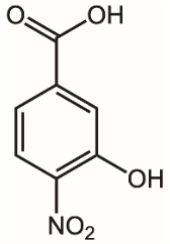
1,1-bi-2-naphthylamine	BNA	284.4	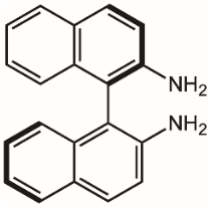
super-DHB	sDHB	-[a]	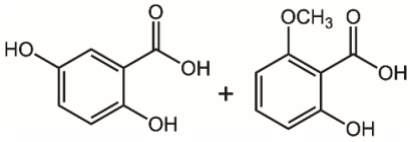

[a] sDHB is a mixture of MSA (168.2 Da) and DHB (154.1 Da).

Substance P acid, RPKPQQFFGLM-OH, a basic peptide that readily ionizes in the positive mode, was analyzed with the nine matrices using the dried droplet and thin-layer method. Cr(III) was added in a 1:10, 1:50, and 1:100 Cr(III)-to-matrix molar ratio. For the thin-layer method, two types of sample spots were created. On one spot Cr(III) and matrix were premixed in an Eppendorf (Enfield, CT, USA) tube before being spotted on the target plate as the seed layer, while in another spot Cr(III) is spotted as a separate layer. Of the nine matrices, an increase in protonation for substance P acid is seen for 2-NPG, THAP, and sDHB using the thin-layer method with Cr(III) and the matrix mixed in a 1:50 molar ratio. The remaining matrices either exhibited no change, loss of signal, or decrease in signal intensity when Cr(III) is added at any concentration. Figure 5.1 contains the MALDI mass spectra for substance P acid using 2-NPG, which shows a 3x increase of $[M + H]^+$ intensity after addition of Cr(III). However, the results are inconsistent and the deviation is large (both with and without the use of Cr(III)). This is also the case with THAP and sDHB. Table 5.2 shows the mean and standard deviations of three independent trials using sDHB, THAP, and 2-NPG without and with Cr(III). These results reveal that the sample-to-sample reproducibility is poor, which is not unusual for MALDI. Thus, the increase in signal intensity that is observed for sDHB, THAP, and 2-NPG may be due to variations in peptide ion signal from different areas on the sample spot and may not necessarily be from the addition of Cr(III).

In addition, Cr(III) changes the crystal morphology for substance P acid when sDHB, THAP, and 2-NPG are used. Figures 5.2 through 5.10 contain images of the sample spots for the different matrices and deposition methods. Crystals produced when Cr(III) and 2-NPG, sDHB, or THAP were premixed and spotted on the target plate were more defined, and the analyte signal was more consistent throughout the sample spot compared to when Cr(III) is not used.

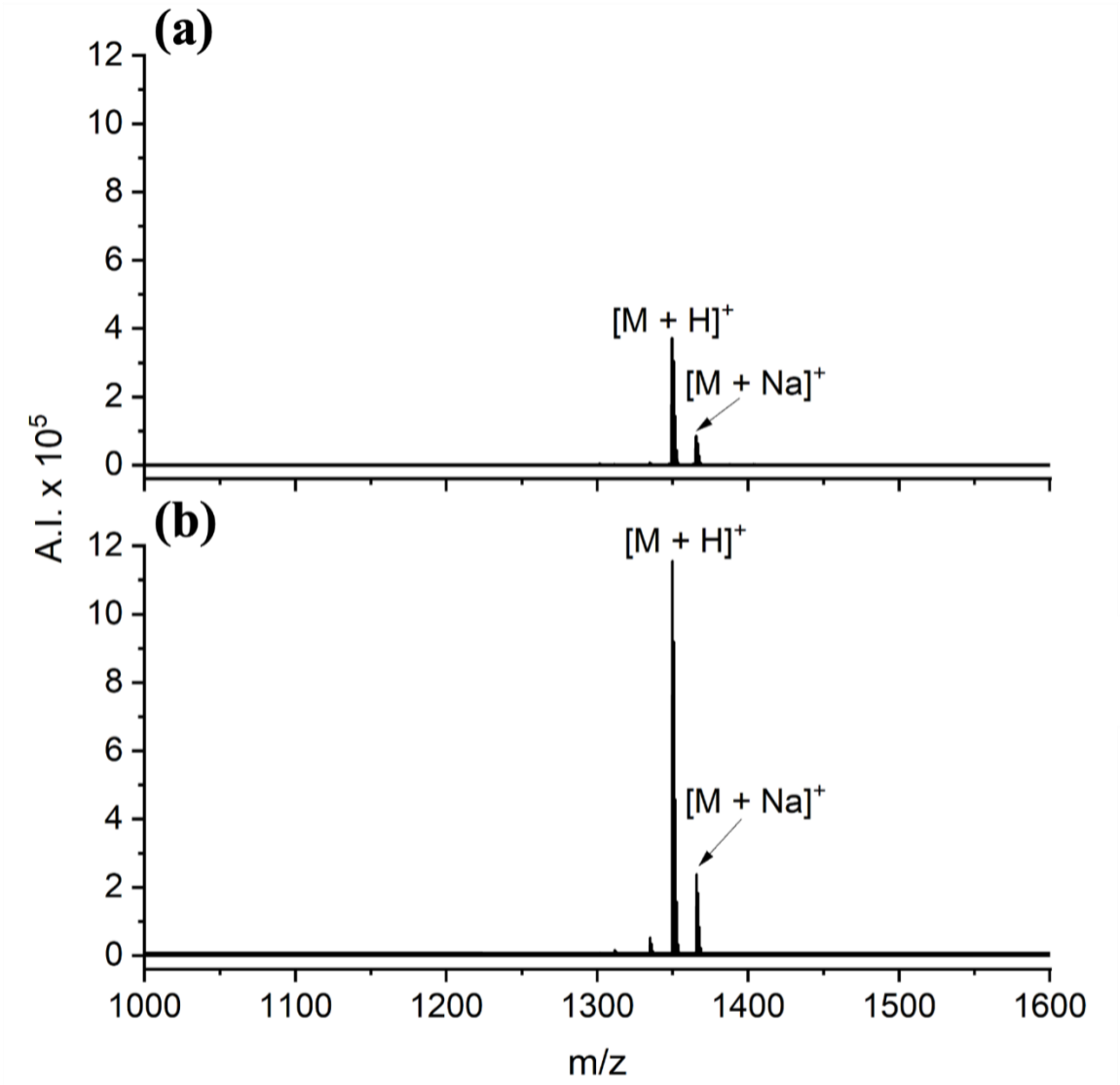

Figure 5.1. MALDI mass spectra of substance P acid containing (a) no Cr(III) and (b) Cr(III) using 2-NPG as the matrix and the thin-layer method with Cr(III) and matrix premixed.

Table 5.2. MALDI results for substance P acid containing the mean and standard deviation of absolute intensities of $[M + H]^+$ without and with Cr(III) using sDHB, THAP, and 2-NPG as the matrix. The thin-layer method with Cr(III) and matrix premixed was used to spot the samples.

	A.I X 10^5		
Matrix	Without Cr(III)	With Cr(III)	Signal increase
sDHB	12 ± 7	25 ± 6	2 ± 1
THAP	0.8 ± 0.8	2.4 ± 0.3	5 ± 5
2-NPG	2 ± 3	12 ± 9	12 ± 11

Cr(III) has less of an impact on crystal formation when using the thin-layer method with the matrix, Cr(III), and the peptide as separate layers than with the dried droplet and Cr(III)/matrix premixed thin-layer method. Figure 5.6 contains images of substance P with THAP as the matrix. Addition of Cr(III) changes the morphology of the crystals for the dried droplet method, Figure 5.6(b) and the thin-layer method with Cr(III) and matrix premixed, Figure 5.6(e). A decrease in the extent of aggregation is observed for the sample. This is also observed with 2-NPG, Figure 5.5, and sDHB, Figure 5.10. Addition of Cr(III) improves the uniformity of the crystals using the thin-layer method with Cr(III) and matrix premixed. Improved crystal uniformity has been linked to better shot-to-shot reproducibility in MALDI,[13,29] but it does not account for day-to-day irreproducibility. Determining whether Cr(III) is the actual cause for the increase in signal intensity observed for substance P acid, which already forms abundant $[M + H]^+$ by MALDI, is difficult.

Heptaalanine amide (A7-NH_2,), a neutral peptide that increased in peptide signal intensity with the addition of Cr(III) in ESI, was analyzed with the nine matrices. A7-NH_2 was selected for

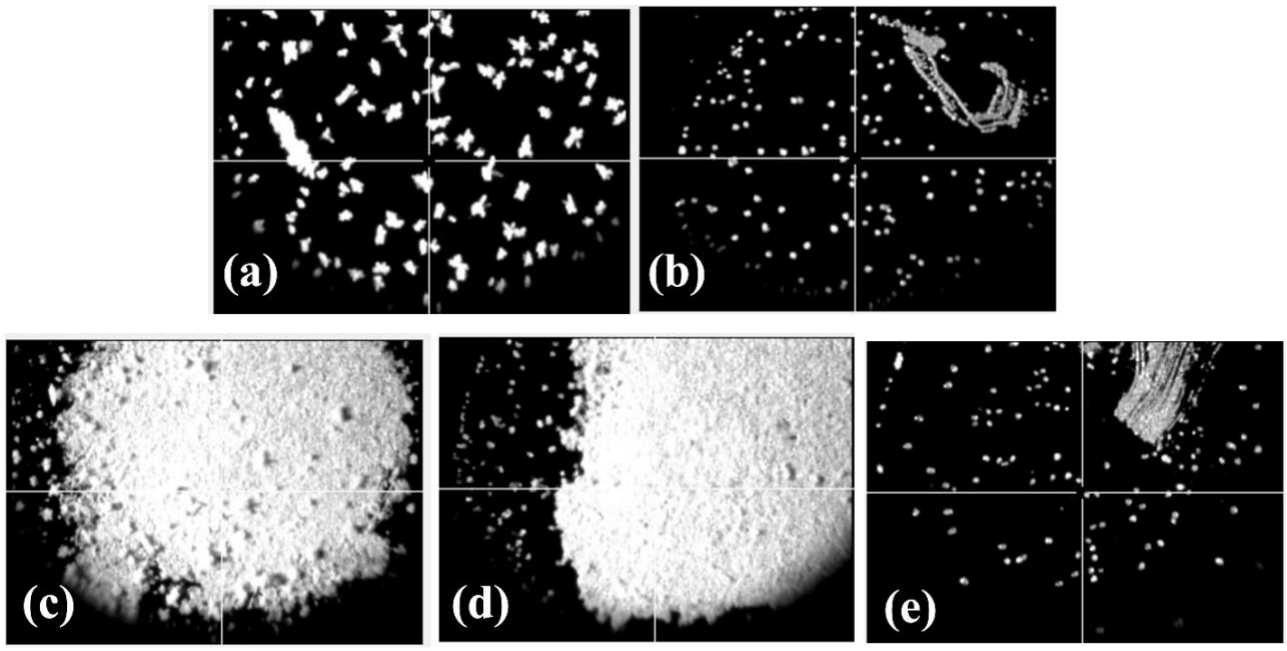

Figure 5.2. Photographic MALDI target plate images of substance P acid using the matrix CHCA. The sample was spotted using the dried droplet method with (a) no Cr(III) and (b) Cr(III), the thin-layer method with (c) no Cr(III) and (d) Cr(III) as a separate layer, and (e) no Cr(III) and matrix mix as a layer.

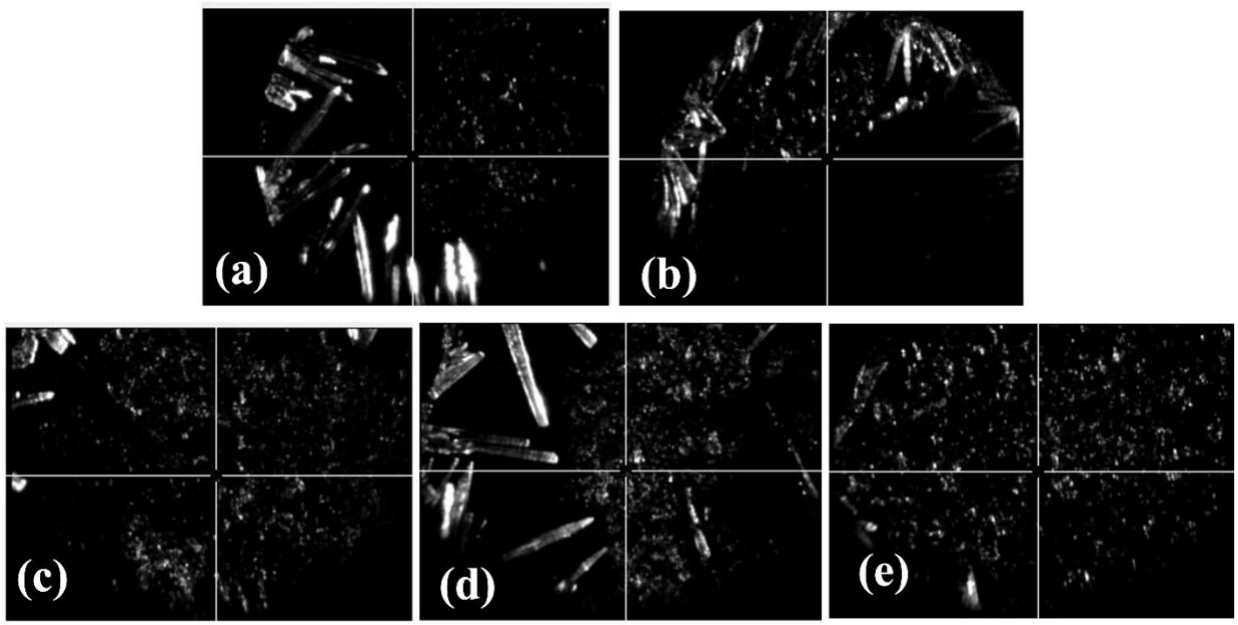

Figure 5.3. Photographic MALDI target plate images of substance P acid using the matrix DHB. The sample was spotted using the dried droplet method with (a) no Cr(III) and (b) Cr(III), the thin-layer method with (c) no Cr(III) and (d) Cr(III) as a separate layer, and (e) no Cr(III) and matrix mix as a layer.

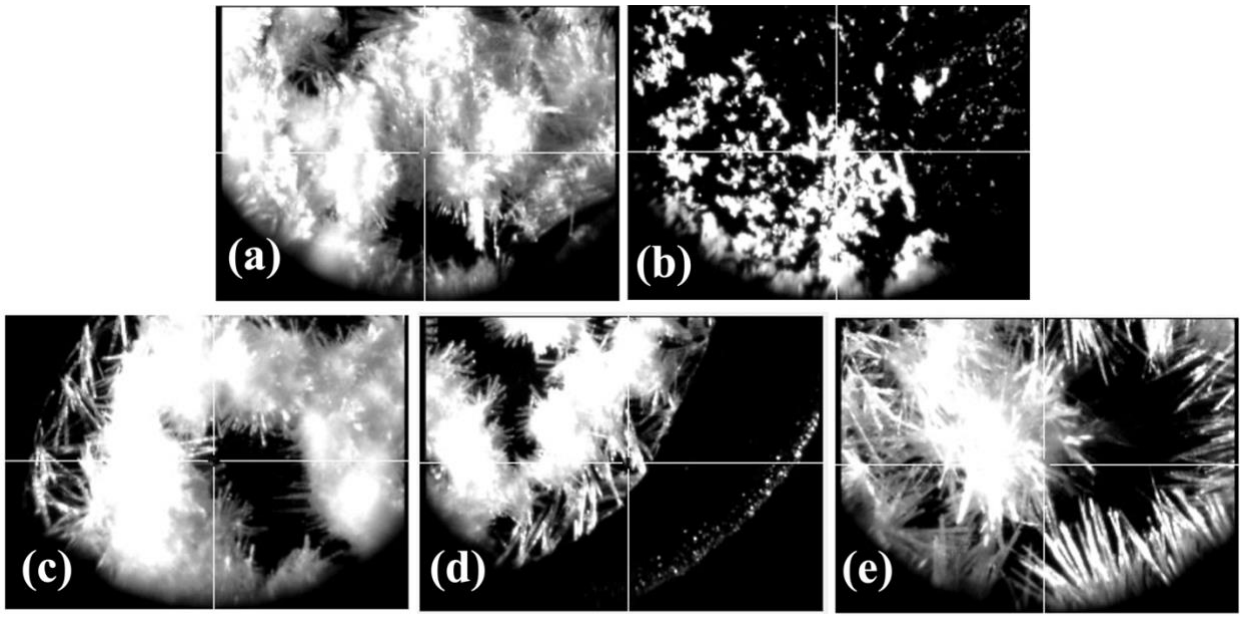

Figure 5.4. Photographic MALDI target plate images of substance P acid using the matrix MSA. The sample was spotted using the dried droplet method with (a) no Cr(III) and (b) Cr(III), the thin-layer method with (c) no Cr(III) and (d) Cr(III) as a separate layer, and (e) no Cr(III) and matrix mix as a layer.

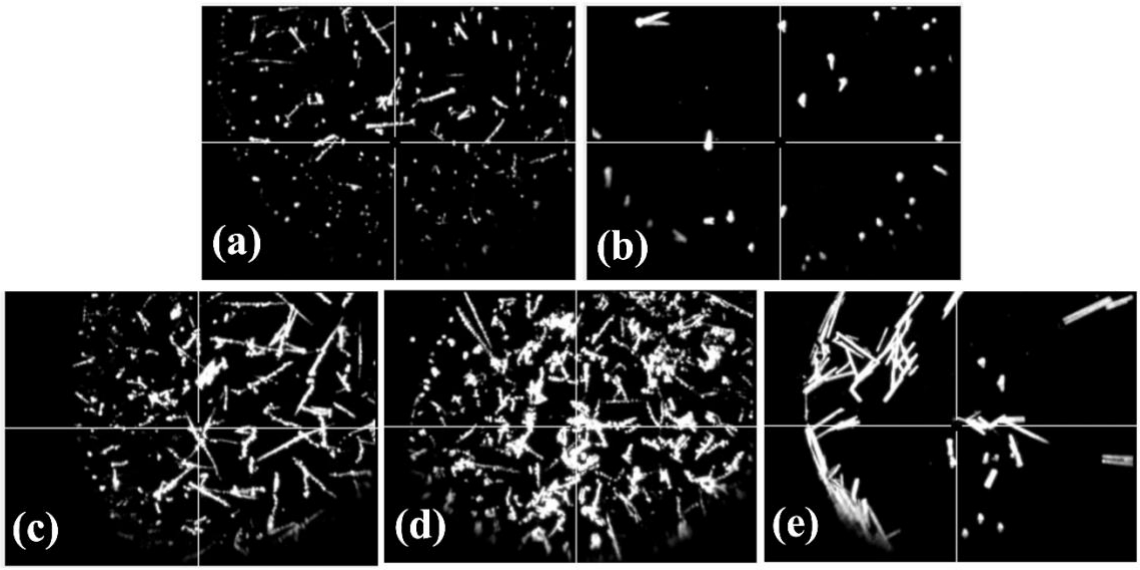

Figure 5.5. Photographic MALDI target plate images of substance P acid using the matrix 2-NPG. The sample was spotted using the dried droplet method with (a) no Cr(III) and (b) Cr(III), the thin-layer method with (c) no Cr(III) and (d) Cr(III) as a separate layer, and (e) no Cr(III) and matrix mix as a layer.

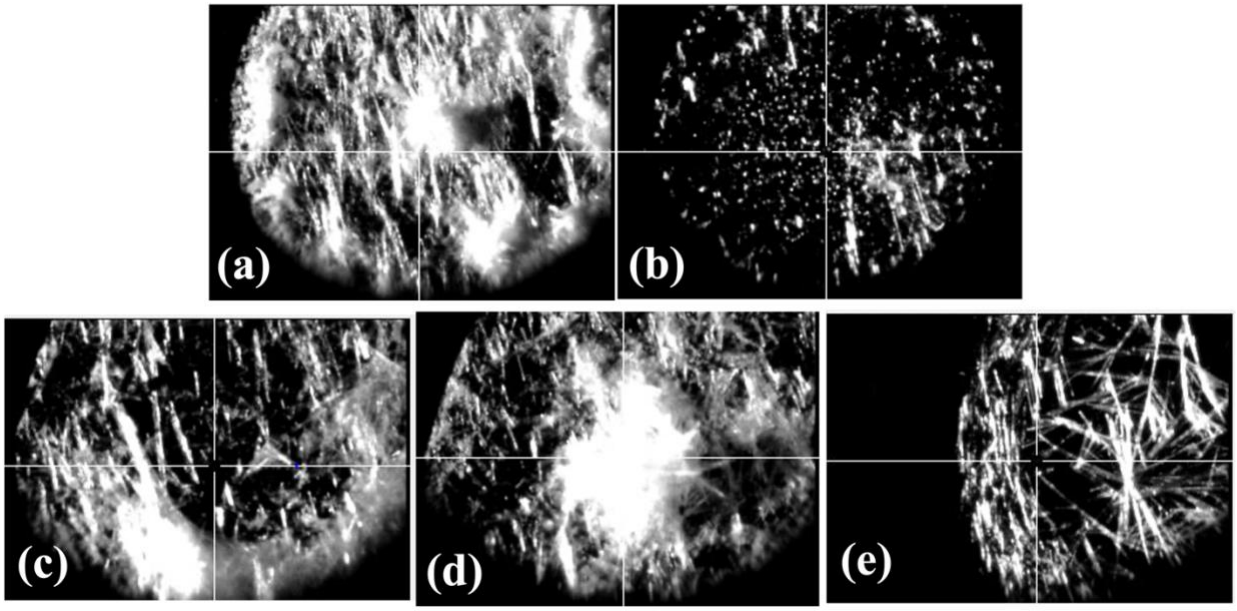

Figure 5.6. Photographic MALDI target plate images of substance P acid using the matrix THAP. The sample was spotted using the dried droplet method with (a) no Cr(III) and (b) Cr(III), the thin-layer method with (c) no Cr(III) and (d) Cr(III) as a separate layer, and (e) no Cr(III) and matrix mix as a layer.

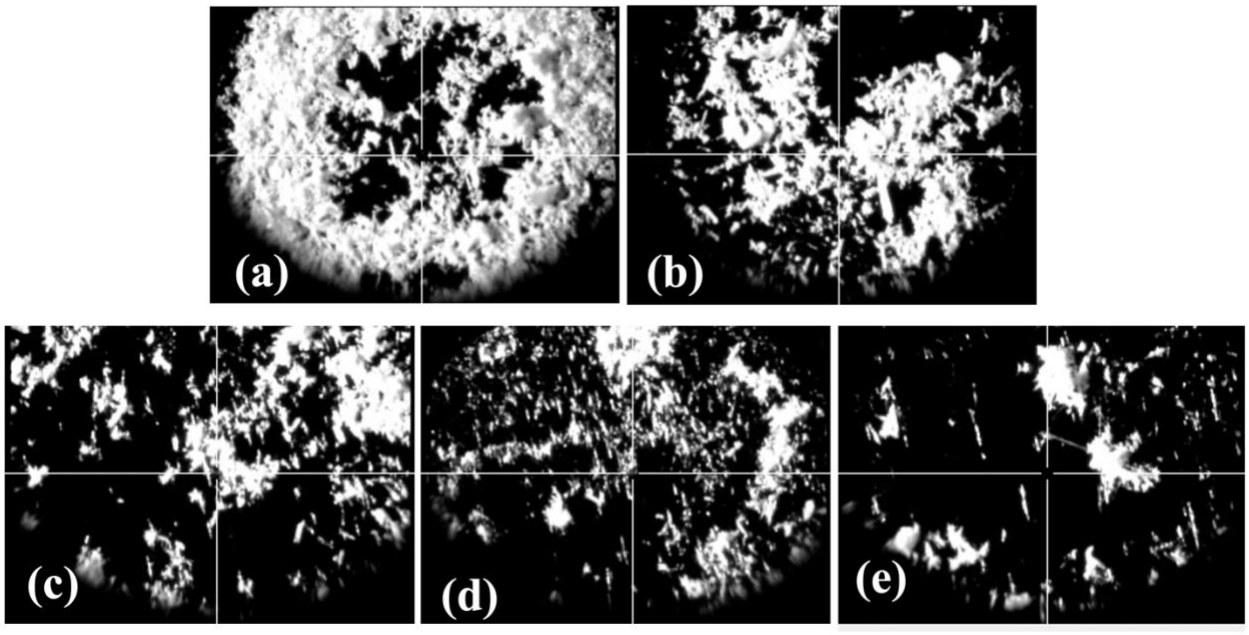

Figure 5.7. Photographic MALDI target plate images of substance P acid using the matrix NNA. The sample was spotted using the dried droplet method with (a) no Cr(III) and (b) Cr(III), the thin-layer method with (c) no Cr(III) and (d) Cr(III) as a separate layer, and (e) no Cr(III) and matrix mix as a layer.

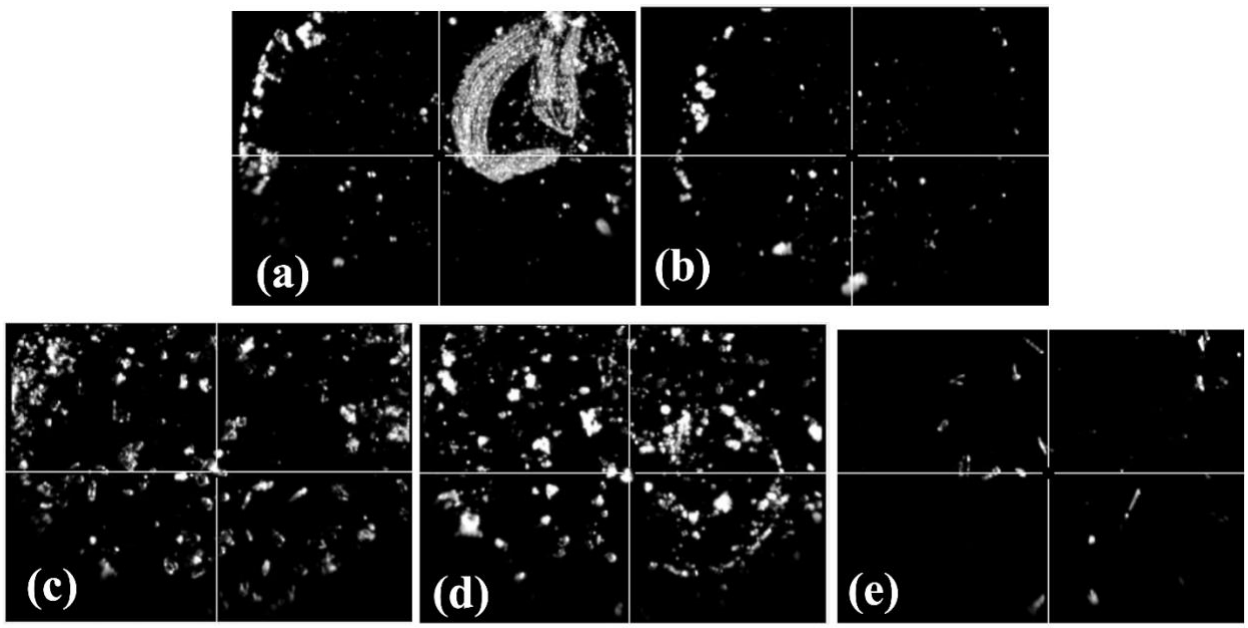

Figure 5.8. Photographic MALDI target plate images of substance P acid using the matrix HNBA. The sample was spotted using the dried droplet method with (a) no Cr(III) and (b) Cr(III), the thin-layer method with (c) no Cr(III) and (d) Cr(III) as a separate layer, and (e) no Cr(III) and matrix mix as a layer.

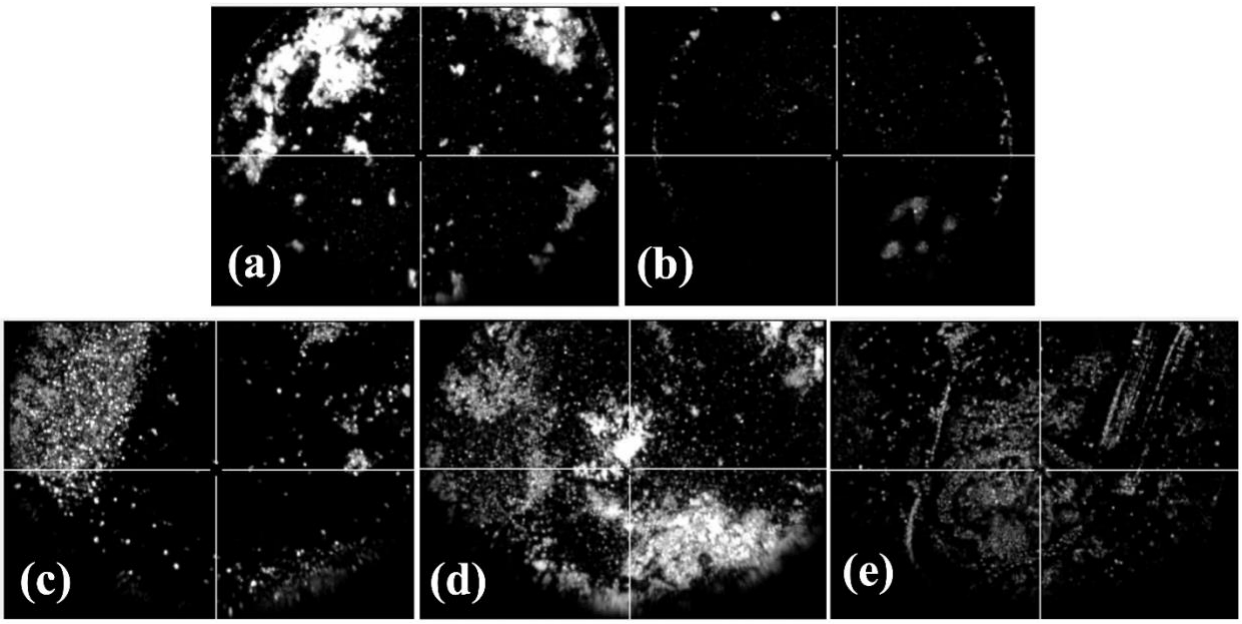

Figure 5.9. Photographic MALDI target plate images of substance P acid using the matrix BNA. The sample was spotted using the dried droplet method with (a) no Cr(III) and (b) Cr(III), the thin-layer method with (c) no Cr(III) and (d) Cr(III) as a separate layer, and (e) no Cr(III) and matrix mix as a layer.

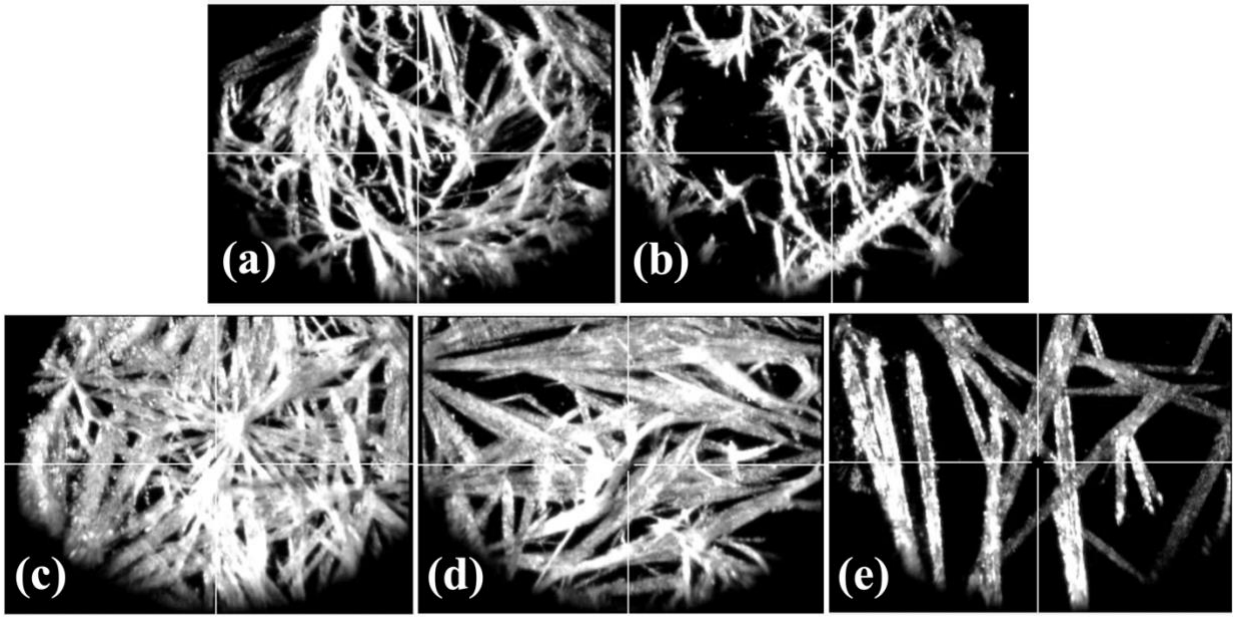

Figure 5.10. Photographic MALDI target plate images of substance P acid using the matrix sDHB. The sample was spotted using the dried droplet method with (a) no Cr(III) and (b) Cr(III), the thin-layer method with (c) no Cr(III) and (d) Cr(III) as a separate layer, and (e) no Cr(III) and matrix mix as a layer.

study because it does not form abundant $[M + H]^+$ by MALDI in the absence of Cr(III). When using NNA, BNA, and THAP as the matrix, no peptide-related ions were observed for A7-NH_2 without and with Cr(III) regardless of the method used to spot the sample. The remaining matrices, produces inconsistent results when using the dried droplet and thin-layer methods. Thus, Cr(III) had no effect on the protonation of A7-NH_2.

The mechanism for Cr(III)-enhanced protonation in ESI may not be applicable to MALDI, because the processes proceed by different mechanisms. The mechanism of ion formation in MALDI is not yet completely understood and may involve multiple processes. Currently two proposed models for ion formation in MALDI exist.[30] The photoexcitation/pooling model assumes that the analyte is neutral when incorporated with the matrix during crystallization.[30,31] Photoionization of the matrix molecules is the first step leading to ionization of the analyte by charge transfer. The more recent model is the cluster model, also termed the "lucky survivor model," which has been studied with proteins.[4,32,33] In this model, ions are said to be preformed and incorporated into the matrix crystal. After laser ablation, clusters including the precharged ions, matrix, and solvent are desorbed off the target plate. Secondary reactions can occur within the laser plume, which includes proton, cation, or electron transfer. Evidence of the cluster model involves MALDI-MS on pH indicator dyes that maintained their pH and, thus, charge state from solution.[34] If the peptide is incorporated into the peptide/matrix crystal as a charged species, then Cr(III) may not impact ionization in MALDI in the manner that it does for ESI. Cr(III) does improve crystal formation of substance P acid using some matrices and can, therefore, make finding "sweet spots" (locations on the sample surface that generate intense ions) less challenging. However, this is dependent on the sample because,

for example, A7-NH_2 did not show any improvement in crystal formation or protonation with Cr(III).

5.4 Conclusions

Ion formation by MALDI is heavily influenced by sample preparation, including the choice of matrix and the method of depositing the sample on the target plate. This often leads to MALDI being an arbitrary process of trial and effort for finding the best method of analyzing a particular analyte. Even when a new method is established, MALDI suffers from poor shot-to-shot and sample-to-sample reproducibility that makes quantitative MALDI difficult. In this study, where ion intensity is being compared, reproducibility is important because of the need to conclusively determine if there is an effect from adding Cr(III). Although an increase in intensity of $[M + H]^+$ is observed for substance P acid using 2-NPG, THAP, and sDHB, the variation in signal intensity is broad and makes it difficult to determine if the increase is due to Cr(III) or to finding a sweet spot on the sample surface. No increase in signal intensity is observed with A7-NH2, which does not readily ionize in MALDI, when Cr(III) is added. Therefore, whether Cr(III) enhances ionization is still not understood, which may be due in part to a lack of a universal understanding of ion formation in MALDI. Cr(III) was seen to improve crystal formation using sDHB, 2-NPG, and THAP for substance P acid, but no improvement was observed for A7-NH_2. Consequently, Cr(III) cannot be recommended as a protonation additive for MALDI.

References

1. Tanaka, K.; Waki, H.; Ido, Y.; Akita, S.; Yoshida, Y.; Yohida, T. Protein and Polymer Analyses Up to M/Z 100,000 by Laser Ionization Time-of-Flight Mass Spectrometry. *Rapid Commun. Mass Spectrom.* **1988**, *2*, 151-153.

2. Karas, M.; Bachmann, D.; Hillenkamp, F. Influence of the Wavelength in High-Irradiance Ultraviolet-Laser Desorption Mass-Spectrometry of Organic-Molecules. *Anal. Chem.* **1985**, *57*, 2935-2939.

3. Bich, C.; Zenobi, R. Mass Spectrometry of Large Complexes. *Curr. Opin. Struct. Biol.* **2009**, *19*, 632-639.

4. Karas, M.; Gluckmann, M.; Schafer, J. Ionization in Matrix-Assisted Laser Desorption/Ionization: Singly Charged Molecular Ions are the Lucky Survivors. *J. Mass Spectrom.* **2000**, *35*, 1-12.

5. Karas, M.; Hillenkamp, F. Laser Desorption Ionization of Proteins with Molecular Masses Exceeding 10,000 Daltons. *Anal. Chem.* **1988**, *60*, 2299-2301.

6. Hoffmann, E. d.; Stroobant, V. *Mass Spectrometry Principles and Applications;* John Wiley & Sons, Ltd: New York, 2007.

7. Leopold, J.; Popkova, Y.; Engel, K. M.; Schiller, J. Recent Developments of Useful MALDI Matrices for the Mass Spectrometric Characterization of Lipids. *Biomolecules* **2018**, *8*, 173.

8. Steven, C. L.; Brian, C. T. Influence of Matrix Solution Conditions on the MALDI-MS Analysis of Peptides and Proteins. *Anal. Chem.* **1996**, *68*, 31-37.

9. Zhang, C.; Zhang, H.; Litchfield, D. W.; Yeung, K. K. CHCA Or DHB? Systematic Comparison of the Two most Commonly used Matrices for Peptide Mass Fingerprint Analysis with MALDI-MS. *Spectroscopy* **2010**, *25*, 48-55.

10. Jing, X. Investigations involving proton/hydrogen transfer in peptides using mass spectrometry. Ph.D. Dissertation, University of Alabama, Tuscaloosa, AL, 2020.

11. Perkins, T.; Puckett, S.; Cassady, C. J. University of Alabama, Tuscaloosa, AL. Unpublished work, **2017.**

12. Wilkinson, W. R.; Gusev, A. I.; Proctor, A.; Houalla, M.; Hercules, D. M. Selection of Internal Standards for Quantitative Analysis by Matrix-Assisted Laser Desorption-Ionization (MALDI) Time-of-Flight Mass Spectrometry. *Fresenius J. Anal. Chem.* **1997**, *357*, 241-248.

13. Nicola, A. J.; Gusev, A. I.; Proctor, A.; Jackson, E. K.; Hercules, D. M. Application of the Fast-evaporation Sample Preparation Method for Improving Quantification of Angiotensin II by Matrix-assisted Laser Desorption/Ionization. *Rapid Commun. Mass Spectrom.* **1995**, *9*, 1164-1171.

14. Garden, R. W.; Sweedler, J. V. Heterogeneity within MALDI Samples as Revealed by Mass Spectrometric Imaging. *Anal. Chem.* **2000**, *72*, 30-36.

15. Dai, Y.; Whittal, R. M.; Li, L. Confocal Fluorescence Microscopic Imaging for Investigating the Analyte Distribution in MALDI Matrices. *Int. J. Comput. Vis.* **1996**, *18*, 2494-2500.

16. Dai, Y.; Whittal, R. M.; Li, L. Two-Layer Sample Preparation: A Method for MALDI-MS Analysis of Complex Peptide and Protein Mixtures. *Anal. Chem.* **1999**, *71*, 1087-1091.

17. Onnerfjord, P.; Ekström, S.; Bergquist, J.; Nilsson, J.; Laurell, T.; Marko-Varga, G. Homogeneous Sample Preparation for Automated High Throughput Analysis with Matrix-Assisted Laser Desorption/Ionisation Time-of-Flight Mass Spectrometry. *Rapid Commun. Mass Spectrom.* **1999**, *13*, 315-322.

18. Fenyo, D.; Wang, Q.; Degrasse, J. A.; Padovan, J. C.; Cadene, M.; Chait, B. T. MALDI Sample Preparation: The Ultra Thin Layer Method. *J. Vis. Exp.* **2007**, *3*, 192.

19. Garcia, B. A.; Heaney, P. J.; Tang, K. Improvement of the MALDI-TOF Analysis of DNA with Thin-Layer Matrix Preparation. *Anal. Chem.* **2002**, *74*, 2083-2091.

20. Dreisewerd, K. Recent Methodological Advances in MALDI Mass Spectrometry. *Anal. Bioanal. Chem.* **2014**, *406*, 2261-2278.

21. Trimpin, S.; Ren, Y.; Wang, B.; Lietz, C. B.; Richards, A. L.; Marshall, D. D.; Inutan, E. D. Extending the Laserspray Ionization Concept to Produce Highly Charged Ions at High Vacuum on a Time-of-Flight Mass Analyzer. *Anal. Chem.* **2011**, *83*, 5469-5475.

22. Inutan, E. D.; Wager-Miller, J.; Mackie, K.; Trimpin, S. Laserspray Ionization Imaging of Multiply Charged Ions using a Commercial Vacuum MALDI Ion Source. *Anal. Chem.* **2012**, *84*, 9079-9084.

23. Choi, H.; Lee, D.; Kim, Y.; Nguyen, H.; Han, S.; Kim, J. Effects of Matrices and Additives on Multiple Charge Formation of Proteins in MALDI–MS Analysis. *J. Am. Soc. Mass Spectrom.* **2019**, *30*, 1174-1178.

24. Chen, B.; Lietz, C. B.; Li, L. In Situ Characterization of Proteins using Laserspray Ionization on a High-Performance MALDI-LTQ-Orbitrap Mass Spectrometer. *J. Am. Soc. Mass Spectrom.* **2014**, *25*, 2177-2180.

25. Distler, A. M.; Allison, J. 5-Methoxysalicylic Acid and Spermine: A New Matrix for the Matrix-Assisted Laser Desorption/Ionization Mass Spectrometry Analysis of Oligonucleotides. *J. Am. Soc. Mass Spectrom.* **2001**, *12*, 456-462.

26. Lee, D.; Cha, S. 5-Methoxysalicylic Acid Matrix for Ganglioside Analysis with Matrix-Assisted Laser Desorption/Ionization Mass Spectrometry. *J. Am. Soc. Mass Spectrom.* **2015**, *26*, 522-525.

27. Lee, C.; Ni, C. Soft Matrix–Assisted Laser Desorption/Ionization for Labile Glycoconjugates. *J. Am. Soc. Mass Spectrom.* **2019**, *30*, 1455-1463.

28. Karas, M.; Ehring, H.; Nordhoff, E.; Stahl, B.; Strupat, K.; Hillenkamp, F.; Grehl, M.; Krebs, B. Matrix-Assisted Laser Desorption/Ionization Mass Spectrometry with Additives to 2,5-Dihydroxybenzoic Acid. *Org. Mass Spectrom.* **1993**, *28*, 1476-1481.

29. Duncan, M. W.; Roder, H.; Hunsucker, S. W. Quantitative Matrix-Assisted Laser Desorption/Ionization Mass Spectrometry. *Brief. funct. genomics proteomics* **2008**, *7*, 355-370.

30. Hillenkamp, F.; Karas, M. *MALDI MS: A Practical Guide to Instrumentation, Methods, and Applications;* Wiley-VCH GmbH: Germany, 2007.

31. Ehring, H.; Karas, M.; Hillenkamp, F. Role of Photoionization and Photochemistry in Ionization Processes of Organic Molecules and Relevance for Matrix-Assisted Laser Desorption Ionization Mass Spectrometry. *Org. Mass Spectrom.* **1992**, *27*, 472-480.

32. Knochenmuss, R. Ion Formation Mechanisms in UV-MALDI. *Analyst* **2006**, *131*, 966-986.

33. Karas, M.; Kruger, R. Ion Formation in MALDI: The Cluster Ionization Mechanism. *Chem. Rev.* **2003**, *103*, 427-439.

34. Krüger, R.; Pfenninger, A.; Fournier, I.; Glückmann, M.; Karas, M. Analyte Incorporation and Ionization in Matrix-Assisted Laser Desorption/Ionization Visualized by pH Indicator Molecular Probes. *Anal. Chem.* **2001**, *73*, 5812-5821.

CHAPTER 6. THE SCOPE OF ENHANCED PROTONATION OF BIOMOLECULES WITH TRIVALENT CHROMIUM IN ELECTROSPRAY IONIZATION

6.1 Introduction

The ability of trivalent chromium, Cr(III), to generate new charge states with acidic and neutral model peptides or increase the intensity for charge states normally produced by electrospray ionization (ESI) of basic peptides is a novel aspect.[1-4] Model peptides (and a few biological peptides) have been used to demonstrate the analytical utility of Cr(III) in enhancing ionization and proposing the mechanism of protonation in ESI. Many of the model peptides used had a limited number of sidechain functional groups. Biological peptides are composed of a myriad of sidechains that can interact with one another and influence the structure and function of the peptide.[5-7] Conformational preferences are dependent on intramolecular interactions (i.e., hydrogen bonding, van der Waals interactions, and electrostatic interactions) between amino acid sidechains.[5,8,9] With model peptides, this aspect of intramolecular interactions is limited. Thus, to gage the analytical utility of Cr(III) in proteomic research, commonly studied peptides with biological activity should be studied.

Along with biological peptides, this chapter will discuss the effect of Cr(III) in enhancing the ionization of other biomolecules. In the published mechanism discussed in Chapter 3,[4] oxygen atoms were shown to be coordination sites for Cr(III). In fact, oxygen atoms bind strongly to Cr(III). This suggests that molecules containing oxygen, which many biomolecules possess, can potentially be good candidates for Cr(III) enhanced protonation in ESI. Lipids are a

diverse group of biological molecules that are soluble in organic solvents, but insoluble in water.[10] Fatty acids are a class of lipids that contain a carboxylic acid functional group with a long-chain hydrocarbon side group. Sterols, another category of lipid, contain four fused saturated rings called cyclopentanoperhydrophenanthrene and a polar hydroxyl group. Most lipids are ionized in the negative ion mode where hydroxyl and carboxyl groups can be deprotonated; in the positive ion mode, derivatizations are typically performed to increase signal intensity.[11-13] Another class of biomolecules, carbohydrates, consist of monosaccharides containing hydroxyl functional groups linked together by glycosidic bonds. Carbohydrates are an essential component of all living organisms.[10] Similar to lipids, carbohydrates are often difficult to protonate in positive ion mode ESI. Derivatization and metalation are commonly performed for ESI analysis of carbohydrates.[14-16]

The work in this chapter will explore the scope of Cr(III) enhanced protonation of a range of biological peptides and will investigate the effects of Cr(III) on the analysis of fatty acids, sterols, and polysaccharides in positive ion mode ESI-MS.

6.2 Experimental

6.2.1 Peptides

All commercial peptides were obtained from either Alfa Aesar (Haverhill, MA, USA) or Bachem (Torrance, CA, USA) except as noted. Substance P free acid was purchased from ThermoFisher (Waltham, MA, USA). Des-Arg^{14}-Glu^{1}-fibrinopeptide B and EDDpYDEEN, were custom synthesized by Biomatik (Cambridge, ON, Canada). All solvents were purchased from VWR (Radnor, PA, USA). Chromium(III) nitrate nonahydrate came from Acros Organics (Fair Lawn, NJ, USA).

6.2.2 Mass spectrometry

The ESI experiments were performed on a Bruker (Billerica, MA, USA) HCTultra PTM Discovery System high-capacity quadrupole ion trap (QIT) mass spectrometer. Samples were directly infused at a flow rate of 3 μL/min into an ESI source with a grounded needle and a voltage of -4.0 kV (positive ion mode) applied to the capillary entrance and end plate. Nitrogen served as both the nebulizer gas and the drying gas. The drying gas had a flow rate of 5-10 L/min and a temperature of 300°C. The nebulizer gas pressure was between 5-10 psi. All spectra shown are the result of signal averaging 300 scans. Reported absolute intensity values are from three replicates obtained on three different days. Final analyte solutions studied were 1-5 μM in 50:50 [v/v] acetonitrile: Milli-Q water. Peptides were mixed with Cr(III) in a 1:10 molar ratio.

6.3 Results and discussion

6.3.1 Biological peptide survey

For this work, a total of 27 biological peptides were studied. Table 6.1 contains the amino acid sequences of all peptides included in the study. Table 6.2 contains the absolute intensities for peptide ions generated by ESI. The addition of Cr(III) to the peptides fibrinopeptide B, des-Arg^{14}-Glu^{1}-fibrinopeptide B, EGFR (985-966), bradykinin (2-9), and hirudin (54-65) results in an increase in the charge state (n) for $[M + nH]^{n+}$ produced by ESI.

Fibrinopeptide B, pEGVNDNEEGFFSAR, is a peptide that is cleaved from the 340 kDa protein fibrinogen.[17,18] Fibrinogen is found in human blood and the polymerization of fibrinogen after cleavage of fibrinopeptide B and A results in the formation of clots.[19] Fibrinopeptide B has a cyclized pyroglutamic acid residue, pE, at the N-terminus, one highly basic arginine (gas-phase basicity of arginine = 240 kcal/mol[20]) residue at the C-terminus, and three acidic amino acid residues within the peptide chain. The peptide forms $[M + nH]^{n+}$, n = 1 and 2 without Cr(III).

Table 6.1. Amino acid sequence and isoelectric point at pH 4.0 of peptides studied. Acidic residues are highlighted in red and basic residues in blue.

Peptide Name	Sequence	Isoelectric Point at pH 4.0[a]
EDDpYDEEN	EDDpYDEEN	-3.03
Des-Arg^{14}-Glu^{1}-fibrinopeptide B	EGVNDNEEGFFSA	-1.05
Glu^{1}-fibrinopeptide B	EGVNDNEEGFFSAR	-0.207
Fibrinopeptide B	pEGVNDNEEGFFSAR	-0.789
EGFR (985-996)	DVVDADEYLIPQ	-1.65
Bradykinin (2-9)	PPGFSPFR	1.20
Bradykinin	RPPGFSPFR	2.20
MUC5AC, analog I fragment	GTTPSPVPTTSTTSAP	0.199
PreproVIP (156-170)	SSEGESPDFPEELEK	-0.587
Hirudin (54-65)	GDFEEIPEEYLQ	-1.25
ACTH (22-39)	VYPNGAEDESAEAFPLEF	-1.03
Somatostatin	AGCKNFFWKTFTSC	2.11
ACTH (1-10)	SYSMEHFRWG	2.06
β -amyloid protein (1-11)	DAEFRHDSGYE	0.619
Amylin (20-29)	SNFGAILSS	0.286
Chemerin (149-157)	YFPGQFAFS	0.286
WP9QY, TNF-alpha antagonist	YCWSQYLCY	0.281
Caerulein	pEQDYTGWMDF-NH_2	0.0727
CEBVB (280-288)	GLCTLVAML	0.346
Angiotensin II	EGVYVHPV	0.900
α-mating factor	WHWLQL	1.34
Gastrin amide	pEGPWLEEEEEAYGWMDF-NH_2	-1.78
Human gastrin (1-14)	pEGPWLEEEEEAYGW	-1.95
Substance P	RPKPQQFFGLM-NH_2	3.00
Substance P acid	RPKPQQFFGLM-OH	2.32
Angiotensin I	DRVYIHPFHL	2.60
ACTH (1-13)	SYSMEHFRWGKPV	3.05

[a]Isoelectric point at pH 4.0 was calculated using the free bioinformatic toolbox Prot pi.[21]

Table 6.2. ESI results of biological peptides studied.

Peptide Name	No Cr(III) A.I[a] x 10^6				Cr(III) A.I x 10^6					
	$[M + H]^+$	$[M + 2H]^{2+}$	$[M + 3H]^{3+}$	$[M +nH]^{n+}$ to $[M + (n-1)H]^{(n-1)+}$ Ratio[b]	$[M + H]^+$	$[M + 2H]^{2+}$	$[M + 3H]^{3+}$	$[M + Cr]^{3+}$	$[M + Cr - H]^{2+}$	$[M +nH]^{n+}$ to $[M + (n-1)H]^{(n-1)+}$ Ratio
EDDpYDEEN	0.6 ± 0.2 [c]	0	0	- [d]	0	0	0	0.44 ± 0.06	0.30 ± 0.01	-
Des-Arg^{14}-Glu^{1}-fibrinopeptide B	7.5 ± 1.8	65 ± 6	0	-	1.1 ± 0.2	34 ± 5	5.7 ± 0.5	20 ± 3	6.9 ± 1.6	0.17 ± 0.01
Glu^{1}-fibrinopeptide B	0	17 ± 6	2.0 ± 0.0	0.13 ± 0.05	0	3.9 ± 1.2	2.4 ± 0.5	0	0	0.64 ± 0.07
Fibrinopeptide B	0.15 ± 0.07	1.7 ± 1.4	0	-	0.01 ± 0.01	7.3 ± 0.9	0.4 ± 0.1	9.1 ± 1.3	2.6 ± 0.4	0.05 ± 0.01
EGFR (985-996)	6.3 ± 1.1	49 ± 6	0	-	0.5 ± 0.0	22 ± 1	6.2 ± 0.4	37 ± 4	7.0 ± 0.2	0.28 ± 0.02
Bradykinin (2-9)	0.4 ± 0.0	48 ± 2	0	-	0.1 ± 0.0	46 ± 8	0.2 ± 0.0	0	0	0.005 ± 0.001
Bradykinin	0	12 ± 2	16 ± 3	1.2 ± 0.1	0	6.6 ± 0.7	14 ± 1	0	0	2.2 ± 0.1
MUC5AC, analog I fragment	1.5 ± 0.5	21 ± 3	0.5 ± 0.1	0.03 ± 0.01	0.1 ± 0.0	12 ± 2	0.4 ± 0.1	9.9 ± 0.5	4.2 ± 0.4	0.03 ± 0.01
PreproVIP (156-170)	0	16 ± 5	1.1 ± 0.5	0.07 ± 0.01	0	3.6 ± 0.3	2.1 ± 0.1	0.8 ± 0.1	0.1 ± 0.0	0.6 ± 0.1
Hirudin (54-65)	2.4 ± 0.8	34 ± 10	0	-	0.2 ± 0.1	13 ± 2	1.7 ± 0.1	24 ± 3	4.6 ± 0.8	0.13 ± 0.01
ACTH (22-39)	1.7 ± 0.4	27 ± 8	1.7 ± 0.9	0.06 ± 0.02	0.1 ± 0.0	12 ± 2	1.2 ± 0.2	12 ± 2	3.4 ± 0.4	0.097 ± 0.001
Somatostatin	0	23 ± 0	11 ± 3	0.5 ± 0.1	0	9.5 ± 0.9	10 ± 1	0.3 ± 0.1	0	1.1 ± 0.1
ACTH (1-10)	0	19 ± 3	32 ± 4	1.7 ± 0.2	0	7.7 ± 0.6	21 ± 1	0	0	2.8 ± 0.1
β-amyloid protein (1-11)	0	12 ± 2	3.9 ± 0.8	0.34 ± 0.05	0	5.1 ± 0.6	5.4 ± 1.1	0.3 ± 0.1	0	1.1 ± 0.3
Amylin (20-29)	0	0.2 ± 0.0	0	-	0	0.9 ± 0.2	0	0.6 ± 0.1	0.1 ± 0.0	-
Chemerin (149-157)	3.9 ± 0.3	12 ± 3	0	3 ± 1	1.0 ± 0.1	27 ± 6	0	16 ± 2	4.4 ± 0.1	26 ± 3
WP9QY, TNFα αntagonist	1.3 ± 0.2	2.2 ± 0.8	0	1.7 ± 0.8	0.3 ± 0.0	6.5 ± 1.5	0	5.3 ± 0.8	2.2 ± 0.2	22 ± 4
Caerulein	0.2 ± 0.1	0.7 ± 0.1	0	5 ± 2	0.2 ± 0.1	0.3 ± 0.0	0	4.6 ± 0.7	4.8 ± 0.8	1.4 ± 0.4
CEBVB(280-288)	3.9 ± 0.8	6.4 ± 1.3	0	1.6 ± 0.1	3.6 ± 1.1	33 ±1	0	15 ± 3	5.4 ± 1.2	10 ± 2
Angiotensin II	0.4 ± 0.1	25 ± 3	0	63 ± 10	0.1 ± 0.0	17 ± 3	0	0	0	210 ± 27
α-mating factor	0.8 ± 0.1	32 ± 1	0	40 ± 3	0.4 ± 0.0	21 ± 3	0	0	0	49 ± 9

Table 6.2. continued.

Peptide Name	No Cr(III) A.I[a] x 10^6				Cr(III) A.I x 10^6					
	$[M + H]^+$	$[M + 2H]^{2+}$	$[M + 3H]^{3+}$	$[M +nH]^{n+}$ to $[M + (n-1)H]^{(n-1)+}$ Ratio[b]	$[M + H]^+$	$[M + 2H]^{2+}$	$[M + 3H]^{3+}$	$[M + Cr]^{3+}$	$[M + Cr - H]^{2+}$	$[M +nH]^{n+}$ to $[M + (n-1)H]^{(n-1)+}$ Ratio
Gastrin amide	0	0.1 ± 0.1	0	-	0	0.1 ± 0.0	0	6.9 ± 0.9	1.7 ± 0.6	-
Human gastrin (1-14)	0	1.4 ± 0.2	0	-	0	0.3 ± 0.1	0	4.3 ± 0.9	5.4 ± 0.2	-
Substance P	0	18 ± 3	24 ± 3	1.3 ± 0.2	0	14 ± 3	33 ± 8	0.3 ± 0.1	0	2.3 ± 0.2
Substance P acid	0	18 ± 2	15 ± 1	0.8 ± 0.6	0	13 ± 2	26 ± 5	0.46 ± 0.13	0	2.0 ± 0.1
	$[M +2H]^{2+}$	$[M + 3H]^{3+}$	$[M + 4H]^{4+}$	$[M +nH]^{n+}$ to $[M + (n-1)H]^{(n-1)+}$ Ratio	$[M + 2H]^{2+}$	$[M + 3H]^{3+}$	$[M + 4H]^{4+}$	$[M + Cr]^{3+}$	$[M + Cr - H]^{2+}$	$[M +nH]^{n+}$ to $[M + (n-1)H]^{(n-1)+}$ Ratio
Angiotensin I	6.0 ± 0.7	15 ± 2	3.7 ± 2.5	0.2 ± 0.1	1.8 ± 0.5	13 ± 0.9	7.5 ± 0.6	0	0	0.6 ± 0.1
ACTH(1-13)	12 ± 2	13 ± 1	8.3 ± 0.6	0.63 ± 0.04	2.6 ± 0.2	11 ± 1	25 ± 4	0	0	2.3 ± 0.1

[a]Absolute intensity
[b]n = the highest protonated charge state observed
[c]Mean ± one standard deviation from three independent replicates
[d] "-" signifies that the ratio is unable to be calculated due to lack of signal

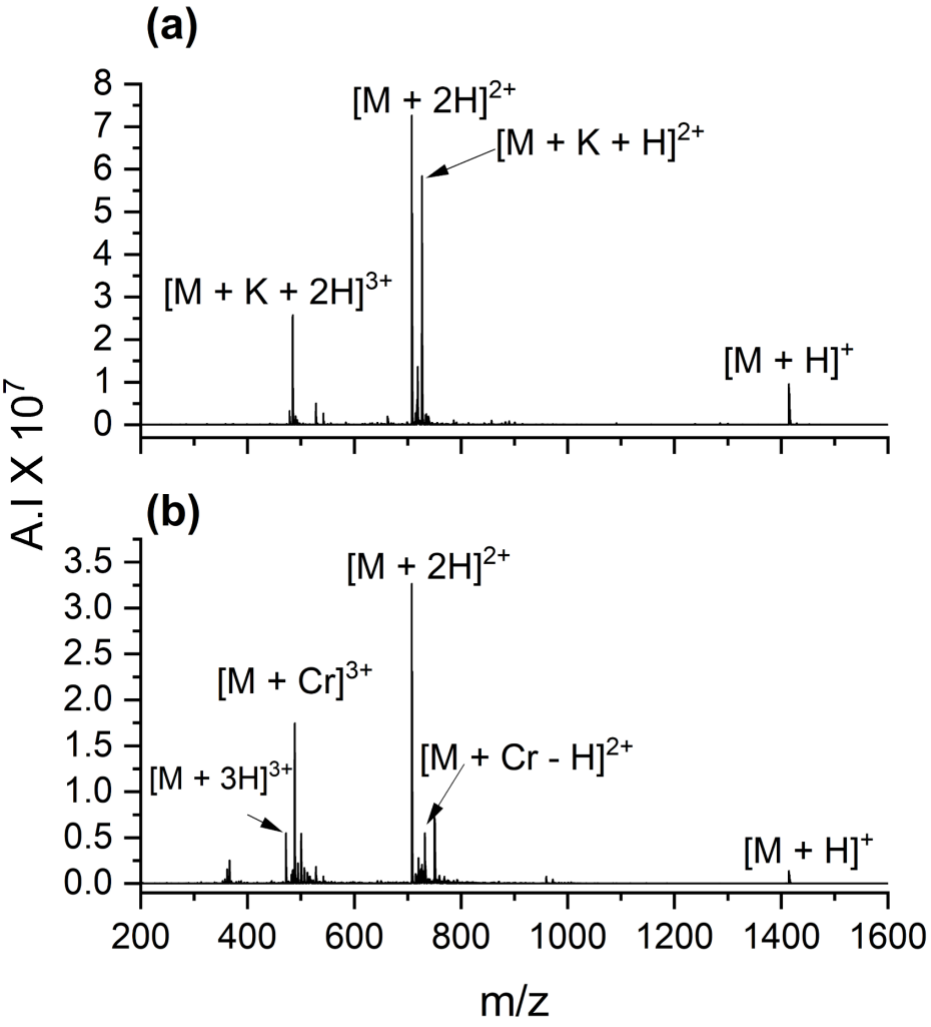

Figure 6.1. ESI mass spectra for des-Arg14-Glu1-fibrinopeptide b with (a) no Cr(III) and (b) Cr(III).

Addition of Cr(III) results in the formation of n = 3 and quadruples the overall intensity of n = 2, ,as shown in Table 6.2. Glu^{1}-fibrinopeptide B, EGVNDNEEGFFSAR, does not have the cyclized N-terminus and forms n = 1-3 without Cr(III) by ESI. Addition of Cr(III) did not form any additional charge states for this peptide.

The isoelectric point (pI) of a peptide is the pH at which the peptide exists in solution as a zwitterion. The lower and more negative the pI is the more acidic the peptide. Table 6.1 includes the pI of the peptides in this study in a solution at pH 4. The pI of des-Arg^{14}-Glu^{1}-fibrinopeptide B, fibrinopeptide B and Glu^{1}-fibrinopeptide B is -1.05, -0.789, and -0.207, respectively. Therefore, des-Arg^{14}-Glu^{1}-fibrinopeptide B is the most acidic of the three peptides. Des-Arg^{14}-Glu^{1}-fibrinopeptide B, EGVNDNEEGFFSA, has an uncyclized N-terminus and no basic arginine residue at the C-terminus. Figure 6.1 contains the ESI mass spectra for des-Arg^{14}-Glu^{1}-fibrinopeptide B in the presence and absence of Cr(III). Addition of Cr(III) to des-Arg^{14}-Glu^{1}-fibrinopeptide B results in the formation of n = 3 that is otherwise not formed by ESI. The peptide also forms the most abundant Cr(III)-adducted peptide ions when compared to fibrinopeptide B and Glu^{1}-fibrinopeptide B. The acidic nature of des-Arg^{14}-Glu^{1}-fibrinopeptide B seemingly increases its binding to Cr(III).

Epidermal growth factor receptor (EGFR) is a tyrosine kinase receptor protein that contains 1,091 residues. The protein binds the several different ligands, also called growth factors.[22,23] Binding of ligands to the receptor signals cell growth and development, tissue turnover and healing, and is essential for animal development.[23,24] Overexpression of EGFR is linked to the development of aggressive cancers in humans.[25-27] The peptide clip of EGFR, EGFR (985-966), is a highly acidic peptide whose sequence is DVVDADEYLIPQ. The peptide

has four acidic residues and no basic residues. In the absence of Cr(III), EGFR (985-966) forms $[M + nH]^{n+}$, n = 1 and 2, Figure 6.2(a). After adding Cr(III), n = 3 forms, Figure 6.2(b).

Hirudin contains 65 amino acids and is an anticoagulant agent isolated from medicinal leeches.[28] Variants of hirudin has been created and approved for clinical use for thrombotic complications.[29,30] The C-terminal end of hirudin contains multiple acidic residues. The clip hirudin (54-65), GDFEEIPEEYLQ, was included in this study because of its acidic nature. Figure 6.3 is the ESI mass spectra for this peptide clip with and without Cr(III). Similar to EGFR (985-996), hirudin (54-65) forms n = 3 only after the addition of Cr(III). Intense Cr(III)-adducted peptide ions, which are characteristic of the ESI spectra for acidic peptides with Cr(III), are also present.

Bradykinin (2-9), PPGFSPFR, was the only basic peptide in this study that adds an additional proton with Cr(III). Full sequence bradykinin, RPPGFSPFR, is a basic peptide that has been associated with inflammation and intense pain.[31,32] Bradykinin forms $[M + nH]^{n+}$, n = 2 and 3 without Cr(III), Table 6.2. No additional protons are added with Cr(III). In contrast, bradykinin (2-9), which is missing the N-terminal arginine residue, forms predominantly $[M + 2H]^{2+}$ and a small amount of $[M + H]^{+}$. Adding Cr(III) leads to the formation of a minute amount of $[M + 3H]^{3+}$.

Another basic peptide, substance P, is a neurotransmitter that is released from the central and peripheral nervous system.[33] The amino acid sequence is RPKPQQFFGLM-NH_2, and it exists naturally with an amide group at the C-terminus (i.e., as a peptide amide). Results presented in Chapter 3 showed that the peptide amides A7-NH_2 and AAAEAAA-NH_2 increased in charge state upon addition of Cr(III). Substance P and its analog substance P acid, RPKPQQFFGLM-OH, were added to this survey to determine if the same effect is observed.

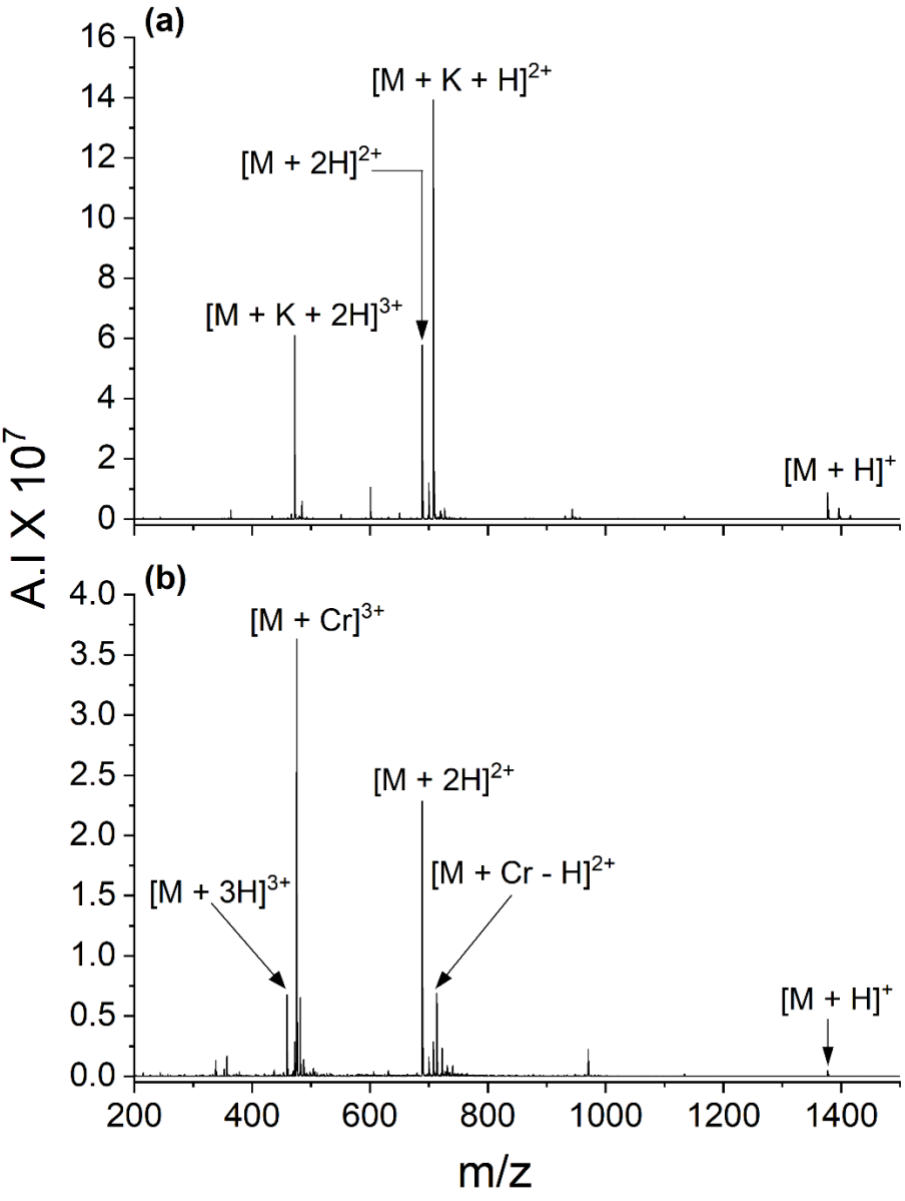

Figure 6.2. ESI mass spectra for EGFR (985-966) with (a) no Cr(III) and (b) Cr(III).

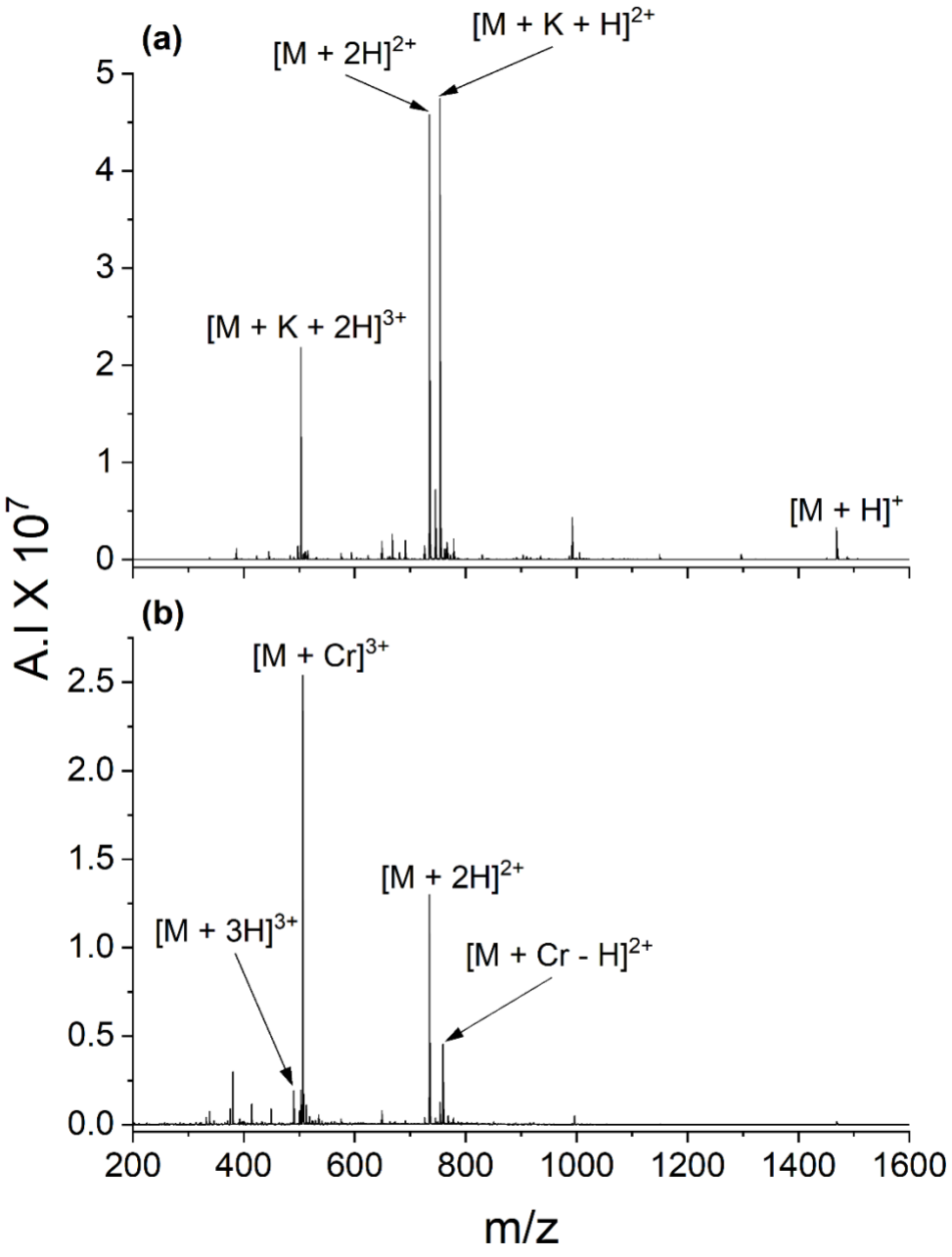

Figure 6.3. ESI mass spectra for hirudin (54-65) with (a) no Cr(III) and (b) Cr(III).

Figure 6.4 and 6.5 contains the mass spectra of substance P amide and acid, respectively. Both peptides form $[M + nH]^{n+}$, n = 2 and 3, by ESI. The addition of Cr(III) shifts the charge distribution towards n = 3 for both peptides but does not add any additional charge states. Although Cr(III) may be able to coordinate to the peptide amide, coordination to the peptide acid results in the protonation being enhanced to a greater extent. For both peptides, only low intensities of Cr(III)-adducted peptide ions form. This agrees with previous results reported by the Cassady group that concluded basic peptides form less intense Cr(III) adduct ions than acidic peptides.[1]

Two other peptide amides were included in the study: human gastrin (1-17) and caerulein. Gastrin (1-17) stimulates gastrin acid secretion and is linked to ulcer disease and gastric cancer.[34] The peptide is highly acidic and difficult to protonate in the positive ion mode but generates abundant ion signal in the negative ion mode.[35] Gastrin (1-17) contains a chain of glutamic acid (E) residues and a cyclized N-terminus pyroglutamic acid residue (pE); its sequence is pEGPWLEEEEEAYGWMDF-NH_2. A clip of the peptide, gastrin (1-14), pEGPWLEEEEEAYGW, was also included in the study. In the absence of Cr(III) both peptides form little $[M + 2H]^{2+}$. After the adding Cr(III) the intensity of $[M + 2H]^{2+}$ decreases for gastrin (1-14) and stays the same for gastrin (1-17), Table 6.2. The peptides form Cr(III)-adducted ions signifying that Cr(III) is interacting with the peptides. This suggest that the multiple carboxylic groups from the sidechain of the acidic residues located near each other may coordinate strongly with Cr(III) and inhibit Cr(III) from being released after binding. This contrasts with previous work by the Cassady group[1] where Cr(III) greatly enhances protonation and charge state for the highly acidic peptide EEEEGDD.

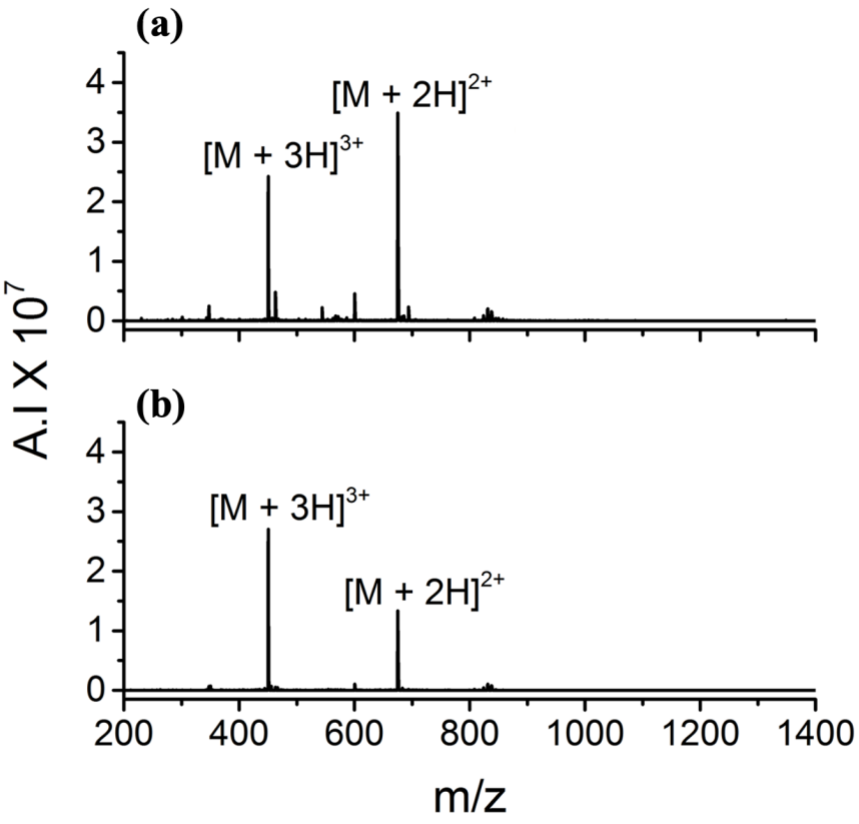

Figure 6.4. ESI mass spectra for substance P amide with (a) no Cr(III) and (b) Cr(III).

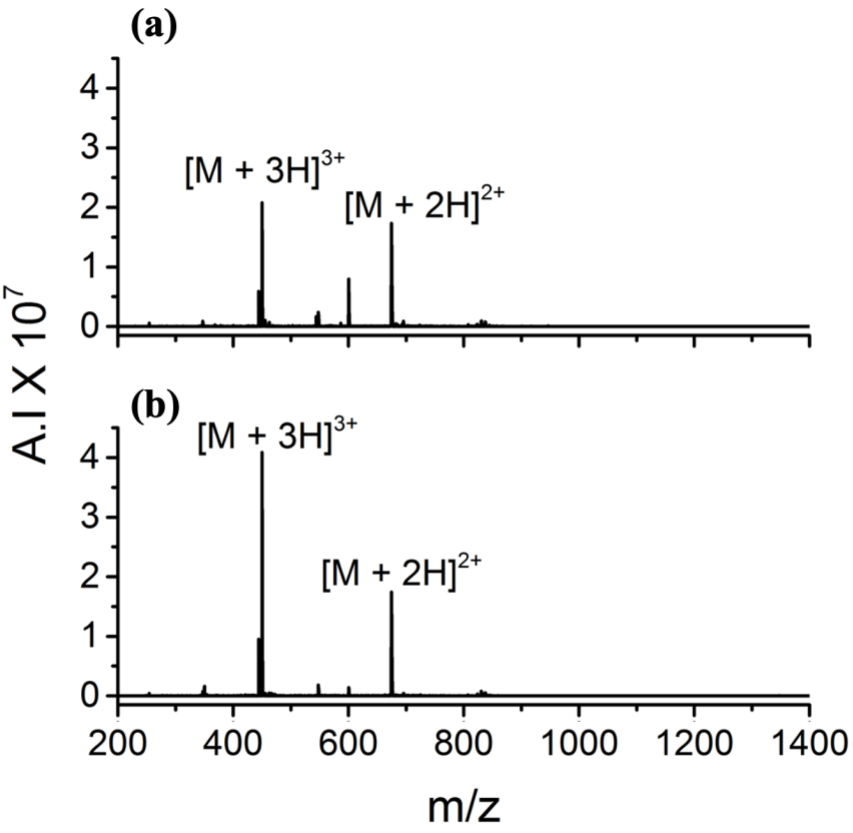

Figure 6.5. ESI mass spectra for substance P acid with (a) no Cr(III) and (b) Cr(III).

Caerulein is a peptide found in the skin of Australian amphibians that causes contractions of the gallbladder and stimulates the production of bile in the intestines. The peptide's sequence is pEQDYTGWMDF-NH_2, with the C-terminus end resembling gastrin (1-17). The tyrosine (Y) residue is sulfated with the hydroxyl group replaced by a sulfate group. In this study, the desulfated peptide is used. Similar to gastrin, caerulein is acidic and produces very little protonated ions, Table 6.2. Without Cr(III), n = 1 and 2 forms at low intensity. The addition of Cr(III) slightly decreases the signal for n = 2. Cr(III) adducted peptide ions are also present with this peptide.

Addition of Cr(III) caused an increase in the signal intensity of protonated ions typically made by ESI for six of the neutral and basic biological peptides in this study, as shown Table 6.3. WP9QY, TNFα antagonist is a neutral cyclic peptide, YCWSQYLCY, with a disulfide bond. The peptide was created to mimic tumor necrosis factor α (TNFα) and prevent binding of TNFα with its receptor.[36] Binding of TNFα to its receptor enhances production of inflammatory diseases and has been associated with rheumatoid arthritis.[37-39] Figure 6.6 is the ESI mass spectra for WP9QY, TNFα antagonist without Cr(III) and with Cr(III). The neutral peptide forms $[M + nH]^{n+}$, n = 1 and 2, by ESI, and the addition of Cr(III) increases n = 2 by a factor of three, which shifts the charge state distribution almost completely to n = 2.

An increase in intensity is also observed with adrenocorticotropic hormone clip (ACTH 1-13) after the addition of Cr(III). ACTH is a hormone that contains 39 amino acids and is produced and secreted by the pituitary gland.[40] The hormone controls the production of corticosteroids from the adrenal glands and have been used as a therapeutic in multiple ailments.[41] The clip ACTH (1-13), SYSMEHFRWGKPV, is a basic peptide with three basic residues and one acidic residue. Figure 6.7 contains the ESI mass spectra for ACTH (1-13) in the

Table 6.3. Peptides that increased in signal intensity but did not add additional protons with Cr(III).

Peptide Name	No Cr(III) A.I[a] x 10^6				Cr(III) A.I x 10^6					
	$[M + H]^+$	$[M + 2H]^{2+}$	$[M + 3H]^{3+}$	$[M +nH]^{n+}$ to $[M + (n-1)H]^{(n-1)+}$ Ratio[b]	$[M + H]^+$	$[M + 2H]^{2+}$	$[M + 3H]^{3+}$	$[M + Cr]^{3+}$	$[M + Cr - H]^{2+}$	$[M +nH]^{n+}$ to $[M + (n-1)H]^{(n-1)+}$ Ratio
WP9QY, TNF-alpha antagonist	1.3 ± 0.2	2.2 ± 0.8	0	1.7 ± 0.8	0.3 ± 0.0	6.5 ± 1.5	0	5.3 ± 0.8	2.2 ± 0.2	22 ± 4
CEBVB(280-288)	3.9 ± 0.8	6.4 ± 1.3	0	1.6 ± 0.1	3.6 ± 1.1	33 ±1	0	15 ± 3	5.4 ± 1.2	10 ± 2
Amylin (20-29)	0	0.2 ± 0.0	0	-	0	0.9 ± 0.2	0	0.6 ± 0.1	0.1 ± 0.0	-[d]
Chemerin (149-157)	3.9 ± 0.3	12 ± 3	0	3 ± 1	1.0 ± 0.1	27 ± 6	0	16 ± 2	4.4 ± 0.1	26 ± 3
Substance P acid	0	18 ± 2	15 ± 1	0.8 ± 0.6	0	13 ± 2	26 ± 5	0.46 ± 0.13	0	2.0 ± 0.1
	$[M +2H]^{2+}$	$[M + 3H]^{3+}$	$[M + 4H]^{4+}$	$[M +nH]^{n+}$ to $[M + (n-1)H]^{(n-1)+}$ Ratio	$[M + 2H]^{2+}$	$[M + 3H]^{3+}$	$[M + 4H]^{4+}$	$[M + Cr]^{3+}$	$[M + Cr - H]^{2+}$	$[M +nH]^{n+}$ to $[M + (n-1)H]^{(n-1)+}$ Ratio
ACTH(1-13)	12 ± 2	13 ± 1	8.3 ± 0.6	0.63 ± 0.04	2.6 ± 0.2	11 ± 1	25 ± 4	0	0	2.3 ± 0.1

[a]Absolute intensity

[b]n = the highest protonated charge state observed

[c]Mean ± one standard deviation from three independent replicates

[d] "-" signifies that the ratio is unable to be calculated due to lack of signal

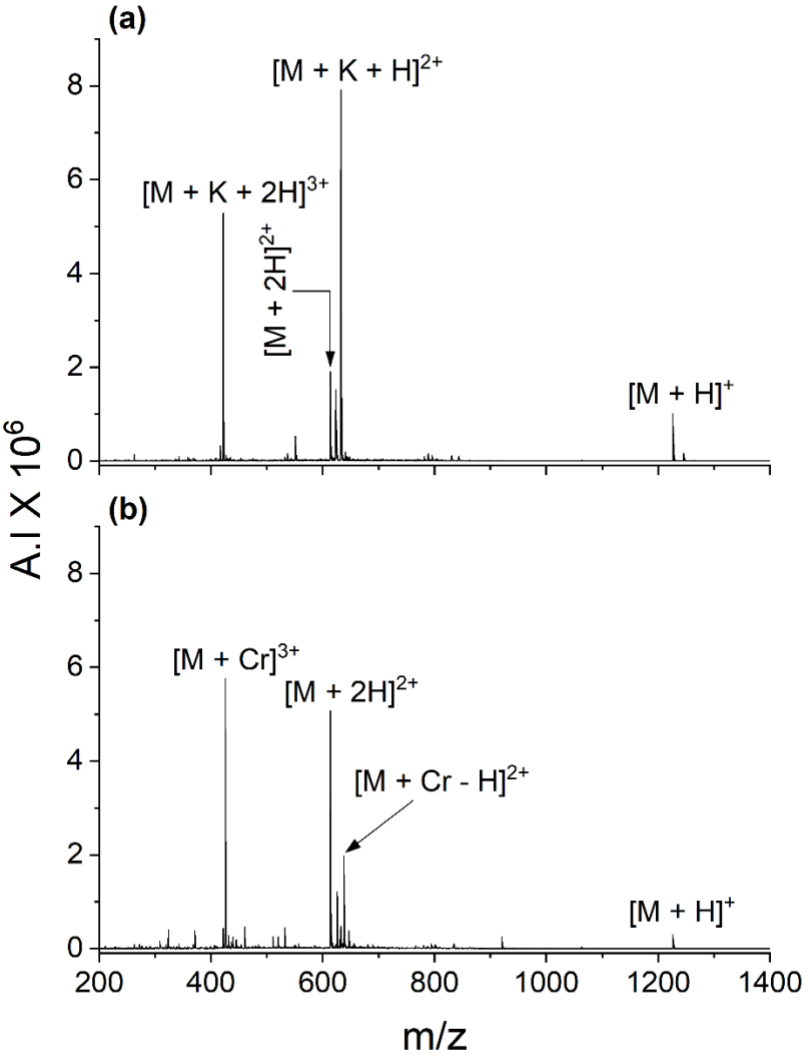

Figure 6.6. ESI mass spectra for WP9QY, TNFα antagonist with (a) no Cr(III) and (b) Cr(III).

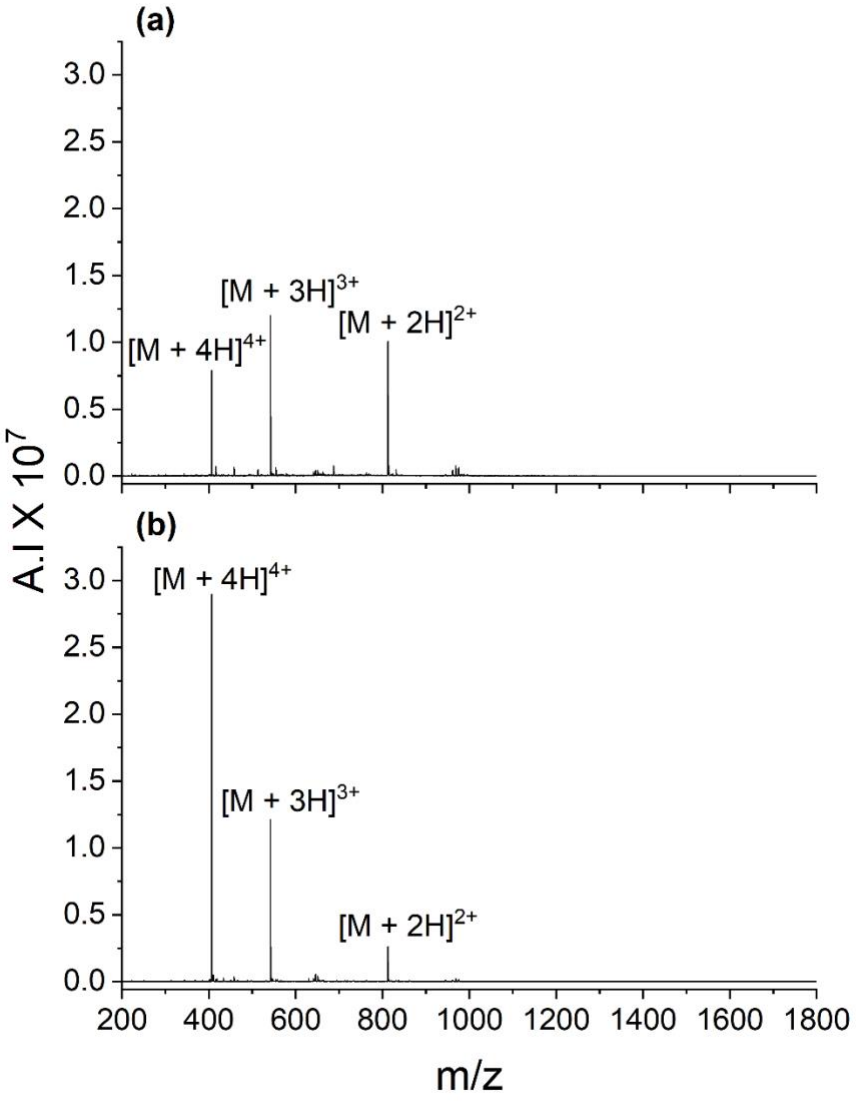

Figure 6.7. ESI mass spectra for ACTH (1-13) with (a) no Cr(III) and (b) Cr(III).

absence and presence of Cr(III). The peptide forms $[M + nH]^{n+}$, n = 2-4, without Cr(III). The addition of Cr(III) shifts the charge state distribution to n = 4 and increases the ion's intensity by three. No Cr(III) adducts form for this basic peptide.

Addition of Cr(III) to the following peptides results in a decrease in the absolute intensity of n = 2: MUC5AC analog I fragment, preproVIP (156-170), ACTH (22-39), somatostatin, β-amyloid (1-11), angiotensin II, and α-mating factor. Unlike the model peptides that were utilized in earlier studies of Cr(III) enhanced protonation, the secondary and tertiary structure of the biological peptides in this study are of higher complexity. Peptide conformations are dictated by their higher order structure. A possibility exist that the conformation of the peptides may be confining Cr(III) and not allowing for dissociation of Cr(III) from the peptide. This also can explain the decrease in intensity for $[M + 2H]^{2+}$ observed for some of the peptides in this study. The mass spectrum for these peptides contains Cr(III) adducts, which confirms the coordination of Cr(III) to the peptide. In addition, for some biological peptides the multiple O- and N-containing sidechains may be resulting in sufficiently strong coordination to inhibit release of Cr(III).

6.3.2 Other biomolecules

A previous Cassady group member, Matthew Mireles, investigated the effect of Cr(III) on lipids; Cr(III) had no impact on the protonation of oleic acid, cholic acid, cholesterol, and hydroxystearic acid.[42] Another Cassady group member, Dr. Ranelle Schaller-Duke, concluded that the addition of Cr(III) to solutions containing carbohydrates had no effect on protonation.[43]

6.4 Conclusions

Of the 27 biological peptides studied, five peptides increased in charge state and protonated ions of six peptides increased in upon addition of Cr(III). All peptides that obtain an

extra proton in the presence of Cr(III) were acidic peptides except for bradykinin (2-9). The increase in signal intensity (but not charge state) is seen with basic and neutral peptides. This is in agreeance with prior studies[1,3] in which Cr(III) was more likely to put on additional protons to acidic peptides and not basic peptides, which, instead, exhibit an increase in signal intensity. Comparison of the biological peptide acids and amides indicates that Cr(III) affects both functional groups the same. Cr(III) suppresses or have no impact on the highly acidic peptides, gastrin 1-17, gastrin 1-14, and EDDpYDEEN suggesting that maybe the presence of too many acidic residues or highly acidic phosphorylated residues may bind tightly to Cr(III) inhibiting the metal ion from dissociating from the peptide. This is evident in the presence of Cr(III) adducts that form in each case. Although Cr(III) did not improve the protonation of all of the peptides studied, it does work well with some. To the contrary, Cr(III) was not observed to increase protonation by ESI for the limited number of lipids, steroids, and carbohydrates that were studied.

References

1. Feng, C.; Commodore, J. J.; Cassady, C. J. The Use of Chromium(III) to Supercharge Peptides by Protonation at Low Basicity Sites. *J. Am. Soc. Mass Spectrom.* **2015**, *26*, 347-358.

2. Commodore, J. J.; Jing, X.; Cassady, C. J. Optimization of Electrospray Ionization Conditions to Enhance Formation of Doubly Protonated Peptide Ions with and without Addition of Chromium(III). *Rapid Commun. Mass Spectrom.* **2017**, *31*, 1129-1136.

3. Jing, X.; Edwards, K. C.; Vincent, J. B.; Cassady, C. J. The Use of Chromium(III) Complexes to Enhance Peptide Protonation by Electrospray Ionization Mass Spectrometry. *J. Mass Spectrom.* **2018**, *53*, 1198-1206.

4. Persaud, R. R.; Dieke, N. E.; Jing, X.; Lambert, S.; Parsa, N.; Hartmann, E.; Vincent, J. B.; Cassady, C. J.; Dixon, D. A. Mechanistic Study of Enhanced Protonation by Chromium(III) in Electrospray Ionization: A Superacid Bound to a Peptide. *J. Am. Soc. Mass Spectrom.* **2020**, *31*, 308-318.

5. Anfinsen Christian, B. Principles that Govern the Folding of Protein Chains. *Science* **1973**, *181*, 223-230.

6. Aebersold, R.; Mann, M. Mass Spectrometry-Based Proteomics. *Nature* **2003**, *422*, 198-207.

7. Aebersold, R.; Goodlett, D. R. Mass Spectrometry in Proteomics. *Chem. Rev.* **2001**, *101*, 269-296.

8. Chakrabarti, P.; Pal, D. The Interrelationships of Side-Chain and Main-Chain Conformations in Proteins. *Prog. Biophys. Mol. Biol.* **2001**, *76*, 1-102.

9. Dill, K. A. Dominant Forces in Protein Folding. *Biochemistry* **1990**, *29*, 7133-7155.

10. Voet, D.; Voet, J. G.; Pratt, C. W. *Fundamentals of Biochemistry: Life at the Molecular Level;* John Wiley & Sons: 2013.

11. Murphy, R. C.; Axelsen, P. H. Mass Spectrometric Analysis of Long-Chain Lipids. *Mass Spectrom. Rev.* **2011**, *30*, 579-599.

12. Wang, M.; Wang, C.; Han, R. H.; Han, X. Novel Advances in Shotgun Lipidomics for Biology and Medicine. *Prog. Lipid Res.* **2016**, *61*, 83-108.

13. Han, X.; Gross, R. W. The Foundations and Development of Lipidomics. *J. Lipid Res.* **2022**, *63*, 100164.

14. Zaia, J. Mass Spectrometry of Oligosaccharides. *Mass Spectrom. Rev.* **2004**, *23*, 161-227.

15. Schaller-Duke, R.; Bogala, M. R.; Cassady, C. J. Electron Transfer Dissociation and Collision-Induced Dissociation of Underivatized Metallated Oligosaccharides. *J. Am. Soc. Mass Spectrom.* **2018**, *29*, 1021-1035.

16. Adamson, J. T.; Håkansson, K. Electron Capture Dissociation of Oligosaccharides Ionized with Alkali, Alkaline Earth, and Transition Metals. *Anal. Chem.* **2007**, *79*, 2901-2910.

17. Riedel, T.; Suttnar, J.; Brynda, E.; Houska, M.; Medved, L.; Dyr, J. E. Fibrinopeptides A and B Release in the Process of Surface Fibrin Formation. *Blood* **2011**, *117*, 1700-1706.

18. Blombäck, B. Fibrinogen and Fibrin--Proteins with Complex Roles in Hemostasis and Thrombosis. *Thromb. Res.* **1996**, *83*, 1-75.

19. Yang, Z.; Mochalkin, I.; Doolittle, R. F. A Model of Fibrin Formation Based on Crystal Structures of Fibrinogen and Fibrin Fragments Complexed with Synthetic Peptides. *Proc. Natl. Acad. Sci. U. S. A.* **2000**, *97*, 14156-14161.

20. Bouchoux, G.; Desaphy, S.; Bourcier, S.; Malosse, C.; Bimbong, R. N. B. Gas-Phase Protonation Thermochemistry of Arginine. *J. Phys. Chem. B* **2008**, *112*, 3410-3419.

21. Prot pi Peptide Tool. *https://www.protpi.ch/Calculator/PeptideTool* (accessed May 21, 2022).

22. Bazley, L. A.; Gullick, W. J. The Epidermal Growth Factor Receptor Family. *Endocr.-Relat. Cancer* **2005**, *12*, S17-S27.

23. Purba, E. R.; Saita, E.; Maruyama, I. N. Activation of the EGF Receptor by Ligand Binding and Oncogenic Mutations: The "Rotation Model". *Cells* **2017**, *6*, 13.

24. Carpenter, G.; Cohen, S. Epidermal Growth Factor. *J. Biol. Chem.* **1990**, *265*, 7709-7712.

25. Hynes, N. E.; Lane, H. A. ERBB Receptors and Cancer: The Complexity of Targeted Inhibitors. *Nat. Rev. Cancer* **2005**, *5*, 341-354.

26. Holbro, T.; Hynes, N. E. ErbB Receptors: Directing Key Signaling Networks Throughout Life. *Annu. Rev. Pharmacol. Toxicol.* **2004**, *44*, 195-217.

27. Hynes, N. E.; Stern, D. F. The Biology of erbB-2/Nue/HER-2 and its Role in Cancer. *Biochim Biophys Acta Rev Cancer* **1994**, *1198*, 165-184.

28. Markwardt, F. Hirudin: The Promising Antithrombotic. *Cardiovasc. Drug Rev.* **1992**, *10*, 211-232.

29. Markwardt, F. The Development of Hirudin as an Antithrombotic Drug. *Thromb. Res.* **1994**, *74*, 1-23.

30. Redwan, E. Animal-Derived Pharmaceutical Proteins. *J. Immunoass. Immunochem.* **2009**, *30*, 262-290.

31. Dray, A.; Perkins, M. Bradykinin and Inflammatory Pain. *Trends Neurosci.* **1993**, *16*, 99-104.

32. Hall, J. M. Bradykinin Receptors. *Vascul. Pharmacol.* **1997**, *28*, 1-6.

33. Harrison, S.; Geppetti, P. Substance P. *Int. J. Biochem. Cell Biol.* **2001**, *33*, 555-576.

34. Ferrand, A.; Wang, T. C. Gastrin and Cancer: A Review. *Cancer Lett.* **2006**, *238*, 15-29.

35. McMillen, C. L.; Wright, P. M.; Cassady, C. J. Negative Ion in-Source Decay Matrix-Assisted Laser Desorption/Ionization Mass Spectrometry for Sequencing Acidic Peptides. *J. Am. Soc. Mass Spectrom.* **2016**, *27*, 847-855.

36. Saito, H.; Kojima, T.; Takahashi, M.; Horne, W. C.; Baron, R.; Amagasa, T.; Ohya, K.; Aoki, K. A Tumor Necrosis Factor Receptor Loop Peptide Mimic Inhibits Bone Destruction to the Same Extent as Anti–tumor Necrosis Factor Monoclonal Antibody in Murine Collagen-Induced Arthritis. *Arthritis Rheum.* **2007**, *56*, 1164-1174.

37. Choy, E. H. S.; Panayi, G. S. Cytokine Pathways and Joint Inflammation in Rheumatoid Arthritis. *N. Engl. J. Med.* **2001**, *344*, 907-916.

38. Brennan, F.; Jackson, A.; Chantry, D.; Maini, R.; Feldmann, M. Inhibitory Effect of TNFα Antibodies on Synovial Cell Interleukin-1 Production in Rheumatoid Arthritis. *Lancet* **1989**, *334*, 244-247.

39. Feldmann, M.; Brennan, F. M.; Maini, R. N. Rheumatoid Arthritis. *Cell* **1996**, *85*, 307-310.

40. Schwyzer, R. ACTH: A Short Introductory Review. *Ann. N. Y. Acad. Sci.* **1977**, *297*, 3-26.

41. Morton, I. K.; Hall, J. M. *Concise Dictionary of Pharmacological Agents: Properties and Synonyms;* Springer Netherlands: Dordrecht, 2012.

42. Mireles, M.; Cassady, C. J. University of Alabama, Tuscaloosa, AL. Unpublished work, **2019.**

43. Schaller-Duke, Ranelle M., Cassady, C.J. University of Alabama, Tuscaloosa, AL. Unpublished work, **2016.**

CHAPTER 7. ELECTRON TRANSFER DISSOCIATION OF MULTIPLY PROTONATED PEPTIDE IONS

7.1 Introduction

Mass spectrometry (MS) is an invaluable tool in peptidomics and proteomic research by providing accurate mass measurements and structural analysis to further understand biological functions and mechanisms.[1-3] Peptide sequence information can be elucidated by utilizing tandem mass spectrometry (MS/MS). The most common method of peptide and protein dissociation is collision-induced dissociation (CID).[4] In CID, precursor ions are activated through collisions with a neutral gas to induce dissociation along the peptide backbone amide bonds. Cleavage at the amide bond generates N-terminal b-ions and C-terminal y-ions, which are characteristic of CID fragmentation. CID can be easily implemented on many commercial mass spectrometers; therefore, the technique is well-known and widespread.

Alternatives to inducing fragmentation are electron-based dissociation techniques such as electron capture dissociation (ECD)[5] and electron transfer dissociation (ETD).[6] Both techniques require multiply charged precursor ions to avoid neutralization of the ion upon the addition of an electron. Unlike CID, ETD is a non-ergodic process, which means that fragmentation is localized and occurs before the energy is randomized. The process involves a low energy electron being transferred to the sample molecule via a reagent ion that is made by means of negative chemical ionization (nCI). The result is cleavage of the N-Cα bonds along the

peptide backbone producing N-terminal c-ions and C-terminal z-ions.[6] Refer to Section 2.5 for peptide fragmentation nomenclature. ETD and CID have been shown to provide complementary information. For example, in glycoprotein MS/MS analysis, CID exclusively cleaves glycosidic bonds while ETD cleaves peptide bonds.[7]

Before dissociation, the sample must be converted into gas-phase ions. The charge and intensity of the precursor ion can influence MS/MS results. Compared to singly protonated ions, higher charge state ions generally require less energy to dissociate and have been shown to increase fragmentation efficiency, thus providing more informative sequence fragmentation by increasing the number of product ions formed.[8-11] In positive ion mode electrospray ionization (ESI) and matrix-assisted laser desorption ionization (MALDI), acidic peptides can be difficult to protonate due to their highly acidic nature and preference for deprotonation.[12,13] Multiple efforts have been made to increase ionization efficiency in ESI. Organic supercharging reagents such as *m*-nitrobenzyl alcohol [14-17] and tetramethylene sulfone[18-20] have been reported to increase the charge state in peptide ions. Another method to generate multiply charged precursor ions from peptides that are normally difficult to protonate is the addition of metal ions to produce metallated peptide cations.[11,21-24] Additionally, trivalent chromium (Cr(III)) salts added to peptide solutions can enhance the signal intensity of protonated peptide ions and in some cases increase the highest charge state observed.[25-28]

The charge state, amino acid composition, and chain length have been shown to affect electron-based dissociation of protonated peptides. Chan and coworkers used ECD to investigate the effects of glutamic acid (Glu) and asparagine (Asn) residues on fragmentation of diarginated peptides.[29] Backbone cleavage was suppressed with the doubly protonated precursor ion as the number of Glu and Asn residues increased, whereas extensive backbone cleavage is seen for the

triply protonated precursor ion. This occurrence was attributed to the stability of the precursor ions caused by the carbonyl oxygen on Glu residue sidechains and the amide backbone stabilizing the proton. In another study by Chan and coworkers,[30] the length of the peptide was determined to be a factor in the suppression of product ions in ECD; they noted a decrease in the intensity of product ions for the longer peptide in their study.

Chalkley and coworkers reported the first statistical analysis of ETD product ions derived from enzymatic cleavage by characterizing the frequency of different ion types based on the charge state and protease used.[31] Doubly protonated precursor ions gave less fragmentations and more hydrogen transfer products than triply protonated precursor ions. The location of the basic residue in the doubly protonated precursor ion was a determinant for the type of product ion formed; this effect is less prevalent with higher charge states that have multiple protonated basic residues. The formation of y-ions, which are characteristic of CID fragmentation, was observed for peptides digested with trypsin and Lys-C. Wysocki, Coon, and coworkers [32] expanded on this work by performing statistical analysis using data mining strategy and K-means clustering on the ETD fragmentation of 11,954 peptides using three different proteases; they observed selective cleavage at lower charge states with intense cleavage N-terminal to arginine, lysine, and glutamic acid, but as the distance between these residues and the C-terminus increases the selectivity decreases. At higher charge states, the preferential cleavage is less significant. Additionally, cleavage N-terminal to proline and carbamidomethylated cysteine were not observed; this was previously reported by Sun and coworkers.[33] In two ETD studies by Karger and coworkers, selective cleavage of disulfide bonds was reported.[34,35]

The current study uses Cr(III) to assist in generation of multiply protonated peptide ions, $[M + nH]^{m+}$, from biologically relevant peptides. Cr(III) can sometimes produce charge states (n)

that are not otherwise formed in sufficient intensity to study by ETD. Therefore, the effects of precursor ion charge on ETD were investigated with regard to the types of product ions produced. The effects of specific residues on ETD fragmentation were also examined.

7.2 Experimental

All ETD experiments were performed using a Bruker (Billerica, MA, USA) HCTultra PTM Discovery System high capacity quadrupole ion trap (QIT) mass spectrometer equipped with ESI. Samples were introduced into the ESI chamber using a KD Scientific syringe pump (Holliston, MA, USA) at a flow rate of 180 µL/hr. Experiments were performed in the positive ion mode with a high voltage of -3.5-4.0 kV applied at the capillary entrance. Nitrogen was the drying and nebulizing gas. The drying gas temperature and flow rate were set to 300ºC and 5-10 L/min, respectively. The pressure of the nebulizer gas was optimized between 10-15 psi. Final spectra are the result of signal averaging 200 scans.

The reagent anion, fluoranthene, was produced by nCI with methane as the nCI reagent gas. To maximize transfer of the electron, the ion charge control (ICC) value was set between 300,000 to 400,000 and the reagent anion accumulation time was set between 5-10 ms. The anion/cation reaction times were set in the range of 110-200 ms. No additional energy was applied to the ions post ETD.

Peptides were purchased from various vendors. Adrenocorticotropic hormone clip (ACTH (4-10)), GLFAVIKKVAKVIKKL, beta-amyloid (1-11), des-Arg^{14}-Glu^{1}-fibrinopeptide B, Glu^{1}-endo-Glu^{7a}-fibrinopeptide B, TDFEAALNTR, and des-Arg^{16}-fibrinopeptide A were obtained from Biomatik USA (Wilmington, Delaware, USA). Hirudin (54-65), prepro vasoactive intestinal polypeptide (preproVIP), epidermal growth factor (EGFR (985-966)), angiotensin I, and fibrinopeptide A were purchased from Bachem Americas (Torrance, CA, USA).

Adrenocorticotropic hormone (ACTH (1-13)), HIF-1{α} (556-574), Glu^1-fibrinopeptide B, and fibrinopeptide B were attained from VWR International (Radnor, PA, USA). Before infusion, peptides were dissolved in 50:50 [v/v] acetonitrile:water. Acetonitrile was purchased from VWR and Ultrapure Milli-Q 18 MΩ water was produced with a Barnstead (Dubuque, IA, USA) E-pure system. Chromium(III) nitrate was purchased from VWR.

7.3 Results and Discussion

7.3.1 Effects of Cr(III) on ETD spectra

All spectra presented are labeled according to the established peptide cleavage nomenclature of Roepstorff and Fohlman[36] as modified by Biemann.[37] This nomenclature is used in the current study to assist in conveying the number of additional hydrogens present in product ions generated from highly protonated precursor ions. Additional hydrogens are denoted by a prime symbol to the right of the ion (i.e., $z_n^{/} = [z_n + H]^+$); whereas, the loss of hydrogens is represented by a prime symbol to the left (i.e., $^{/}c_n = [c_n - H]^+$). In the figures, the following color code is used to label ions: z-ions = red, c-ions = blue, y-ions = green, undissociated precursor ion = purple, and neutral loss/electron transfer without dissociation (ETnoD) ions = black.

Sixteen peptides were chosen to study their fragmentation patterns at different charge states in ETD. The peptides and their sequences are provided in Table 7.1, along with the protonated ions formed during ESI and the fragment ions produced by ETD. The peptides range in size from 7-19 amino acid residues. For peptides that only form $[M + H]^+$ during ESI or multiply protonated ions with weak intensities, chromium(III) nitrate was added to the peptide solution in a 5:1 or 10:1 Cr(III) to peptide molar ratio to increase the signal intensity of the multiply charged protonated ion, $[M + nH]^{n+}$.

Our computational and experimental research into the mechanism by which Cr(III) enhances the protonation of peptides[27,28] suggests that the use of Cr(III) should not influence the ETD spectra. To confirm this, ETD spectra of peptide solutions with Cr(III) were compared with ETD spectra of peptide solutions without Cr(III). The work of Chapter 6 and previous Cassady group work demonstrates that Cr(III) is especially useful for the analysis of acidic and neutral peptides by ESI.[25] Neutral peptides are defined as peptides with an equal number of basic and acidic sites. Basic sites include the N-terminus and sidechain of basic amino acids (arginine, lysine, and histidine). Acidic sites on peptides are the C-terminus and sidechain of acidic amino acids (glutamic and aspartic acid).

The ETD spectra for des-Arg^{14}-Glu^{1}-fibrinopeptide B are presented in Figure 7.1. ETD of $[M + 2H]^{2+}$ from des-Arg^{14}-Glu^{1}-fibrinopeptide B with acetic acid, Figure 7.1(a), and with Cr(III), Figure 7.1(b), generates the same product ions. The spectra are identical, with des-Arg^{14}-Glu^{1}-fibrinopeptide B producing c- and z-type product ions. In both cases, the c-series consist of $c_{2, 9\text{-}12}^{+}$ and the z-series is z_{11}^{+} and $z_{12}^{/+}$. Human epidermal growth factor fragment (EGFR (985-996)) without any additive forms only $[M + nH]^{n+}$, n = 1-2, by ESI. Addition of Cr(III) forms n = 3, which is comparable to the ESI spectrum of EGFR (985-996) with 0.1% acid added to the peptide solution. ETD performed on $[M + 3H]^{3+}$ produced by the addition of Cr(III) results in the same product ions being formed as ETD on $[M + 3H]^{3+}$ produced with the addition of acetic acid. The product ions formed are of the z, c, and y-series and consist of $z_{3\text{-}11}^{/+}$, $z_{8\text{-}9,11}^{//+}$, $c_{2\text{-}11}^{+}$, $c_{3\text{-}9,\,11}^{/+}$, and y_{2}^{+}. Hirudin (54-65) is a highly acidic peptide that forms $[M + nH]^{n+}$, n = 1-2, with acid, while with Cr(III) n = 3 forms. Comparison of the ETD spectra of $[M + 2H]^{2+}$ with acid and Cr(III) shows the same product ions are formed: $z_{11}^{/+}$, $z_{11}^{//+}$, $c_{9\text{-}11}^{+}$, $c_{11}^{/+}$, and $y_{9\text{-}10}^{+}$.

Table 7.1. ESI ion formation and corresponding ETD product ions.

Peptide Sequence	Precursor ion formed by ESI	Number of fragment ions	z_n-ions	c_n-ions	y_n-ions
DRVYIHPFHL Angiotensin I	$[M + 2H]^{2+}$	4	$z_n^{\cdot/+}$, n=9 $z_n^{//+}$, n=9	c_n^{+}, n=7-8 $c_n^{\cdot/+}$, n=8-9	
	$[M + 3H]^{3+}$	13	$z_n^{\cdot/+}$, n=2-3, 5, 7-9 $z_n^{//+}$, n=9	c_n^{+}, n=2-5, 7-9	
	$[M + 4H]^{4+}$	11	$z_n^{\cdot/+}$, n=2, 5, 7-8 $z_n^{//+}$, n=7-9	c_n^{+}, n=2-3, 5, 7-8 $c_n^{\cdot/+}$, n=9	
GDFEEIPEEYLQ Hirudin (54-65)	$[M + 2H]^{2+}$	6	$z_n^{\cdot/+}$, n=11 $z_n^{//+}$, n=11	c_n^{+}, n=9-11 $c_n^{\cdot/+}$, n=11	y_n^{+}, n=9-10
	$[M + 3H]^{3+}$	20	$z_n^{\cdot/+}$, n=2-11 $z_n^{//+}$, n=2-11	c_n^{+}, n=3-11 $c_n^{\cdot/+}$, n=3-5, 7-11	y_n^{+}, n=6
DLDLEMLAPYIPMDDDFQL HIF-1{α} (556-574)	$[M + 2H]^{2+}$	18	$z_n^{\cdot/+}$, n=8, 12, 14, 16, 18 $z_n^{//+}$, n=12, 15-18	c_n^{+}, n=9-10, 12-18 $c_n^{\cdot/+}$, n=15-18	y_n^{+}, n=8,11
	$[M + 3H]^{3+}$	22	$z_n^{\cdot/+}$, n=2-7, 9, 12 $z_n^{//+}$, n=2-4, 6, 10, 12, 14	c_n^{+}, n=6-7, 9-10, 12-18 $c_n^{\cdot/+}$, n=7, 10, 12-18	y_n^{+}, n=8,11
GLFAVIKKVAKVIKKL	$[M + 2H]^{2+}$	6	$z_n^{\cdot/+}$, n=13-15 $z_n^{//+}$, n=13-15	c_n^{+}, n=13-15 $c_n^{\cdot/+}$, n=14-15	
	$[M + 3H]^{3+}$	17	$z_n^{\cdot/+}$, n=3, 5, 9, 11-15 $z_n^{//+}$, n=3, 5, 9, 11-15	c_n^{+}, n=7-15 $c_n^{\cdot/+}$, n=7, 10-15	
	$[M + 4H]^{4+}$	25	$z_n^{\cdot/+}$, n=2-4, 6-7, 9-15 $z_n^{//+}$, n=2, 4, 6-7, 9-15	c_n^{+}, n=2-7, 9-15 $c_n^{\cdot/+}$, n=3-7, 9-15	
MEHFRWG ACTH (4-10)	$[M + 2H]^{2+}$	7	$z_n^{\cdot/+}$, n=3-6 $z_n^{//+}$, n=4	c_n^{+}, n=5-6 $c_n^{\cdot/+}$, n=4	
	$[M + 3H]^{3+}$	9	$z_n^{\cdot/+}$, n=3-6 $z_n^{//+}$, n=5-6	c_n^{+}, n=2-6 $c_n^{\cdot/+}$, n=5-6	
SYSMEHFRWGKPV ACTH (1-13)	$[M + 2H]^{2+}$	2	$z_n^{//+}$, n=10	$c_n^{\cdot/+}$, n=12	
	$[M + 3H]^{3+}$	17	$z_n^{\cdot/+}$, n=3-7 $z_n^{//+}$, n=8-11 z_n^{2+}, n=11	c_n^{+}, n=6-9, 12 c_n^{2+}, n=12	y_n^{+}, n=4-5, 11 y_n^{2+}, n=11
	$[M + 4H]^{4+}$	21	$z_n^{\cdot/+}$, n=3-7, 10-11 $z_n^{/2+}$, n=7-8, 10-11 $z_n^{//+}$, n=8-9	c_n^{+}, n=2-10 c_n^{2+}, n=8,10,12 c_n^{3+}, n=12	y_n^{2+}, n=7, 11

Table 7.1. continued.

Peptide Sequence	Precursor ion formed by ESI	Number of fragment ions	z_n-ions	c_n-ions	y_n-ions
DAEFRHDSGYE β-amyloid (1-11)	$[M + 2H]^{2+}$	2	$z_n^{//+}$, n=10	c_n^{+}, n=10	
	$[M + 3H]^{3+}$	15	$z_n^{/+}$, n=5-10 $z_n^{//+}$, n=5, 9-10	c_n^{+}, n=2-10 $c_n^{/+}$, n=4-8, 10	
EGVNDNEEEGFFSAR Glu[1]-endo-Glu[7a]-fibrinopeptide B	$[M + 2H]^{2+}$	11	$z_n^{/+}$, n=4-14 $z_n^{//+}$, n=4-14		
	$[M + 3H]^{3+}$	25	$z_n^{/+}$, n=1-9, 11-14 $z_n^{//+}$, n=1-2, 6-8, 11-14	c_n^{+}, n=3-14 $c_n^{/+}$, n=4-5, 7-8, 10-14	
SSEGESPDFPEELEK PreproVIP (156-170)	$[M + 2H]^{2+}$	2		c_n^{+}, n=14 $c_n^{/+}$, n=14	y_n^{+}, n=9
	$[M + 3H]^{3+}$	33	$z_n^{/+}$, n=2-5, 7-8, 10-13 $z_n^{//+}$, n=8, 11-14	c_n^{+}, n=3-5, 7-8, 10-14 $c_n^{/+}$, n=3-4, 7, 10, 13-14	y_n^{+}, n=2-13
DVVDADEYLIPQ EGFR (985-996)	$[M + 2H]^{2+}$	3		c_n^{+}, n=8-9, 11 $c_n^{/+}$, n=9, 11	
	$[M + 3H]^{3+}$	20	$z_n^{/+}$, n=3-11 $z_n^{//+}$, n=8-9, 11	c_n^{+}, n=2-11 $c_n^{/+}$, n=3-9, 11	y_n^{+}, n=2
EGVNDNEEGFFSA Des-Arg[14]-Glu[1]-fibrinopeptide B	$[M + 2H]^{2+}$	7	z_n^{+}, n=11 $z_n^{/+}$, n=12	c_n^{+}, n=2, 9-12	
	$[M + 3H]^{3+}$	22	$z_n^{/+}$, n=2-12 $z_n^{//+}$, n=2-12	c_n^{+}, n=2-12 $c_n^{/+}$, n=4-12	
EGVNDNEEGFFSAR Glu[1]-fibrinopeptide B	$[M + 2H]^{2+}$	13	$z_n^{/+}$, n=8-13 $z_n^{//+}$, n=3-13	c_n^{+}, n=11, 13	
	$[M + 3H]^{3+}$	32	$z_n^{/+}$, n=1-13 $z_n^{//+}$, n=8-10, 12-13	c_n^{+}, n=2-13 $c_n^{/+}$, n=10-13	y_n^{+}, n=1-6, 10
pEGVNDNEEGFFSAR Fibrinopeptide B	$[M + 2H]^{2+}$	11	$z_n^{//+}$, n=3-13		
	$[M + 3H]^{3+}$	24	$z_n^{/+}$, n=1-8, 10 $z_n^{//+}$, n=9, 11-13	c_n^{+}, n=3-13	

Table 7.1. continued.

Peptide Sequence	Precursor ion formed by ESI	Number of fragment ions	z_n-ions	c_n-ions	y_n-ions
ADSGEGDFLAEGGGV Des-Arg^{16}-fibrinopeptide A	$[M + 2H]^{2+}$	12	$z_n^{//+}$, n=8, 12-14	$c_n^{//+}$, n=2-3 c_n^{+}, n=9-14	
	$[M + 3H]^{3+}$	24	z_n^{+}, n= 3-5 $z_n^{/+}$, n=6-13 $z_n^{//+}$, n=13-14	c_n^{+}, n=2-12, 14 $c_n^{/+}$, n=13	
ADSGEGDFLAEGGGVR Fibrinopeptide A	$[M + 2H]^{2+}$	18	$z_n^{/+}$, n=5-6, 8-15 $z_n^{//+}$, n=2-15	c_n^{+}, n=11, 14 $c_n^{/+}$, n=14	y_n^{+}, n=5, 14
	$[M + 3H]^{3+}$	35	$z_n^{/+}$, n=1-7, 9-13, 15 $z_n^{//+}$, n= 10-15	c_n^{+}, n=3-15 $c_n^{/+}$, n=10-15	y_n^{+}, n=2-5, 10-13
TDFEAALNTR	$[M + 2H]^{2+}$	7	$z_n^{/+}$, n=5-9 $z_n^{//+}$, n=3-6, 8-9		
	$[M + 3H]^{3+}$	14	$z_n^{/+}$, n=2-9	c_n^{+}, n=4-9	

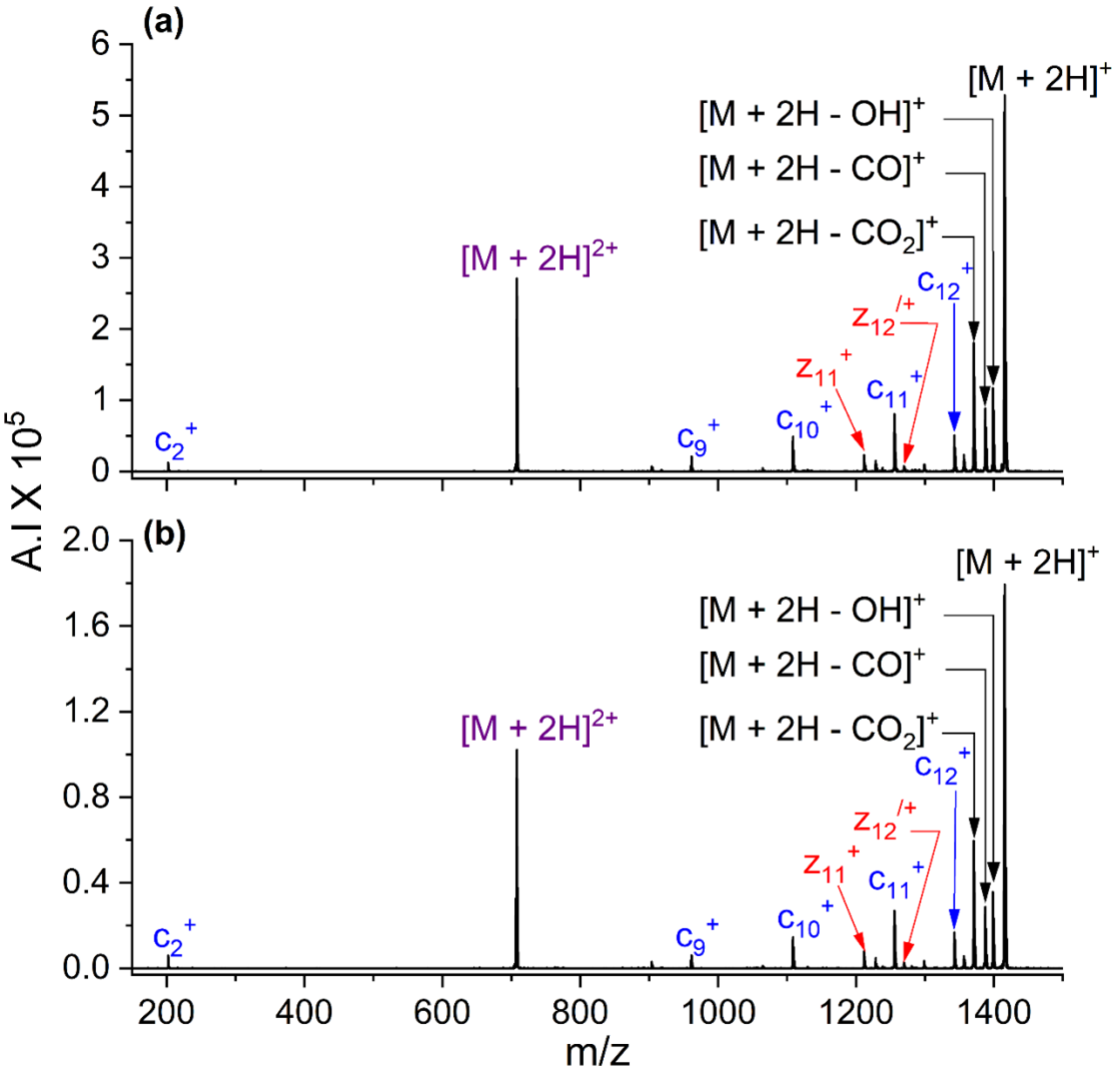

Figure 7.1. ETD mass spectra of $[M + 2H]^{2+}$ for des-Arg^{14}-Glu^{1}-fibrinopeptide B (a) with acetic acid and (b) with Cr(III). In the figures, the following colors are used to label the ions: z-ions = red, c-ions = blue, y-ions = green, undissociated precursor ion = purple, and neutral loss/electron transfer without dissociation (ETnoD) ions = black. Additional hydrogens are denoted by a prime symbol to the right of the ion (i.e., $z_n^{/} = [z_n + H]^+$); whereas, the loss of hydrogens is represented by a prime symbol to the left (i.e., $^{/}c_n = [c_n - H]^+$). All peaks are shown to scale.

As expected, the addition of Cr(III) had no impact on the ETD fragmentation. The same ions representing ETD product ions were formed for the precursor ions with and without Cr(III) at the same relative intensities. The process of isolating the protonated precursor ion prior to performing dissociation in the QIT prohibits Cr(III) from participating in the dissociation process because Cr(III) is not present in the isolated precursor ion. Also, the final step of the mechanism in which Cr(III) enhances protonation involves the separation of Cr(III) from the protonated peptide.[27] Therefore, the impact of Cr(III) is only observed in the ionization step and does not play a role during dissociation.

One thing to note, for these biological peptides, is the absolute intensity of all protonated ions decreased with the addition of Cr(III). (That is not true for model peptides and some biological peptides, that have been previously studied, including the work in Chapter 6.[25,26,28]) In single stage MS, Cr(III)-adducted peptide ions are observed, which competes with protonation for the generation of precursor ions and decreases the amount of the peptide available for protonation.

7.3.2 Effect of charge state

With the knowledge that Cr(III), which is used for increasing protonated ion signal and charge, does not impact fragmentation, the number of peptides studied was increased to explore fragmentation patterns at different charge states (n) in ETD. The number of distinct fragment ions formed at different charge states during ETD is listed for each peptide in Table 7.1. All peptides studied formed $[M + nH]^{n+}$, n = 1-3, during ESI except for angiotensin I, ACTH (1-13), and GLFAVIKKVAKVIKKL, which also formed n = 4. In cases where Cr(III) was added to aid in protonation, the precursor ion generated from the Cr(III)-containing solution was used for this study.

Des-Arg^{16}-fibrinopeptide A contains four acidic residues and no basic residues and forms $[M + nH]^{n+}$, n = 1-3, by ESI. Figure 7.2(a) shows the ETD spectrum of $[M + 2H]^{2+}$ for des-Arg^{16}-fibrinopeptide A. The most prominent ions are c-ions, $c_{2-3}^{//+}$ and c_{9-14}^{+}. Some higher mass z-ions are present, $z_{8,12-14}^{//+}$. All of the product ions are singly charged, and the spectrum contains neutral losses involving CO and OH. Dissociation of the precursor ion is poor with a significant amount of ETnoD product and the charge reduced product, $[M + 2H]^{+}$, remaining. In comparison, Figure 7.2(b) shows the ETD spectrum of $[M + 3H]^{3+}$ for des-Arg^{16}-fibrinopeptide A. The spectrum contains about an equal mixture of c- and z-ions. Ions present of the z-series are z_{3-5}^{+}, $z_{6-13}^{/+}$, and $z_{13-14}^{//+}$. The c-series consists of $c_{2-12,14}^{+}$, and $c_{13}^{/+}$. There is still a substantial amount of ETnoD product remaining although more fragmentation is observed for 3+. Lower mass c- and z-type ions appear at 3+ that are not formed from 2+. Cleavage occurs at every residue besides the low mass z_{1-2} and c_1 positions.

ACTH (1-13) is a basic peptide that forms $[M + nH]^{n+}$, n = 2-4, by ESI. Figure 7.3(a) contains the ETD spectrum of $[M + 2H]^{2+}$ for ACTH (1-13). Similar to des-Arg^{16}-fibrinopeptide A, ETD of $[M + 2H]^{2+}$ gives extensive ETnoD and charge reduced product. Only two product ions form: $c_{12}^{/+}$ and $z_{10}^{//+}$. ETD of $[M + 3H]^{3+}$, Figure 7.3(b), yields a mixture of c-, z-, and y-ions. Ions present of the c-series are $c_{6-9,12}^{+}$ and c_{12}^{2+}. The z-series consist of $z_{3-7}^{/+}$, $z_{8-11}^{//+}$, and $z_{11}^{//2+}$. The y-ions that form are $y_{4,5,11}^{+}$ and y_{11}^{2+}. The formation of y-ions results from cleavage of the peptide bond, which is usually associated with CID. Although rare, y-ions have been observed in electron-based dissociation techniques.[38-40] More product ions are observed with the n = 3 precursor ion than with n = 2, but the spectrum is still dominated by the ETnoD and charge reduced ions $[M + 3H]^{2+}$ and $[M + 3H]^{+}$. Figure 7.3(c) shows the ETD spectrum for the n = 4 precursor ion. Compared to n = 3, n = 4 produces more ions of the c-series. The product

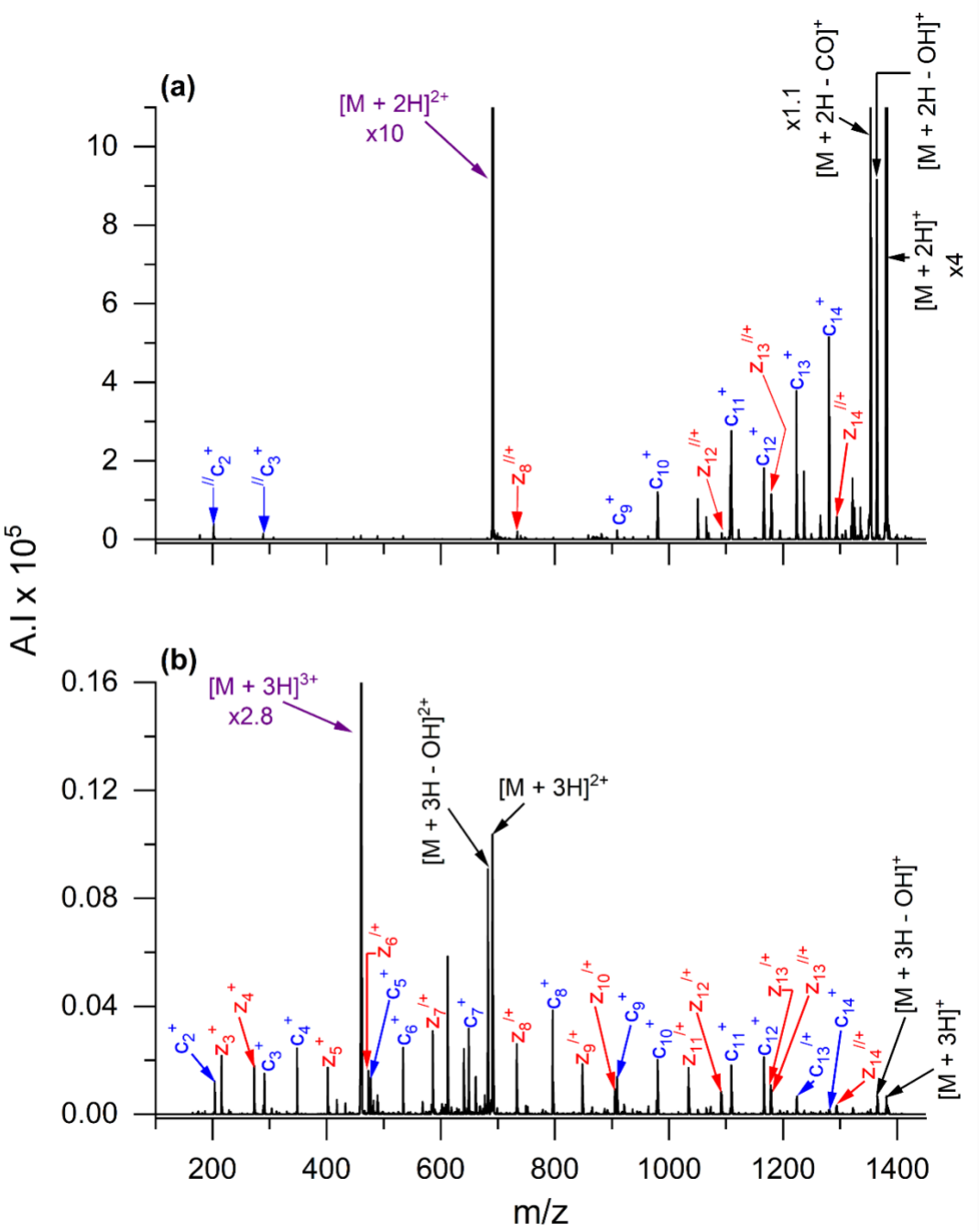

Figure 7.2. ETD mass spectra of (a) $[M + 2H]^{2+}$ and (b) $[M + 3H]^{3+}$ for des-Arg^{16}-fibrinopeptide A. In the figures, the following colors are used to label the ions: z-ions = red, c-ions = blue, y-ions = green, undissociated precursor ion = purple, and neutral loss/electron transfer without dissociation (ETnoD) ions = black. Additional hydrogens are denoted by a prime symbol to the right of the ion (i.e., zn/ = [zn + H]+); whereas, the loss of hydrogens is represented by a prime symbol to the left (i.e., /cn= [cn – H]+). There is an expansion of the y-axis.

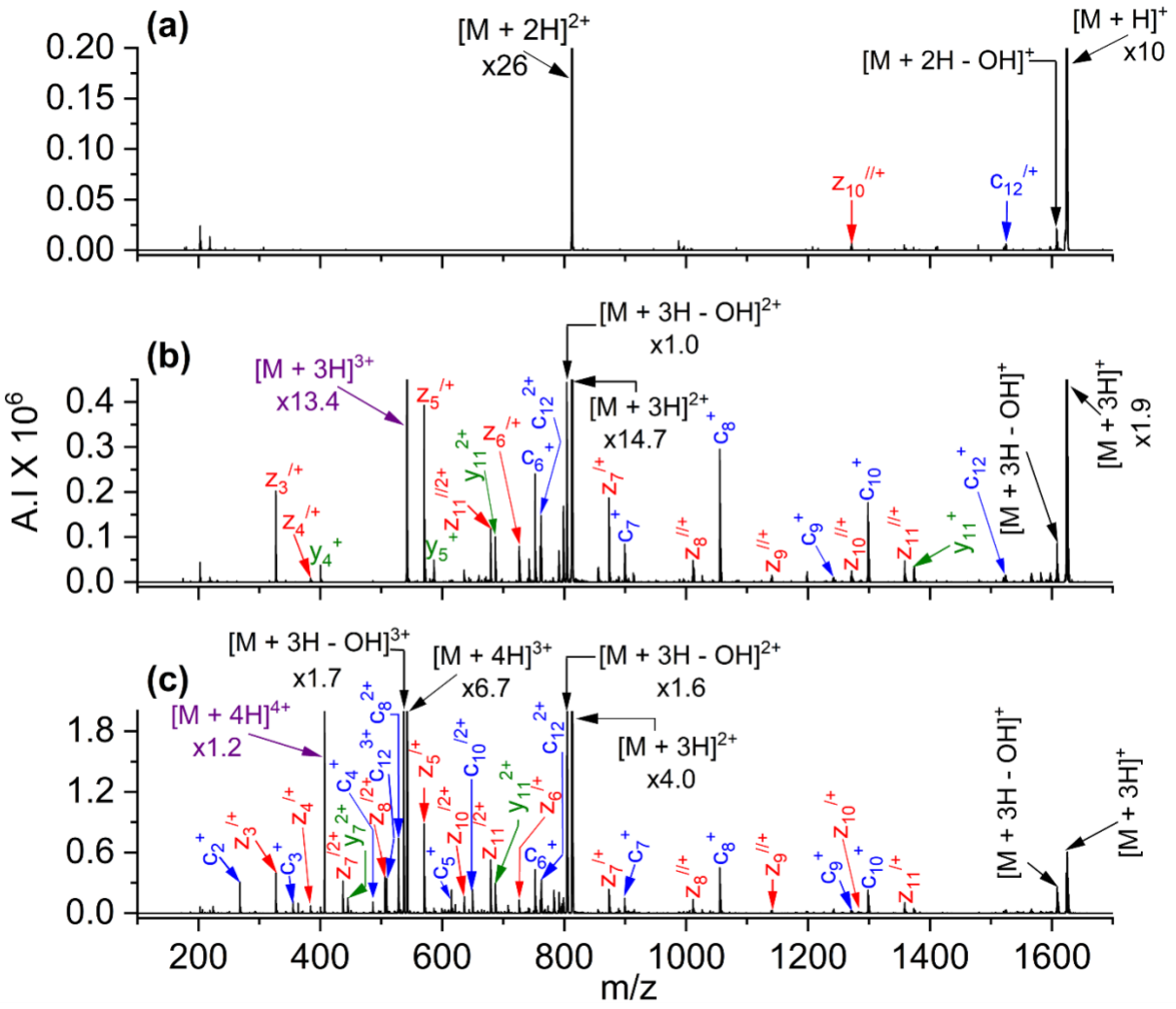

Figure 7.3. ETD mass spectra of (a) $[M + 2H]^{2+}$, (b) $[M + 3H]^{3+}$, and (c) $[M + 4H]^{4+}$ for ACTH (1-13). In the figures, the following colors are used to label the ions: z-ions = red, c-ions = blue, y-ions = green, undissociated precursor ion = purple, and neutral loss/electron transfer without dissociation (ETnoD) ions = black. Additional hydrogens are denoted by a prime symbol to the right of the ion (i.e., $z_n^{/} = [z_n + H]^+$); whereas, the loss of hydrogens is represented by a prime symbol to the left (i.e., $^{/}c_n = [c_n - H]^+$). There is an expansion of the y-axis.

ions formed for 4+ are $c_{2\text{-}10}^{+}$, $c_{8,10,12}^{2+}$, c_{12}^{3+}, $z_{3\text{-}7,10\text{-}11}^{/+}$, $z_{8\text{-}9}^{//+}$, $z_{7\text{-}8,10\text{-}11}^{/2+}$, and $y_{7,11}^{2+}$. Multiply charged product ions are observed for the n = 3and n = 4 precursor ion. ETD of $[M + 3H]^{3+}$ forms $z_{11}^{/2+}$, c_{12}^{2+}, and y_{11}^{2+}, while ETD of 4+ forms $z_{7\text{-}8,10\text{-}11}^{/2+}$, $c_{8,10,12}^{2+}$, and c_{12}^{3+}. The number of multiply charged product ions increases with charge state, which is not unexpected from basic peptides that contain multiple basic residues (i.e., arginine, lysine, and histidine) that can potentially sequester a proton at the sidechain. This is evident based on the location of the cleavages. All multiply charged product ions that are present in the spectra contain at least two basic residues in the product ion's sequence.

Table 7.2 summarizes the ETD results. Compared to n = 2, more fragmentation is generated with n = 3 and 4. The increase in product ion formation with charge state is consistent with previous ETD studies of protonated and metallated peptide precursor ions.[29,31,41,42] For all peptides in this study, ETD of n = 2 yields extensive ETnoD and charge-reduced products with minimal fragmentation. Liu and McLuckey reasoned that the lack of fragmentation observed for n = 2 might be due to the lack of internal electrostatic repulsion after electron transfer.[41] Post-activation methods have been utilized to increase ETD product ion formation.[11,24,43,44] The Bruker HCTultra PTM Discovery system that was utilized for the experiments in this chapter has a "smart decomposition" feature that applies resonant excitation (very low energy CID) to break hydrogen and non-covalent bonds that keeps the ion intact. Unfortunately, this feature is not working properly (breaking midway through this project), and manual excitation could not be performed. This did not prevent acquisition of ETD spectra, but it did limit fragmentation efficiency. In cases where adding supplemental energy is not available, n = 3 yields the best sequence informative results.

Table 7.2. Summary of ETD fragmentation at different precursor ion charge states.

Peptides	Precursor ions	Peptide sequence and fragmentation[b]
Angiotensin I	$[M + 2H]^{2+}$	
	$[M + 3H]^{3+}$	
Hirudin (54-65)	$[M + 2H]^{2+}$	
	$[M + 3H]^{3+}$	
HIF-1{α} (556-574)	$[M + 2H]^{2+}$	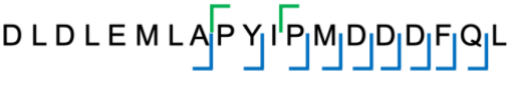
	$[M + 3H]^{3+}$	
GLFAVIKKVAKVIKKL	$[M + 2H]^{2+}$	
	$[M + 3H]^{3+}$	
	$[M + 4H]^{4+}$	
ACTH (4-10)	$[M + 2H]^{2+}$	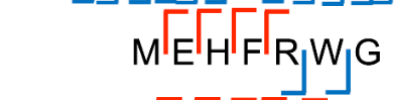
	$[M + 3H]^{3+}$	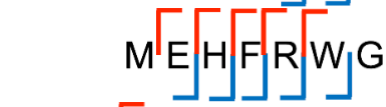
ACTH (1-13)	$[M + 2H]^{2+}$	
	$[M + 3H]^{3+}$	
	$[M + 4H]^{4+}$	
β-amyloid (1-11)	$[M + 2H]^{2+}$	
	$[M + 3H]^{3+}$	

Table 7.2. continued.

Peptides	Precursor ions	Peptide sequence and fragmentation
Glu[1]-endo-Glu[7a]-fibrinopeptide	$[M + 2H]^{2+}$	
	$[M + 3H]^{3+}$	
PreproVIP (156-170)	$[M + 2H]^{2+}$	
	$[M + 3H]^{3+}$	
EGFR 985-996	$[M + 2H]^{2+}$	
	$[M + 3H]^{3+}$	
Des-Arg[14]-Glu[1]-fibrinopeptide B	$[M + 2H]^{2+}$	
	$[M + 3H]^{3+}$	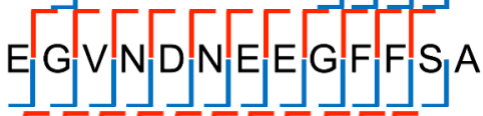
Glu[1]-fibrinopeptide B	$[M + 2H]^{2+}$	
	$[M + 3H]^{3+}$	
Fibrinopeptide B	$[M + 2H]^{2+}$	
	$[M + 3H]^{3+}$	
Des-Arg[16]-fibrinopeptide A	$[M + 2H]^{2+}$	
	$[M + 3H]^{3+}$	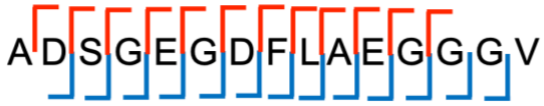

Table 7.2. continued.

Peptides	Precursor ions	Peptide sequence and fragmentation
Fibrinopeptide A	$[M + 2H]^{2+}$	
	$[M + 3H]^{3+}$	
TDFEAALNTR	$[M + 2H]^{2+}$	
	$[M + 3H]^{3+}$	

[b]The colors are z-ions in red, c-ions in blue, and y-ions in green.

7.3.3 Formation of c-ions

The amino acid composition and charge on the precursor ion can have a significant impact on formation of the c-ion series. Performing ETD on $[M + 2H]^{2+}$ from fibrinopeptide B, Glu^{1}-fibrinopeptide B, and Glu^{1}-endo-Glu^{7a}-fibrinopeptide B generates an extensive z-series that is majority $z^{//+}$; whereas, des-$Arg1^{4}$-Glu^{1}-fibrinopeptide B, EGVNDNEEGFFSA, which does not have a C-terminal arginine residue unlike the aforementioned peptides, formed only two z-ions, both of which are $z^{/+}$.

In Figure 7.4(a) for ETD on $[M + 2H]^{2+}$ for fibrinopeptide B, pEGVNDNEEGFFSAR, $z_{3\text{-}13}^{//+}$ forms. In contrast, ETD on $[M + 3H]^{3+}$, Figure 7.4(b), forms $z_{1\text{-}8,10}^{/+}$ and $z_{9,\,11\text{-}13}^{//+}$ and $c_{3\text{-}13}^{+}$. The emergence of c-ions with the higher charge state indicates that the C-terminal arginine is involved in directing fragmentation at the lower charge state but is insignificant at higher charge states. All product ions resulting from ETD of 2+ from fibrinopeptide B are singly charged.

The lack of a c-series for $[M + 2H]^{2+}$ signifies that the proton is located at the arginine residue for all the product ions formed. The gas-phase basicity of arginine is 240 kcal/mol, and it is the most basic amino acid.[45] The effects of basic residues on ETD fragmentation has been reported with studies focused on ETD of Lys-N and trypsin digested proteins and peptides.[46-48] The enzyme Lys-N, which cleaves at the N-terminal side of lysine, has been shown to produce predominantly c-ions.[46] Trypsin protease cleaves proteins on the C-terminal side of lysine and arginine, which leaves a basic residue at the C-terminus of the resulting peptide.[47,48] CID spectra of peptides digested by trypsin have been reported to predominantly generate y-ions that contain the basic residue.[49] The sidechains of basic residues are known to sequester protons because of their high gas-phase basicity, which explains spectra dominated by product ions containing the basic residue. At higher charge states, the impact of the basic residue is negligible due to the presence of additional protons that can mobilize and promote randomized backbone cleavage.

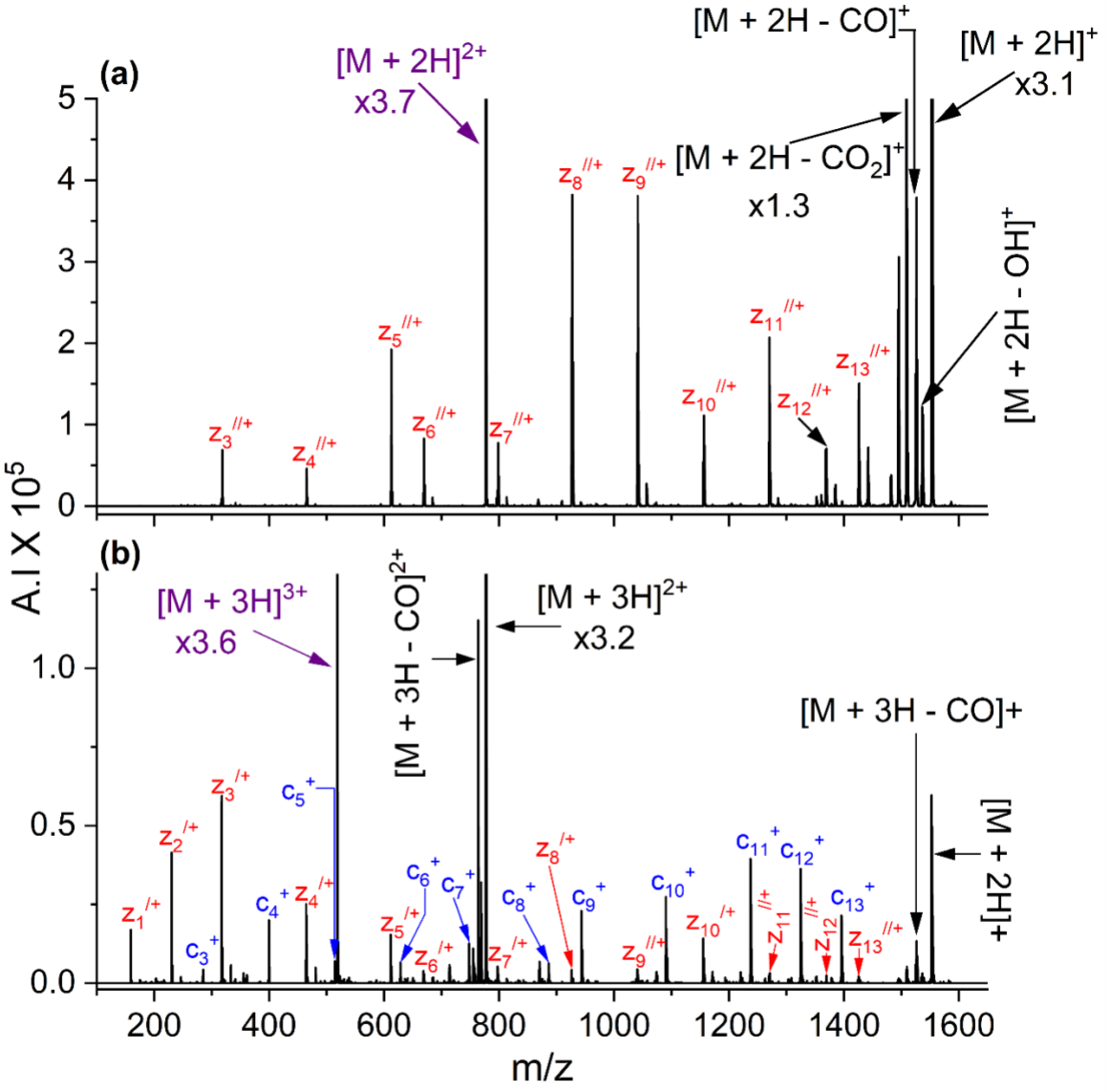

Figure 7.4. ETD mass spectra of (a) $[M + 2H]^{2+}$ and (b) $[M + 3H]^{3+}$ from fibrinopeptide B. In the figures, the following colors are used to label the ions: z-ions = red, c-ions = blue, y-ions = green, undissociated precursor ion = purple, and neutral loss/electron transfer without dissociation (ETnoD) ions = black. Additional hydrogens are denoted by a prime symbol to the right of the ion (i.e., $z_n^{/} = [z_n + H]^+$); whereas, the loss of hydrogens is represented by a prime symbol to the left (i.e., $^{/}c_n = [c_n - H]^+$). There is an expansion of the y-axis.

7.3.4 Proline effects

Six of the 17 peptides studied contained at least one proline residue. Cleavage of the N-Cα bond on the N-terminal side of proline is often absent in the ECD and ETD mass spectra due to the sidechain of proline forming a pyrrolidine ring with the adjacent amide nitrogen along the peptide backbone.[5,50-52] Although the N-Cα bond is broken by ETD, the peptide is still covalently held together, which results in fragmentation not being observed. The peptides in this study that contain proline are angiotensin I, hirudin (54-65), ACTH (1-13), preproVIP (156-170), EGFR (985-996), and HIF-1{α} (556-574). Fragmentation N-terminal to proline was not observed for ACTH (1-13) and angiotensin I, which contain three basic residues in their sequence. ETD of $[M + 3H]^{3+}$ for hirudin (54-65) results in the formation of $z_6^{/+}$, y_6^+, and c_6^+, which corresponds to cleavage N-terminal to proline. PreproVIP (156-170) generates y_9^+ for both the 2+ and 3+ precursor ion. In addition to y_9^+, c_6^+ and y_6^+ are observed with the 3+ precursor ion. N-terminal proline cleavage is only seen when performing ETD on the 3+ charge state for EGFR (985-996); the product ions y_2^+ and c_{10}^+ are formed. ETD of HIF-1{α} (556-574) produces y_8^+ for both 2+ and 3+.

In ETD of peptides containing proline, formation of y-ions N-terminal to proline residues are favored when cleavage is observed. This can be explained by the proline effect that is known in CID of proline-containing peptides. The proline effect describes the presence of abundant y-ions in CID spectra indicative of the amide bond cleavage N-terminal to proline residues.[53-55] The relatively high gas-phase basicity of proline (213.3 kcal/mol)[56] is one factor that encourages cleavage at the amide bond N-terminal to the proline residue. The lack of N-terminal proline cleavage for basic peptides may be the result of the highly basic residues immobilizing the protons that can otherwise promote backbone cleavage. In the case of acidic peptides that lack basic residues, the mobile proton model[8] that explains fragmentation in CID may encourage the

formation of the y-ions in ETD. Due to the absence of basic residues, the proton added can become mobilized and migrate to the backbone amide nitrogen, which weakens the bond and triggers cleavage of the amide bond leading to y-ion formation.[57] The formation of y-ions containing proline was observed for all the proline containing peptides in this study except for angiotensin I, which contains multiple basic residues.

Extensive y-ion formation is seen with ETD of $[M + 3H]^{3+}$ of the highly acidic peptide preproVIP. PreproVIP contains six acidic residues and one basic residue at the C-terminus. Based on the sequence, two of the three protons added most likely are originally located at the N-terminus and the lysine residue at the C-terminus. The third proton does not have a definite location to reside on the peptide chain and therefore might be acting as a mobile proton. Previous ETD studies reported y-ion formation in peptides containing aspartic and glutamic acid residues.[57-61] The presence of multiple acidic residues and the mobile proton might promote extensive y-ion formation that is seen with preproVIP.

7.4 Conclusions

As expected, Cr(III) can be used to enhance the ionization of peptides without disrupting ETD fragmentation. Performing ETD experiments on higher charge states yields more fragmentation compared to the doubly protonated peptide ion, which generated little to no fragmentation without any supplemental activation following the ETD process. Formation of c-ions were inhibited for n = 2 when basic residues were located at the C-terminus. The high gas-phase basicity of the basic residue immobilizes the proton and promotes z-ion formation. At higher charge states, additional protons are mobile, which leads to more random fragmentation and the appearance of c-ions. Proline containing peptides form y-ions N-terminal to the proline

residue; this effect is less prevalent with peptides containing multiple basic residues that sequesters protons. The formation of y-ions are also promoted by multiple acidic residues.

References

1. Coon, J., J.; Syka, J. E. P.; Shabanowitz, J.; Hunt, D. F. Tandem Mass Spectrometry for Peptide and Protein Sequence Analysis. *BioTechniques* **2005**, *38*, 519-523.

2. Trauger, S. A.; Webb, W.; Siuzdak, G. Peptide and Protein Analysis with Mass Spectrometry. *Spectroscopy* **1900**, *16*, 320152.

3. Zhang, G.; Annan, R. S.; Carr, S. A.; Neubert, T. A. Overview of Peptide and Protein Analysis by Mass Spectrometry. *Curr. Protoc. Protein Sci.* **2010**, *62*, 16.1.1-16.1.30.

4. Hayes, R. N.; Gross, M. L. Collision-Induced Dissociation. *Meth. Enzymol.* **1990**, *193*, 237-263.

5. Zubarev, R. A.; Kelleher, N. L.; McLafferty, F. W. Electron Capture Dissociation of Multiply Charged Protein Cations. A Nonergodic Process. *J. Am. Chem. Soc.* **1998**, *120*, 3265-3266.

6. Syka, J. E. P.; Coon, J. J.; Schroeder, M. J.; Shabanowitz, J.; Hunt, D. F. Peptide and Protein Sequence Analysis by Electron Transfer Dissociation Mass Spectrometry. *Proc. Natl. Acad. Sci. USA* **2004**, *101*, 9528-9533.

7. Hogan, J. M.; Pitteri, S. J.; Chrisman, P. A.; McLuckey, S. A. Complementary Structural Information from a Tryptic N-Linked Glycopeptide Via Electron Transfer Ion/Ion Reactions and Collision-Induced Dissociation. *J. Proteome Res.* **2005**, *4*, 628-632.

8. Dongre, A. R.; Jones, J. L.; Somogyi, A.; Wysocki, V. H. Influence of Peptide Composition, Gas-Phase Basicity, and Chemical Modification on Fragmentation Efficiency: Evidence for the Mobile Proton Model. *J. Am. Chem. Soc.* **1996**, *118*, 8365-8374.

9. Kjeldsen, F.; Giessing, A. M. B.; Ingrell, C. R.; Jensen, O. N. Peptide Sequencing and Characterization of Post-Translational Modifications by Enhanced Ion-Charging and Liquid Chromatography Electron-Transfer Dissociation Tandem Mass Spectrometry. *Anal. Chem.* **2007**, *79*, 9243-9252.

10. Madsen, J. A.; Brodbelt, J. S. Comparison of Infrared Multiphoton Dissociation and Collision-Induced Dissociation of Supercharged Peptides in Ion Traps. *J. Am. Soc. Mass Spectrom.* **2009**, *20*, 349-358.

11. Commodore, J. J.; Cassady, C. J. Effects of Acidic Peptide Size and Sequence on Trivalent Praseodymium Adduction and Electron Transfer Dissociation Mass Spectrometry. *J. Mass Spectrom.* **2017**, *52*, 218-229.

12. Gao, J.; Cassady, C. J. Negative Ion Production from Peptides and Proteins by Matrix-Assisted Laser Desorption/Ionization Time-of-Flight Mass Spectrometry. *Rapid Commun. Mass Spectrom.* **2008**, *22*, 4066-4072.

13. Huzarska, M.; Ugalde, I.; Kaplan, D. A.; Hartmer, R.; Easterling, M. L.; Polfer, N. C. Negative Electron Transfer Dissociation of Deprotonated Phosphopeptide Anions: Choice of Radical Cation Reagent and Competition between Electron and Proton Transfer. *Anal. Chem.* **2010**, *82*, 2873-2878.

14. Iavarone, A. T.; Williams, E. R. Collisionally Activated Dissociation of Supercharged Proteins Formed by Electrospray Ionization. *Anal. Chem.* **2003**, *75*, 4525-4533.

15. Iavarone, A. T.; Williams, E. R. Supercharging in Electrospray Ionization: Effects on Signal and Charge. *Int. J. Mass Spectrom.* **2002**, *219*, 63-72.

16. Iavarone, A. T.; Jurchen, J. C.; Williams, E. R. Supercharged Protein and Peptide Ions Formed by Electrospray Ionization. *Anal. Chem.* **2001**, *73*, 1455-1460.

17. Sterling, H. J.; Williams, E. R. Origin of Supercharging in Electrospray Ionization of Noncovalent Complexes from Aqueous Solution. *J. Am. Soc. Mass Spectrom.* **2009**, *20*, 1933-1943.

18. Douglass, K. A.; Venter, A. R. Investigating the Role of Adducts in Protein Supercharging with Sulfolane. *J. Am. Soc. Mass Spectrom.* **2012**, *23*, 489-497.

19. Lomeli, S. H.; Peng, I. X.; Yin, S.; Ogorzalek Loo, R. R.; Loo, J. A. New Reagents for Increasing ESI Multiple Charging of Proteins and Protein Complexes. *J. Am. Soc. Mass Spectrom.* **2010**, *21*, 127-131.

20. Sterling, H. J.; Daly, M. P.; Feld, G. K.; Thoren, K. L.; Kintzer, A. F.; Krantz, B. A.; Williams, E. R. Effects of Supercharging Reagents on Noncovalent Complex Structure in Electrospray Ionization from Aqueous Solutions. *J. Am. Soc. Mass Spectrom.* **2010**, *21*, 1762-1774.

21. Asakawa, D.; Wada, Y. Electron Transfer Dissociation Mass Spectrometry of Peptides Containing Free Cysteine using Group XII Metals as a Charge Carrier. *J. Phys. Chem. B* **2014**, *118*, 12318-12325.

22. Asakawa, D.; Takeuchi, T.; Yamashita, A.; Wada, Y. Influence of Metal–Peptide Complexation on Fragmentation and Inter-Fragment Hydrogen Migration in Electron Transfer Dissociation. *J. Am. Soc. Mass Spectrom.* **2014**, *25*, 1029-1039.

23. Dong, J.; Vachet, R. W. Coordination Sphere Tuning of the Electron Transfer Dissociation Behavior of Cu(II)-Peptide Complexes. *J. Am. Soc. Mass Spectrom.* **2012**, *23*, 321-329.

24. Commodore, J. J.; Cassady, C. J. The Effects of Trivalent Lanthanide Cationization on the Electron Transfer Dissociation of Acidic Fibrinopeptide B and its Analogs. *J. Am. Soc. Mass Spectrom.* **2016**, *27*, 1499-1509.

25. Feng, C.; Commodore, J. J.; Cassady, C. J. The use of Chromium(III) to Supercharge Peptides by Protonation at Low Basicity Sites. *J. Am. Soc. Mass Spectrom.* **2015**, *26*, 347-358.

26. Commodore, J. J.; Jing, X.; Cassady, C. J. Optimization of Electrospray Ionization Conditions to Enhance Formation of Doubly Protonated Peptide Ions with and without Addition of Chromium(III). *Rapid Commun. Mass Spectrom.* **2017**, *31*, 1129-1136.

27. Persaud, R. R.; Dieke, N. E.; Jing, X.; Lambert, S.; Parsa, N.; Hartmann, E.; Vincent, J. B.; Cassady, C. J.; Dixon, D. A. Mechanistic Study of Enhanced Protonation by Chromium(III) in Electrospray Ionization: A Superacid Bound to a Peptide. *J. Am. Soc. Mass Spectrom.* **2020**, *31*, 308-318.

28. Jing, X.; Edwards, K. C.; Vincent, J. B.; Cassady, C. J. The use of Chromium(III) Complexes to Enhance Peptide Protonation by Electrospray Ionization Mass Spectrometry. *J. Mass Spectrom.* **2018**, *53*, 1198-1206.

29. Chan, W. Y. K.; Chan, T. W. D. Natural Structural Motifs that Suppress Peptide Ion Fragmentation After Electron Capture. *J. Am. Soc. Mass Spectrom.* **2010**, *21*, 1235-1244.

30. Wong, P. S. J.; Chen, X.; Deng, L.; Wang, Z.; Li, W.; Wong, Y. L. E.; Chan, T. W. D. Suppression of Peptide Ion Dissociation Under Electron Capture: Role of Backbone Amide Hydrogen. *Rapid Commun. Mass Spectrom.* **2015**, *29*, 1757-1764.

31. Chalkley, R. J.; Medzihradszky, K. F.; Lynn, A. J.; Baker, P. R.; Burlingame, A. L. Statistical Analysis of Peptide Electron Transfer Dissociation Fragmentation Mass Spectrometry. *Anal. Chem.* **2010**, *82*, 579-584.

32. Li, W.; Song, C.; Bailey, D. J.; Tseng, G. C.; Coon, J. J.; Wysocki, V. H. Statistical Analysis of Electron Transfer Dissociation Pairwise Fragmentation Patterns. *Anal. Chem.* **2011**, *83*, 9540-9545.

33. Sun, R.; Dong, M.; Song, C.; Chi, H.; Yang, B.; Xiu, L.; Tao, L.; Jing, Z.; Liu, C.; Wang, L.; Fu, Y.; He, S. Improved Peptide Identification for Proteomic Analysis Based on Comprehensive Characterization of Electron Transfer Dissociation Spectra. *J. Proteome Res.* **2010**, *9*, 6354-6367.

34. Wu, S.; Jiang, H.; Lu, Q.; Dai, S.; Hancock, W. S.; Karger, B. L. Mass Spectrometric Determination of Disulfide Linkages in Recombinant Therapeutic Proteins using Online LC−MS with Electron-Transfer Dissociation. *Anal. Chem.* **2009**, *81*, 112-122.

35. Wu, S.; Jiang, H.; Hancock, W. S.; Karger, B. L. Identification of the Unpaired Cysteine Status and Complete Mapping of the 17 Disulfides of Recombinant Tissue Plasminogen Activator using LC−MS with Electron Transfer Dissociation/Collision Induced Dissociation. *Anal. Chem.* **2010**, *82*, 5296-5303.

36. Roepstorff, P.; Fohlman, J. Proposal for a Common Nomenclature for Sequence Ions in Mass Spectra of Peptides. *Biomed. Mass Spectrom.* **1984**, *11*, 601.

37. Biemann, K. Contributions of Mass-Spectrometry to Peptide and Protein-Structure. *Biomed. Environ. Mass Spectrom.* **1988**, *16*, 99-111.

38. Zubarev, R. A.; Kruger, N. A.; Fridriksson, E. K.; Lewis, M. A.; Horn, D. M.; Carpenter, B. K.; McLafferty, F. W. Electron Capture Dissociation of Gaseous Multiply-Charged Proteins is Favored at Disulfide Bonds and Other Sites of High Hydrogen Atom Affinity. *J. Am. Chem. Soc.* **1999**, *121*, 2857-2862.

39. Cooper, H. J. Investigation of the Presence of B Ions in Electron Capture Dissociation Mass Spectra. *J. Am. Soc. Mass Spectrom.* **2005**, *16*, 1932-1940.

40. Marek, A.; Pepin, R.; Peng, B.; Laszlo, K. J.; Bush, M. F.; Tureček, F. Electron Transfer Dissociation of Photolabeled Peptides. Backbone Cleavages Compete with Diazirine Ring Rearrangements. *J. Am. Soc. Mass Spectrom.* **2013**, *24*, 1641-1653.

41. Liu, J.; McLuckey, S. A. Electron Transfer Dissociation: Effects of Cation Charge State on Product Partitioning in Ion/Ion Electron Transfer to Multiply Protonated Polypeptides. *Int. J. Mass Spectrom.* **2012**, *330-332*, 174-181.

42. Chen, X.; Wang, Z.; Li, W.; Wong, Y. L. E.; Chan, T. W. D. Effect of Structural Parameters on the Electron Capture Dissociation and Collision-Induced Dissociation Pathways of Copper(II)-Peptide Complexes. *Eur. J. Mass Spectrom.* **2015**, *21*, 649-657.

43. Riley, N. M.; Westphall, M. S.; Coon, J. J. Activated Ion-Electron Transfer Dissociation Enables Comprehensive Top-Down Protein Fragmentation. *J. Proteome Res.* **2017**, *16*, 2653-2659.

44. Frese, C. K.; Altelaar, A. F.; van den Toorn, H.; Nolting, D.; Griep-Raming, J.; Heck, A. J.; Mohammed, S. Toward Full Peptide Sequence Coverage by Dual Fragmentation Combining Electron-Transfer and Higher-Energy Collision Dissociation Tandem Mass Spectrometry. *Anal. Chem.* **2012**, *84*, 9668-9673.

45. Bouchoux, G.; Desaphy, S.; Bourcier, S.; Malosse, C.; Bimbong, R. N. B. Gas-Phase Protonation Thermochemistry of Arginine. *J. Phys. Chem. B* **2008**, *112*, 3410-3419.

46. Taouatas, N.; Drugan, M. M.; Heck, A. J. R.; Mohammed, S. Straightforward Ladder Sequencing of Peptides using a Lys-N Metalloendopeptidase. *Nat. Methods* **2008**, *5*, 405-407.

47. Olsen, J. V.; Ong, S. E.; Mann, M. Trypsin Cleaves Exclusively C-Terminal to Arginine and Lysine Residues. *Mol. Cell. Proteomics* **2004**, *3*, 608-614.

48. Picotti, P.; Aebersold, R.; Domon, B. The Implications of Proteolytic Background for Shotgun Proteomics. *Mol. Cell. Proteomics* **2007**, *6*, 1589-1598.

49. Tabb, D. L.; Huang, Y.; Wysocki, V. H.; Yates, J. R. Influence of Basic Residue Content on Fragment Ion Peak Intensities in Low-Energy Collision-Induced Dissociation Spectra of Peptides. *Anal. Chem.* **2004**, *76*, 1243-1248.

50. Syrstad, E. A.; Tureček, F. Toward a General Mechanism of Electron Capture Dissociation. *J. Am. Soc. Mass Spectrom.* **2005**, *16*, 208-224.

51. Zubarev, R. A.; Horn, D. M.; Fridriksson, E. K.; Kelleher, N. L.; Kruger, N. A.; Lewis, M. A.; Carpenter, B. K.; McLafferty, F. W. Electron Capture Dissociation for Structural Characterization of Multiply Charged Protein Cations. *Anal. Chem.* **2000**, *72*, 563-573.

52. Hayakawa, S.; Hashimoto, M.; Matsubara, H.; Turecek, F. Dissecting the Proline Effect: Dissociations of Proline Radicals Formed by Electron Transfer to Protonated Pro-Gly and Gly-Pro Dipeptides in the Gas Phase. *J. Am. Chem. Soc.* **2007**, *129*, 7936-7949.

53. Bleiholder, C.; Suhai, S.; Harrison, A. G.; Paizs, B. Towards Understanding the Tandem Mass Spectra of Protonated Oligopeptides. 2: The Proline Effect in Collision-Induced Dissociation of Protonated Ala-Ala-Xxx-Pro-Ala (Xxx = Ala, Ser, Leu, Val, Phe, and Trp). *J. Am. Soc. Mass Spectrom.* **2011**, *22*, 1032-1039.

54. Vaisar, T.; Urban, J. Probing the Proline Effect in CID of Protonated Peptides. *J. Mass Spectrom.* **1996**, *31*, 1185-1187.

55. Schwartz, B. L.; Bursey, M. M. Some Proline Substituent Effects in the Tandem Mass Spectrum of Protonated Pentaalanine. *Biol. Mass Spectrom.* **1992**, *21*, 92-96.

56. Ewing, N. P.; Zhang, X.; Cassady, C. J. Determination of the Gas-Phase Basicities of Proline and its Di- and Tripeptides with Glycine: The Enhanced Basicity of Prolylproline. *J. Mass Spectrom.* **1996**, *31*, 1345-1350.

57. Sargaeva, N. P.; Lin, C.; O'Connor, P. B. Unusual Fragmentation of B-Linked Peptides by ExD Tandem Mass Spectrometry. *J. Am. Soc. Mass Spectrom.* **2011**, *22*, 480-491.

58. Li, X.; Lin, C.; O'Connor, P. B. Glutamine Deamidation: Differentiation of Glutamic Acid and Γ-Glutamic Acid in Peptides by Electron Capture Dissociation. *Anal. Chem.* **2010**, *82*, 3606-3615.

59. Li, X.; Lin, C.; Han, L.; Costello, C. E.; O'Connor, P. B. Charge Remote Fragmentation in Electron Capture and Electron Transfer Dissociation. *J. Am. Soc. Mass Spectrom.* **2010**, *21*, 646-656.

60. O'Connor, P. B.; Cournoyer, J. J.; Pitteri, S. J.; Chrisman, P. A.; McLuckey, S. A. Differentiation of Aspartic and Isoaspartic Acids using Electron Transfer Dissociation. *J. Am. Soc. Mass Spectrom.* **2006**, *17*, 15-19.

61. Chan, W. Y. K.; Chan, T. W. D.; O'Connor, P. B. Electron Transfer Dissociation with Supplemental Activation to Differentiate Aspartic and Isoaspartic Residues in Doubly Charged Peptide Cations. *J. Am. Soc. Mass Spectrom.* **2010**, *21*, 1012-1015.

CHAPTER 8. CONCLUDING REMARKS

In mass spectrometry (MS) analysis, the first step is conversion of the analyte into gas-phase ions. For peptide and protein studies, this is often accomplished with electrospray ionization (ESI). Fundamental studies of the ionization of peptides and proteins is of importance, and many techniques have been developed to improve ionization efficiency in ESI by increasing charge state.[1-5] The focus of supercharging in ESI has been with proteins. Dr. Heather Watson, a previous Cassady group member, discovered that the addition of trivalent chromium, Cr(III), to peptide solutions undergoing ESI enhances the protonation of the peptide.[6] This discovery was further studied by Dr. Changgeng Fang,[7] Dr. Juliette Commodore,[8] and Dr. Xinyao Jing.[9] The work in this dissertation builds upon these studies and investigates the scope of Cr(III) enhanced protonation of peptides.

In Chapter 3, experimental studies were carried out with model peptides to gain an understanding of the mechanism of Cr(III) enhanced protonation by probing properties of peptides. The ESI results reveal that the position of acidic residues (i.e., glutamic acid and aspartic acid) affects the extent of enhanced protonation using Cr(III). Acidic residues near the C-terminus generate the largest 2+ to 1+ ratio indicating the importance of the carboxyl group in the mechanism. The carboxyl group can be located on the sidechain of acidic residues or at the C-terminus. The amino acids, proline and tyrosine, were determined to have no effect on enhanced protonation using Cr(III). In contrast, addition of Cr(III) does not enhance the protonation of phosphorylated peptides, but rather suppresses its ionization. This can be attributed to Cr(III) and phosphate groups forming insoluble salts.

Experimental and computational studies were employed to elucidate the mechanism of enhanced protonation using Cr(III). Computational studies using density functional theory were performed by Dr. Rudradatt Persaud of the Dixon group.[10] The mechanism involves the loss of water from the Cr(III) complex, which shifts the pKa of the complex into the range of superacids. The highly acidic Cr(III) complex coordinates with a carboxylic acid group. In ESI experiments of the peptide amides A7-NH_2 and A3EA3-NH_2 methyl ester, where no carboxyl group exists, enhanced protonation is observed. In this case, amide groups, which can deprotonate[11-13] and coordinate metal ions,[14] may act as a site of Cr(III) coordination. A proton can then be transferred to an amide site on the peptide backbone followed by dissociation of Cr(III) from the peptide.

In Chapter 4, the test peptide heptaalanine was employed to investigate alternative methods of adding Cr(III) in peptide analysis by MS. The focus was on post-column addition of Cr(III) because liquid chromatography (LC) MS studies by Matthew Mireles[15] showed that using Cr(III) as a mobile phase additive had a negative impact on chromatographic resolution and separation. Three post-column methods were studied. The most promising methods are the use of a tee connection to introduce the Cr(III) solution in parallel to the peptide solution and the doping of the nebulizing gas with Cr(III). Another method, depositing Cr(III) onto the ESI spray shield, enhances the protonation of A7 by forming $[M + 2H]^{2+}$, but in order to obtain continuing effects a constant supply of Cr(III) is necessary. In addition, depositing Cr(III) on the spray shield requires a high concentration of Cr(III) that can clog the ESI capillary and decrease signal intensity. Doping the nebulizing gas with Cr(III) also necessitates a high concentration of Cr(III) to observe formation of $[M + 2H]^{2+}$, which causes a decrease in overall signal intensity of $[M + H]^{+}$. Perhaps the most important feature of these latter two methods is they demonstrate that

Cr(III) does not have to be present in the peptide solution in order to induce enhanced protonation; instead, Cr(III) can be introduced during the ESI desolvation stage.

The work presented in Chapter 4 serves as preliminary data to give future direction on incorporating Cr(III) into the LC-MS bottom-up proteomics workflows. Using a tee union to add Cr(III) into the ESI source region generates the largest ratio of 2+ to 1+ of 2:1. To expand on this work, further optimization should be done to improve on these results including finding the optimal flow rate for the sample as well as the drying gas flow and nebulizing gas pressure, which are critical factors in Cr(III) enhanced protonation in ESI. Additionally, the method of doping the nebulizing gas with Cr(III) should be optimized. Instead of a solution of Cr(III), the nebulizing gas can be passed through solid Cr(III). Lastly, to better reflect real-world MS applications, a peptide mixture should be analyzed using LC-MS with post-column addition of Cr(III).

In Chapter 5, the ability of Cr(III) to enhance the ionization of peptides in matrix-assisted laser desorption ionization (MALDI) was studied. Dr. Xinyao Jing determined that Cr(III) is not suitable for use as a MALDI matrix.[16] The work presented in this chapter studied Cr(III) as an additive to improve protonation. Based upon the postulated mechanism for Cr(III) enhanced protonation (which involves coordination of Cr(III) to carboxyl groups) and routine peptide analysis in MALDI, nine matrices with varying properties were investigated with Cr(III). Two common methods of depositing the sample on the MALDI target plate was also studied.

Enhanced protonation in MALDI using Cr(III) was inconclusive. Some promising enhancements in peptide protonation were observed although the results were not always reproducible. It is well established that MALDI suffers from poor sample-to-sample and shot-to-shot reproducibility. In a study such as this one, where absolute ion intensities are being

compared, reproducibility is essential. The thin-layer method produced more reproducible results than the dried droplet method, although the standard deviations were still large in both methods. Addition of Cr(III) to substance P does improve the homogeneity of the crystal sizes in the thin-layer method, but it had no effect on heptaalanine amide.

In Chapter 6, the focus reverts to Cr(III) enhanced protonation in ESI with a survey of biological peptides. Work presented in previous chapters utilized model peptides and a few biological peptides to study the effect Cr(III) has on protonation. This study included twenty-seven acidic, basic, and neutral biological peptides to study the utility of Cr(III) in proteomic research. Of the peptides studied, five peptides added an additional charge state (n) upon addition of Cr(III) to the peptide solution undergoing ESI. Three of the peptides that added an additional proton, fibrinopeptide B, des-Arg^{14}-Glu^{1}-fibrinopeptide B, and EGFR (985-966), were acidic in nature. Bradykinin (2-9) was the only basic peptide that added an additional charge state. The peptides ACTH (1-13), WP9QY, TNFα Antagonist, CEBVB (280-288), amylin (20-29), chemerin (149-157), and substance P acid did not add an additional proton, but an increase in ion intensity for the highest charge state formed by ESI is observed with Cr(III). These results agree with previous studies that showed that acidic peptides are more likely to add an additional proton with Cr(III), while basic peptides are more likely to experience an increase in signal intensity.[7,9] Unlike model peptides, the biological peptides in this study contain a myriad of sidechains that can interact and influence higher order structures of the peptide. There is a possibility that interactions between functional groups can prevent Cr(III) from coordinating efficiently with the peptide. In addition, interactions of Cr(III) with multiple functional groups simultaneously could hinder the ability of Cr(III) to detach from the peptide during formation of $[M + nH]^{n+}$.

The work presented in Chapter 7 studies the electron transfer dissociation (ETD) of multiply protonated peptide ions. ETD is a tandem mass spectrometry (MS/MS) technique that is used in peptide sequencing and requires multiply charged precursor ions. Th ETD fragmentation of protonated precursor ions produced with Cr(III) was the same as the ETD of the precursor ion produced with 1% acetic acid. Thus, the use of Cr(III) as an ESI additive is not affecting the gas-phase peptide ion structures. Performing ETD on higher charge states (n) provides better sequence coverage. The presence of a basic residue (i.e. arginine or lysine) at the C-terminus leads to the ETD mass spectra of $[M + 2H]^{2+}$ being dominated by z-ions containing the basic residue. At n = 3 and n = 4, the effect of the basic residue on fragmentation is diminished. The mobile proton model of protonated peptide fragmentation[17] can be used to explain this trend. At higher n values, the additional protons are mobilized and can induce more random fragmentation compared to n = 2. Another observation is the formation of y-ions in ETD, which seems to be influenced by the presence of proline and acidic residues. The formation of y-ions is a characteristic of collision-induced dissociation (CID) but has been observed in ETD experiments.[18] For future work, the formation of y-ions in ETD can be further investigated using model peptides containing proline and acidic residues. The N-terminal N-Cα bond adjacent to proline does not cleave during the ETD process due to the side chain of proline being cyclized onto the peptide backbone amide group. The formation of y-ions could help in indicating the presence of proline in the peptide sequence if there is, in fact, a correlation.

The ETD of $[M + 2H]^{2+}$ results in an extensive amount of charge reduced and ETnoD products. This is typically remedied by adding supplemental energy after the ETD process to disrupt any hydrogen or noncovalent bonding that holds the cleaved peptide fragments intact at the mass-to-charge ratio of the precursor ion. The Bruker HCTultra PTM Discovery System

mass spectrometer has a “smart decomposition” function that applies resonant excitation (very low energy CID) to overcome these attractive forces. Unfortunately, this function stopped working on the instrument and applying supplemental energy manually could not be accomplished due to software limitations. Expansion of this work should include repeating ETD on $[M + 2H]^{2+}$ using supplemental energy.

The work presented in this dissertation gives an overall perspective of the analytical utility of Cr(III)-enhanced protonation of peptides in MS. This contribution increases the knowledge on the mechanism in which Cr(III) enhances protonation in ESI and describes its limitations. The ability of Cr(III) to enhance the protonation of peptides is a novel aspect that can be beneficial to bottom-up ESI-MS and MS/MS analysis.

References

1. Iavarone, A. T.; Jurchen, J. C.; Williams, E. R. Supercharged Protein and Peptide Ions Formed by Electrospray Ionization. *Anal. Chem.* **2001**, *73*, 1455-1460.

2. Iavarone, A. T.; Williams, E. R. Supercharging in Electrospray Ionization: Effects on Signal and Charge. *Int. J. Mass Spectrom.* **2002**, *219*, 63-72.

3. Lomeli, S. H.; Peng, I. X.; Yin, S.; Ogorzalek Loo, R. R.; Loo, J. A. New Reagents for Increasing ESI Multiple Charging of Proteins and Protein Complexes. *J. Am. Soc. Mass Spectrom.* **2010**, *21*, 127-131.

4. Flick, T. G.; Williams, E. R. Supercharging with Trivalent Metal Ions in Native Mass Spectrometry. *J. Am. Soc. Mass Spectrom.* **2012**, *23*, 1885-1895.

5. Sterling, H. J.; Cassou, C. A.; Susa, A. C.; Williams, E. R. Electrothermal Supercharging of Proteins in Native Electrospray Ionization. *Anal. Chem.* **2012**, *84*, 3795-3801.

6. Watson, H. M. Effects of Transition Metal Cationization on Peptide Dissociation by Mass Spectrometry. Ph.D. Dissertation, The University of Alabama, Tuscaloosa, AL, USA, 2011.

7. Feng, C.; Commodore, J. J.; Cassady, C. J. The use of Chromium(III) to Supercharge Peptides by Protonation at Low Basicity Sites. *J. Am. Soc. Mass Spectrom.* **2015**, *26*, 347-358.

8. Commodore, J. J.; Jing, X.; Cassady, C. J. Optimization of Electrospray Ionization Conditions to Enhance Formation of Doubly Protonated Peptide Ions with and without Addition of Chromium(III). *Rapid Commun. Mass Spectrom.* **2017**, *31*, 1129-1136.

9. Jing, X.; Edwards, K. C.; Vincent, J. B.; Cassady, C. J. The use of Chromium(III) Complexes to Enhance Peptide Protonation by Electrospray Ionization Mass Spectrometry. *J. Mass Spectrom.* **2018**, *53*, 1198-1206.

10. Persaud, R. R.; Dieke, N. E.; Jing, X.; Lambert, S.; Parsa, N.; Hartmann, E.; Vincent, J. B.; Cassady, C. J.; Dixon, D. A. Mechanistic Study of Enhanced Protonation by Chromium(III) in Electrospray Ionization: A Superacid Bound to a Peptide. *J. Am. Soc. Mass Spectrom.* **2020**, *31*, 308-318.

11. Bokatzian-Johnson, S. S.; Stover, M. L.; Dixon, D. A.; Cassady, C. J. A Comparison of the Effects of Amide and Acid Groups at the C-Terminus on the Collision-Induced Dissociation of Deprotonated Peptides. *J. Am. Soc. Mass Spectrom.* **2012**, *23*, 1544-1557.

12. Plummer, C. E.; Stover, M. L.; Bokatzian, S. S.; Davis, J. T. M.; Dixon, D. A.; Cassady, C. J. An Experimental and Computational Study of the Gas-Phase Acidities of the Common Amino Acid Amides. *J. Phys. Chem. B* **2015**, *119*, 9661-9669.

13. Li, Z.; Matus, M. H.; Velazquez, H. A.; Dixon, D. A.; Cassady, C. J. Gas-Phase Acidities of Aspartic Acid, Glutamic Acid, and their Amino Acid Amides. *Int. J. Mass Spectrom.* **2007**, *265*, 213-223.

14. Sigel, H.; Martin, R. B. Coordinating Properties of the Amide Bond. Stability and Structure of Metal Ion Complexes of Peptides and Related Ligands. *Chem. Rev.* **1982**, *82*, 385-426.

15. Mireles, M.; Cassady, C. J. University of Alabama, Tuscaloosa, AL. Unpublished work, **2019.**

16. Jing, X. Investigations involving proton/hydrogen transfer in peptides using mass spectrometry. Ph.D. Dissertation, University of Alabama, Tuscaloosa, AL, 2020.

17. Dongre, A. R.; Jones, J. L.; Somogyi, A.; Wysocki, V. H. Influence of Peptide Composition, Gas-Phase Basicity, and Chemical Modification on Fragmentation Efficiency: Evidence for the Mobile Proton Model. *J. Am. Chem. Soc.* **1996**, *118*, 8365-8374.

18. Marek, A.; Pepin, R.; Peng, B.; Laszlo, K.; Bush, M.; Tureček, F. Electron Transfer Dissociation of Photolabeled Peptides. Backbone Cleavages Compete with Diazirine Ring Rearrangements. *J. Am. Soc. Mass Spectrom.* **2013**, *24*, 1641-1653.